FLIGHT RESEARCH LABORATORY

THE UNIVERSITY OF KANSAS CENTER FOR RESEARCH, INC.
2291 Irving Hill Drive
Lawrence, Kansas 66045-2969

AN INVESTIGATION OF FIGHTER AIRCRAFT AGILITY

KU-FRL-831-7
5 November 1993

FINAL TECHNICAL REPORT
NCC 2-588 Phases I-V, 01/01/89 - 12/31/93

John Valasek
and
David R. Downing, Principal Investigator

THE UNIVERSITY OF KANSAS CENTER FOR RESEARCH, INC.
Flight Research Laboratory
2291 Irving Hill Drive
Lawrence, Kansas 66045
(913) 864-3043

prepared for
Joseph Gera and Robert Clarke, Technical Monitors
NASA Ames Research Center
Dryden Flight Research Facility

ABSTRACT

This report attempts to unify in a single document the results of a series of studies on fighter aircraft agility funded by the NASA Ames Research Center, Dryden Flight Research Facility and conducted at the University of Kansas Flight Research Laboratory during the period January 1989 through December 1993. New metrics proposed by pilots and the research community to assess fighter aircraft agility are collected and analyzed. The report develops a framework for understanding the context into which the various proposed fighter agility metrics fit in terms of application and testing. Since new metrics continue to be proposed, this report does not claim to contain every proposed fighter agility metric. Flight test procedures, test constraints, and related criteria are developed. Instrumentation required to quantify agility via flight test is considered, as is the sensitivity of the candidate metrics to deviations from nominal pilot command inputs, which is studied in detail. Instead of supplying specific, detailed conclusions about the relevance or utility of one candidate metric versus another, the authors have attempted to provide sufficient data and analyses for readers to formulate their own conclusions. Readers are therefore ultimately responsible for judging exactly which metrics are "best" for their particular needs. Additionally, it is not the intent of the authors to suggest combat tactics or other actual operational uses of the results and data in this report. This has been left up to the user community.

Twenty of the candidate agility metrics were selected for evaluation with high fidelity, nonlinear, non real-time flight simulation computer programs of the F-5A Freedom Fighter, F-16A Fighting Falcon, F-18A Hornet, and X-29A. The information and data presented on the 20 candidate metrics which were evaluated will assist interested readers in conducting their own extensive investigations. The report provides i) a definition and analysis of each metric; ii) details of how to test and measure the metric, including any special data reduction requirements; iii) typical values for

the metric obtained using one or more aircraft types, and iv) a sensitivity analysis if applicable.

The report is organized as follows. The first chapter in the report presents a historical review of air combat trends which demonstrate the need for agility metrics in assessing the combat performance of fighter aircraft in a modern, all-aspect missile environment. The second chapter presents a framework for classifying each candidate metric according to time scale (transient, functional, instantaneous), further subdivided by axis (pitch, lateral, axial). The report is then broadly divided into two parts, with the transient agility metrics (pitch lateral, axial) covered in chapters three, four, and five, and the functional agility metrics covered in chapter six. Conclusions, recommendations, and an extensive reference list and biography are also included. Five appendices contain a comprehensive list of the definitions of all the candidate metrics collected by the investigators; a description of the aircraft models and flight simulation programs used for testing the metrics; several relations and concepts which are fundamental to the study of lateral agility; an in-depth analysis of the axial agility metrics; and a derivation of the relations for the instantaneous agility metrics and their approximations, including an example of their use.

PREFACE

This report is a summary of fighter agility metrics research conducted by the University of Kansas Flight Research Laboratory from the period January 1989 through December 1993. This work was conducted by several researchers, and resulted in five reports, six theses, five conference papers, and two journal articles. The objective of this report was to collect the individual reports and theses and supplement them with new material in order to present a comprehensive and coherent overview. In addition to the authors, the researchers who have contributed to this report are Randall K. Liefer, David P. Eggold, Brian W. Cox, George W. Ryan III, and Frank H. Liu.

In the course of this study, the researchers have received assistance and many valuable suggestions. The authors extend their appreciation and thanks to the following persons: Joseph Gera, Robert Clarke, and Joseph Wilson of the NASA Ames Research Center, Dryden Flight Research Facility; Edward D. Onstott of the Northrop Corporation, Aircraft Division; Herbert H. Hickey Jr., G. Thomas Black, and William T. Thomas of the Air Force Wright Research and Development Center; Major Bob Vosburgh and Major Dale A. Nagy, United States Air Force; Major Steven Grohsmeyer, United States Marine Corps.

TABLE OF CONTENTS

LIST OF FIGURES

LIST OF TABLES

NOMENCLATURE

ADI	attitude direction indicator	
AIM	aircraft interception missile	
AOA	angle of attack	degrees
A_{cent}	centripetal acceleration	feet/sec^2
alpha	angle of attack	degrees
ATHP	aircraft time history program	
b	wing span	feet
beta	sideslip angle	degrees
BVR	beyond visual range	
$C_{L_{max}}$	maximum lift coefficient	
C_{m_α}	variation of pitching moment coefficient due to angle of attack	
C_{m_δ}	variation of pitching moment coefficient due to pitch control effectors	
CCT	combat cycle time metric	seconds
CG	center of gravity	
$\bar{c}$	mean aerodynamic chord	feet
D	drag	pounds
DEG	degrees	
DT	product of crossrange and time metric	feet-seconds
EM	energy maneuverability	
FCS	flight control system	
FS	fuselage station	inches
GLOC	g induced loss of consciousness	

g	gravitational acceleration	feet/sec^2
H	altitude	feet
HARV	high angle of attack research vehicle	
HUD	head up display	
h_e	specific energy height	feet
IR	infrared	
I_{XZ}	XZ product of inertia	slug-feet^2
I_{XX}, I_{YY}, I_{ZZ}	moment of inertia about X, Y, Z axes	slug-feet^2
KIAS	indicated airspeed	knots
KTAS	true airspeed	knots
KU/FRL	University of Kansas Flight Research Laboratory	
k	x10^3	
L	lift	pounds
L	rolling moment	foot-pounds
LEX	leading edge extension	
lbf	pounds force	
M	pitching moment	foot-pounds
M	Mach number	
M_{ic}	pitching moment due to inertial coupling	foot-pounds
M_{start}	starting or initial Mach number	
M_{test}	test Mach number	
MGC	mean geometric chord	
MvN	some quantity "M" versus some quantity "N"	

M_δ	dimensional variation of pitching moment due to pitch control effectors	$seconds^{-2}$
N	yawing moment	foot-pounds
NASA	national aeronautics and space administration	
N_z	normal load factor	g's
n	normal load factor	g's
n(+), n(-)	upper and lower boundaries of n in the service flight envelope	g's
n_X	axial load factor	g's
n_Y	lateral load factor	g's
n_Z	normal load factor	g's
OTIS	optimal trajectories by implicit simulation	
P	body axis roll rate	degress/second
$P_{man\ plane}$	maneuver plane roll rate	degrees/second
P_S	specific excess power	feet/second
P_{stab}	stability axis roll rate	degrees/second
p	perturbed body axis roll rate	degrees/second
Q	body axis pitch rate	degrees/second
q	perturbed body axis pitch rate	degrees/second
$\bar{q}$	dynamic pressure	$pounds/feet^2$
R	body axis yaw rate	degrees/second
REF	reference	
r	perturbed body axis yaw rate	degrees/second
S	wing area	$feet^2$
SEC	seconds	

SLS	sea level static	
T	thrust	pounds
TEP	time-energy penalty metric	feet-seconds
TO	take off	
TR	turn rate	degrees/second
$T_{max\ g}$	time to achieve maximum normal load factor metric	seconds
T_{RC}	time to roll and capture a bank angle near 90°	seconds
T_{RC90}	time to roll and capture a 90° bank angle change metric	seconds
T_{RC180}	time to roll and capture a 180° bank angle change metric	seconds
T_{TR90}	time to roll through a 90° bank angle metric	seconds
T_{unload}	time to pitch from maximum normal load factor to 0g metric	seconds
T_{90}	time to roll through a 90° bank angle change metric	seconds
t	time	seconds
t_k	time to kill	seconds
V	total velocity	feet/second
VIFFING	vectoring in forward flight	
V_c	corner speed	feet/second, knots
V_t	true airspeed	feet/second, knots
W	weight	pounds
WVR	within visual range	
X	aircraft longitudinal axis	
Y	aircraft lateral axis	
Y	crossrange	feet
Z	aircraft transverse axis	

α	angle of attack	degrees
β	sideslip angle	degrees
γ	pitch angle or flight path angle in Serret-Frenet reference plane	degrees
Δ	incremental value	
Θ, θ	pitch attitude angle	degrees
τ_r	roll subsidence mode time constant	seconds
Φ, ϕ	bank angle	degrees
χ	heading angle in Serret-Frenet reference plane	degrees
Ψ, ψ	heading angle	degrees
ω	turn rate	degrees/second
Я	roll angle in Serret-Frenet reference plane	degrees
1v1	one-verus-one	

SUBSCRIPTS

B, body	body fixed axes
max	maximum value
min	minimum value
n	normal component
S, stab	stability axes
W, wind	relative wind axes
x	axial component

SUPERSCRIPTS

$\dot{}$	derivative with respect to time

1. INTRODUCTION

1.1 BACKGROUND OF AGILITY METRIC RESEARCH

Fighter flying qualities and combat capabilities are currently measured and compared in terms relating to vehicle energy, angular rates and sustained acceleration. Criteria based on these measurable quantities have evolved over the past several decades and are routinely used to design aircraft structures, aerodynamics, propulsion and control systems. While these criteria, or metrics, have the advantage of being well understood, easily verified and repeatable during test, they tend to measure the steady state capability of the aircraft and not its ability to transition quickly from one state to another (REF. 1, 2, 3).

Figure 1.1 displays historical trends in the close or within-visual-range (WVR) air combat arena. In the past, the necessity of achieving stable, rear quarter firing solutions led to extended engagement times and steady state maneuvering. Traditional measures of merit such as maximum level speed, turn rate, rate of climb, and maximum normal load factor were found to be adequate for quantifying aircraft capabilities. Recently, the introduction of lethal, reliable, all-aspect, short range missiles such as the AIM-9L Sidewinder have diminished the emphasis on sustained maneuvering capability. Engagement times have been decreased by nearly an order of magnitude as pilots need only to point their weapons at the target in order to achieve a high probability of kill.
The emphasis now is to "point and shoot" first (REF. 4).

Point and shoot requires an instantaneous maneuver capability (translational and rotational accelerations) and nonsymmetric or uncoordinated dynamic maneuvers (sideslip $\neq 0$, sideforce $\neq 0$). As a result the capability to change aircraft states as quickly as possible has become an important factor for success in modern air combat. This means the modern fighter pilot is required to execute the *same* number of state changes faster, or change a *greater* number of states in the same length of

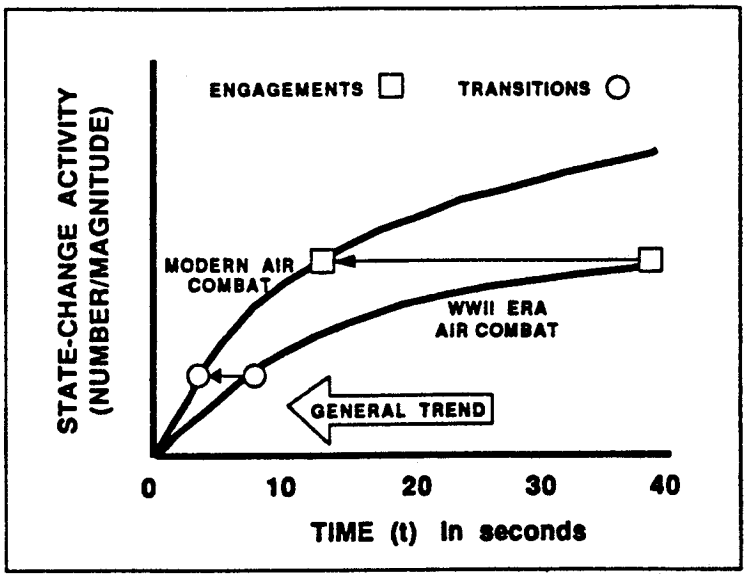

Figure 1.1 Historical Trends in Air Combat (REF. 5)

time, or both, than his predecessors of twenty years ago (REF. 5). This trend identified the need for new performance measures which focus specifically on the bottom left corner of Figure 1.1. This extended set of new performance measures, termed *agility metrics*, have been proposed by both pilots and analysts throughout government and the industry. The basic goals of agility metrics analysis (REF. 6) are to i) measure and compare previously neglected capability, ii) correlate agility metrics to combat capability, and iii) understand how to design for agility. The proposed agility metrics are not intended to replace existing performance measures but to supplement them in quantifying previously unidentified transient capabilities.

Although no universally accepted, specific definition of agility exists, it is generally agreed that agility is concerned with transient capability as opposed to sustained capability. Agility might be described as an unspecified function of maneuverability, controllability (REF. 6), nose pointing ability, accelerations, dynamics, and flying qualities (REF. 5). With respect to these characteristics, it has been suggested that an agility metric should possess the following qualities (REF. 7):

1) OPERATIONAL RELEVANCE - a proposed maneuver should be similar to an actual combat maneuver, not just a pure flight test or airshow maneuver.

2) SIX DEGREES-OF-FREEDOM - aircraft models must be realistic and not constrained to 2-dimensions.

3) TRANSIENT CAPABILITY - should not be overly dependent upon or dominated by steady state qualities.

4) NON-AIRCRAFT SPECIFIC - a proposed maneuver should not be so specialized that either a conventional or a non-conventional aircraft cannot perform it.

5) TESTABLE AND REPEATABLE - a proposed maneuver should be safe to fly and repeatable in a flight test environment without undue pilot workload.

6) DESIGN RELEVANT - should highlight capabilities useful for aircraft and flight control system design and analysis.

Agility studies should be performed closed loop, with the airframe-flight control system-pilot as a complete unit. It is an oversimplification to assume that the nature of agility can be gleaned simply by examining the nonlinear six degree-of-freedom equations of motion to discover the "agility terms" or "agility coefficients" (REF. 5). This type of open loop analysis by itself is fruitless because flight control systems can greatly modify the open loop dynamics. In addition, analysis of the flight control system by itself also yields little useful information without taking into account airframe dynamics.

Although flight testing is ultimately required to accurately measure the agility of real aircraft, nonlinear, non real-time, unmanned flight simulations are useful for a priori evaluation of testing methods and data reduction techniques. All analysis and results presented in this report were obtained by either i) hand calculation, ii) non real-time, nonlinear six degree-of-freedom flight simulation computer programs (e.g., REF. 8), or iii) the Optimal Trajectories by Implicit Simulation (OTIS) computer program (REF. 9, 10). The non real-time flight simulation and trajectory optimization programs require pre-determined pilot commands and pre-determined general trajectories respectively.

This necessitates analysis of deviations from the nominal pilot command inputs, so where applicable these sensitivities are included in this report.

Although the scope of this report is extensive, it does not encompass areas which are of interest to all agility researchers. The specific topics not covered in this report are i) multiple engagements, ii) maneuvering at high angles of attack, iii) flight testing experiences, and iv) agility improvement. Three different types of fighter aircraft are used in the analyses (Appendix B), but restrictions inherent to these simulations required that the aircraft be tested singly and not in groups. Thus there are no one-versus-one (1v1) or multiple engagement (MvN) results in this report. For discussions of 1v1 or MvN results, the interested reader should consult References 11 through 20.

There is also a great deal of interest in controlled flight at angles of attack well beyond that for maximum lift. High rate maneuvering in the low speed, high angle of attack part of the envelope is popularly referred to as *supermaneuverability*. While an agile airplane is also desirable in this flight regime, supermaneuverability is not addressed in this report. For discussions of supermaneuverability, the interested reader should consult References 11, 16, 21, 22, and 23.

Preliminary flight test experience dealing with agility metrics has shown that sufficient accuracy and repeatability can in practice be difficult to obtain. Since flight test experience and results must determine whether or not the simulation methods provide sufficient accuracy to warrant their use in future agility research, all readers are strongly encouraged to familiarize themselves with References 24 and 25.

The agility an aircraft possess is determined by a combination of elements in the aircraft configuration and the flight control system. Any one of these elements can potentially limit the agility of the total aircraft system. By implementing simple changes that do not affect the basic functioning of the flight control system or the validity of the aircraft model, tangible improvements in agility can be obtained. The research that the University of Kansas Flight Research Laboratory (KU/FRL) has

conducted in improving the agility of an existing aircraft is not contained in this report, but is presented in References 26, 27, and 28.

1.2 REPORT OBJECTIVE

This report attempts to compile in a single document the results of a series of studies supported by the NASA Ames Dryden Flight Research Facility and conducted at the KU/FRL during the period January 1989 through July 1993. The majority of the results presented in this report were obtained by several KU/FRL investigators, and comments on experiences and results of the investigations are limited to work performed solely by them. The authors have generated new unpublished results to compliment and unify the previously published data. The intent of the authors is not to suggest combat tactics or other actual operational uses of the results and data in this report. This has been left up to the user community.

The report provides a framework for understanding the context into which the various proposed fighter agility metrics fit in terms of application and testing. Since new metrics continue to be proposed, this report does not claim to contain every agility metric. Results for those candidate metrics which were investigated are usually presented for only a small number of flight conditions, since this research was intended to identify candidate agility metrics and investigate their characteristics, rather than perform exhaustive analyses over the entire operational flight envelope. However, the information and data presented in this report should be sufficient to permit interested readers to conduct their own extensive investigations. Readers interested in investigating a particular metric should be able to locate i) a definition of the metric; ii) an explanation of how to test and measure the metric, including any special data reduction requirements; iii) typical values for the metric obtained using one or more aircraft types, and iv) a sensitivity analysis if applicable.

Instead of supplying specific, detailed conclusions about the relevance or utility of particular metrics, the authors have attempted to provide sufficient data and analyses for readers to formulate their own conclusions. Readers are ultimately responsible for judging exactly which metrics are "best" for their particular needs.

1.3 REPORT ORGANIZATION

This report is broadly divided into two parts; the transient agility metrics are covered in Chapters 2 through 5, and the functional agility metrics are covered in Chapter 6. Chapter 2 presents a framework for classifying the candidate agility metrics investigated. Chapters 3 through 6 each examine a particular class of metrics, according to the framework established in Chapter 2. In each chapter a definition, background discussion, testing methods, and data reduction methods are presented. Typical results and a discussion of sensitivity to testing errors are also presented where appropriate. Pitch agility is investigated in Chapter 3, lateral agility in Chapter 4, and axial agility in Chapter 5. Functional agility is investigated in Chapter 6. Conclusions and recommendations are presented in Chapters 7 and 8 respectively. A comprehensive list of all of the candidate metrics investigated in this report is contained in Appendix A. Appendix B contains a description of the aircraft models and flight simulation programs used for the investigations. Appendix C develops several relations and concepts which are fundamental to the study of lateral agility. Appendix D examines the axial agility metrics in depth. Appendix E derives the relations for the instantaneous agility metrics and their approximations, and demonstrates their use.

2. CLASSIFICATION OF AGILITY METRICS

2.1 BACKGROUND

Since the pilots, engineers and researchers now involved in agility have, as yet, not reached a commonly accepted definition of the term, it is not surprising that the proposed agility metrics deal with many different aspects of fighter capability. The various metrics proposed to measure agility deal in units of time, velocity, angular rate, distance and combinations of time, rate and distance. One of the first tasks undertaken in this research was the establishment of a method to classify the numerous metrics suggested by researchers from industry and government laboratories. Although not unique, the following classification framework has been found to be useful.

2.2 CLASSIFICATION FRAMEWORK

After collecting and reviewing the candidate metrics now available in the literature, it is apparent that they may be divided into two categories or classes. First, the candidate metrics can be grouped by time scale into classes referred to by some authors as *functional* and *transient* (REF. 24, 29). Secondly, the metrics may be classified according to type of motion involved, e.g. translational (axial), longitudinal, and lateral.

Each of these two schemes of metric classification are discussed below. The resulting framework is then presented in a matrix format.

2.2.1 Transient, Functional, Potential

Regardless of the motion variables involved or the units chosen, all of the proposed agility metrics can be grouped into one of two time scales. Agility in the context of the short time scale, on the order of one to three seconds, is frequently called transient agility (REF. 4, 18, 29). The transient

agility metrics are a means to quantify a fighters ability to generate controlled angular motion and to transition quickly between minimum and maximum levels of specific excess power.

A second group of time dependent metrics called large amplitude metrics (REF. 29) or functional agility metrics (REF. 24) deals with a longer time scale of ten to twenty seconds. This class seeks to quantify how well the fighter executes rapid changes in heading or rotations of the velocity vector. The emphasis is on energy lost during turns through large heading angles and the time required to recover kinetic energy after unloading to zero normal load factor. Many of these functional metrics involve maneuvers made up of a sequence of brief segments of transient agility metrics. For example, the *combat cycle time* metric (REF. 30) consists of a pitch to maximum normal load factor, a turn at maximum normal load factor to some specified new heading angle, a pitch down to zero normal load factor and an acceleration to the original airspeed. The net effect of combining a sequence of maneuvers and flight segments into a single metric is that conventional aircraft performance, that is, thrust to weight ratio and sustained normal load factor or turn rate capability, tend to dominate the metric. In addition to measuring the aircraft capability, these functional agility metrics also depend heavily on complex pilot inputs which are in turn influenced by the pilot's skill, experience, the aircraft's flying qualities and the effect of cockpit displays and cues.

A third group of metrics has appeared which are independent of time and so are neither transient or large amplitude in nature. These metrics deal not with the aircraft characteristics demonstrated via flight test or simulation but with the agility potential that results from sizing and configuration choices. These *agility potential* metrics serve to highlight the (sometimes obvious) relationships between thrust, weights, inertias, control power and agility. While they have the advantage of using data available early in the aircraft design cycle, they tend not to reflect the impact of cross axis nonlinearity or flight control system response characteristics (REF. 31).

2.2.2 Lateral, Pitch, Axial

Agility metrics may also be classified according to the type of aircraft motion being studied independent of time scale. *Lateral* agility metrics include those that deal primarily with rolling motion, especially rolling at high angles of attack. *Longitudinal* or pitch agility metrics involve only pitching motion and normal acceleration. Finally, a number of metrics have been proposed to quantify the ability of the aircraft to transition between energy states or specific excess power (P_s) levels. These are commonly referred to as *axial* agility metrics and involve only translational motion.

2.2.3 Agility Classification Matrix

When these two classes of agility metrics are combined (REF. 1), the result is a matrix as seen in Figure 2.1.

	TRANSIENT (1 - 5 SECONDS)	FUNCTIONAL (> 5 SECONDS)	POTENTIAL
LATERAL	T_{90} TORSIONAL	ROLL REVERSAL PARAMETER	LATERAL AGILITY CRITERIA
LONGITUDINAL	$T_{MAX\ G}$ T_{UNLOAD} LOAD FACTOR RATE	POINTING MARGIN	PITCH AGILITY CRITERIA
AXIAL	POWER ONSET POWER LOSS	COMBAT CYCLE TIME DYNAMIC SPEED TURN RELATIVE ENERGY STATE	AGILITY POTENTIAL

Figure 2.1 Proposed Classification Framework (REF. 1)

Nearly all of the candidate agility metrics can be placed in a unique position in the matrix. For instance, *pointing margin* is a functional agility metric concerned with the longitudinal aircraft axis. The two exceptions are *torsional* agility and agility *potential.* Torsional agility is deliberately formulated to mix pitching and rolling characteristics and is the ratio of turn rate to the time to roll and capture a 90° bank angle change (REF. 18). The other exception, agility potential, is the ratio of two traditional performance metrics: wing loading, which is related to longitudinal maneuverability, and thrust to weight ratio.

Beginning with Chapter 3, each matrix element will be discussed. The order of presentation is pitch (longitudinal) agility in Chapter 3, lateral agility in Chapter 4, axial agility in Chapter 5, functional agility in Chapter 6, instantaneous agility in Chapter 7, and agility improvement in Chapter 8.

3. PITCH AGILITY

3.1 BACKGROUND

Pitch agility metrics are intended to quantify the motions in the vertical plane or longitudinal capabilities of fighter aircraft. This class of metrics typically involve only pitching motions and normal acceleration. This chapter defines the candidate metrics and then details the method of testing used. The methods used to compare results are also presented. For the results contained in this chapter, pitch agility is quantified using nonlinear, non real-time, six degree-of-freedom flight simulation computer programs. Results and analysis are presented for the F-5A, F-16A, and F-18A. Experiments consist of pre-specified maneuvers designed to quantify the pitch agility of the aircraft. The acceptability of such maneuvers to an operational pilot, the associated issues of flying qualities, pilot discomfort, and g-induced loss of consciousness are not addressed in this report.

3.2 CANDIDATE PITCH AGILITY METRICS

Numerous metrics have been proposed to quantify pitch agility including:.

1) maximum positive and negative pitch rate from steady level flight
2) maximum positive pitch rate from an initial angle of attack
3) maximum negative pitch rate from an initial angle of attack
4) time to pitch to maximum normal load factor
5) time to pitch down from maximum load factor to zero load normal factor
6) maximum positive normal load factor rate
7) maximum negative normal load factor rate
8) average pitch rate

9) time to capture a specified angle of attack

10) time to change pitch attitude

11) pitch agility criteria

12) maximum initial pitch acceleration

All of these candidate metrics are investigated with the exception of *time to capture a specified angle of attack, time to change pitch attitude, pitch agility criteria,* and *maximum initial pitch acceleration.* These metrics are not investigated in this report because of unsatisfactory results from previous testing, or because they have been generally rejected by agility researchers (Appendix A).

3.3 PITCH AGILITY TESTING AND DATA REDUCTION TECHNIQUES

The candidate pitch agility metrics listed in Section 3.2 which are tested using non real-time simulation at altitudes of 500 feet, 15,000 feet and 30,000 feet, and at subsonic Mach numbers ranging from 0.4 to 0.9. The Mach numbers and altitudes are selected to be representative of those at which fighter aircraft are most likely to be engaged in within visual range air combat. The metrics investigated in this report are evaluated in both the nose up and nose down directions.

During subsequent testing of each candidate pitch agility metric (REF. 1, 2, 3), it was determined that a value for each metric at a given test point could be obtained from a single data collection run, using a standardized pilot command. This technique simplifies the task for both the pilot and flight test engineer. The standardized pilot command input consists of an abrupt step input which is held for two seconds, after which the step command is abruptly taken back out (Figure 3.1). The duration of the step input is sufficiently long enough for various maximum values and maximum rates to be achieved. Thus the pilot is not burdened with having to determine whether he has achieved

the maximum values and rates. This gives the test engineer clearly defined reference points for measuring the "time to" metrics, using the time at which the pitch-up is initiated, and the time at which the pitch-down is initiated. Generalizing the command inputs for each candidate pitch agility metric to a single standardized input sequence is an approximation, but it simplifies the test procedure and considerably reduces the number of data collection runs.

At each flight condition investigated, the aircraft is trimmed to straight and level flight. Step inputs of maximum aft stick deflection are applied to the longitudinal stick and held for two seconds. Forward stick was then applied to pitch down to zero normal load factor. Figure 3.1. is a typical simulation time history from a data collection run, showing how the time to load, unload and the associated pitch rates and load factor rates are extracted. Note especially that the time to pitch down to zero normal load factor is calculated from the time forward stick is commanded, not from the time that normal load factor begins to decay due to airspeed loss. This method minimizes the influence of aircraft drag characteristics on pitch agility measurements and emphasizes nose down pitch authority.

The test technique described above is adequate only for aircraft like the F-16A and F-18A whose flight control systems incorporate pitch rate and load factor limiters. Applying full aft stick in aircraft such as the F-5, F-4, or F-15 will at many flight conditions over stress the pilot and aircraft. In these types of aircraft, the pilot must limit pitch rate and normal load factors manually. As a result, care must be taken when directly comparing the pitch agility of two aircraft like the F-5 and F-18A, whose flight control systems are fundamentally different. One option is to define the maximum surface deflection permissible for each aircraft at a given flight condition, and then base the agility measurement on that deflection instead of maximum stick input. This would make flight test much more difficult since information about surface position is not available to the pilot during flight. Also, this method would not account for the effects of control surfaces such as maneuvering flaps. These

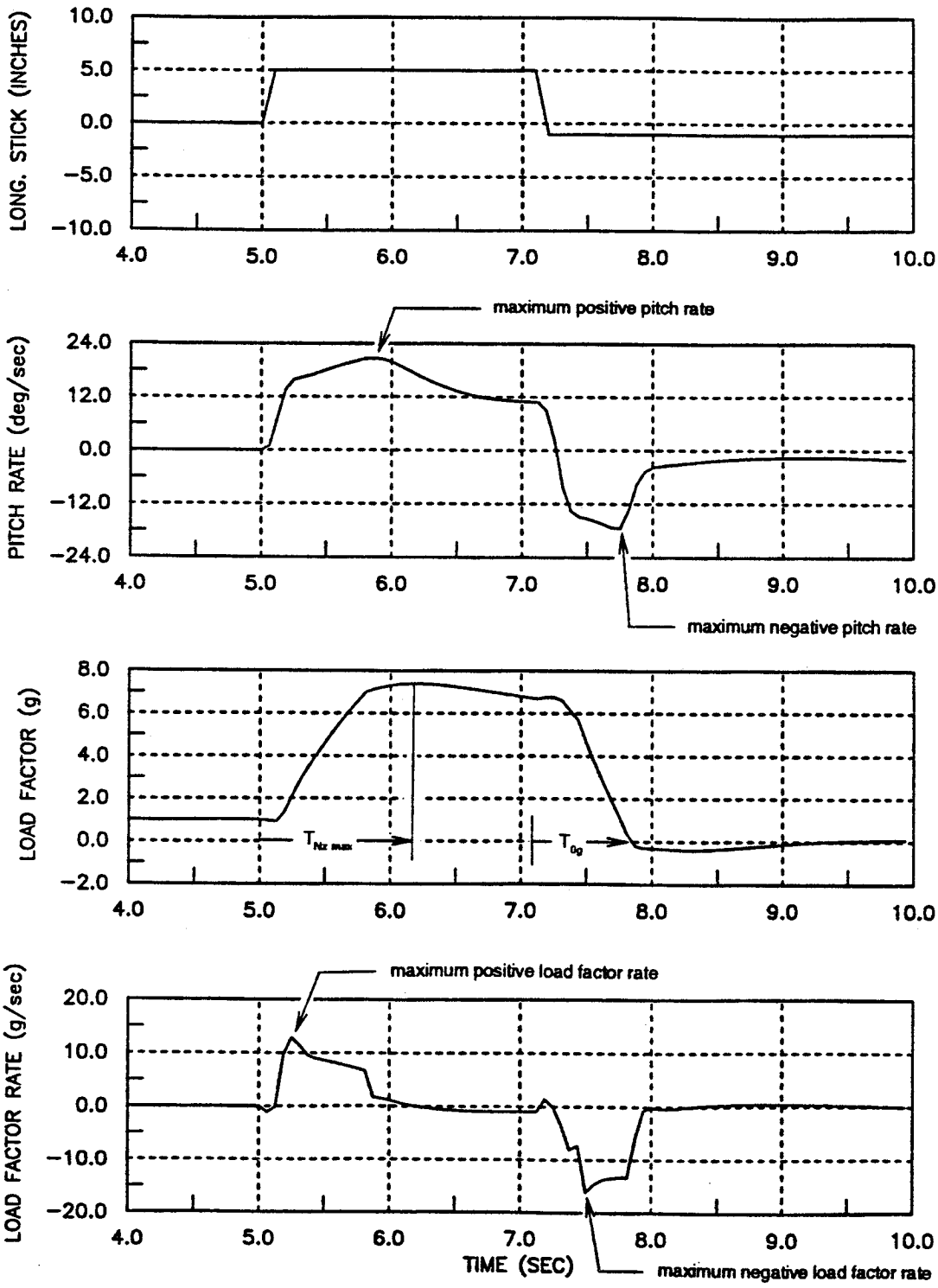

Figure 3.1 Typical Pilot Stick Input Commands And Data Extraction Points Used For Evaluating Pitch Agility Metrics

surfaces are present on the F-18A but are not installed on the generic F-5A.

The *time rate of change of normal load factor* and *average pitch rate* are not available either as a term in the dynamic models of the aircraft or as an output of a modelled sensor. A simple differencing scheme is used to measure the normal load factor rate. A similar approach would be needed to obtain this data from a flight test maneuver. In the simulations used with no random atmospheric inputs, buffeting, or sensor noises, the differencing algorithm produced usable normal load factor rate data. Application of a differencing scheme to obtain normal load factor rate information from flight test might require extensive smoothing and may not be feasible.

Values for the *average pitch rate* metric are computed numerically using simulation or flight data and the equation

$$\text{Average Pitch Rate} = \frac{\int_{t_1}^{t_2} q \, dt}{t_2 - t_1} \tag{3.1}$$

where

q = body axis pitch rate (deg/sec)

t_1 = time at which pitch command input is initiated

t_2 = completion time of the interval of interest

The interval of interest is selected based upon engineering judgement and experience. In most cases the interval of interest is readily apparent. For example, initiating and maintaining a full aft stick input from level flight results in a pitch up maneuver which will eventually result in a repeated set of either stalls or complete loops. From the standpoint of "point and shoot" transient agility, such a long term, non-task oriented maneuver is probably not meaningful. However, the portion of the maneuver consisting of the initial pitch up plus two or three seconds is probably realistic and meaningful.

The generic F-18A simulation is used to assess the sensitivity of the pitch agility metrics. It is important to note that *these sensitivity results are specific to the generic F-18A* ***only****, and cannot be generalized to all fighter aircraft.* The intent here is simply to determine in a broad sense how sensitive the pitch agility metrics can be to pilot inputs, and to demonstrate one way in which an analysis of this type can be conducted. If Figure 3.1 represents the nominal pilot command input, then the actual pilot command input can deviate from the nominal in the following ways (REF. 1):

1. The initial aft stick input can be applied at a slower rate.
2. The aft stick input can be less than a full deflection command.
3. The forward stick input can be applied at a slower rate.
4. The magnitude of the forward stick input may be too large.

Each of these errors in the input time histories is imposed, one at a time, on the generic F-18A during the pitch maneuvers used to evaluate the candidate pitch agility metrics. The magnitudes of the introduced deviations are displayed in Table 3.1.

Table 3.1 Deviations For Pitch Sensitivity Testing

Error Type	Magnitude
Aft Stick Rate	Reduced 20%
Aft Stick Deflection	Reduced 20%
Forward Stick Rate	Reduced 20%
Forward Stick Deflection	Increased 20%

Since this analysis is simply intended to show typical behavior, the sensitivity tests are limited to a single altitude of 15,000 feet. Note that forward stick deflection (deviation four) is **increased** rather than reduced; this is because reducing the forward deflection by 20% resulted in failure to achieve the

zero normal load factor as required by the metric definitions.

Not all of the input errors listed in Table 3.1 will affect both the pitch up and pitch down portions of the test maneuver. Only the aft stick command deviations (one and two) influence the *time to maximum normal load factor, positive normal load factor rate, and maximum positive pitch rate* metrics. Considering the pitch down portion of the metrics, only the aft stick command rate (deviation one) is not influential since the rate at which the initial nose up command is applied has no effect on the pitch down maneuvers. However, the magnitude of the initial aft stick deflection (deviation two) does affect the attitude from which the pitch down is initiated.

3.4 CANDIDATE PITCH AGILITY METRICS RESULTS

In this section each of the eight pitch agility metrics will be presented. Each metric is defined and then typical results are presented.

3.4.1 **Maximum Positive Pitch Rate** (REF. 18)

3.4.1.1 Definition

The maximum value of positive pitch rate attainable in transitioning from a 1g flight condition to maximum lift angle of attack.

3.4.1.2 Discussion and Typical Results

The maximum positive pitch rates for the generic F-5A, F-16A, and F-18A from steady level 1g flight are displayed in Figures 3.2, 3.3, and 3.4. Maximum aft stick deflections are used for the generic F-16A and generic F-18A since the full authority flight control systems on these aircraft prevent overstressing of the airframe. Since the generic F-5A does not have a full authority flight control system, the magnitude of the aft stick deflections must be selected to prevent overstressing.

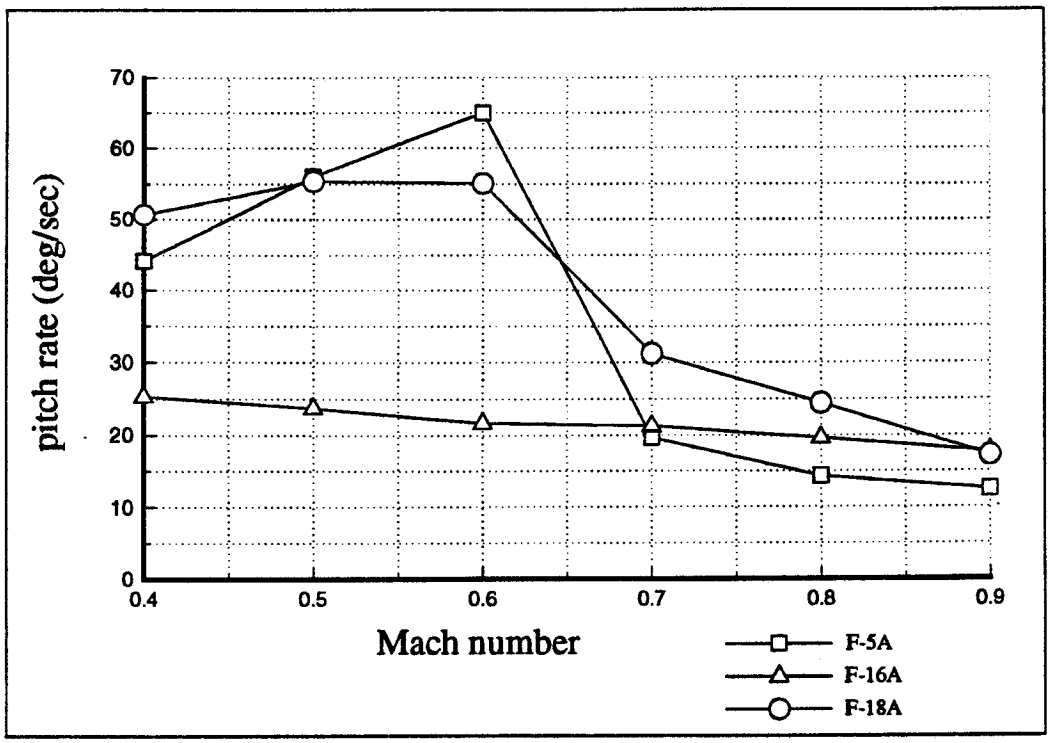

Figure 3.2 Generic F-5A, F-16A, And F-18A *Maximum Positive Pitch Rate* From Level Flight, H = 500 feet

Figure 3.2 shows that at an altitude of 500 feet, the generic F-5A and generic F-18A exhibit similar behavior in that the maximum positive pitch rate capability decreases with increasing Mach number due to normal load factor limiter in the control system. The maximum positive pitch rate capability of the generic F-16A is lower at low Mach numbers, but unlike that of the generic F-5A and generic F-18A, exhibits little variation over the range of Mach numbers tested. This is a result of the flight control system having a pitch rate limiter. The employment of pitch rate limiters tends to have a marked effect on pitch agility. In the case of the generic F-16A, the pitch rate limiter is intended to (REF. 18):

i) create a uniform pitch rate capability across the range of subsonic Mach numbers

ii) offset a reduction in nose down pitching moment with increasing angle of attack

iii) avoid a deep stall tendency

The maximum positive pitch rate capability for the three aircraft at an altitude of 15,000 feet is displayed in Figure 3.3.

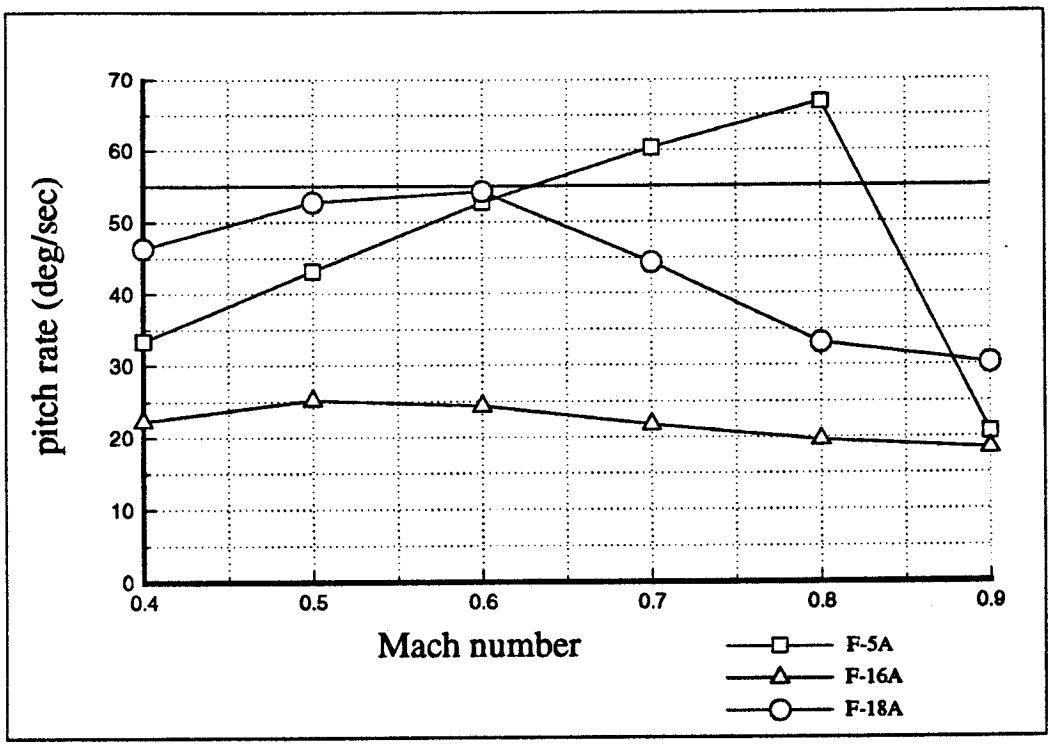

Figure 3.3 Generic F-5A, F-16A, And F-18A *Maximum Positive Pitch Rate* From Level Flight, H = 15,000 feet

Compared to the 500 feet altitude case, the generic F-5A is seen to extend the Mach number at which maximum positive pitch rate capability is achieved from 0.6 up to 0.8, without overstressing the airframe. The generic F-18A still experiences pitch rate limiting, but is not restricted as much here. Again, the generic F-16A exhibits a nearly constant maximum positive pitch rate capability across the Mach number range.

At an altitude of 40,000 feet all three aircraft are limited by available lift so that the normal load factors are well below their maximum structural limits (Figure 3.4). Thus, neither the flight

control system nor the pilot need to impose any pitch rate limiting. For the generic F-18A at this altitude, the limited lift translates into a somewhat greater values of maximum positive pitch rate over the subsonic Mach number range than at the lower altitudes. Figure 3.4 also shows that the generic F-18A maximum positive pitch rate is almost constant across the entire range of Mach numbers tested, similar to that of the generic F-16A. At 40,000 feet, the generic F-5A maximum positive pitch rate capability increases with Mach number up to Mach 0.9.

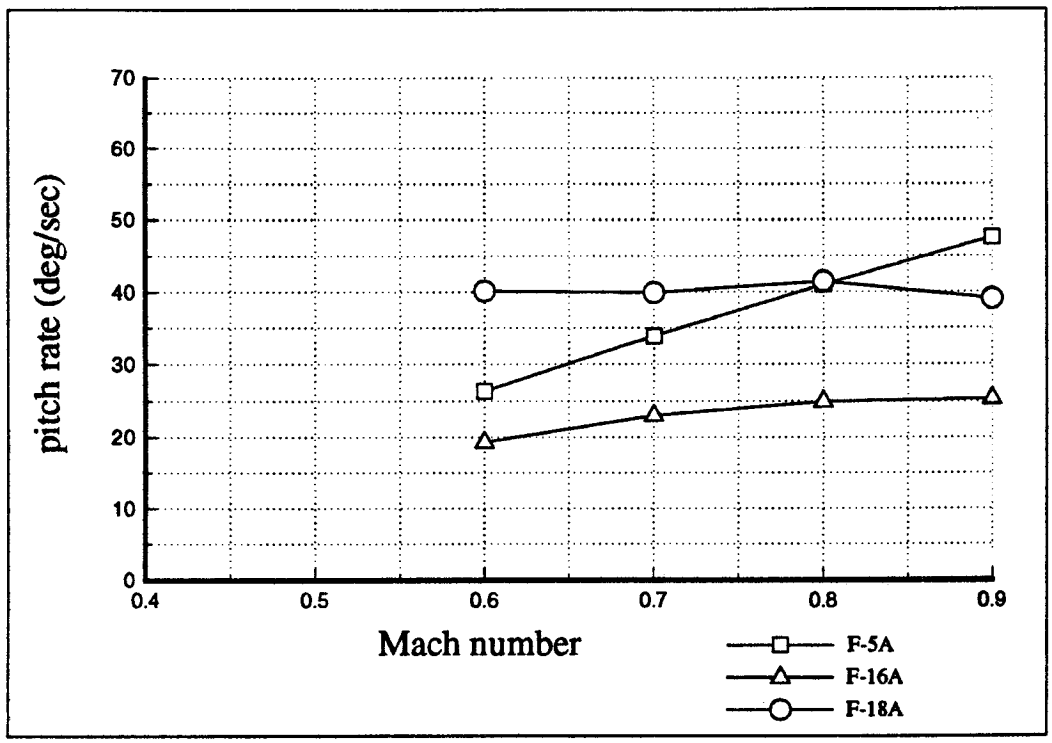

Figure 3.4 Generic F-5A, F-16A, And F-18A *Maximum Positive Pitch Rate* From Level Flight, H = 40,000 feet

3.4.1.3 Maximum Positive Pitch Rate Sensitivity

As seen in Figure 3.5, reduced aft stick rate has little effect on the maximum pitch rate generated by the generic F-18A during the pitch up. However, when the maximum aft stick deflection

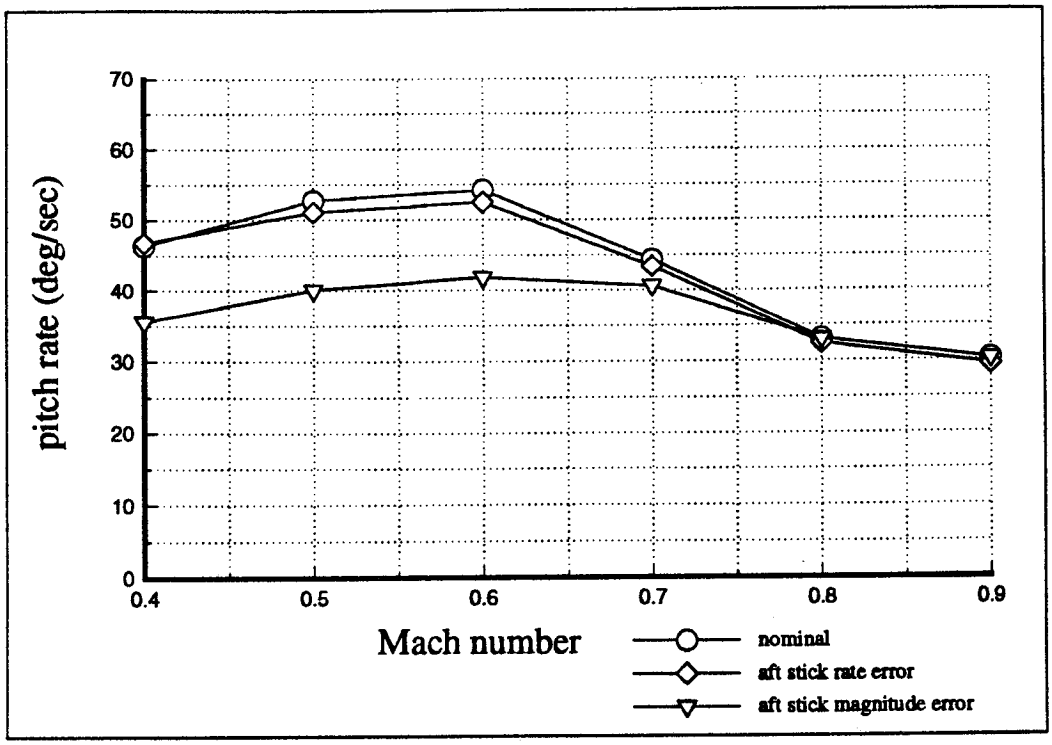

Figure 3.5 Generic F-18A *Maximum Positive Pitch Rate* Sensitivity, H = 15,000 feet

is reduced 20%, the maximum positive pitch rate is significantly reduced in the range of lower Mach numbers. This deviation tends to have a pronounced effect on maximum positive pitch rate, but little to no impact on the other metrics. This is because the value of each different pitch agility metric is established at a different point in the time history of the maneuver. For example, maximum positive normal load factor rate occurs very early in the maneuver, at a time when maximum positive pitch rate is still relatively small. Also, the peak positive normal load factor is achieved later in the maneuver, when normal load factor rate is zero, and after positive pitch rate has peaked and is declining.

3.4.1.4 Summary

The *maximum positive pitch rate* metric is a direct measure of a task-oriented maneuver. It has the additional benefit of being easy to measure. A drawback may be that the maneuver is open loop, and does not adequately address flying qualities concerns. The results for all three aircraft can be summed up as follows:

1. At 500 feet (low altitudes) each aircraft exhibits pitch rate limiting at the higher Mach numbers due to high dynamic pressures.

2. At 15,000 feet (intermediate altitudes) the capability of generating large maximum positive pitch rates is present, but is usually limited because of normal load factor constraints.

3. At 40,000 feet (high altitudes) each aircraft is limited by available lift (due to low dynamic pressures), which obviates the need for pitch rate limiting. As a result maximum positive pitch rate capability at the higher Mach numbers is greater than it is at the lower altitudes.

4. As will be seen for other metrics, the detailed characteristics of the flight control system tend to significantly influence vehicle capabilities.

In the nose up direction, positive pitch rate is reduced by approximately ten degrees per second if four inches of aft stick is applied rather than the maximum of five.

3.4.2 **Maximum Negative Pitch Rate** (REF. 18)

3.4.2.1 Definition

The maximum negative pitch rate attainable in transitioning from maximum positive normal load factor to zero normal load factor.

3.4.2.2 Discussion and Typical Results

Figures 3.6, 3.7, and 3.8 display the maximum negative pitch rates for the generic F-5A, F-16A, and F-18A from steady level 1g flight. Figure 3.6 indicates that all three aircraft follow the same general trend with increasing Mach number, even though the generic F-5A does not have the pitch limiting inherent to a full authority automatic flight control system. Each aircraft achieves its best negative pitch rate capability somewhere in the lower end of the Mach number range, before gradually falling off in the high Mach number range. This trend is similar to the nose-up pitch rate trend in Figure 3.2, except that there the generic F-16A nose-up pitching capability is more constant over the range of Mach numbers.

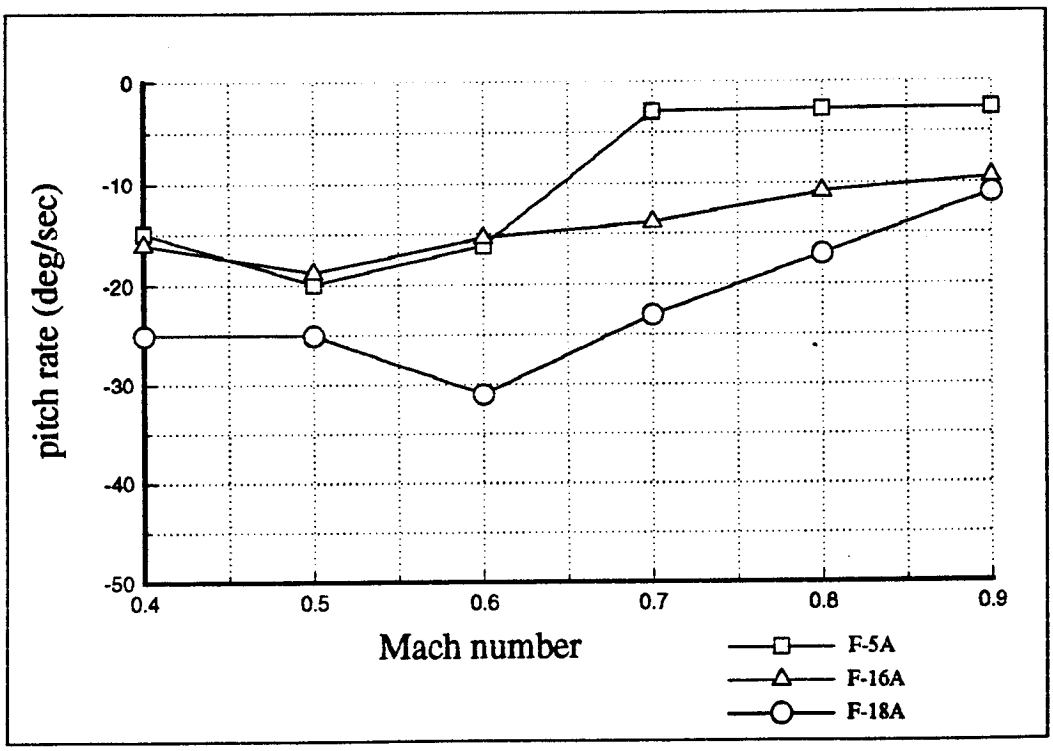

Figure 3.6 Generic F-5A, F-16A, And F-18A
Maximum Negative Pitch Rate, H = 500 feet

Compared to the 500 feet altitude case, the nose-down pitching capability for the three aircraft at an altitude of 15,000 feet shows more consistency across the Mach number range (Figure 3.7). At

this altitude there is also a greater disparity between the three aircraft. The generic F-16A and generic F-18A once again exhibit the effects of pitch limiting, but in terms of magnitude the generic F-18A nose-down pitch capability is actually better at this altitude. The generic F-16A capability at this altitude is virtually unchanged from the lower altitude, both in terms of magnitude and trend with Mach number. As is the case for nose-up pitch rate capability on the generic F-5A, increasing altitude has the effect of extending the Mach number at which maximum negative pitch rate capability is achieved.

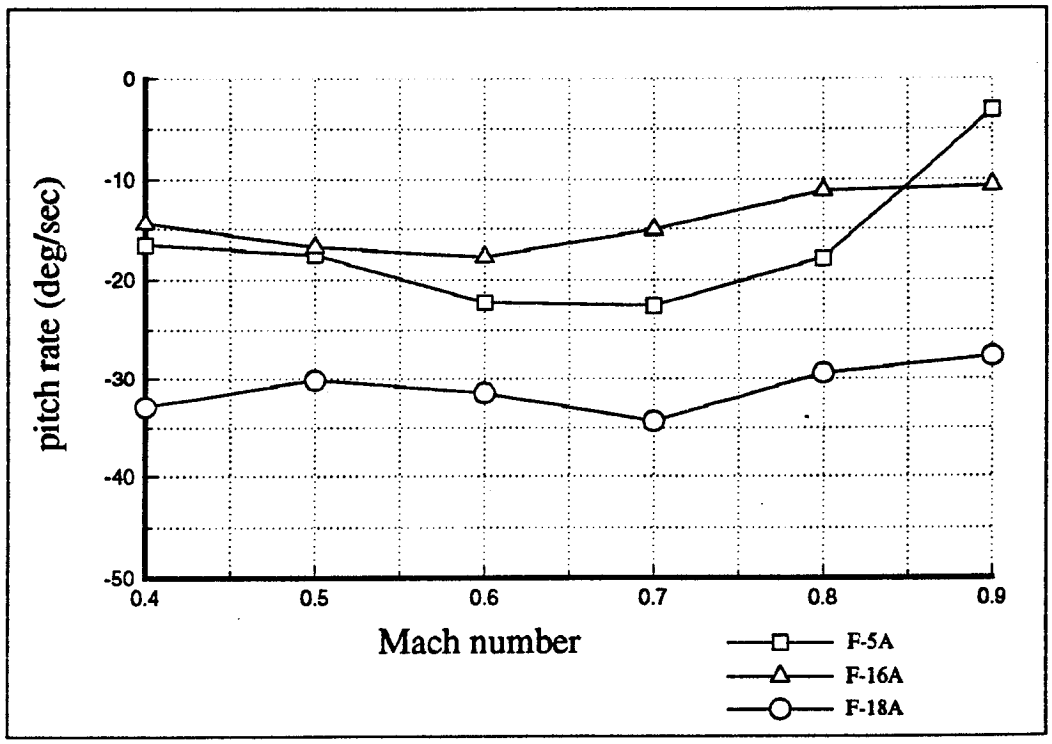

Figure 3.7 Generic F-5A, F-16A, And F-18A
Maximum Negative Pitch Rate, H = 15,000 feet

At an altitude of 40,000 feet neither the flight control system nor the pilot need to impose any pitch rate limiting. Figure 3.8 shows very little change over Figure 3.7, except that the generic F-5A has a nearly constant negative pitch rate capability across the Mach number range like the other two

aircraft. The generic F-18A has a slightly greater negative pitch rate capability at this altitude than it does at the lower altitudes.

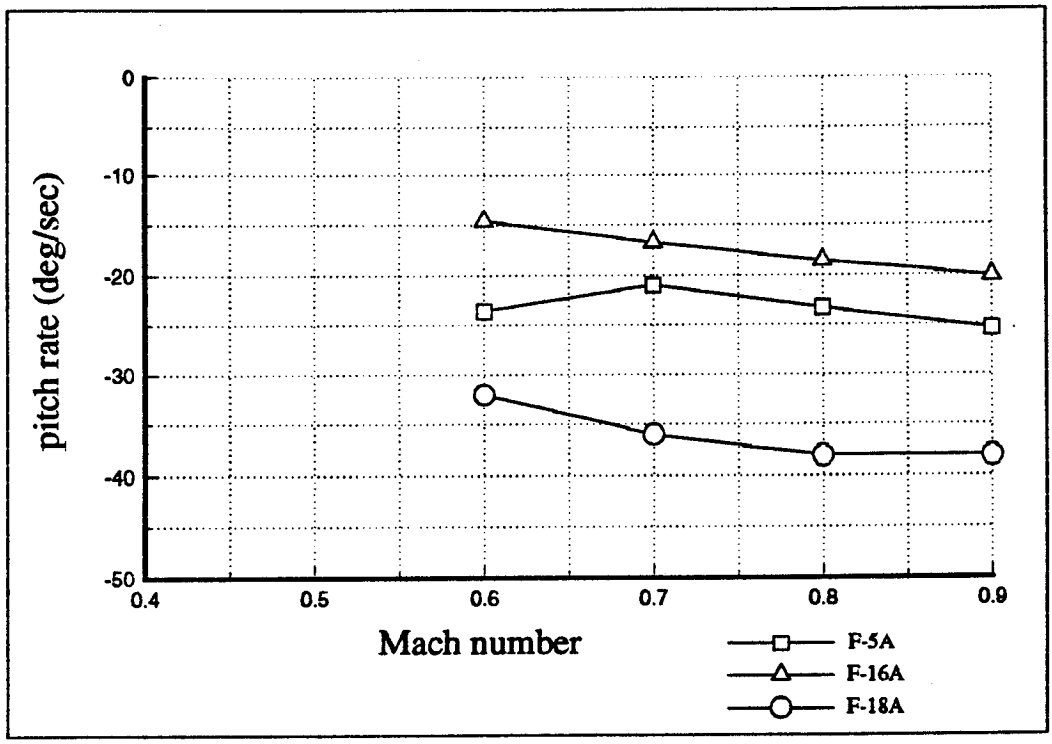

Figure 3.8 Generic F-5A, F-16A, And F-18A
Maximum Negative Pitch Rate, H = 15,000 feet

3.4.2.3 Maximum Negative Pitch Rate Sensitivity

The sensitivity of the *maximum negative pitch rate* metric to deviations in forward stick rate, aft stick magnitude and forward stick magnitude for the generic F-18A are shown in Figure 3.9. It is seen that commanding more than the nominal forward stick deflection causes slightly larger negative pitch rates, while applying the stick input at a slower rate reduces the magnitude of the resulting pitch. In no case, however, are the changes large or unpredictable.

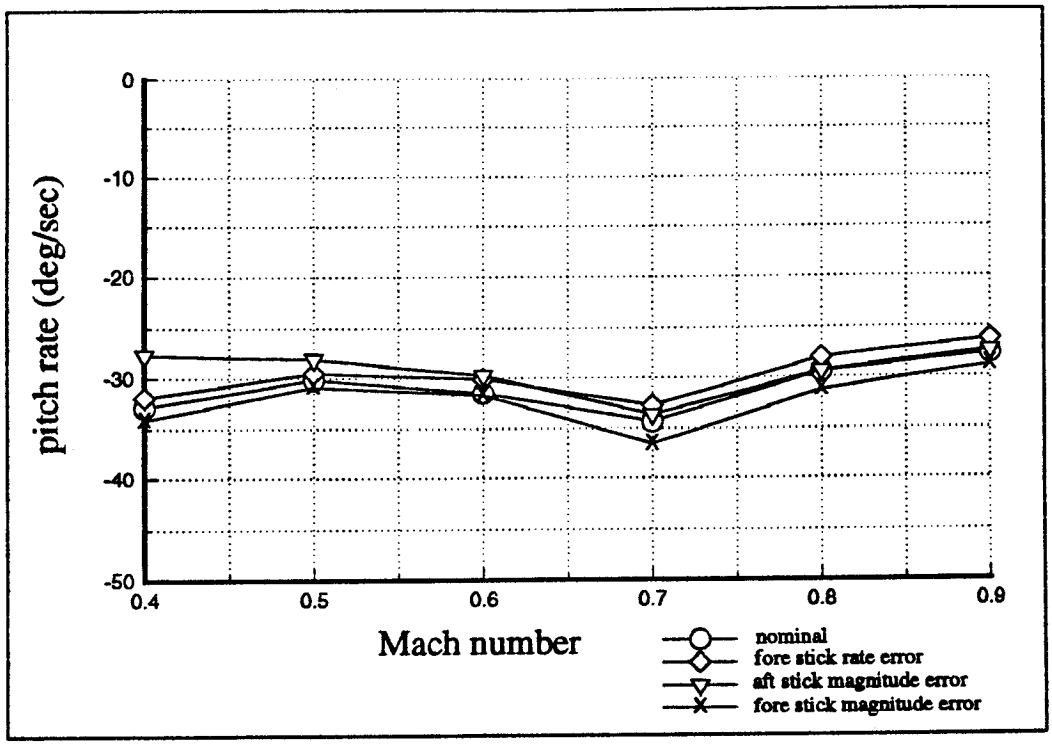

Figure 3.9 Generic F-18A *Maximum Negative Pitch Rate* Sensitivity, H = 15,000 feet

3.4.2.4 Summary

The *maximum negative pitch rate* metric, when combined with the *maximum positive pitch rate* metric, provide a general overview of pitching capability. Not surprisingly, the results of Sections 3.4.1 and 3.4.2 indicate that in general the three aircraft tested tend to have greater nose-up than nose-down pitch rate capability. The generic F-16A is a slight exception, since its pitch rate capability in both directions remains essentially constant with Mach number, and very nearly constant with altitude. Althoughof an air is a direct measure of a task-oriented maneuver, and is easy to test and measure. This feature provides the pilot with very consistant and predictable responses to command inputs in the range of flight conditions where air combat is usually conducted.

3.4.3 Maximum Positive And Negative Pitch Rate From An Initial Angle Of Attack

3.4.3.1 Definition

The maximum positive or negative pitch rate attained from pitching up or down from a specified initial angle of attack.

3.4.3.2 Discussion and Typical Results

If maximum positive and negative pitch rates are used to quantify pitch agility, then the flight maneuver used previously is not adequate to fully evaluate this capability. A full deflection aft stick input followed by pitch down to zero load factor results in pitch rate data at only one angle of attack for each flight condition. A more complete picture would show pitch rate versus initial angle of attack at representative flight conditions. A proposed flight test maneuver consists of pitching the aircraft with incremental longitudinal stick inputs. Then full aft (or forward if nose down rates are being studied) stick is applied. Maximum pitch rate is recorded and plotted against the angle of attack from which the maximum rate command was initiated. The full deflection inputs should follow the initial incremental steps quickly enough that aircraft Mach and altitude remain within acceptable flight test tolerances.

The simulation results from this procedure using the generic F-18A at 15,000 feet is shown in Figure 3.10. The trends for each Mach number show that as the initial angle of attack is increased, the pitching moment authority remaining available to generate nose up pitch rate is reduced. Figure 3.10 shows the effect of the flight control system limiting the pitch rates at Mach equals 0.8 to prevent the generic F-18A from exceeding its structural limit. At Mach equals 0.4 and 0.6 at an altitude of 15,000 feet, because the value of maximum lift will not overstress the aircraft, there is no need to limit the pitch rate.

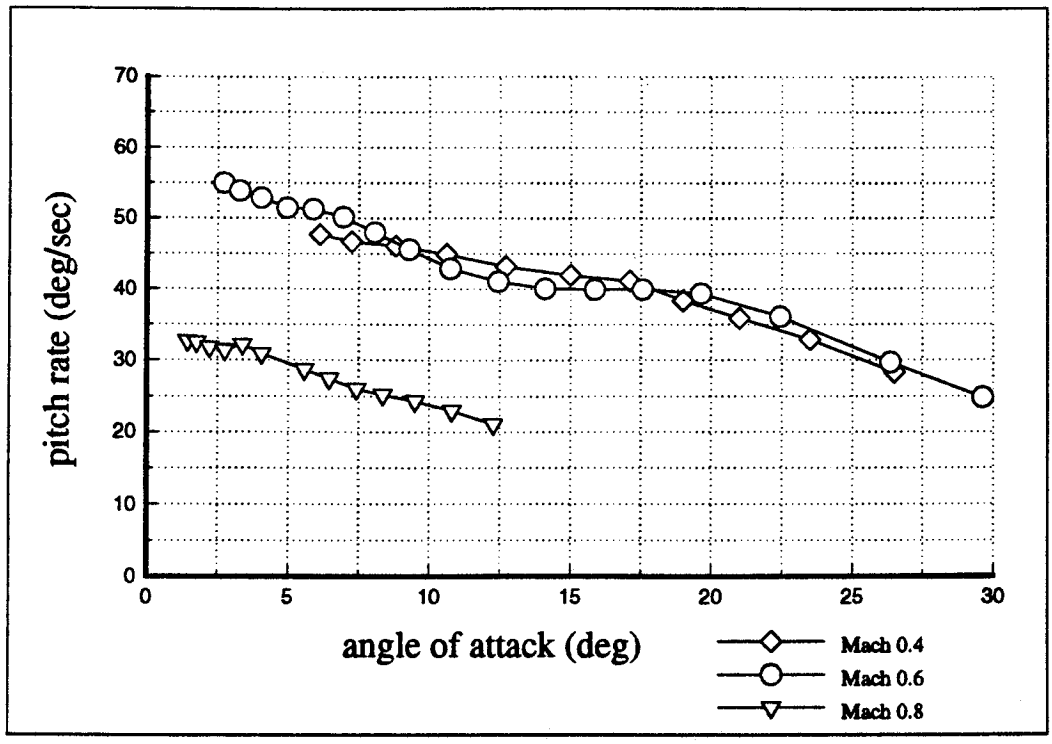

Figure 3.10 Generic F-18A *Maximum Positive Pitch Rate From An Initial Angle Of Attack*, H = 15,000 feet

Figure 3.11 shows that the available nose down pitch rate on the generic F-18A is greater when the maneuver is initiated at a higher angles of attack. This is due both to the natural stability of the aircraft (negative Cm_α) and the larger net pitch control surface deflections made when pitching down from higher angles of attack. Some pitch rate limiting is also evident in Figure 3.11 since nose down pitch rates at Mach equals 0.8 are consistently slower than for Mach equals 0.6.

A sensitivity study for this metric is not conducted because of the similarity to the *maximum positive and negative pitch rate* metrics.

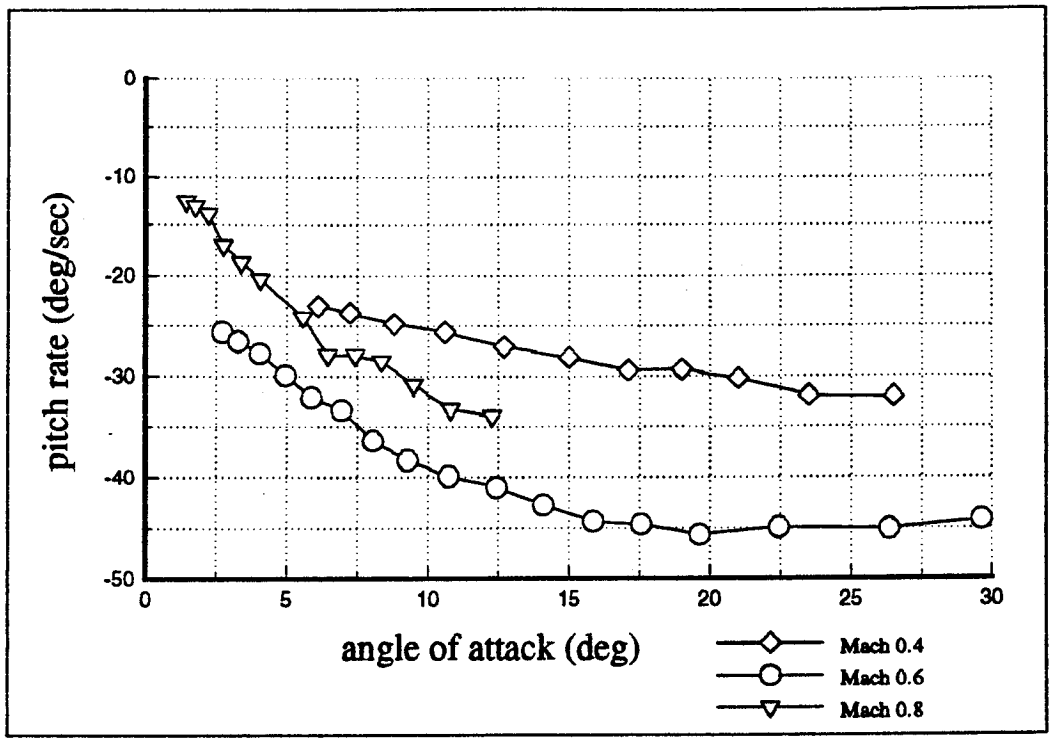

Figure 3.11 Generic F-18A *Maximum Negative Pitch Rate From An Initial Angle Of Attack*, H = 15,000 feet

3.4.3.3 Summary

The advantages of the *maximum positive and negative pitch rate from an initial angle of attack* are that a more complete picture of nose pointing ability is available, and the pilot inputs are simpler and more repeatable. Since the pilot is not required to capture a specific angle of attack or normal load factor, aircraft characteristics are highlighted and the impact of individual pilot technique is minimized. The ability to quickly and accurately capture a desired pitch attitude is important, but is nevertheless a flying qualities problem as well as an agility issue.

3.4.4 **Time To Pitch To Maximum Positive Normal Load Factor** (REF. 18)

3.4.4.1 Definition

The sum of:

time to pitch from a 1g flight condition to maximum lift coefficient or normal load factor

and

time to pitch down from maximum lift coefficient or normal load factor to 0g

3.4.4.2 Discussion and Typical Results

This definition of pitch agility correctly implies that both nose up and nose down pitch agility are important. There are, however, a number of questions this definition raises including:

1. If the times associated with nose up and nose down pitch maneuvers are to be summed, should the two be equally weighted?
2. Is the time to pitch up significantly different than the time to pitch down?
3. Does an aircraft with better positive pitch agility necessarily have better negative pitch agility?

Since these questions remain to be resolved by the engineering and pilot communities, in the current research values of this metric associated with nose up pitch maneuvers are treated separately from values associated with nose down pitch maneuvers. The nose up pitch maneuver is the *time to pitch up to maximum normal load factor* and the nose down pitch maneuver is the *time to pitch down from maximum normal load factor to 0g*.

Figures 3.12, 3.13, and 3.14 show that the *time to pitch up to maximum normal load factor* is a strong function of Mach number and altitude. For the generic F-5A at the altitudes tested, normal acceleration due to angle of attack tends to increase with increasing Mach number. The resulting time to load is smaller, even in cases where the pitch rates at each Mach number are nearly the same.

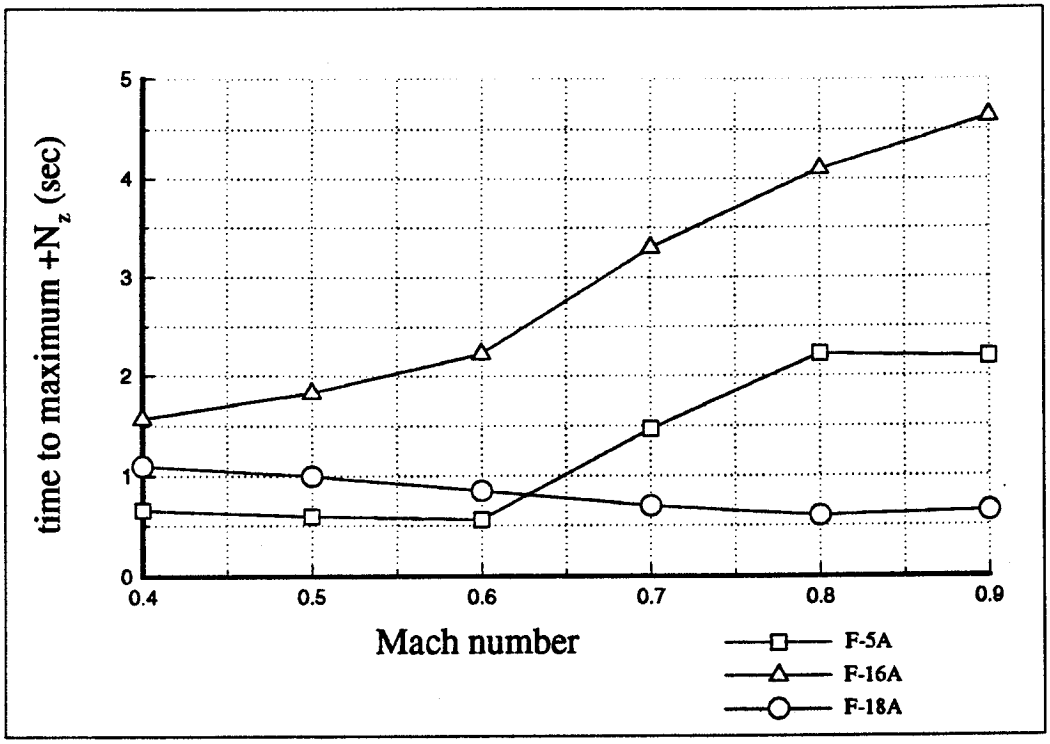

Figure 3.12 Generic F-5A, F-16A, And F-18A *Time To Pitch Up To Maximum Normal Load Factor*, H = 500 feet

However, Figure 3.12 shows that at the high dynamic pressure flight conditions (Mach numbers between 0.6 and 0.9), the time to load increases. This is because the magnitude of the pitch stick input must be reduced by the pilot to avoid over-stressing the airframe. This is also the cause for the data point at Mach 0.9 in Figure 3.13. The generic F-18A follows this trend also. Since the time to load is seen to vary only slightly, the flight control system on the generic F-18A is providing the pilot with consistent and predictable pitch-up characteristics (in terms of time to load) across the range of subsonic Mach numbers and altitudes which were tested. Figures 3.12 and 3.13 show that for altitudes of 500 feet and 15,000 feet, the F-16A's time to load to maximum load factor increases with increasing Mach number. For these altitudes the generic F-5A and the generic F-18A to not exhibit this Mach number dependency. At 40,000 feet, all three airplanes do not show this Mach number

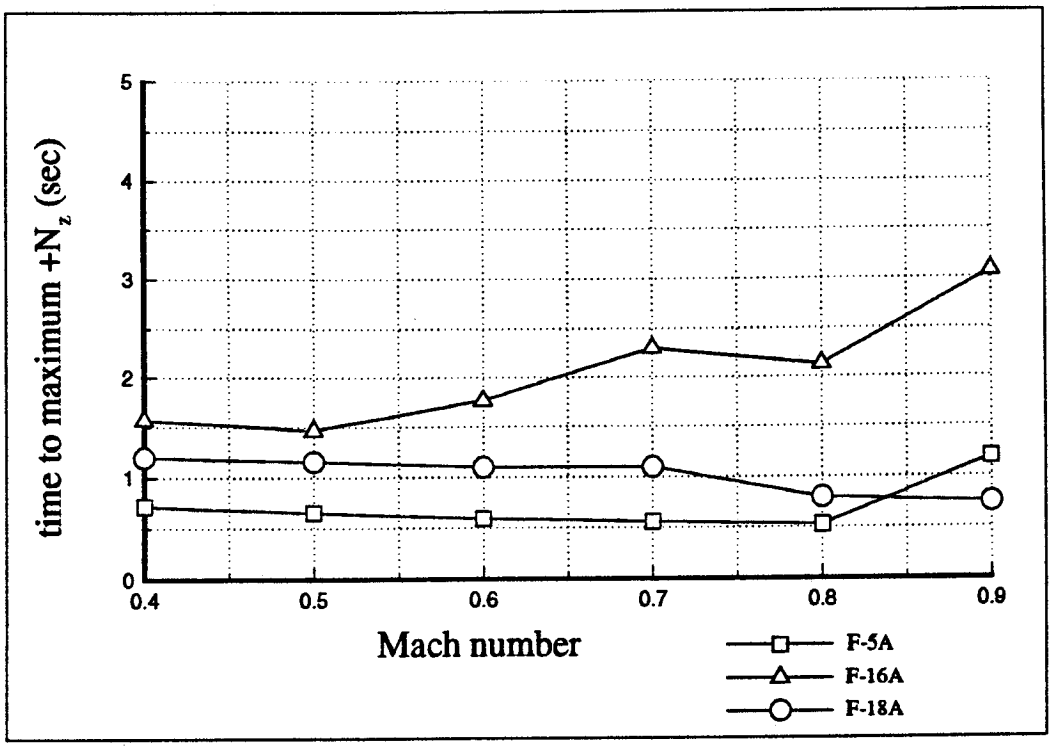

Figure 3.13 Generic F-5A, F-16A, And F-18A *Time To Pitch Up To Maximum Normal Load Factor*, H = 15,000 feet

dependency. This characteristic results from the F-16A requiring both pitch rate and normal load factor limiting to avoid overstressing the airframe and/or pilot. The results for all three aircraft again indicate that time to load is not purely dependent upon the pitching capability inherent in the airframe but are effected by the design of the automatic flight control systems. Care must be taken when interpreting the *time to pitch up to maximum normal load factor* metric. Contrary to the indications of Figure 3.13, the generic F-18A is not slower in pitching to maximum normal load factor at Mach equals 0.7 than it is at Mach equals 0.6. The load factor onset is actually faster at Mach equals 0.7, but the maximum peak load factor is higher. Thus the time required to achieve that peak is slightly longer, e.g. 1.1 seconds compared to 1.05 seconds.

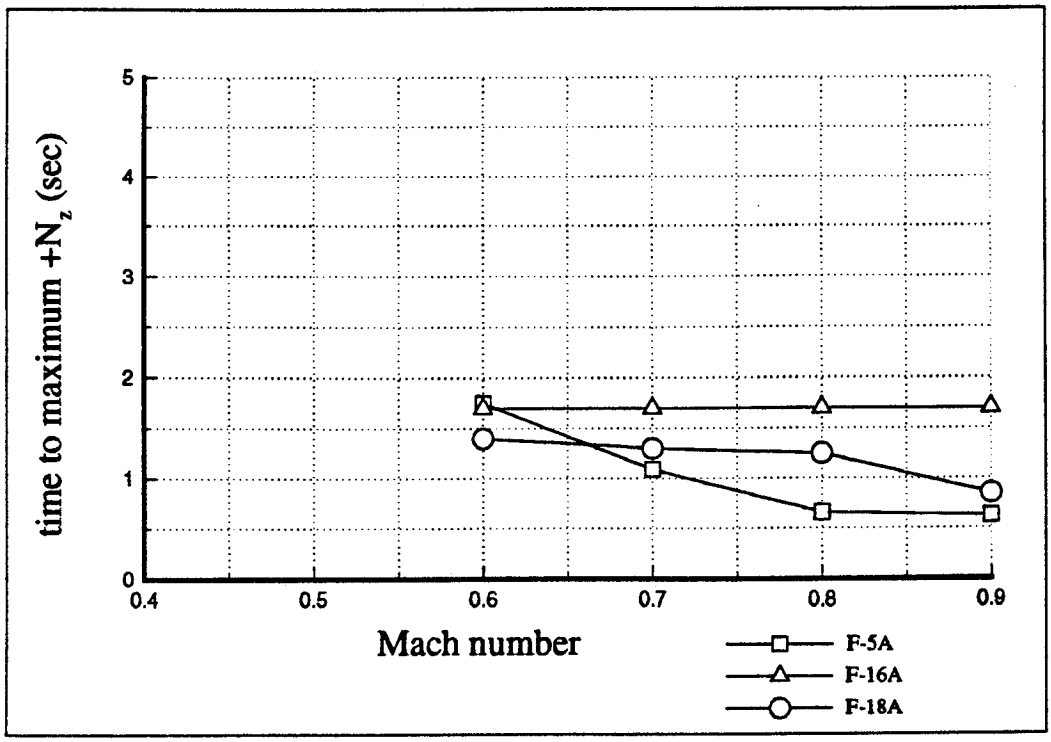

Figure 3.14 Generic F-5A, F-16A, And F-18A *Time To Pitch Up To Maximum Normal Load Factor*, H = 40,000 feet

3.4.4.3 Time To Pitch Up To Maximum Normal Load Factor Sensitivity

The effect of deviations from the generic F-18A nominal stick inputs on the *time to pitch up to maximum normal load factor* metric is displayed in Figure 3.15. The results indicate that this metric is generally not sensitive to the introduced deviations. As expected, reducing the aft stick deflection rate 20% increases the measured value of the metric, but the maximum change is only 0.15 seconds. Applying four inches of aft stick deflection instead of the maximum of five inches has an even smaller effect. This is because this metric measures only the **time** to achieve maximum normal load factor, and not the magnitude of the normal load factor itself.

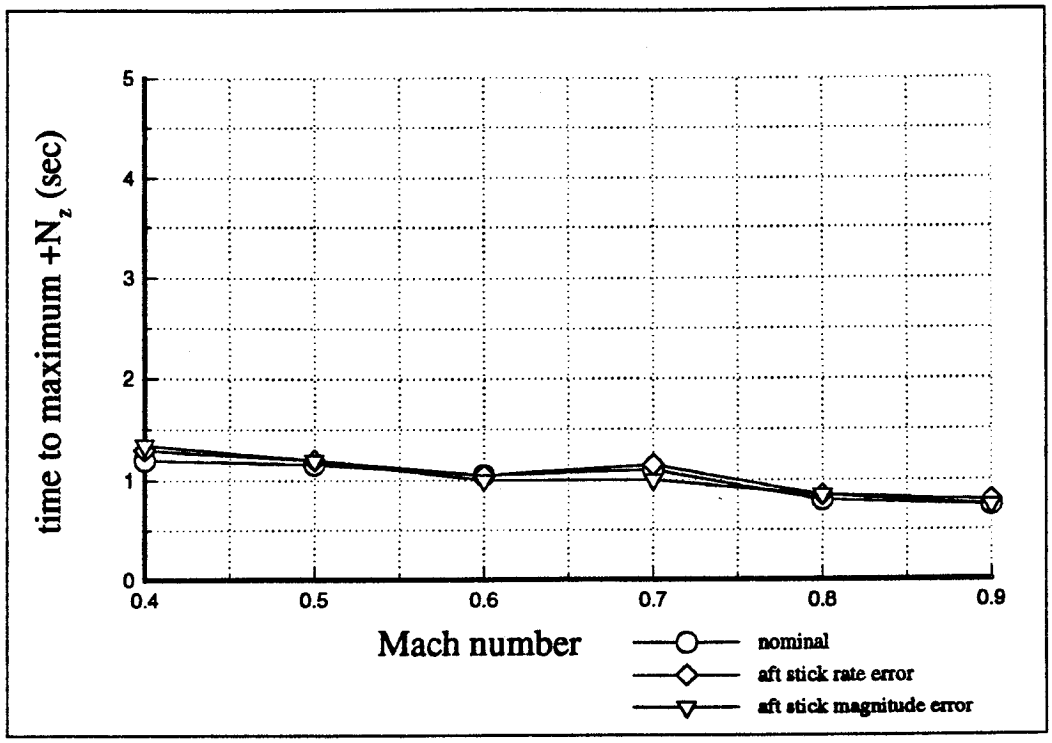

Figure 3.15 Generic F-18A *Time To Pitch Up To Maximum Normal Load Factor* Sensitivity, H = 15,000 feet

3.4.4.4 Summary

Normal load factor onset can significantly affect the measured values of the *time to pitch up to maximum normal load factor* metric. This information is not directly available when this metric is presented as in Figures 3.12, 13, and 14. If this metric is used to compare the agility of dissimilar aircraft, misleading results could occur at flight conditions where the maximum normal load factors of the respective aircraft are different. This metric is generally not sensitive to deviations in pilot command inputs.

3.4.5 Time To Pitch Down From Maximum Normal Load Factor To 0g (REF. 18)

3.4.5.1 Definition

The sum of:

time to pitch from a 1g flight condition to maximum lift coefficient or normal load factor

and

Time to pitch down from maximum lift coefficient or normal load factor to 0g

3.4.5.2 Discussion and Typical Results

Figures 3.16, 3.17, and 3.18 show the *time to pitch down from maximum normal load factor to 0g* at altitudes of 500, 15,000, and 40,000 feet. Compared to Figures 3.12, 3.13, and 3.14, these figures suggest that the generic F-18A is significantly more agile in pitch for nose up pitching than in nose down pitching.

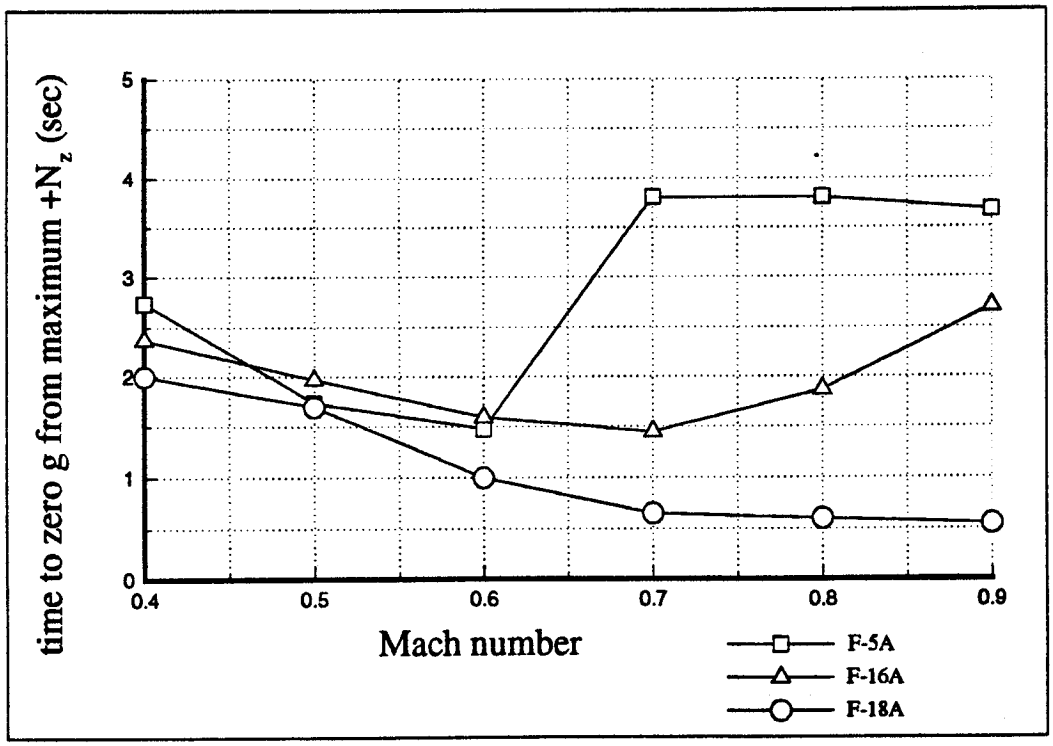

Figure 3.16 Generic F-5A, F-16A, And F-18A *Time To Pitch Down From Maximum Normal Load Factor To 0g*, H = 500 feet

At lower Mach numbers, the generic F-18A requires about twice as much time to unload from maximum normal load factor to zero normal load factor, as it does to pitch from straight and level flight to maximum normal load factor. This result was also noted by Reference 18. In that analysis of several current fighter aircraft, it was concluded that modern fighter aircraft tend to possess much less nose down pitch agility than nose up pitch agility. If pitch agility in both directions is important to an operational pilot, then nose down pitch authority is a promising candidate for improvement. The results presented here for the generic F-16A are very similar to the generic F-18A, and seem to bear out the conclusion of Reference 18.

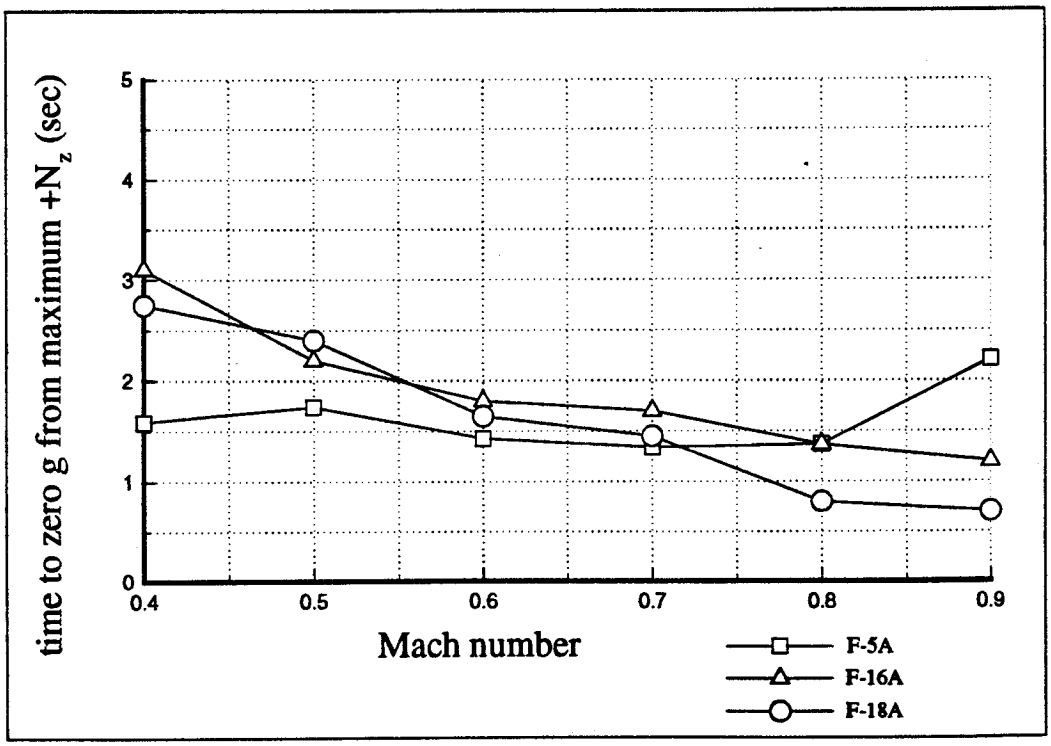

Figure 3.17 Generic F-5A, F-16A, And F-18A *Time To Pitch Down From Maximum Normal Load Factor To 0g*, H = 15,000 feet

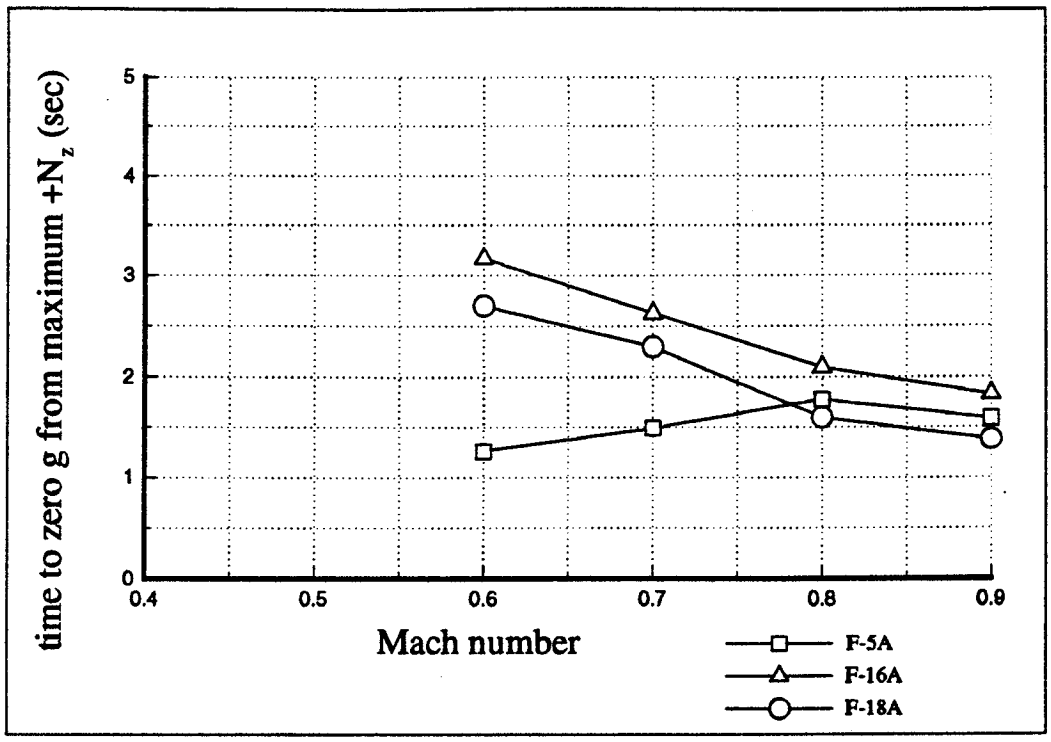

Figure 3.18 Generic F-5A, F-16A, And F-18A *Time To Pitch Down From Maximum Normal Load Factor To 0g*, H = 40,000 feet

Interestingly, the generic F-5A has nearly constant times to unload across the subsonic Mach number range tested, at both the low and intermediate altitudes. At the higher altitude, the time to unload is again roughly constant across the Mach number range, but with slightly greater times, as is expected for a low dynamic pressure flight condition.

3.4.5.3 Time to Pitch Down From Maximum Normal Load Factor to 0g Sensitivity

For the generic F-18A, all of the deviations tested except reduced aft stick rate have an effect on the nose down portion of the pitch agility metrics. However, only one of these deviations causes a significant change in the *time to pitch down from maximum normal load factor to 0g* (Figure 3.19).

As expected, applying 20% more forward stick than for the nominal case permits the aircraft to reach zero normal load factor more quickly at the lower Mach numbers. Otherwise, for the generic F-18A this metric is generally insensitive to deviations from the nominal stick commands.

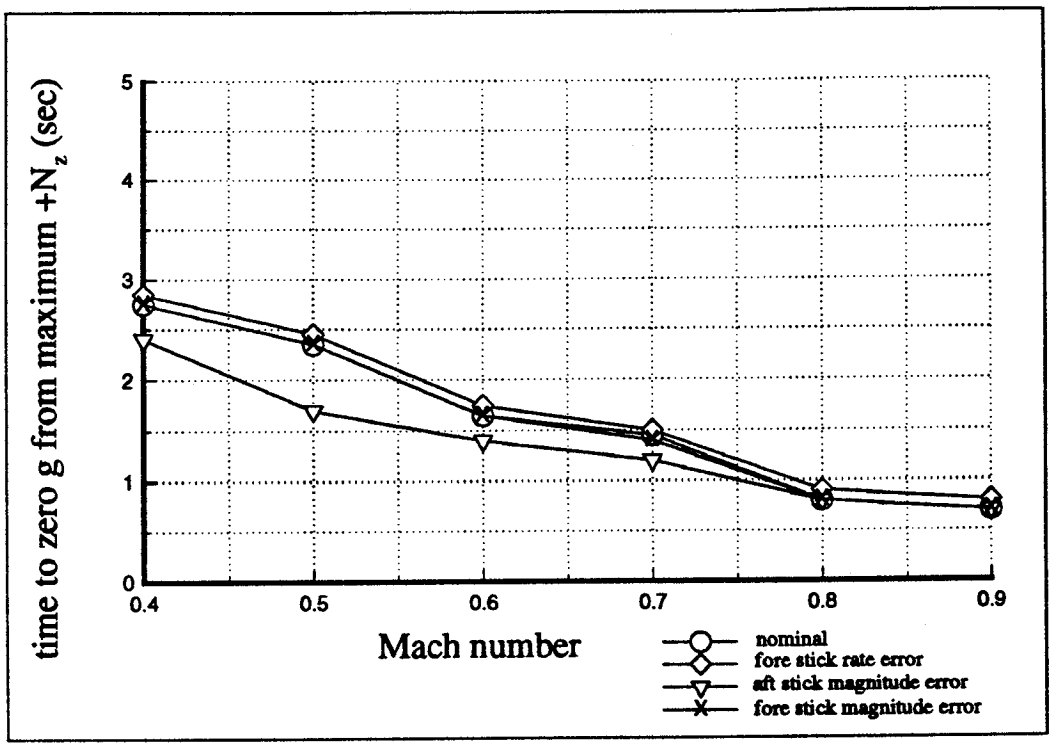

Figure 3.19 Generic F-18A *Time To Pitch Down From Maximum Normal Load Factor To 0g* Sensitivity, H = 15,000 feet

3.4.5.4 Summary

Though the *time to pitch to maximum normal load factor* and the *time to pitch down from maximum normal load to 0g* are conceptually simple, testing these two metrics revealed that at many flight conditions, maximum normal load factor cannot be held during the two second input step. In these cases, aircraft deceleration causes normal load factor to decrease immediately after the peak is achieved and before the pitch down command is initiated. The time to pitch down as shown in Figure

3.1 is calculated from the time forward stick is input, not from the time that normal load factor begins to decay due to airspeed loss. This method minimizes the influence of aircraft drag characteristics on pitch agility measurements and emphasizes nose down pitch authority.

While it is easy to initiate the pitch up from steady level flight conditions, the pitch down from positive normal load factor may start from a condition where airspeed and altitude are rapidly changing. If pitch agility is to be plotted against flight condition, the choice of flight condition may often be somewhat arbitrary. Also, because of flight control and aerodynamic nonlinearities, the normal load factor response will often not be well damped. Determining the times to maximum normal load factor can be subjective when no steady state value is reached, or the maximum value is approached asymptotically.

3.4.6 **Positive Normal Load Factor Rate** (REF. 32)

3.4.6.1 Definition

The positive time rate of change of normal load factor, for a given maneuver.

3.4.6.2 Discussion and Typical Results

The maximum positive normal load factor rate generated during a pitch up maneuver is plotted against Mach number and altitude in Figures 3.20, 3.21, and 3.22. These figures reflect the same dependence on Mach number and altitude as the metrics in the previous sections. Figure 3.20 shows that all three aircraft are capable of roughly the same positive normal load factor rate at Mach equals 0.4, after which the generic F-5A and generic F-18A are superior to the generic F-16A. The generic F-5A generates its largest value at Mach equals 0.6, after which it falls off sharply to the level of the generic F-16A. This is because the generic F-5A, having no load factor or pitch rate limiters, cannot

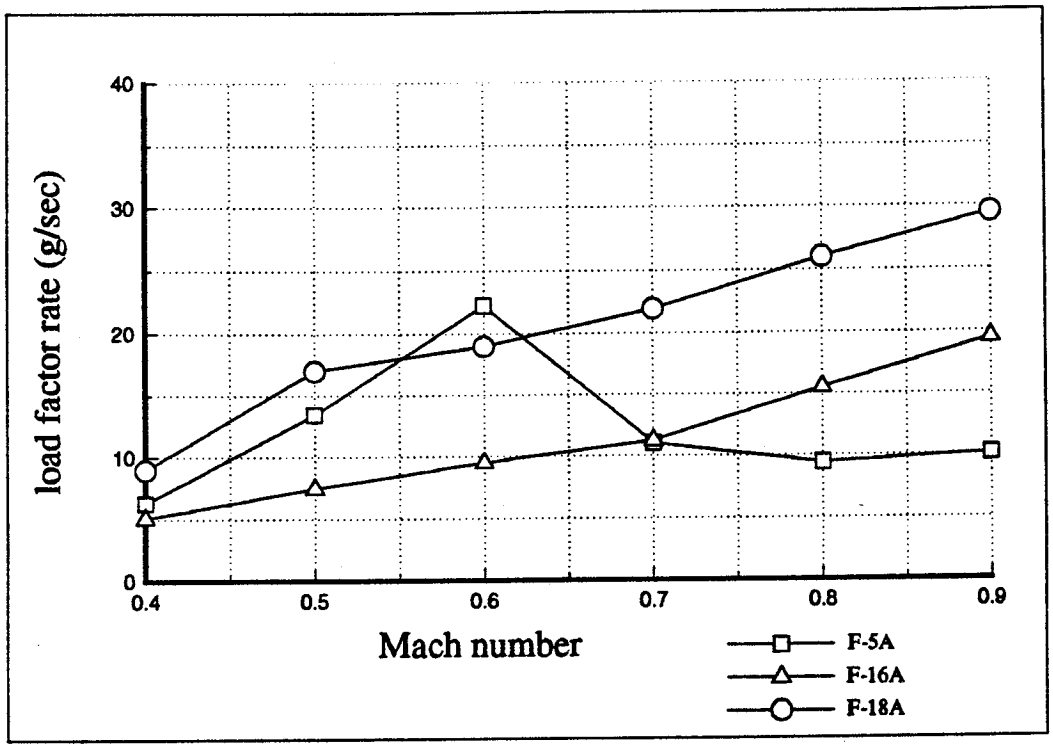

Figure 3.20 Generic F-5A, F-16A, And F-18A *Positive Normal Load Factor Rate*, H = 500 feet

limiters, cannot utilize full aft stick deflections at these higher dynamic pressure flight conditions without overstressing the airframe. Examination of Figure 3.20 indicates that the generic F-16A and generic F-18A each have very consistent and predictable maximum normal load factor rate performance across the range of subsonic Mach numbers tested. This is once again a result of the full authority flight control systems on each aircraft. Figure 3.21 shows the same trends for each aircraft as in Figure 3.20, except that the Mach number at which the generic F-5A cannot use full aft stick deflections is increased to Mach equals 0.8, as is expected for a higher altitude. Figure 3.22 shows all three aircraft to have essentially identical normal load factor rate performance over the range of subsonic Mach numbers tested at this altitude.

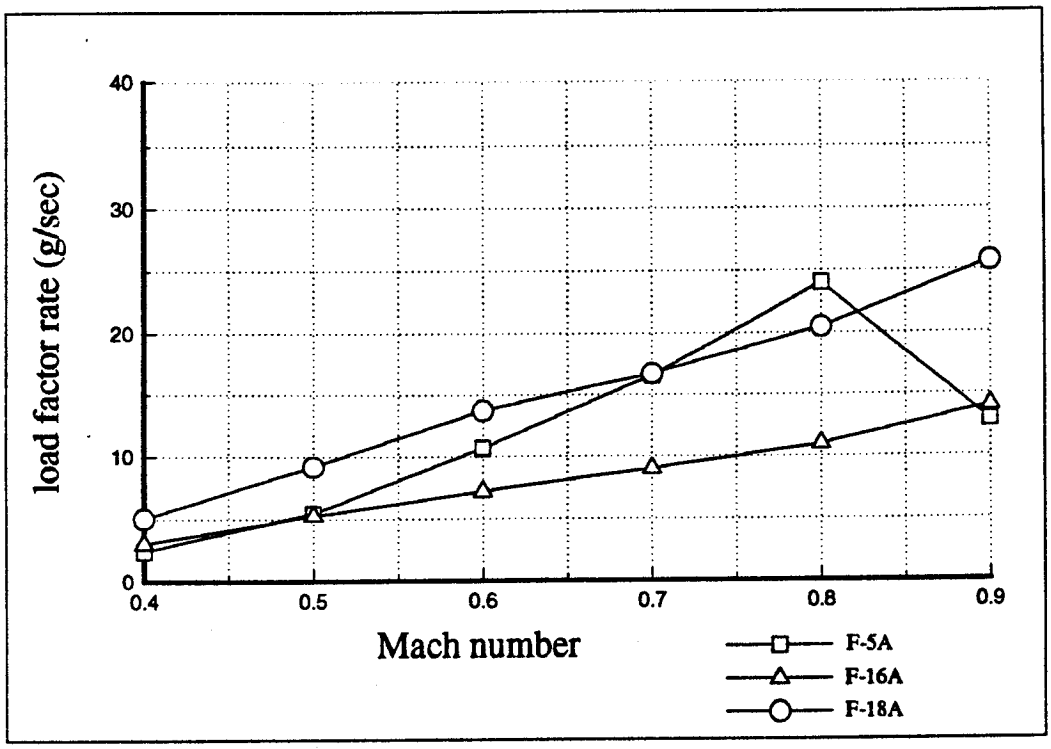

Figure 3.21 Generic F-5A, F-16A, And F-18A *Positive Normal Load Factor Rate*, H = 15000 feet

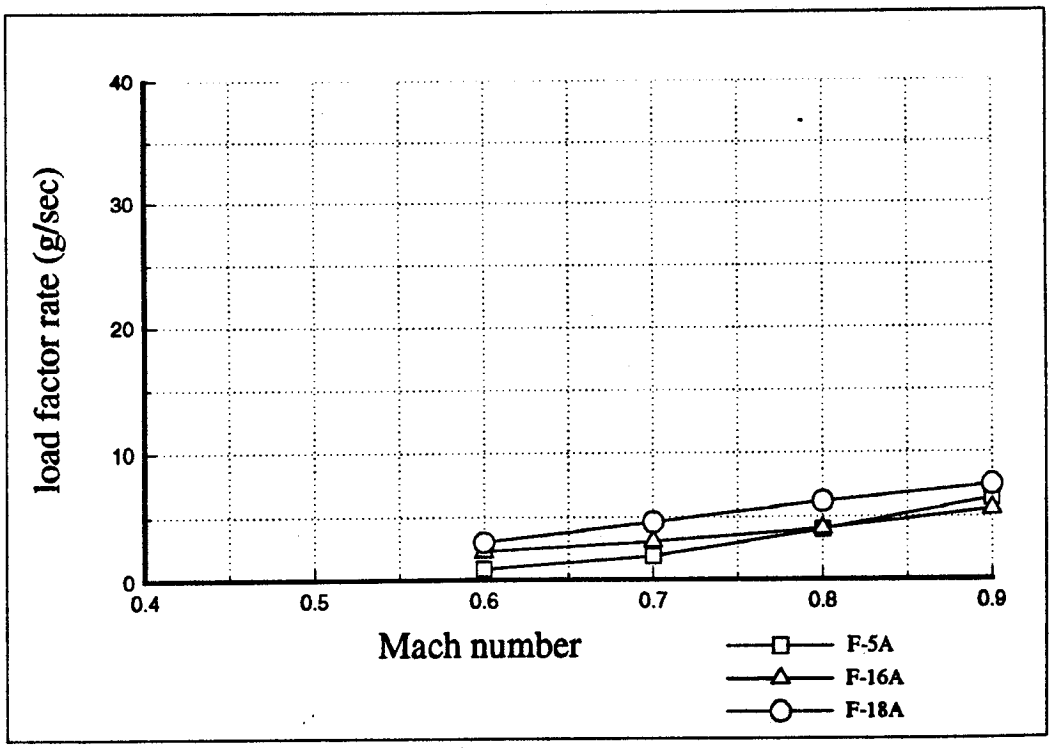

Figure 3.22 Generic F-5A, F-16A, And F-18A *Positive Normal Load Factor Rate*, H = 40000 feet

3.4.6.3. Positive Normal Load Factor Rate Sensitivity

Figure 3.23 shows that the maximum positive normal load factor rate generated by the generic F-18A in the pitch up portion of the maneuver is virtually unchanged by deviations in either aft stick rate or aft stick magnitude. This metric is judged to be essentially insensitive to introduced deviations from the nominal stick inputs.

3.4.6.4 Summary

The positive time derivative of normal load factor, though difficult to measure directly, can in theory be extracted from flight test or simulation time histories. Flight control systems affect this metric, since values of this metric can vary considerably for aircraft which do not employ pitch rate or normal load factor rate limiting. This metric is essentially insensitive to introduced deviations from the nominal stick inputs.

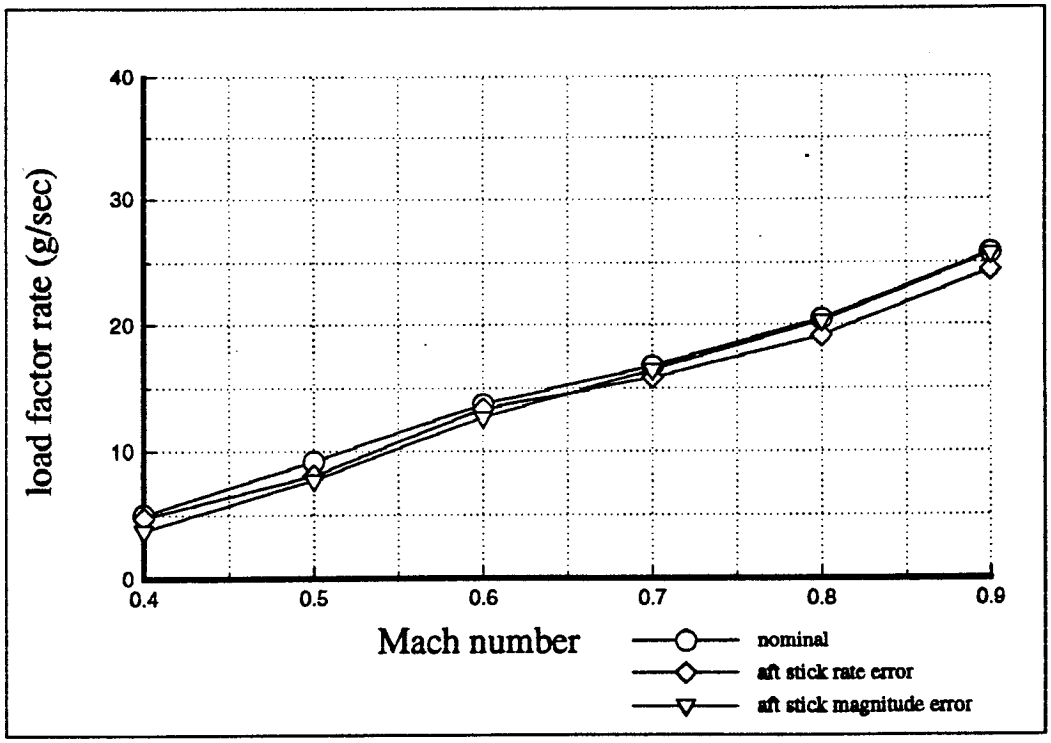

Figure 3.23 Generic F-18A *Positive Normal Load Factor Rate* Sensitivity, H = 15,000 feet

3.4.7 **Negative Normal Load Factor Rate** (REF. 32)

3.4.7.1 Definition

The negative time rate of change of normal load factor, for a given maneuver.

3.4.7.2 Discussion and Typical Results

The *negative normal load factor rate* generated during a pitch down (unloading) maneuver is plotted against Mach number and altitude in Figures 3.24, 3.25, 3.26. As before, the results show the now familiar dependency on Mach number and altitude. However, the maximum negative normal load factor rates generated are not equivalent for the pitch up maneuvers at all Mach numbers. Figures 3.24 and 3.25 show that for nose down pitching the generic F-5A does not suffer from the limitation of reducing the magnitude of the longitudinal stick input, as it did for pitch up maneuvers. For the higher Mach numbers at a given altitude, the maximum positive and negative normal load

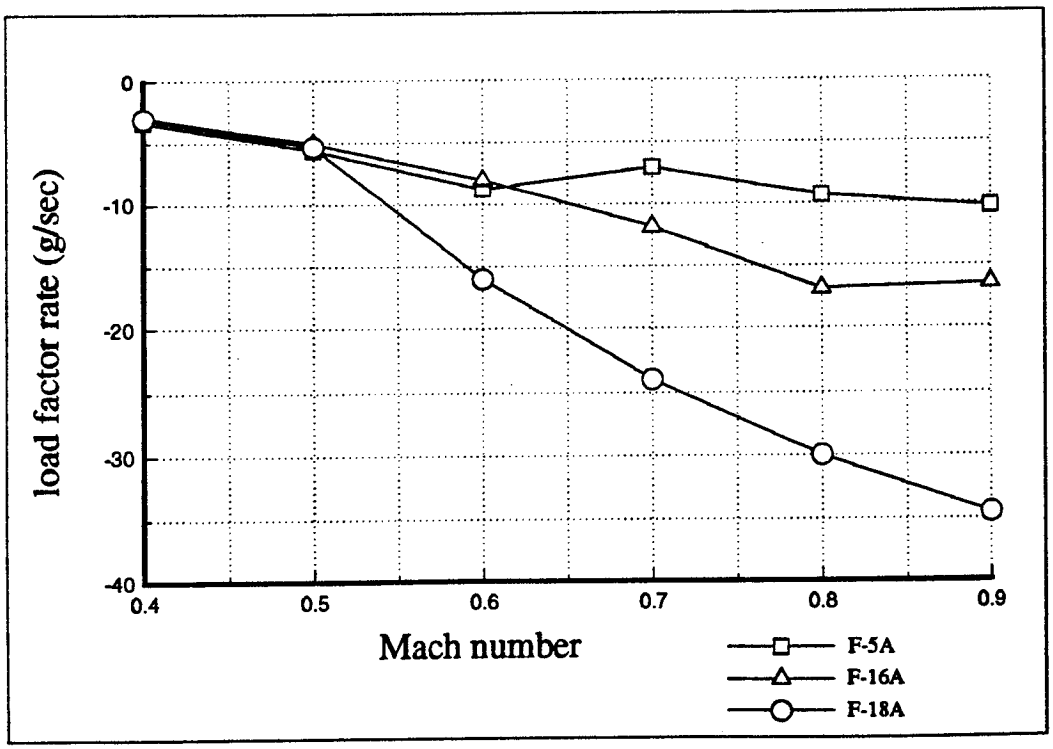

Figure 3.24 Generic F-5A, F-16A, And F-18A *Negative Normal Load Factor Rate*, H = 500 feet

factor rates for a specific aircraft tend to be equivalent. At the lower Mach numbers for a given altitude, the maximum negative normal load factor rate can be significantly less than the positive normal load factor rate for some aircraft. Using the generic F-18A as an example, at Mach equals 0.5 at 500 feet the maximum negative normal load factor rate (Figure 3.24) is approximately one third of the maximum positive normal load factor rate at the same flight condition (Figure 3.20). Based upon the results of this metric, the aircraft tested generally possess more pitch up capability than pitch down capability.

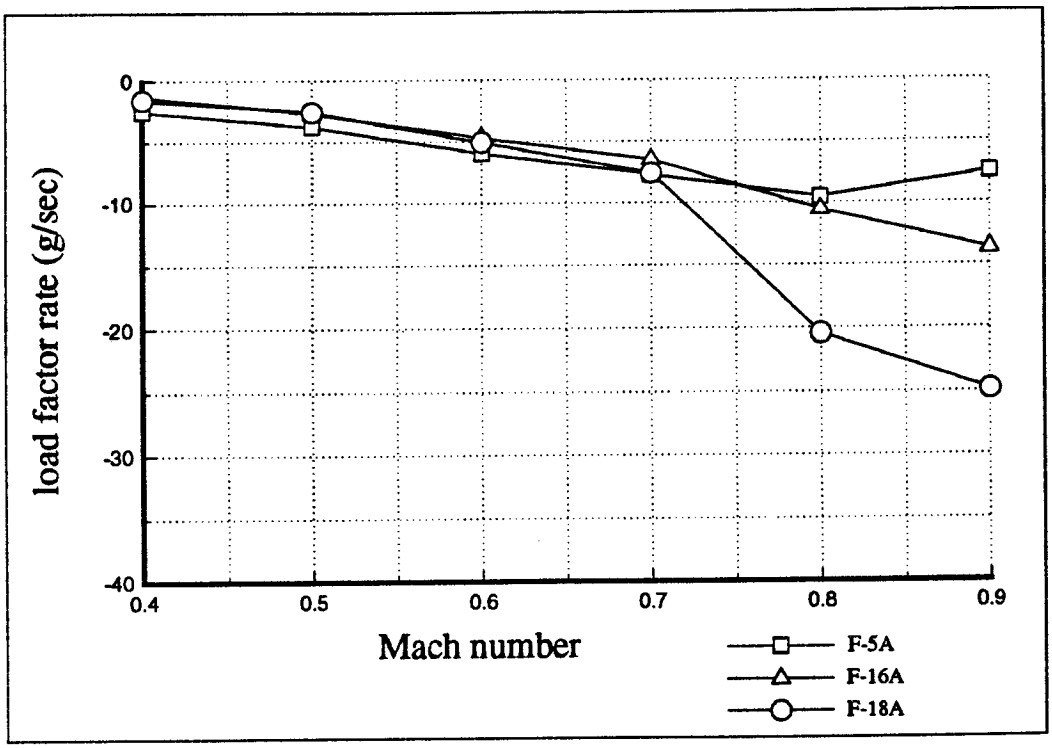

Figure 3.25 Generic F-5A, F-16A, And F-18A
Negative Normal Load Factor Rate, H = 15,000 feet

3.4.7.3 Negative Normal Load Factor Rate Sensitivity

Figure 3.27 shows that the *negative normal load factor rate* metric is generally insensitive to any of the deviations for the generic F-18A.

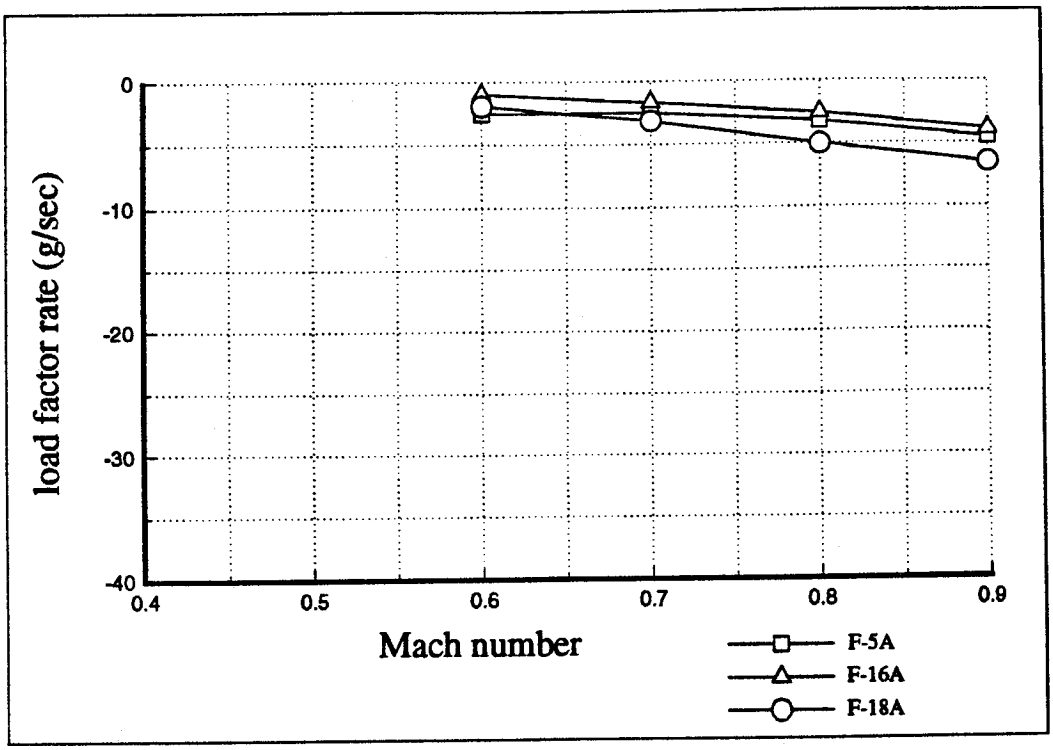

Figure 3.26 Generic F-5A, F-16A, And F-18A
Negative Normal Load Factor Rate, H = 40,000 feet

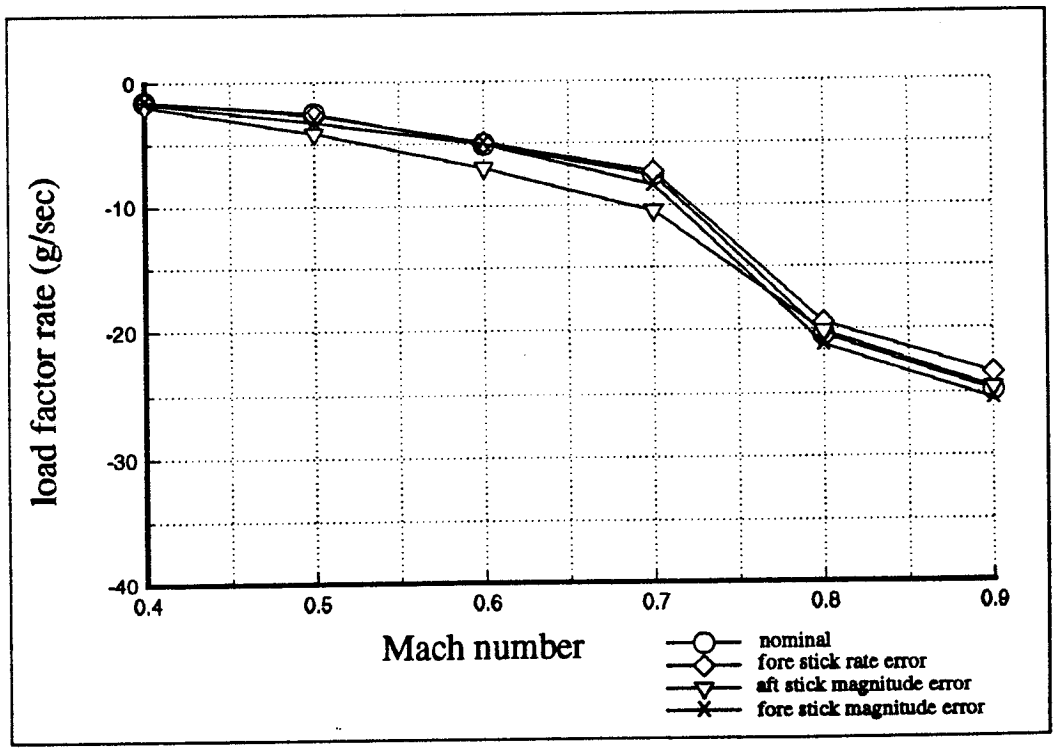

Figure 3.27 Generic F-18A *Negative Normal Load Factor Rate* Sensitivity, H = 15,000 feet

3.4.7.4 Summary

Since pitch down capability is as tactically important as pitch up capability, the *negative normal load factor rate* during a pitch down maneuver was investigated in this report. This metric is basically analogous to the *positive normal load factor rate* metric. At the higher Mach numbers, results for the two metrics are essentially equivalent, while at the lower Mach numbers values for *negative normal load factor rate* tend to be lower than the *positive normal load factor rate*. Sensitivity results indicate that both of these metrics are insensitive to the deviations applied in this study. It has been shown in Reference 32 that time histories of normal load factor rate and the *curvature agility* metric of Reference 33 are virtually identical when scaled to account for different units. A derivation and numerical example is supplied in Appendix E.

3.4.8 **Average Pitch Rate**

3.4.8.1 Definition

$$\text{Average Pitch Rate} = \frac{\int_{t_1}^{t_2} q \, dt}{t_2 - t_1}$$

where q is pitch rate, t_1 is the time at which the pitch-up is executed, and t_2 is the time at which the pitch-up maneuver is completed. The completion time t_2 is selected at the discretion of the tester. Usually, t_2 is selected from a common sense point of view for the particular task which is being performed.

3.4.8.2 Discussion and Typical Results

Referring to Figure 3.3 in Section 3.4.1, for a Mach number of 0.7 and an altitude of 15,000 feet, the generic F-5A has the largest maximum positive pitch rate measured. Based solely upon the maximum pitch rate criteria of Section 3.4.1, the generic F-5A would be judged to be the most agile

of the three airplanes in pitch for this flight condition. A potential problem exists because simply plotting the maximum value achieved versus Mach number reveals nothing about the character of the pitch rate response. Consider the pitch rate time histories of the generic F-5A, F-16A, and F-18A at Mach equals 0.7 at 15,000 feet in Figure 3.28.

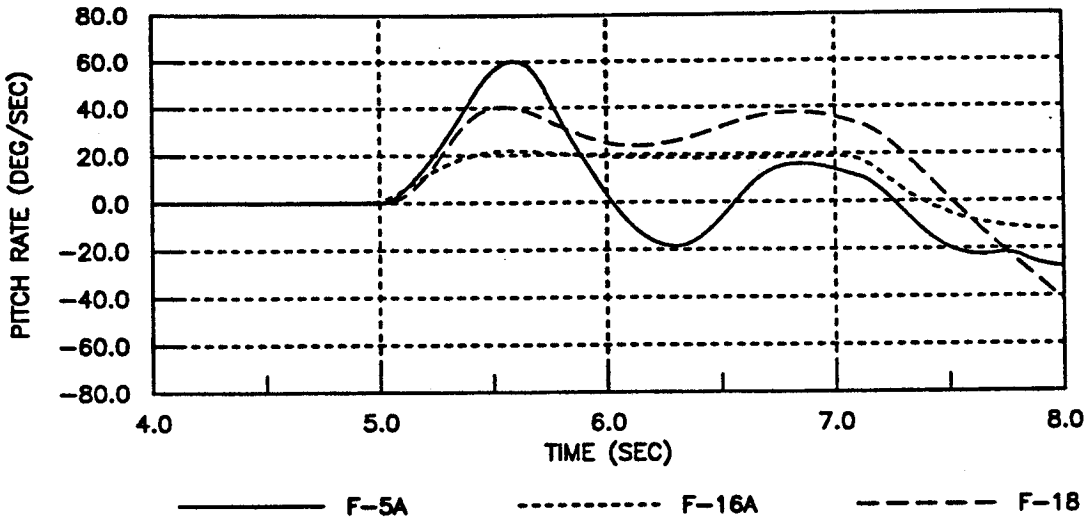

Figure 3.28 Generic F-5A, F-16A, And F-18A Pitch Rate From Level Flight Time History, Mach = 0.7, H = 15,000 feet

For the purpose of illustration, the command to each aircraft is a pitch-up step input only; unlike the commands given to test each of the previous metrics, the nose-down step input is not commanded. Figure 3.28 shows that at this test point the generic F-5A pitch rate falls off to values well below those of the generic F-16A and generic F-18A pitch rates shortly after the initial peak. Although the generic F-16A and generic F-18A can maintain a larger average pitch rate over the duration of the test maneuver, the *maximum positive pitch rate* metric alone does not highlight this capability. If the pitch rate time histories of Figure 3.28 are averaged over the time interval from three to five seconds, the generic F-5A is no longer indicated to be superior in pitch to the generic F-16A and the generic F-

18A. The average pitch rates for the generic F-5A, F-16A, and F-18A at this test point are 6.67, 11.52, and 19.6 degrees per second respectively. This example serves to illustrate that although the generic F-18A does not achieve the largest pitch rate of the three aircraft, it is able to maintain a larger average value of pitch rate over the time interval considered. Thus merit is given to the aircraft which can maintain the largest values of pitch rate over a specified period of time, instead of just at a large, momentary value at a point.

Values for the *average pitch rate* metric are calculated using the same testing technique used to obtain the maximum positive pitch rate data of Section 3.4.1. Values for the generic F-5A, F-16A, and F-18A from steady level 1g flight are displayed in Figures 3.29, 3.30, and 3.31. Figure 3.29 shows that although the generic F-18A *average pitch rate* is larger than the other aircraft at the lower Mach numbers, the reverse is true at the higher Mach numbers. The generic F-18A degenerates to values approximately equal to the generic F-5A, while the generic F-16A maintains a roughly constant

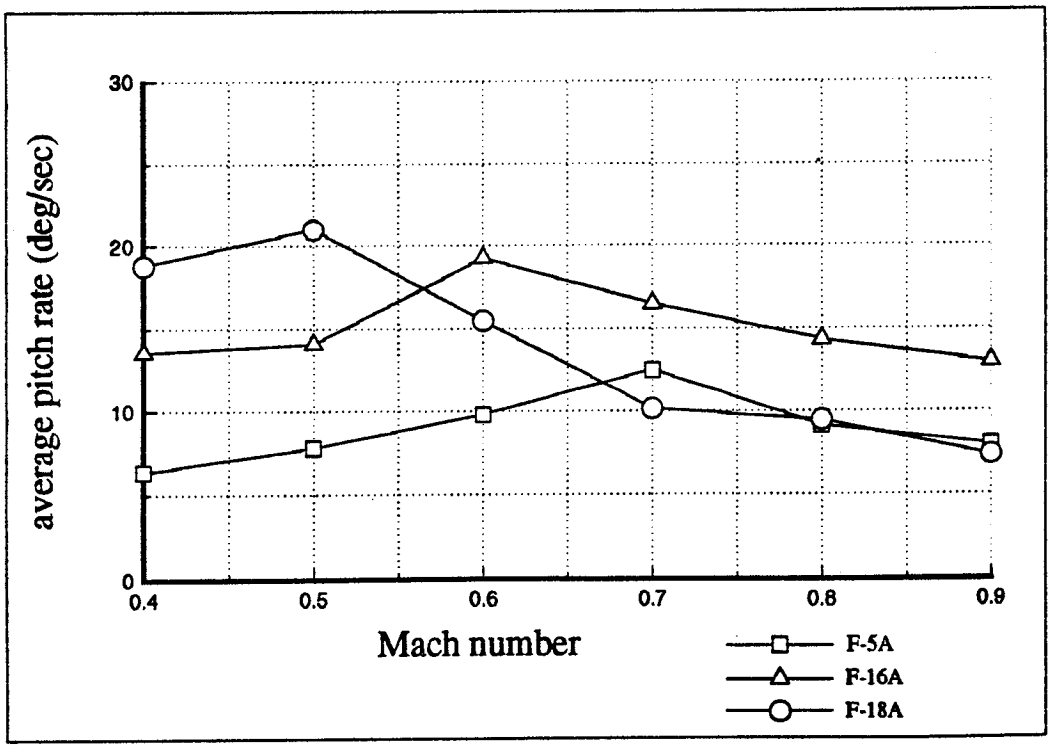

Figure 3.29 Generic F-5A, F-16A, And F-18A
Average Pitch Rate From Level Flight, H = 500 feet

value of 15 degrees per second across the range of Mach numbers. Comparing Figure 3.29 to Figure 3.2 of Section 3.4.1.2, the generic F-16A and generic F-18A exhibit the same basic trends with respect to Mach number, in spite of the generic F-16A being better in *average pitch rate* than in *maximum positive pitch rate*. The generic F-5A however shows considerable differences since the *average pitch rate* is considerably lower than the peak maximum pitch rate.

At 15,000 feet, the trends in *average pitch rate* are similar to the low altitude results in Figure 3.29, except that the Mach number at which the generic F-18A *average pitch rate* is extended from Mach equals 0.5 to Mach equals 0.7 (Figure 3.30). Compared to the *maximum positive pitch rate* results for this same altitude in Figure 3.3, the *average pitch rate* results of Figure 3.30 once again show the generic F-16A and generic F-18A trends to be very similar for the two different pitch rate metrics. Values of *average pitch rate* for the generic F-5A are also once again vastly inferior to those for the *maximum positive pitch rate*.

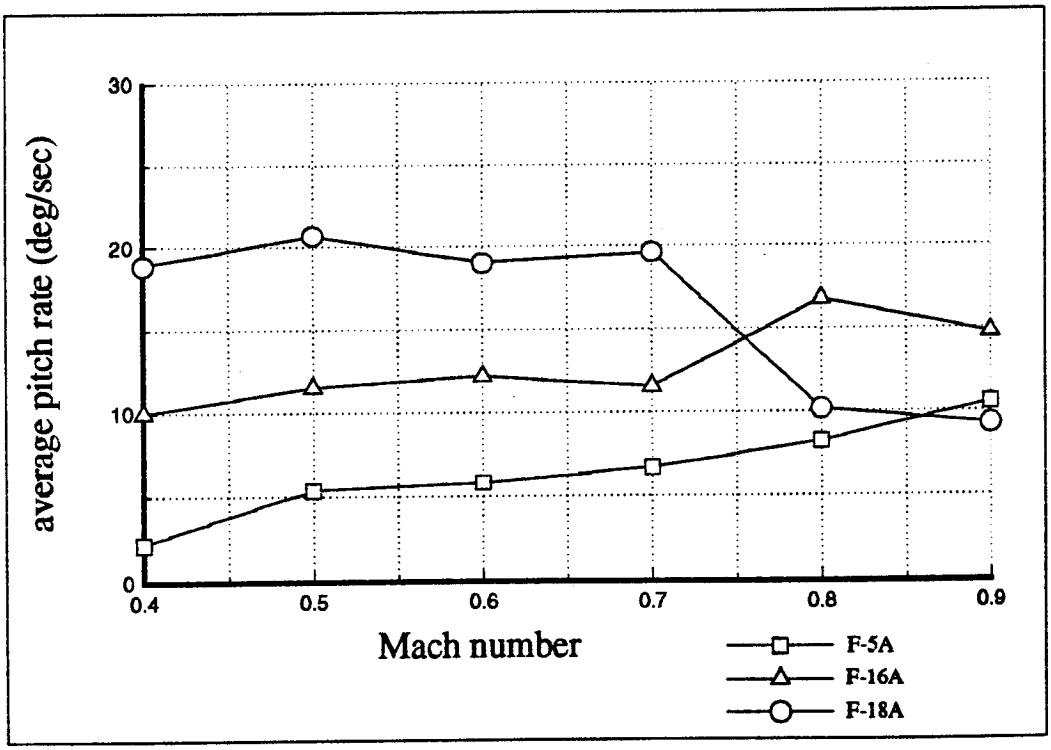

Figure 3.30 Generic F-5A, F-16A, And F-18A
Average Pitch Rate From Level Flight, H = 15,000 feet

At an altitude of 40,000 feet, the generic F-18A *average pitch rate* values of Figure 3.31 are remarkably similar to those at 15,000 feet, including the decrease in values at Mach equals 0.7. The generic F-16A fairs just slightly worse at this higher altitude, as does the generic F-5A. Compared to the *maximum positive pitch rate* values at this altitude in Figure 3.4, the trends for the generic F-16A and generic F-18A are in general proportion to each other for both metrics. The generic F-5A is once again better in *maximum positive pitch rate* than in *average pitch rate.*

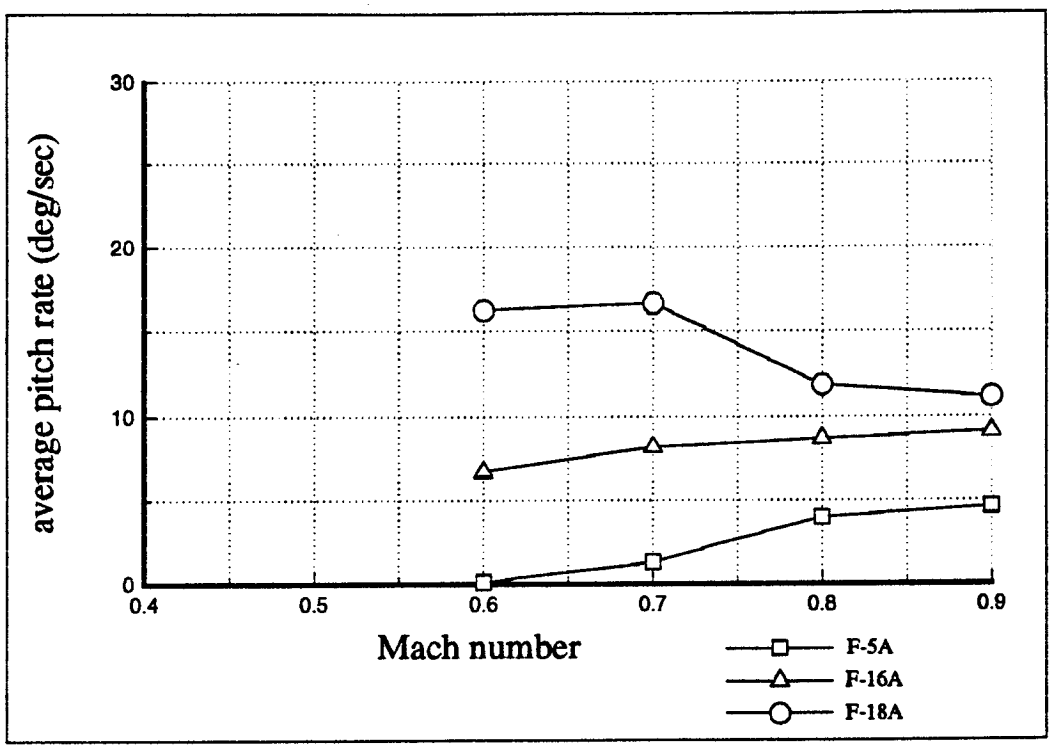

Figure 3.31 Generic F-5A, F-16A, And F-18A
Average Pitch Rate From Level Flight, H = 40,000 feet

3.4.8.3 Average Pitch Rate Sensitivity

The generic F-18A *average pitch rate* sensitivity of Figure 3.32 is very similar to the *maximum positive pitch rate* sensitivity in Figure 3.5. This is to be expected as the results above demonstrate that the general trends and behaviours of the generic F-18A is the same for both metrics.

The only sensitivity noted is that resulting from a 20% reduction in the magnitude of the aft stick command. This result is to be expected as less *average pitch rate* is measured since less pitch rate is being commanded. At the higher Mach numbers the sensitivity disappears because of the pitch rate limiting of the FCS.

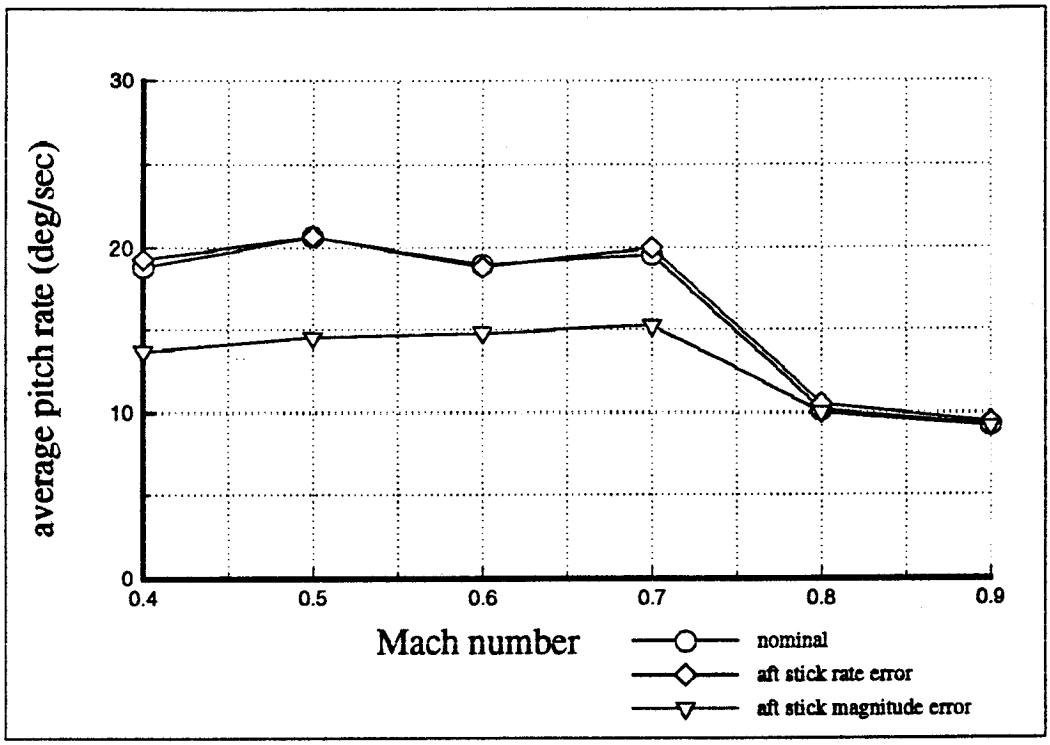

Figure 3.32 Generic F-18A *Average Pitch Rate* From Level Flight Sensitivity, H = 15,000 feet

3.4.8.4 Summary

A pilot usually commands pitch rate to point the nose of the aircraft or to achieve a desired load factor or turn rate. Ideally, pitch agility metrics should be task oriented. Considering only the *maximum positive or negative pitch rate* is often misleading for the purpose of comparing aircraft, since very large values can usually be generated only momentarily. Also, measuring only the *maximum positive or negative pitch rate* does not directly relate to either the aircraft's ability to point

the nose or to achieve a desired load factor. From this task oriented point of view, it is the *average pitch rate* which is desirable to measure.

3.5 SUMMARY

The *time to pitch to maximum load factor* and the *time to unload to zero normal load factor* metrics contain inherent limitations for comparison among dissimilar aircraft or even among various flight conditions for the same aircraft because the maximum normal load factors can be very different at the same flight condition. For example, consider two dissimilar aircraft. The first (aircraft A) with a 5g maximum normal load factor capability at a certain flight condition, and the second (aircraft B) with a 9g capability at that same flight condition. If both are equally agile in terms of positive normal load factor rate, then aircraft A will have a shorter time to achieve it's maximum normal load factor since the maximum normal load factor is a lower value. Likewise, results of the generic F-18A simulation at an altitude of 15,000 feet demonstrate the same *time to pitch to maximum normal load factor* at Mach equals 0.6 and at Mach equals 0.7. The reason for this apparent anomaly is that at Mach equals 0.7, the aircraft has **both** a higher normal load factor **rate** and a higher **value** of maximum normal load factor.

Maximum positive and negative pitch rate is only an indirect measure of the ability of an aircraft to generate normal accelerations and to unload quickly to zero normal load factor. Additionally, differences in lift curve slopes are neglected as they would be in measuring the time to capture angle of attack. Pitch rate is a direct measure of pilot ability to point the nose of the aircraft, which is a significant capability during within-visual-range engagements. Although limited because of the "more is better" property of this metric, assessing pitch agility by plotting *maximum positive and negative pitch rate* versus angle of attack also appears to have some merit. Some advantages of

this approach are :

1. Since the pilot is not required to capture a specific angle of attack or normal load factor, his inputs are simpler and more repeatable. As a result aircraft characteristics are highlighted, and the impact of individual pilot technique is minimized.

2. A more complete picture of the aircraft's nose pointing ability is presented than with other metrics.

In summary, the sensitivity analysis indicates that as tested using the generic F-18A, none of the candidate pitch agility metrics tested are unusually sensitive to deviations from the nominal sequence of stick input commands. In the nose up direction, positive pitch rate is reduced by approximately ten degrees per second if four inches of aft stick is applied rather than the maximum of five. During the pitch down portion of the maneuvers, zero normal load factor is achieved more quickly when additional forward stick is applied. Except for these two instances, the input deviations studied here had no significant effect on the values of the metrics. This would appear to indicate that ,at least for the generic F-18A, useful data for the *time to maximum normal load factor* and *maximum normal load factor rate* metrics possess a reasonable tolerance to variations in pilot input. These sensitivities could apply when using other fighter aircraft to obtain data, but naturally with differing magnitudes of errors. Additionally, when attempting to collect data to measure *maximum positive or negative pitch rate*, or the *time to achieve zero normal load factor*, unique cockpit displays may be helpful to allow more precise inputs.

The interaction of flying qualtities and pitch agility metrics becomes especially important when manned simulators and actual flight testing are used instead of the unmanned non real-time simulations used for these investigations. For coverage of this aspect of pitch agility the reader is encouraged to consult Reference 34.

4. LATERAL AGILITY

4.1 BACKGROUND

Lateral agility is concerned primarily with rolling maneuvers, usually at intermediate or high angles of attack, and elevated normal load factors. The purposes of this chapter is to analyze the particular aircraft characteristics which enhance/degrade lateral agility; demonstrate methods for testing and measuring lateral agility using candidate lateral agility metrics; and compare the lateral agility of the F-5A, F-16A, and F-18A.

Bank angle capture criteria are developed in order to quantify those candidate lateral agility metrics which require the capture of a target bank angle. The required pilot command inputs, and the sensitivity of the candidate lateral agility to deviations in the pilot command inputs is presented. The lateral agility metrics are evaluated using the University of Kansas Flight Research Laboratory's generic F-5A and generic F-18A aircraft simulations (Appendix B). All roll angles discussed in this chapter are in the wind axis coordinate system (Appendix C).

4.2 CANDIDATE LATERAL AGILITY METRICS

In recent years agility researchers have proposed numerous metrics to quantify the lateral agility of fighter aircraft. The proposed metrics include:

1) time through 90° roll angle (T_{TR90})
2) 90° roll angle capture (T_{RC90})
3) 180° roll angle capture (T_{RC180})
4) torsional agility

5) roll reversal capture

6) defensive roll reversal agility parameter

7) roll transient

All seven candidate lateral agility metrics are defined in Appendix A. In the current study, results are presented for only the *time through 90 degree roll angle* (T_{TR90}), the *90 degree roll angle capture* (T_{RC90}), and the *180 degree roll angle capture* (T_{RC180}). The *torsional agility* metric is discussed in Appendix A and Reference 18. The remaining candidate lateral agility metrics have been fully addressed in detail by other researchers. For a discussion of the *roll reversal capture* metric, the reader is directed to Reference 25. The *defensive roll reversal agility parameter* is defined in Reference 35, and the *roll transient* metric is defined in Reference 25.

4.3 LATERAL AGILITY TESTING AND DATA REDUCTION TECHNIQUES

The lateral agility metrics are measured by performing rolling maneuvers at the corner speed (V_C) at a particular altitude. Test points consist of either specified initial positive angles of attack, or specified initial normal load factors from 1 to n_{MAX}, or specified values of longitudinal stick deflection. The test cases are conducted at Mach numbers which roughly correspond to the corner speed for each aircraft. All results presented here are obtained at an altitude of 15,000 feet, which is considered a typical altitude for high subsonic WVR air combat. Additionally, a number of agility metrics in the open literature have been evaluated at this altitude (REF. 1, 2, 3, 4, 18, 19).

Although not explicitly a part of the definition of any metric, a set of constraints is established in order to define an acceptable or realistic maneuver. This consideration is particularly important for the agility metrics which involve rolling, since large undesirable cross-axis responses such as

adverse/proverse sideslip can be generated inadvertently. The constraints also provide a level of standardization and repeatability. For this investigation, the constraint boundaries are established using standard flight test procedures (REF.36), and the previous experience of other researchers from the F-18 high angle of attack research vehicle (HARV) flight tests (REF. 37). The enforced constraints consist of the following:

1) constant altitude: ± 2000 feet

2) Mach number excursion: ± 0.2

3) maximum angle of attack excursion: $\leq \pm 6^{\circ}$

4) maximum adverse sideslip: $\leq 7^{\circ}$

5) maximum proverse sideslip: $\leq 1^{\circ}$

6) maximum lateral acceleration: ± 2g

At each flight condition investigated, the aircraft is trimmed to straight and level flight. With the trim point established, pilot command inputs required to measure the lateral agility metrics are applied. The longitudinal stick command is ramped in over one second and then held, until angle of attack approaches a relatively steady value. Lateral stick is then commanded to either roll through or capture a specified value of bank angle. Mach number and angle of attack are then averaged over this same time. The throttle is applied to hold Mach number constant when possible. When full afterburner is not sufficient to hold speed, the initial Mach number is increased to provide the average Mach number desired for the test point.

Lateral and longitudinal stick are the only pilot command inputs used unless stated otherwise. All pilot command inputs used in this investigation consist of steps and/or doublets, and are ramped in and ramped out over a minimum of 0.1 seconds. This is an approximation of the time required for a human operator to affect an abrupt control input or "stick grab" (REF. 3). The pilot command

inputs for the generic F-5A are similar to the generic F-16A and generic F-18A, except that care must be taken to prevent overstressing of the airframe.

Although several pilot techniques can be used to generate the necessary bank angle displacements, only two different classes of pilot command input strategies are used in this investigation. In the first class, if testing a metric requires only a measurement of the minimum time to achieve a certain value of a variable such as bank angle, then a simple full throw or step of the stick is commanded (Figure 4.1).

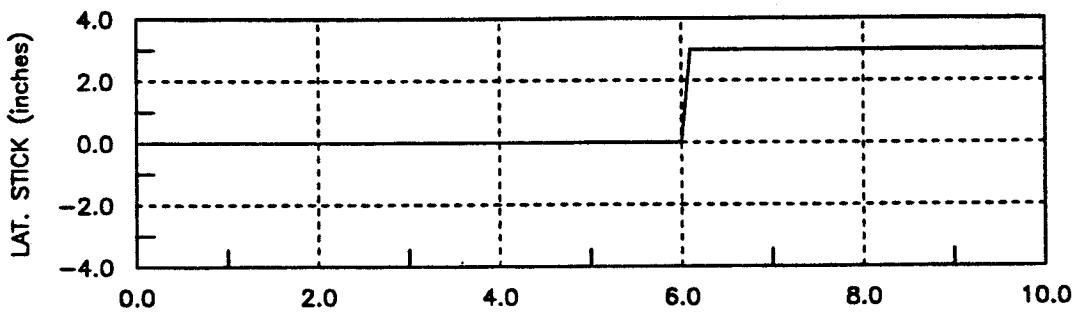

Figure 4.1 Typical Lateral Stick Time
History Used To Roll Through A Target Bank Angle

The second class is used when a metric requires the aircraft to capture a commanded value of a variable such as bank angle. In this class, a doublet is required to initiate and then arrest the roll, thereby accomplishing the capture. A typical lateral stick time history for this test case is shown in Figure 4.2. Full lateral stick is ramped in to begin the roll, followed by full opposite stick to arrest the roll. The times t_1 and t_2 of Figure 4.2 are iterated so that the aircraft stops rolling near a bank angle of 90°. The stick position is then held as closely as possible. Although this command input strategy results in the capture of some value of bank angle, criteria are required to determine if the test aircraft has captured the **correct** target bank angle. Of the two techniques used in this investigation, one is arbitrarily selected for testing the *90° roll angle capture*, and the other capture

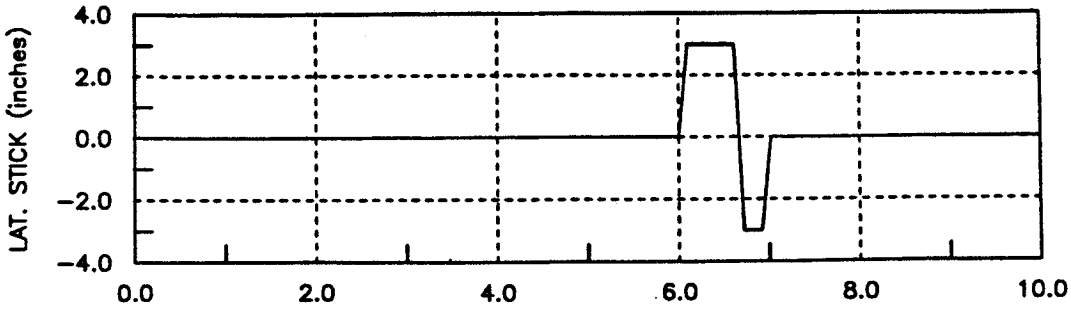

Figure 4.2 Typical Lateral Stick Time
History Used To Capture A Target Bank Angle

technique is used for testing the *180° roll angle capture.*

4.3.1 Measurement Criteria For The Time Through 90° Roll Angle Metric

For testing the T_{TR90} metric, after setting up the aircraft trimmed at the desired Mach number and angle of attack, full lateral stick is ramped in and held for the duration of the maneuver (Figure 4.1). The time through a target value of bank angle is measured from the time of application of lateral stick, to the crossing of $\phi_{wind} = 90°$ (Figure 4.3).

4.3.2 Capture Criteria For The 90° Roll Angle Capture Metric

The T_{RC90} metric is tested in the same manner as the T_{TR90} metric, except that opposite maximum lateral stick is commanded to arrest the roll near the target bank angle (Figure 4.2). The time to capture is approximated numerically using a normalization algorithm. Reference 18 proposed a capture algorithm formulated in terms of parameters in the body axes. Reference 28 modified this algorithm to relate the time to capture in terms of bank angle and roll rate in the wind axes:

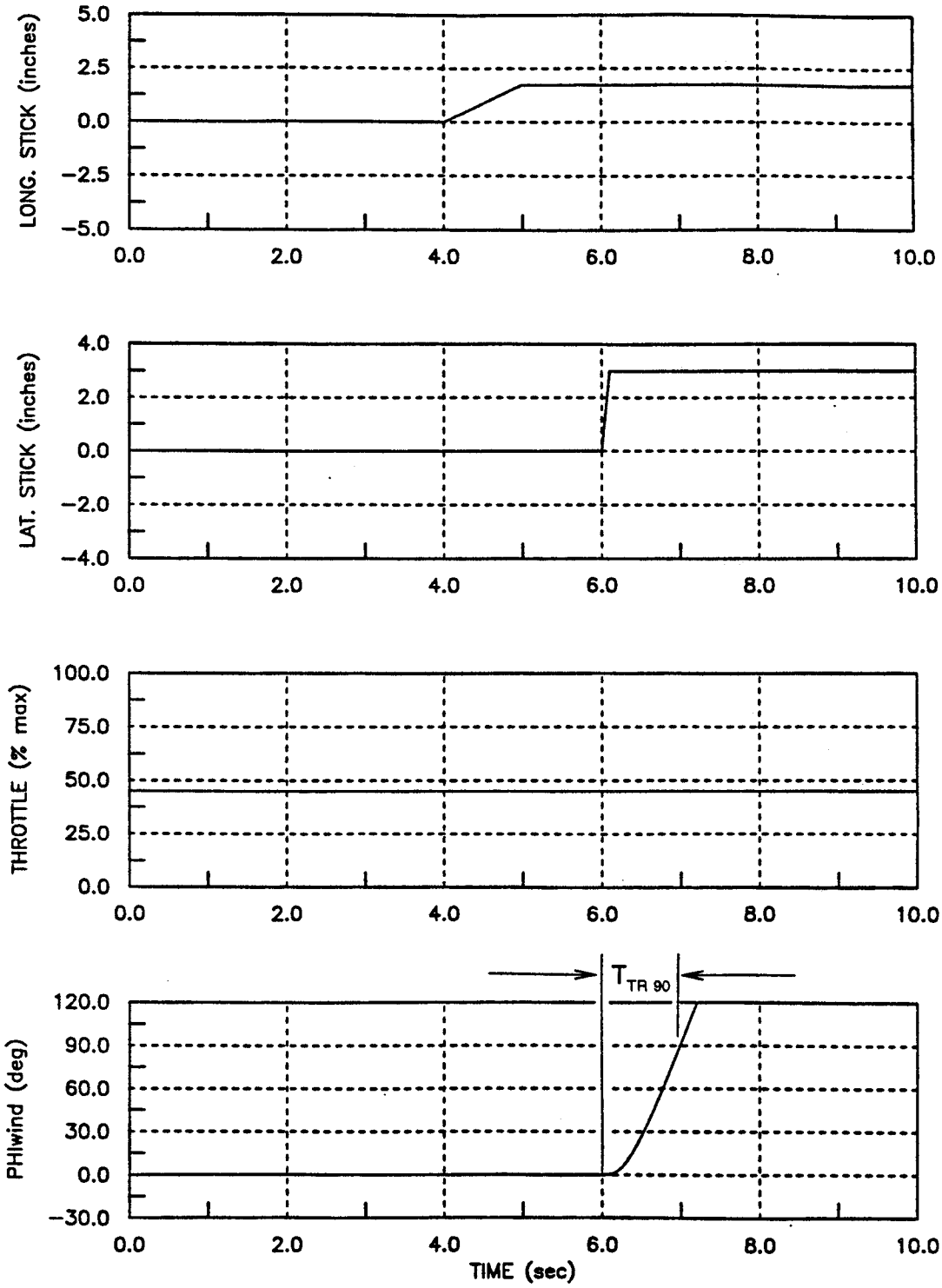

Figure 4.3 Typical Pilot Stick Input Commands And Data Extraction Points Used For Testing The *Time Through 90° Roll Angle* Metric

$$T_{RC90} = T_{RC} + \frac{90° - (\phi_{wind})_{max}}{(P_{wind})_{max}} \quad (4.1)$$

The times are normalized to a bank angle displacement of exactly 90°. Precise capture of the target bank angle is not required. Instead, only the capture of a bank angle close to the target angle (approximately ± 10°) is required. Equation 4.1 takes the amount of ϕ_{wind} overshoot or undershoot and computes the time it would have taken to traverse that angle at the maximum rate (P_{wind}) achieved during the roll. The time is then added or subtracted from the measured time (T_{RC}), defined as the time from the application of lateral stick until roll rate reaches zero, to get the normalized time (Figure 4.4).

To see how accurate the normalization procedure is, the time at which the stick deflection was reversed was varied up to ± 0.1 seconds. This created a range of overshoots and undershoots of 90°. Figure 4.5 shows that despite overshoots and undershoots of more than 10°, consistent T_{RC90} data can be predicted.

When using non real-time unmanned simulations, the capture algorithm technique is only effective for evaluating roll angle capture metrics such as T_{RC90} and T_{RC180} when sideslip angles are relatively small. Figure 4.6 shows a generic F-18A time history of a 12° angle of attack roll where capturing the target bank angle is not possible. Kinematic coupling during the roll acceleration and deceleration generate large sideslip angles, and the rudder actuators are not fast enough to follow the rudder deflection commands. Although the rudders are riding their rate limits almost continuously three seconds after the roll is initiated, the transients cannot be eliminated, and the target bank angle cannot be captured.

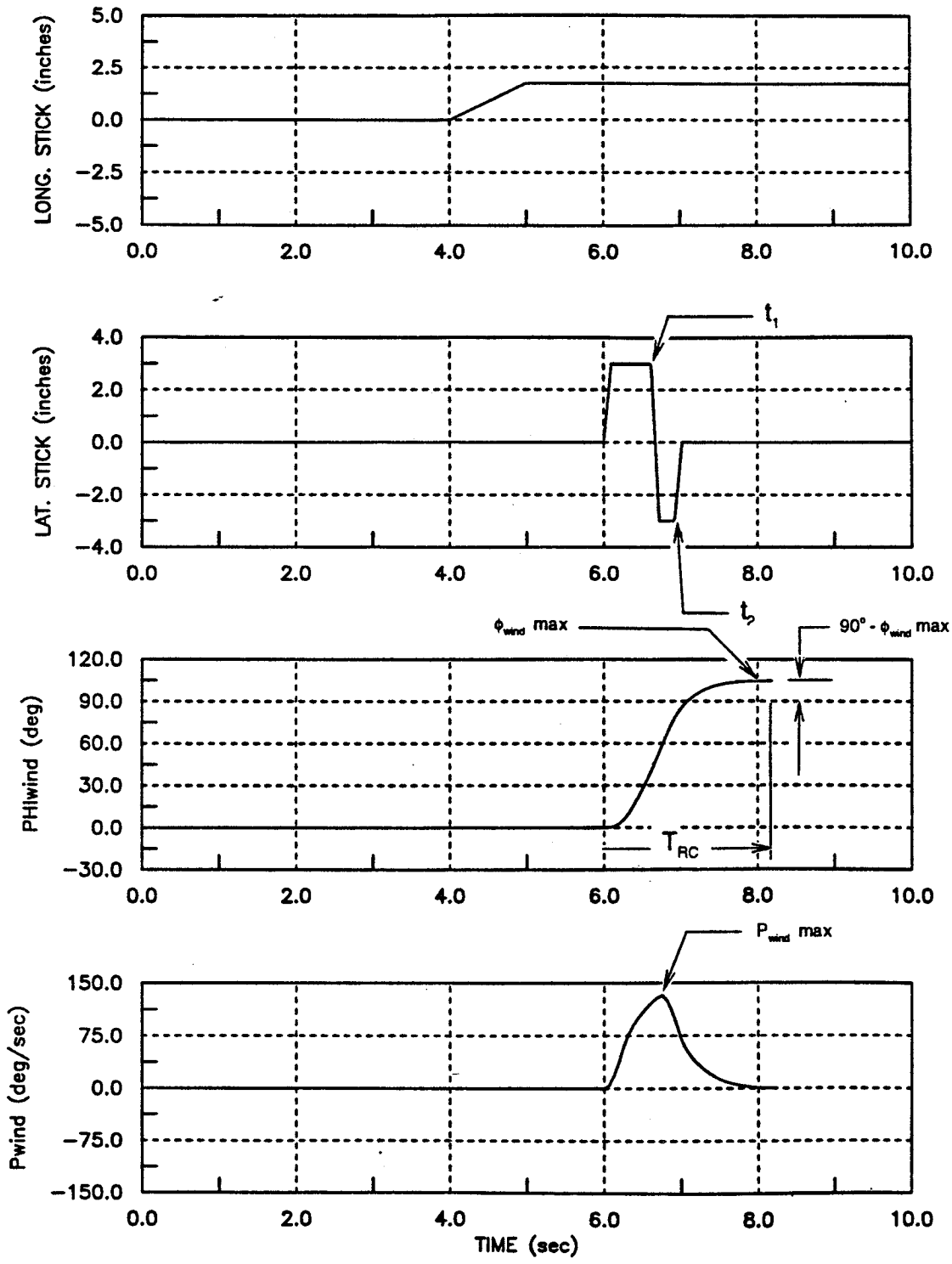

Figure 4.4 Typical Pilot Stick Input Commands And Data Extraction Points Used For Testing The *90° Roll Angle Capture* Metric

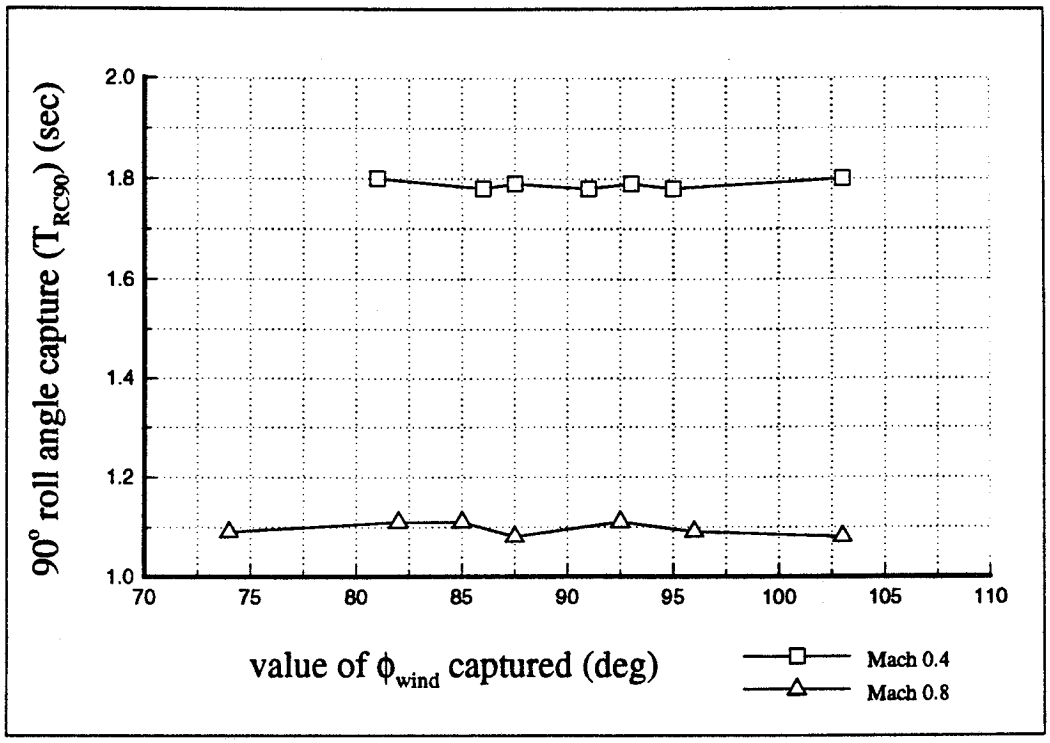

Figure 4.5 Effect Of Normalization On The Time To Roll And Capture 90°, Generic F-18A, Mach = 0.4, H = 15,000 feet

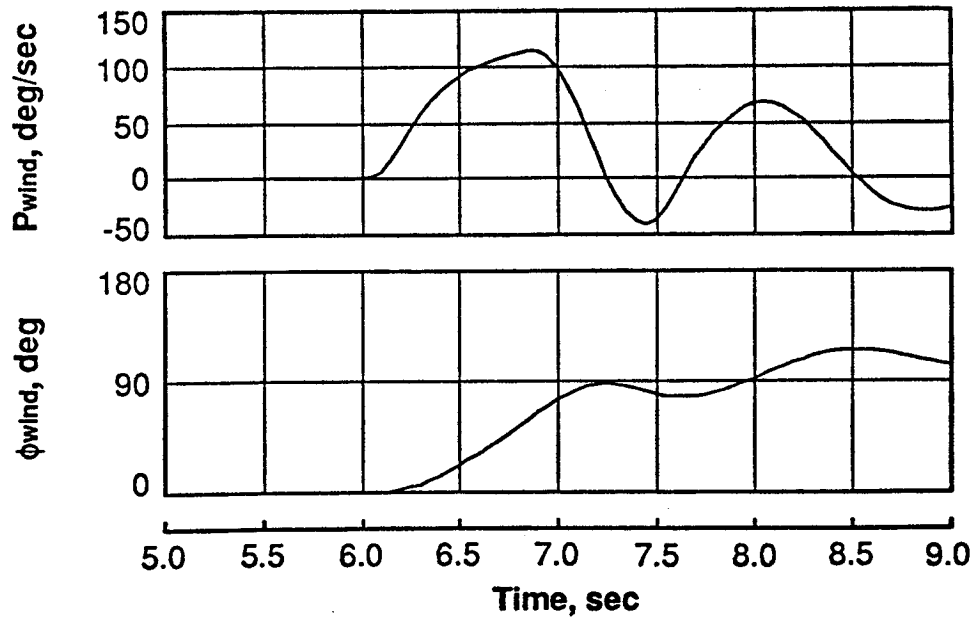

Figure 4.6 Generic F-18A Unsatisfactory Target Bank Angle Capture For The *90° Roll Angle Capture* Metric, H = 15,000 feet

4.3.3 180° Roll Angle Capture Metric

The T_{RC180} metric is tested by first trimming the aircraft to straight and level 1g flight. Lateral stick is then commanded to set the aircraft at the desired -90° bank angle. At time equals five seconds, sufficient longitudinal stick is applied to set the aircraft at the angle of attack specified for the test point. With the aircraft now banked -90° and at the desired angle of attack, the maneuver commences with the first application of lateral stick, which occurs at time equals seven seconds for all test cases. Full positive lateral stick is applied and held, then reversed to capture the +90° bank angle (Figure 4.7). Instead of using an algorithm like the one described in Section 4.3.2, bank angle capture criteria are used to for measuring T_{RC180}. The criteria are defined as (REF. 7, 38):

1) maximum overshoot: ± 3° after achieving the target bank angle

2) hold time: 2 seconds after achieving the target bank angle

For a 180° roll angle capture maneuver (ϕ_i = -90°, ϕ_f = +90°), the interpretation of the criteria above is that bank angle must first achieve +90°, and then remain there within a six degree band, $87° \leq \phi \leq 93°$, for two full seconds. The band is 3% of the total angular displacement of 180°. Figure 4.8 shows application of the criteria for a typical successful capture.

A modification of this criteria is required for bank angle responses which decrease monotonically after achieving the target bank angle. If after achieving the target bank angle, the response decays monotonically outside the six degree band before two seconds have elapsed, the time to capture is defined as

$$t_{capture} = t_{achieve\,\phi\,target} + 2 \text{ seconds} \qquad (4.2)$$

This assumption is justifiable in the case of monotonic bank angle decay because a real-time pilot in the loop should be able to keep the bank angle within the required six degree band. This is an

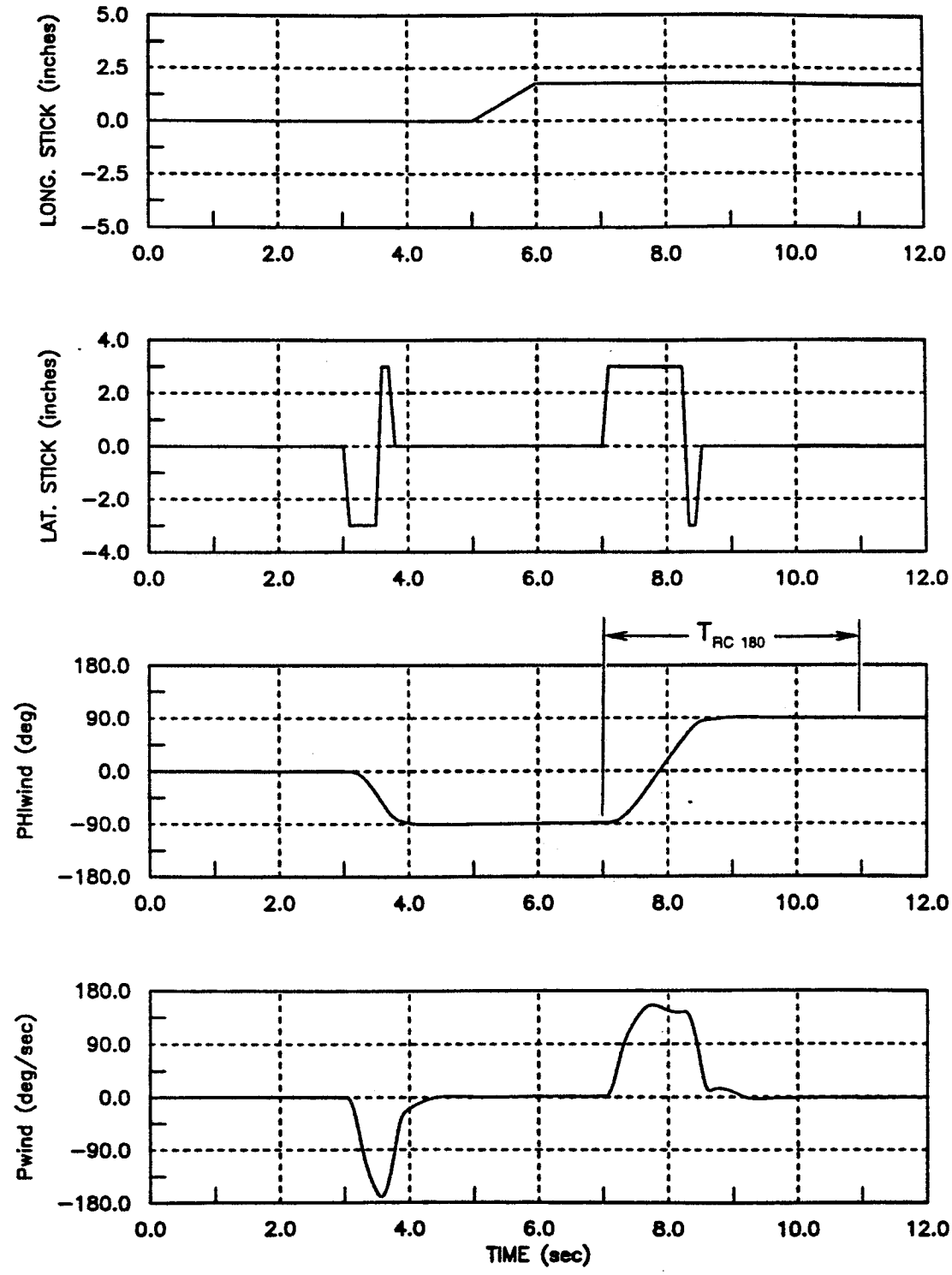

Figure 4.7 Typical Pilot Stick Input Commands And Data Extraction Points Used For Testing The *180° Roll Angle Capture* Metric

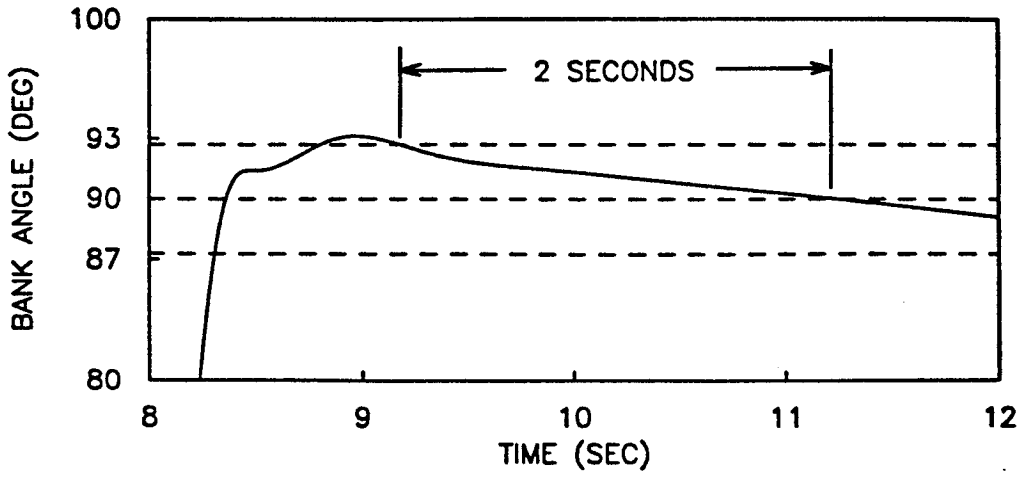

Figure 4.8 Application Of The Bank Angle Capture Criteria
For Testing The *180° Roll Angle Capture* Metric (REF. 7)

abstraction, but it is realistic.

Reference 25 proposes a slightly different set of capture criteria for this similar maneuver, defined as ± 10° of target bank angle held for one second. For a 180° roll angle capture maneuver this overshoot band is 11% of the total angular displacement. The band is relatively large to permit a pilot to easily capture the target bank angle, since the pilot must use the attitude direction indicator (ADI) to visually track bank angle during the maneuver instead of a dedicated display on the HUD. An advantage of using the ADI to track bank angle for this particular maneuver is that the pilot's wings level reference line is normal to the horizon reference line upon completion of a 90° bank angle capture. Using this assumption, the overshoot band might be reduced to 3% of the total angular displacement without causing the pilot undue difficulty.

The *90° and 180° roll angle capture* metrics, as with any closed loop piloted maneuver, are susceptible to deviations in pilot command inputs. A major problem in attempting to capture a target bank angle at even moderate angles of attack is that adverse sideslip increases to the point where the dihedral effect induces large roll rate oscillations. The use of non real-time simulation only

compounds the problem.

The generic F-18A simulation is used to assess the sensitivity of the lateral agility metrics. It is important to note that *these sensitivity results are specific to the generic F-18A **only**, and cannot be generalized to all fighter aircraft.* The intent here is simply to determine in a broad sense how sensitive the lateral agility metrics can be to pilot inputs, and to demonstrate one way in which an analysis of this type can be conducted. Since this analysis is simply intended to show typical behavior, the sensitivity tests are limited to a single altitude of 15,000 feet. The sensitivity of the *time through roll angle* metric is not analyzed since the pilot stick input command consists of a single maximum magnitude step which is held for the duration of the maneuver (Figure 4.1). The nominal sequence of pilot command inputs are defined here as those inputs which generate the best *roll angle capture* performance. If Figure 4.2 represents the nominal pilot command inputs for the *roll angle capture* metrics, then the actual pilot command input can deviate from the nominal inputs in five ways (REF. 3):

1) Aft stick position relaxed during the roll instead of being held constant. This deviation was prevalent during F-18A agility flight testing.

2) Less than full lateral stick is applied to initiate the roll.

3) Less than full opposite lateral stick is applied to arrest the roll.

4) Longitudinal and lateral stick inputs are applied at incorrect rates.

5) Full opposite lateral stick held too long before arresting the roll.

Deviations two and five are not tested. If less than full lateral stick is applied to initiate the roll, while the timing of all inputs is the same as the nominal case, as in number two above, the target bank angle is never achieved. The effect of a deviation like number five above is that the aircraft captures a bank angle greater than the target bank angle. Figure 4.5 represents the effect of this deviation using the

normalization algorithm of Section 4.3.2, and this devitation makes the capture criteria of Section 4.3.3 impractical to enforce. As a result, a sensitivity analysis is performed using deviations one, three, and four. The magnitudes of the introduced deviations is contained in Table 4.1.

Table 4.1 Errors And Magnitudes For Roll Angle Capture Metrics Sensitivity Analysis

Error	Magnitude
Aft Stick Position	Reduced 50%
Lateral Stick To Arrest Roll	Reduced 20%
Longitudinal-Lateral Stick Rates	Reduced 50%

4.4 CANDIDATE LATERAL AGILITY METRICS RESULTS

In this section results for the candidate lateral agility metrics are presented. Each metric is defined and then typical results are given.

4.4.1 Time Through 90° Roll Angle (T_{TR90}) (REF. 24, 27)

4.4.1.1 Definition

The time required to roll through a target bank angle of 90° at various angles of attack.

4.4.1.2 Discussion and Results

Results for the *time through 90° roll angle* metric (T_{TR90}) are presented in the form of plots of T_{TR90} versus average angle of attack for various Mach numbers. The altitude used for this investigation is 15,000 feet. Results for the generic F-5A, F-16A, and F-18A are provided in Figures 4.9 through 4.11. Figure 4.9 shows that the generic F-5A T_{TR90} values are a strong function of both

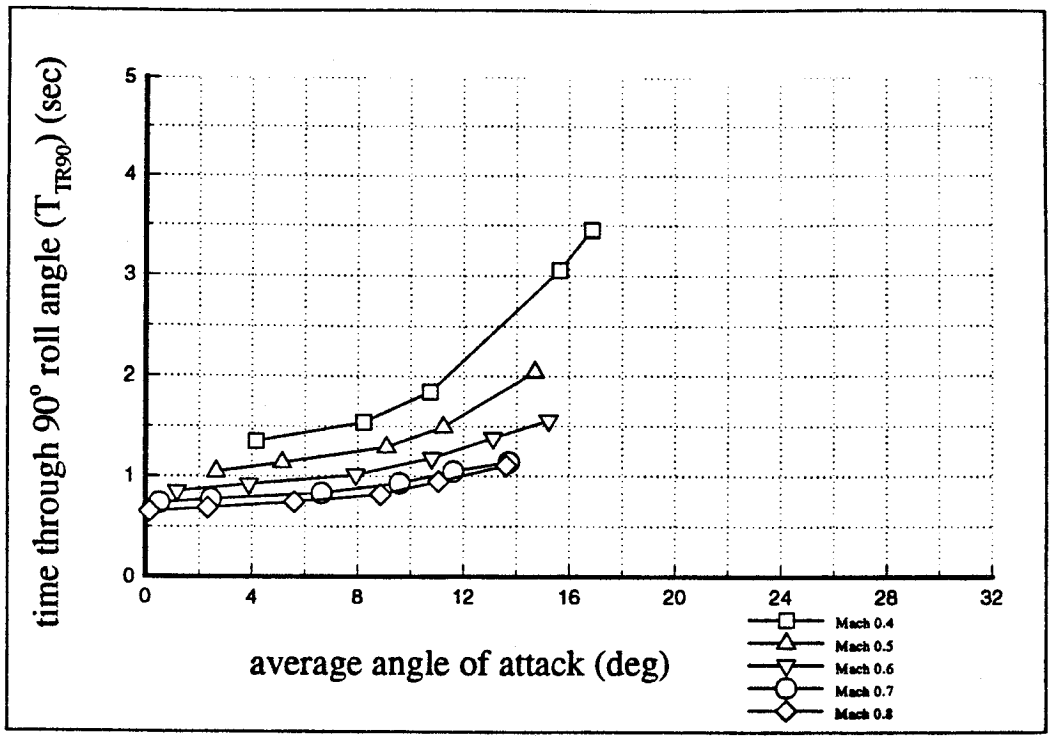

Figure 4.9 Generic F-5A *Time Through 90° Roll Angle* Metric Results, H = 15,000 feet

angle of attack and Mach number. This result is consistent for an aircraft which does not have a full authority FCS, since there is a marked disparity between T_{TR90} values at the lower Mach numbers and T_{TR90} values at the higher Mach numbers. The T_{TR90} values are increased significantly at the higher angles of attack at Mach equals 0.4.

The generic F-16A T_{TR90} results are in Figure 4.10. Unlike the generic F-5A, Figure 4.11 shows that this aircraft exhibits exceptional consistency across the range of both angles of attack and Mach numbers. This can be directly attributed to the full authority FCS. Although the generic F-16A can roll faster at the higher speeds, the FCS is designed to provide consistent flying qualities at all speeds. The utility of the predictable bank angle responses to a pilot engaged in WVR air-to-air combat is readily apparent. If desired, workload previously allocated to anticipating and adjusting vehicle response to variations in flight conditions may be devoted to combat.

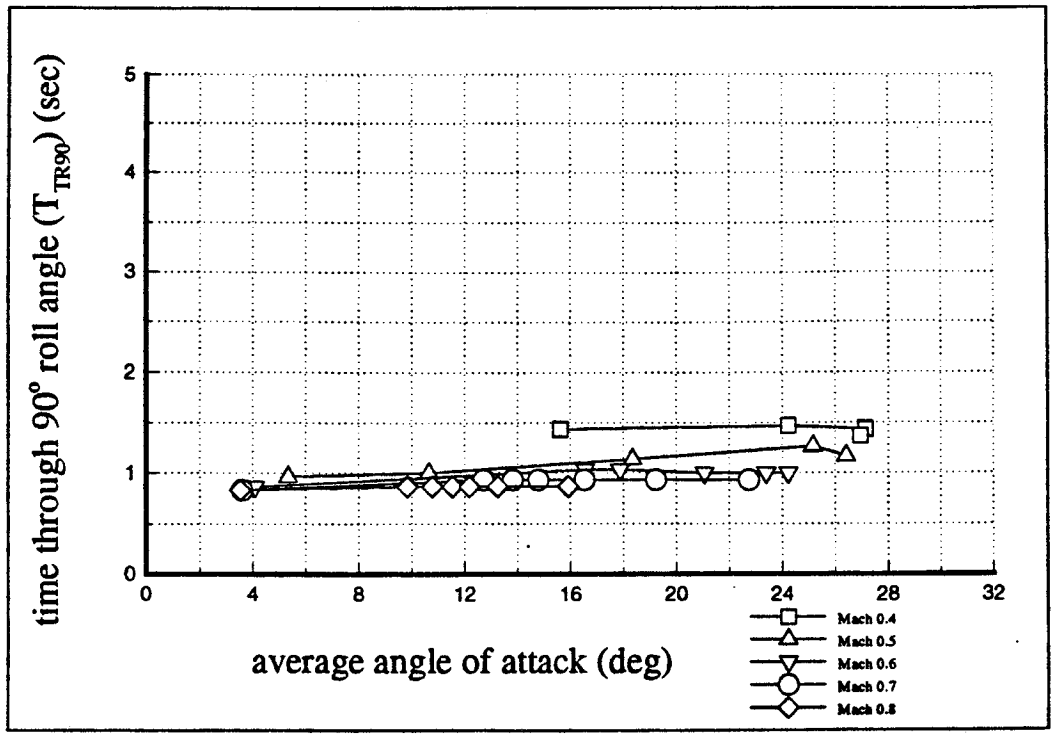

Figure 4.10 Generic F-16A *Time Through 90° Roll Angle* Metric Results, H = 15,000 feet

Figure 4.11 shows that values of T_{TR90} for the generic F-18A are also consistent across the Mach number range for angles of attack below approximately 15°. For angles of attack above 15°, T_{TR90} varies proportionally with angle of attack. Note also that a dependence on speed appears for angles of attack of 10° and above on this aircraft. At these flight conditions the surface deflection limits begin to limit the available roll control power. The deflection limits are reached at the lowest angle of attack at Mach equals 0.4, and at higher angles of attack at Mach equals 0.5 and 0.6. The maximum angles of attack tested at Mach equals 0.7 and 0.8 are limited by the normal load factor limit of the airplane. As is the case for the generic F-16A, the FCS is seen to have a marked effect on the agility of this aircraft also.

Although it is not mandatory for obtaining values of T_{TR90}, it is instructive to examine the behavior of normal load factor and maximum sideslip angle during a maneuver of this type The

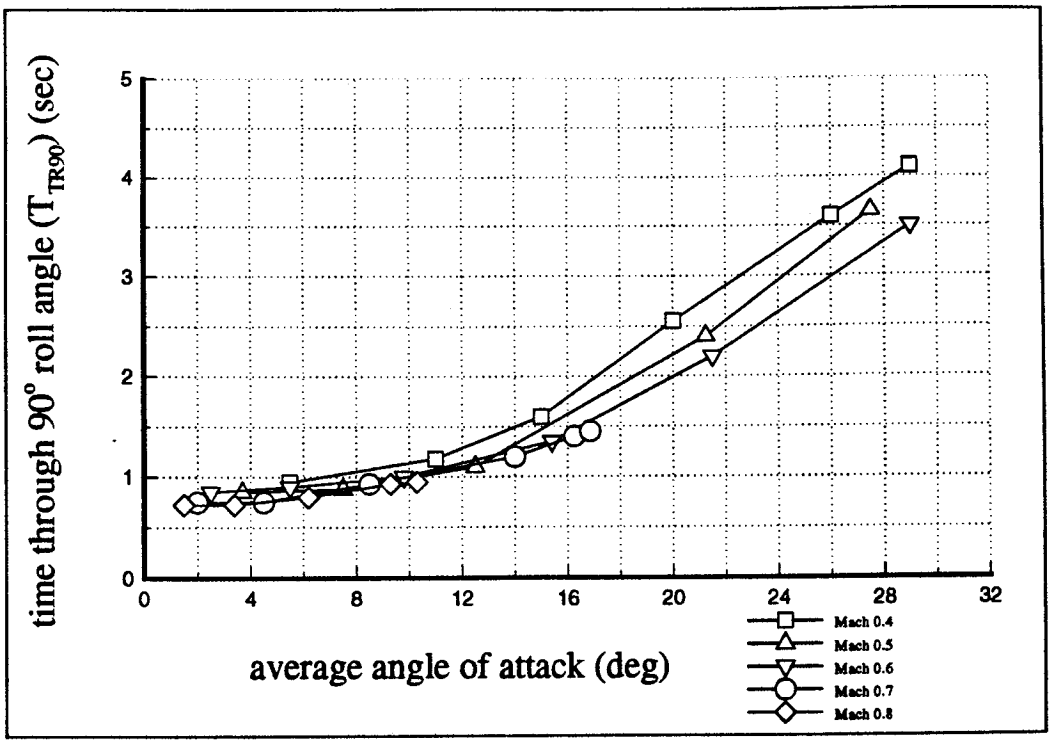

Figure 4.11 Generic F-18A *Time Through 90° Roll Angle* Metric Results, H = 15,000 feet

generic F-18A is arbitrarily selected for this part of the analysis. Figure 4.12 shows the generic F-18A average normal load factor during the T_{TR90} maneuver. The data is obtained from the same test cases used to construct Figure 4.11. A plot of this type can be useful to pilots in situations where normal load factor is of more concern than angle of attack. The lines for the lower speeds approach the vertical because the average angles of attack of these maneuvers are near the angle of attack for maximum lift. As the average angle of attack of the maneuver increases above 15°, the amount of additional lift decreases while the time to roll through ϕ_{wind} equals 90° increases sharply.

Figure 4.13 displays the maximum value of sideslip angle generated by the generic F-18A during the rolls through ϕ_{wind} equals 90°. This data is also obtained from the same test cases used to construct Figure 4.11. It is desirable that sideslip angle be zero or at least a minimum during maneuvers like the T_{TR90} so that the roll (not the turn!) is coordinated (Appendix C). For the generic

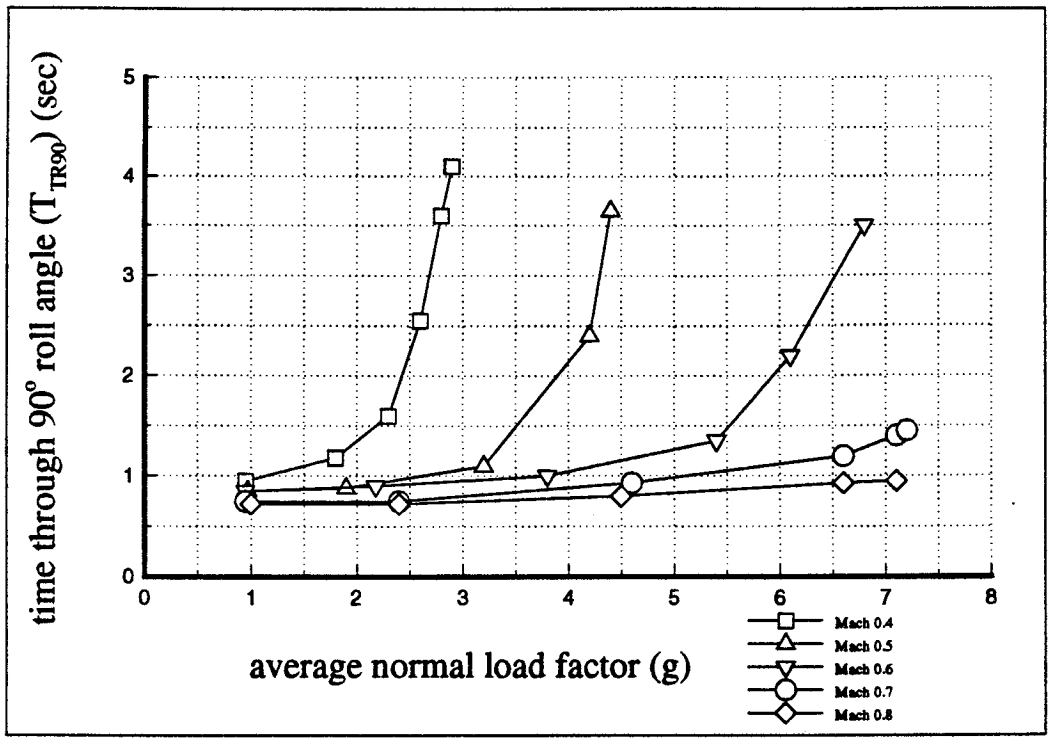

Figure 4.12 Generic F-18A Average Normal Load Factor During A *Time Through 90° Roll Angle* Maneuver, H = 15,000 feet

F-18A, the largest sideslip angles are generated during the rolls at angles of attack between 10° and 20° for all of the Mach numbers tested. The shape of the curves is the result of the generic F-18A FCS scheduling of the roll command gain and roll command limiter. The fact that sideslip angles of six to eight degrees are allowed by the FCS might indicate that it was not originally designed to coordinate abrupt, full-stick rolls.

4.4.1.3 Time Through 90° Roll Angle Sensitivity

The sensitivity of the *time through 90° roll angle* metric is not analyzed since the pilot stick input command consists of a single maximum magnitude step which is held for the duration of the maneuver (Figure 4.1).

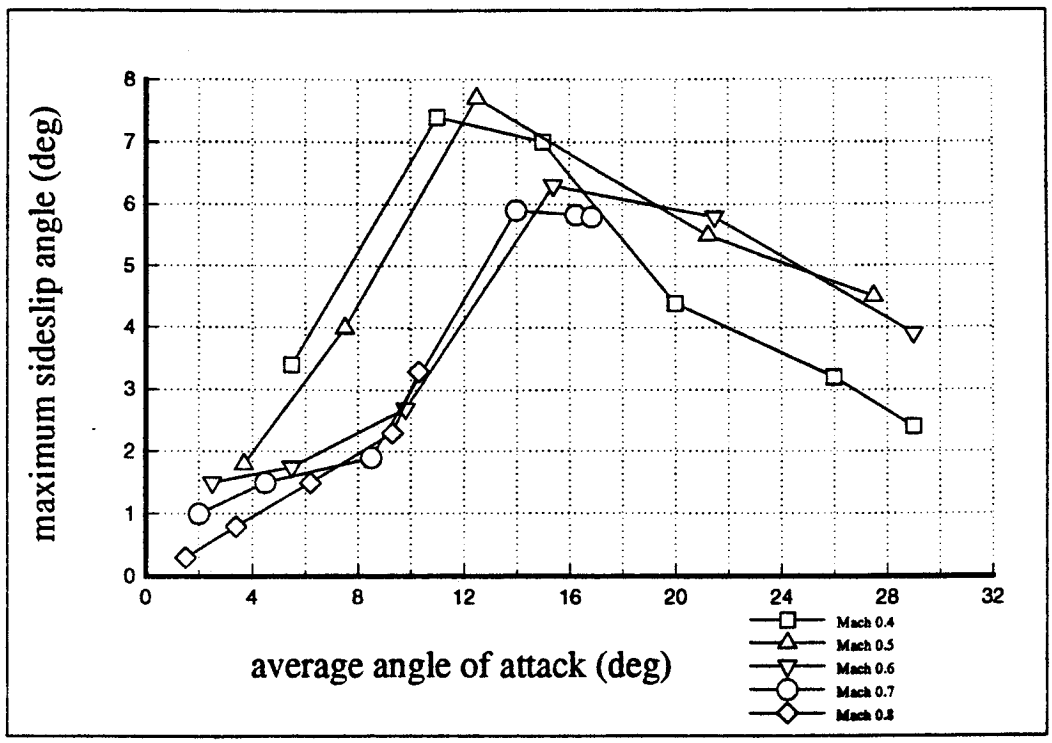

Figure 4.13 Generic F-18A Maximum Sideslip Angle During A *Time Through 90° Roll Angle* Maneuver, H = 15,000 feet

4.4.1.4 Summary

The T_{TR90} metric appears to provide useful insight into the transient performance aspect of lateral agility. It is easy to test, and is repeatable. Since this metric only passes through and does not "capture" a target bank angle, the controllability aspect of arresting the roll after the 90° bank angle change has been achieved is not addressed. Examining the average normal load factor and maximum sideslip angle behavior during the maneuver is useful in determining the nature of cross-axis responses. When the effect of flying qualities during a maneuver such as this is desired, the 90° or 180° *roll angle capture* metric discussed in the next two subsections should be used.

4.4.2 90° Roll Angle Capture (T_{RC90}) (REF. 18, 25)

4.4.2.1 Definition

The time required to roll and capture $\Delta\phi = 90°$ at various angles of attack.

4.4.2.2 Discussion and Typical Results

The *90° roll angle capture* metric (T_{RC90}) is a measure of an aircraft's ability to transition and capture a 90° roll angle. To evaluate this metric, the aircraft is exercised with a two step lateral stick command, i.e. roll left command followed by a roll right command. The command input time history uses the normalization algorithm described in Section 4.3.2. Figure 4.14 shows that the T_{RC90} results for the generic F-5A are similar to the T_{TR90} results for this aircraft in Figure 4.9. The T_{RC90} metric is largely a function of angle of attack, and higher Mach numbers result in slightly lower values.

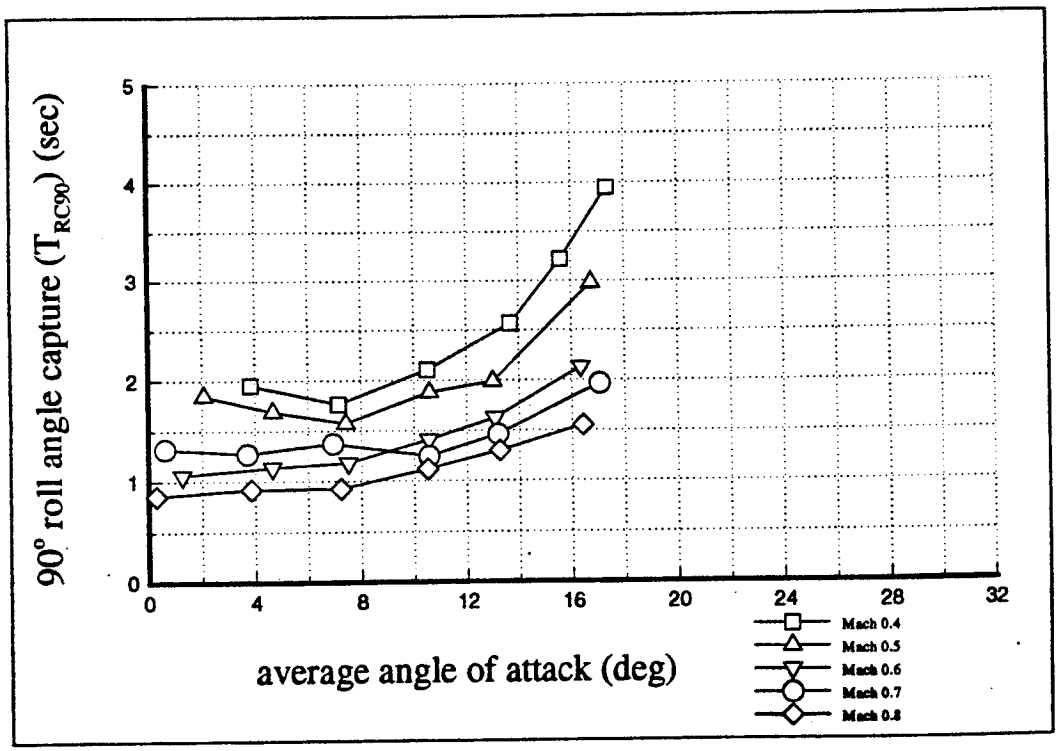

Figure 4.14 Generic F-5A *90° Roll Angle Capture* Metric Results, H = 15,000 Feet

The results for angles of attack above 10° are not very accurate because of the difficulty in capturing and holding a target bank angle using only step inputs. The sideslip angle that is generated by kinematic coupling causes roll rate oscillations which prevent a good roll angle capture. Damping these oscillations in roll rate with additional stick inputs can be extremely difficult, and is probably beyond the scope of this unpiloted simulation study.

Figure 4.15 contains the generic F-16A T_{RC90} values. There is a slight dependency on speed as the values for Mach equals 0.4 and 0.5 are distinct from those at Mach equals 0.6 through 0.8. Note also that a variation in T_{RC90} with angle of attack exists for the lower Mach numbers. This is attributed to the reduction in roll control power available at the lower Mach numbers to **arrest** the roll rate and capture the target bank angle. Note that a plateau in T_{RC90} values is reached at approximately 23° angle of attack for all Mach numbers.

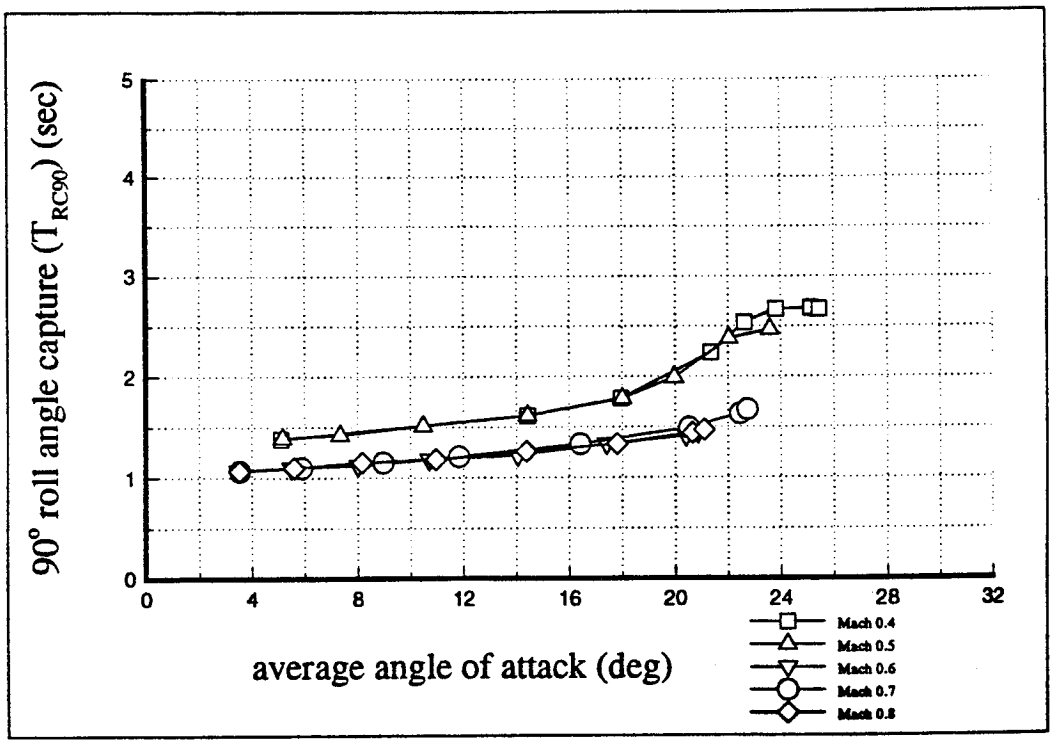

Figure 4.15 Generic F-16A *90° Roll Angle Capture* Metric Results, H = 15,000 Feet

The T_{RC90} results for the generic F-18A in Figure 4.16 are almost identical to the T_{TR90} results for this aircraft in Figure 4.11. Once again, the influence of the FCS in providing a nearly uniform roll capability across the low to intermediate angle of attack range can be seen. Mach number has an effect on the values of T_{RC90} only for the Mach equals 0.4 test points, and even this effect is small. Like the generic F-16A, the FCS on the generic F-18A has a definite impact on the lateral agility of the entire vehicle.

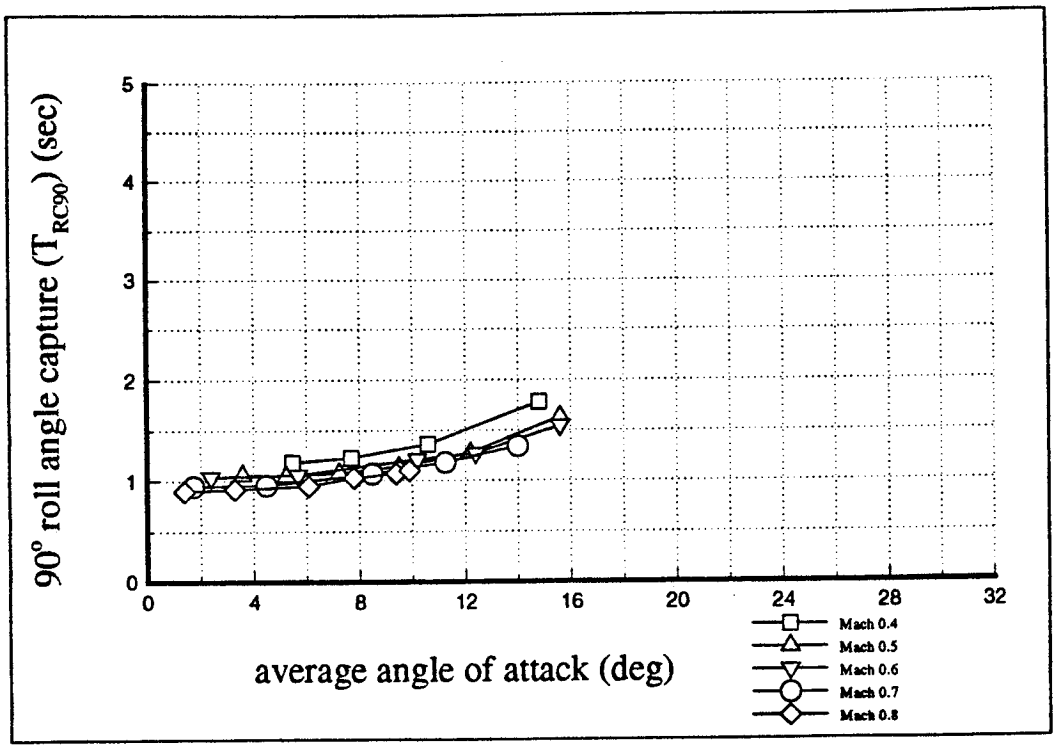

Figure 4.16 Generic F-18A *90° Roll Angle Capture* Metric Results, H = 15,000 Feet

4.4.2.3 90° Roll Angle Capture Sensitivity

The sensitivity of the *90° roll angle capture* metric to deviations in pilot stick input commands is shown in Figure 4.17. All test cases for the T_{RC90} sensitivity analysis use the normalization algorithm of Section 4.3.2. Since Reference 3 indicates that there is little variation in T_{RC90} sensitivity

results with respect to Mach number, the sensitivities presented here are limited to a single Mach number of 0.7. All time points for the deviations in pilot stick input commands listed in Table 4.1 are identical to the nominal generic F-18A inputs.

The first error introduced is the relaxed aft longitudinal stick position. Aft stick position required to maintain the required normal load factor is held until the application of full opposite lateral stick used to arrest the roll. At this point, aft longitudinal stick is ramped down to 50% of the nominal value, at which point it remains constant through capture. Figure 4.17 indicates that this input error produces deviations from the nominal generic F-18A T_{RC90} values of less than 2%. Closer inspection of the simulation results show that peak adverse sideslip occurs early in the roll before the aft stick command is reduced. As a result, the forward stick motion does little to speed the roll

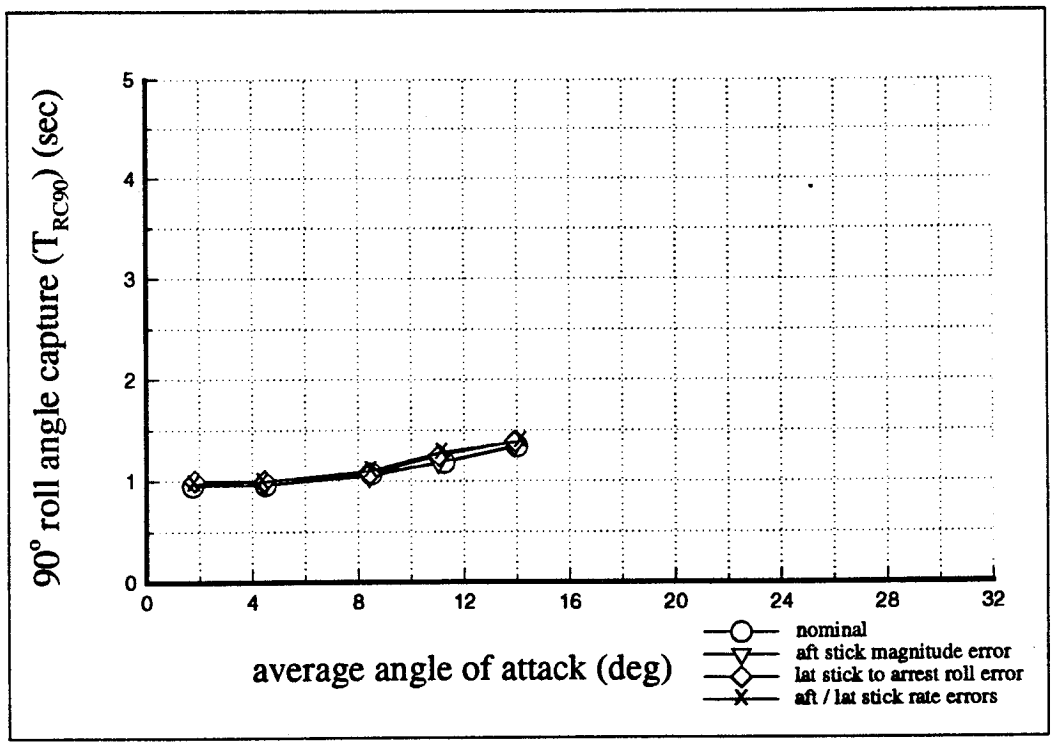

Figure 4.17 Generic F-18A *90° Roll Angle Capture* Sensitivity, H = 15,000 Feet

response even though angle of attack is reduced during the last half of the maneuver.

The second deviation, reduced lateral stick to arrest the roll, is introduced by simply reducing lateral stick magnitude to 20% of the maximum deflection of ± 3 inches for the generic F-18A. Again, all time points are the same as the nominal case. As expected, this deviation resulted in a captured bank angle greater than the nominal 90°. Over the range of angles of attack, the captured bank angle exceeded 90° by an average of 13°. Because the maximum roll rates experienced here are the same as in the nominal cases (since the initial roll commands are the same), the normalization algorithm accurately corrects for the error in final bank angle. The calculated T_{RC90} values for all test points varied from the nominal values by less than 2%.

A 50% reduction in all lateral stick rates, both ramping in and ramping out, constitutes the third error. The initiation time points for all of the pilot stick input commands remains the same as for the nominal case. While this deviation results in the captured bank angle being smaller than the nominal target bank angle of 90°, the normalization algorithm largely corrects for this difference as it does for both of the other deviations described earlier in this section. Specifically, reducing the lateral stick rate by 50% for each of the test cases changes the values of the T_{RC90} by an average of only 3.%.

4.4.2.4 Summary

The *90° roll angle capture* metric is easy to test for angles of attack below approximately 10°. Compared to the *time through 90° roll angle* metric, the *90° roll angle capture* metric provides limited but useful information about the controllability aspect of capturing the target bank angle. The iterative normalization algorithm works well for unmanned flight simulation programs, provided the sideslip angles due to roll rate oscillations are small. If the sideslip angles are large, then the bank angle

capture criteria of Section 4.3.3 might be used.

The T_{RC90} metric is not overly sensitive to deviations in pilot stick input commands. Provided the roll is initiated with full lateral stick deflection, the normalization algorithm successfully normalizes the maneuver to a 90° bank angle change and thereby compensates for deviations introduced by the pilot.

4.4.3 **180° Roll Angle Capture** (REF. 18, 25)

4.4.3.1 Definition

The time required to roll and capture $\Delta\phi = 180°$ at various angles of attack.

4.4.3.2 Discussion and Typical Results

The *180° roll angle capture* metric (T_{RC180}) is analogous to the *90° roll angle capture*, except that the roll angle displacement is 180°. It is tested in this report using the testing technique outlined in Section 4.3.3, e.g. by first rolling the aircraft to a 90° bank angle, pulling to the desired angle of attack for the test point, and then rolling to the opposite 90° bank holding aft stick constant. The bank angle capture criteria described in that section is used for determining capture.

Figure 4.18 shows T_{RC180} for the generic F-5A and generic F-18A over a range of angles of attack at Mach equals 0.7 at 15,000 feet. Results are not presented for the generic F-16A as this simulation was not available at the time T_{RC180} was investigated. The generic F-18A is able to accomplish the maneuver over a relatively wide range of angles of attack, while the generic F-5A cannot above an angle of attack of approximately seven degrees. The reason for this apparent anomaly is indicated in Figure 4.19, which is a plot of T_{RC180} versus normal load factor. The generic F-5A is below corner speed at Mach equals 0.7 at 15,000 feet, so normal load factor is limited by available maximum lift at this flight condition to only 4g. Even during a maximum pitch up

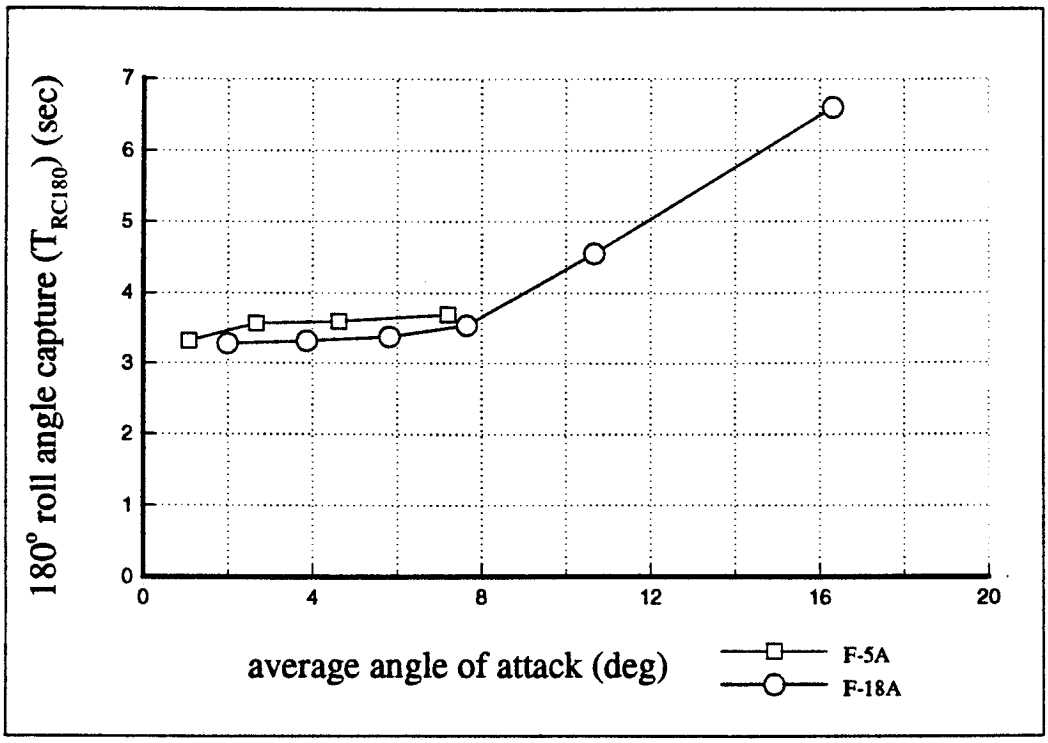

Figure 4.18 Generic F-5A And Generic F-18A
180° Roll Angle Capture Metric Results, H = 15,000 Feet

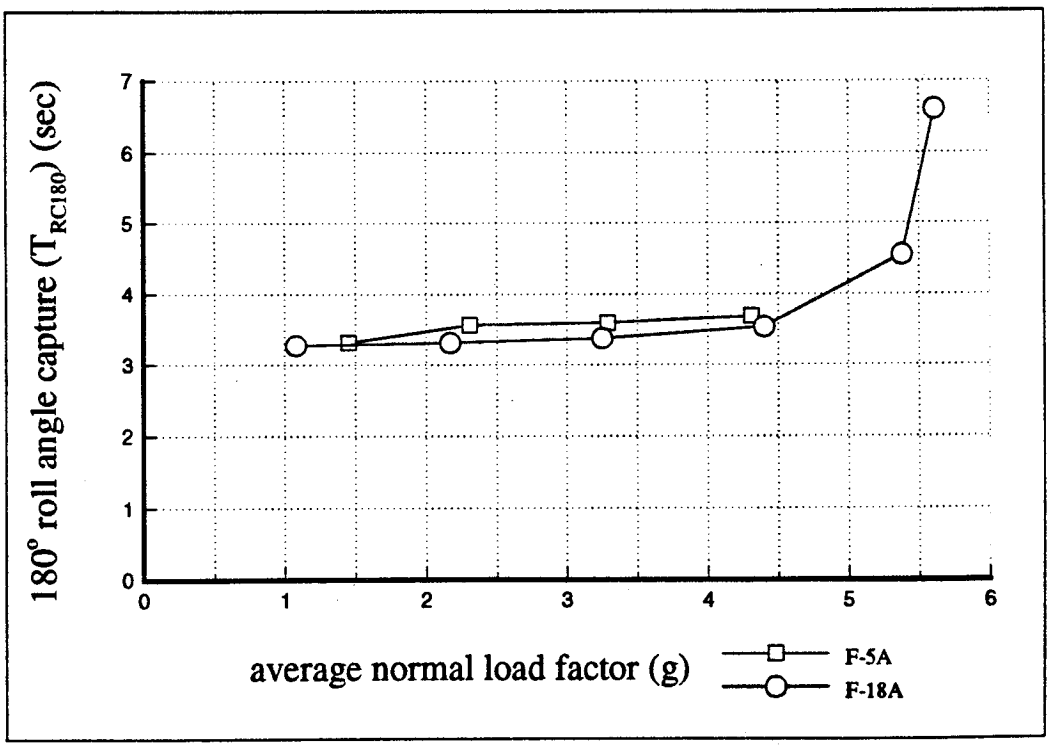

Figure 4.19 Generic F-5A And Generic F-18A Average Normal Load Factor During A *180° Roll Angle Capture* Maneuver, H = 15,000 Feet

maneuver from wings level flight, 4.7g is the maximum normal load factor that the generic F-5A can generate, and even then only momentarily. Simulation results in Reference 38 clearly demonstrate this behavior, and the F-5A performance data in Reference 39 confirms it. The generic F-18A is not as severely limited in normal load factor, since it is very near corner speed at this particular flight condition. However, it is only capable of generating a normal load factor of 6g.

Time histories for the generic F-5A and generic F-18A 7° average angle of attack test point are contained in Figure 4.20. The absence of a throttle ramp input is the only significant difference in pilot command inputs between the two aircraft for this test point. The bank angle responses in Figure 4.20 show that the generic F-5A completes the 180° transition by achieving the 90° bank angle at about the same time as the generic F-18A, even though the generic F-18A is experiencing high-g roll rate limiting. The generic F-5A also appears to be much better damped in pitch during this maneuver, as both normal load factor and angle of attack are only slightly oscillatory. Note that the generic F-18A angle of attack required to sustain 4g is 18% greater than the same angle of attack required for the generic F-5A. The corresponding sustained turn rates for both aircraft are 11 degrees per second. With regard to sideslip angle, the generic F-5A is again well damped, but hits a slightly greater peak value than the generic F-18A. The maximum lateral acceleration at the pilot's head for the generic F-5A is 1.1g, and that for the generic F-18A 1.5g.

The complete trajectory of the generic F-18A from trim, to maneuver initiation, to capture for the 7° average angle of attack test point is displayed in Figure 4.21. Note that Figure 4.21 indicates the trajectory of the center of mass only, and therefore does not depict angular displacements such as rolling or yawing. The projection of the trajectory in the XZ plane shows that the generic F-18A begins losing altitude before the maneuver is initiated. At the initiation point, the sustained turn rate is 10 degrees per second at a crossrange displacement of 211 feet. The target bank angle is captured with the aircraft 8,300 feet downrange and 435 feet below the test altitude. The XY projection of the

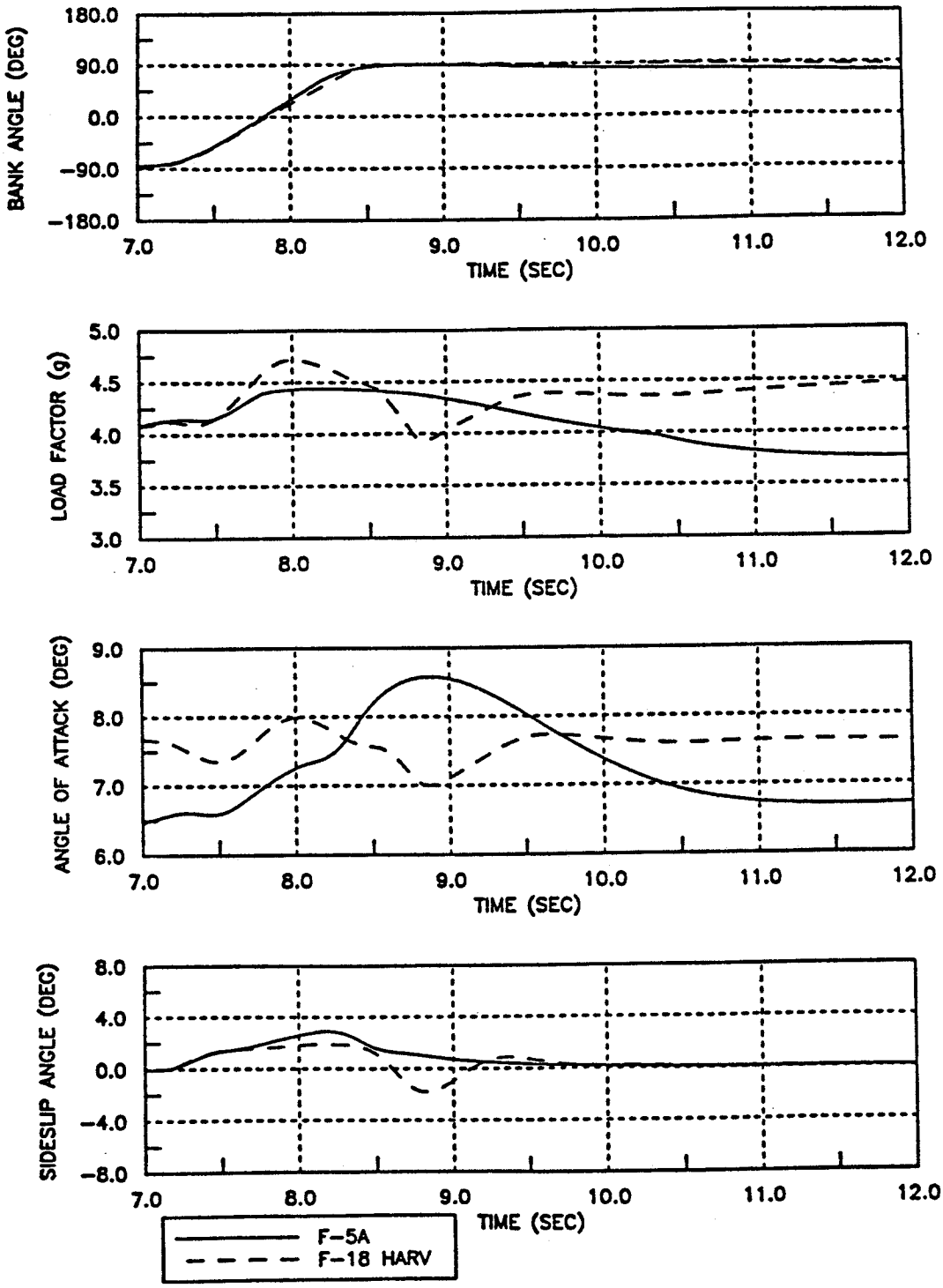

Figure 4.20 Comparison Of Generic F-5A And Generic F-18A Parameters During A *180° Roll Angle Capture*, Average Angle Of Attack 7°, 0.7/15k (REF. 7)

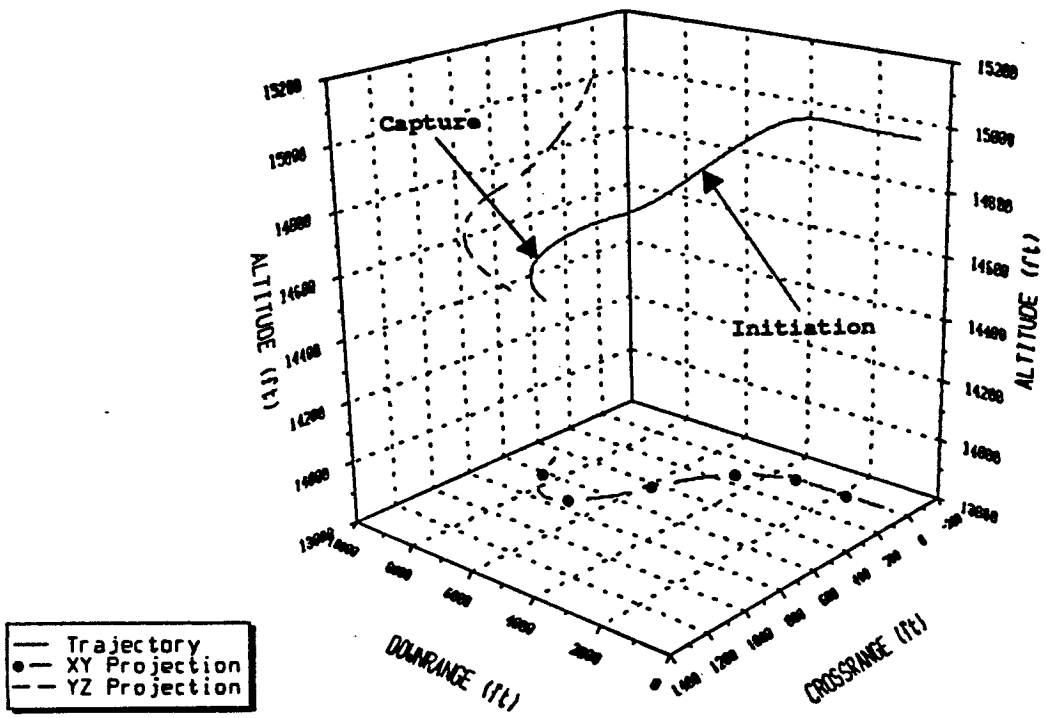

Figure 4.21 Generic F-18A *180° Roll Angle Capture*
Trajectory, Average Angle Of Attack 7°, 0.7/15k (REF. 7)

trajectory describes a turn reversal with its characteristic "S" shape.

It was shown in Section 4.4.1 and 4.4.2 that the FCS, or in the case of the generic F-5A the lack of a FCS, tends to have a marked effect on the lateral agility of a given aircraft. This result is easier to perceive for the T_{RC180} metric by examining time histories of generic F-18A aerodynamic parameters (Figure 4.22) and control surface parameters (Figure 4.23) corresponding to the 16° average angle of attack test point of Figure 4.18. Figure 4.22 shows that the bank angle response for this test point is sluggish, and demonstrates difficulty in sustaining bank angle rate at time equals 7.8 seconds. A roll reversal does not occur, but bank angle becomes oscillatory as the lateral stick command is taken out at time equals nine seconds, before damping out. The resulting motions make the 90° bank angle difficult to capture. Normal load factor drops to 4g by the conclusion of the maneuver, and angle of attack is divergent. This is the only test case where the 90° bank angle is successfully

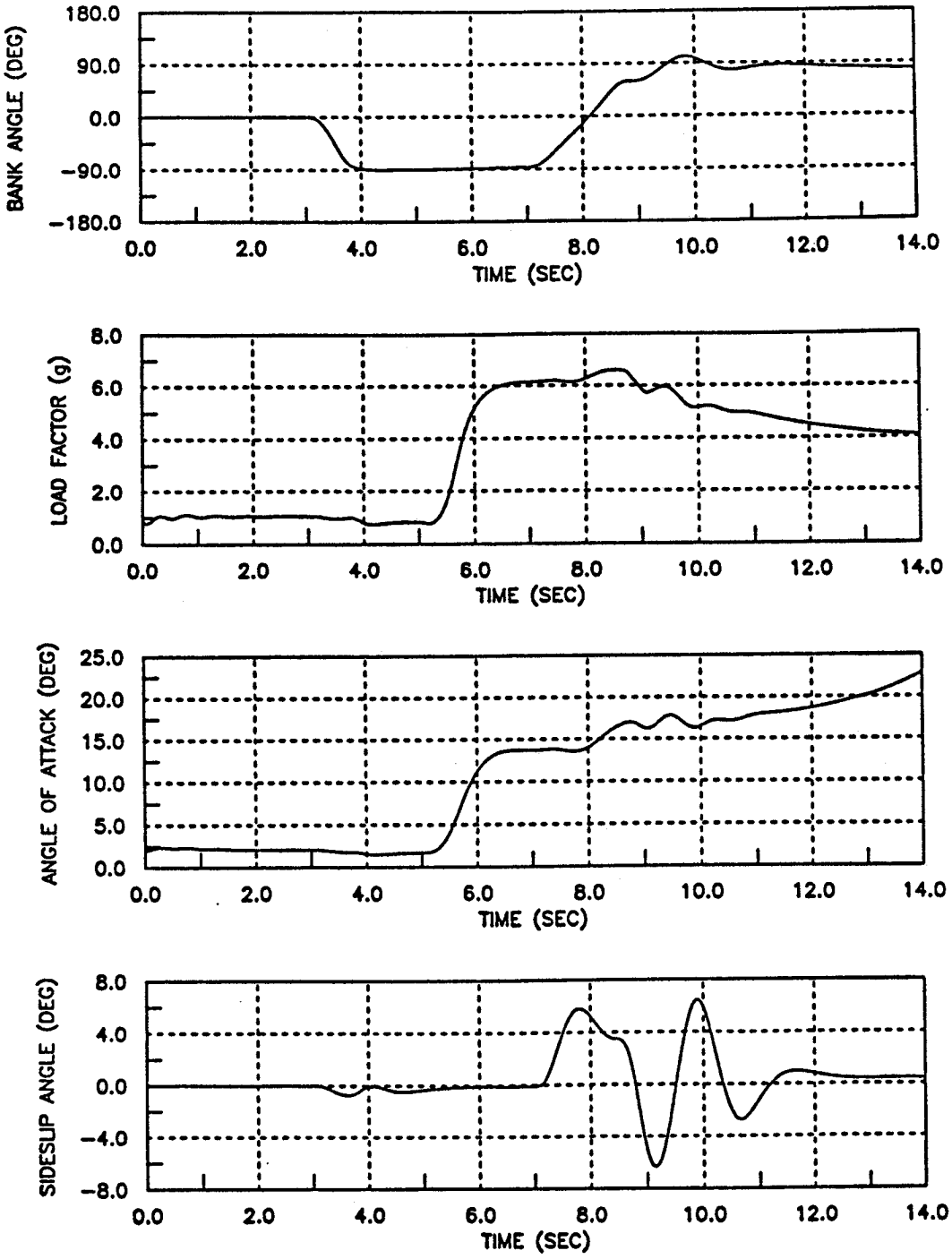

Figure 4.22 Generic F-18A Parameters During A *180° Roll Angle Capture*, Average Angle Of Attack 16°, 0.7/15k (REF. 7)

captured but the angle of attack constraint is violated. Sideslip angle builds to its largest peak values for this test point, achieving seven degrees both adverse and proverse. This exceeds both maximum sideslip test constraints. The sideslip angle time history shows that the Dutch Roll mode has been excited with an equivalent natural frequency of approximately 3.5 radians per second. This natural frequency meets the applicable Mil-Standard requirement in Reference 40. The equivalent Dutch Roll damping ratio of approximately 0.28 does not. The resultant sideslip oscillations drive the roll oscillations at the end of the maneuver, and the capture criteria is not satisfied. The effect of these oscillations is that the lateral stick command must be reversed at a point where bank angle is approximately 30° short of the target bank angle. While direct comparisons cannot be made with the sideslip excursion requirements in full stick rolls in paragraph 4.6.2 of Reference 40, and the roll rate oscillation requirements of Paragraph 4.5.1.4, both appear to be violated. Although the aircraft can successfully complete the task of capturing the target bank angle, the total flying qualities seem to be less than desirable. This result is in agreement with a similar result in Reference 34.

In Figure 4.23, the generic F-18A FCS is seen to use the stabilators, trailing edge flaps, and ailerons in unison to generate and coordinate the required roll forces. The trailing edge flaps are not used at all during at this test point, and both stabilators and ailerons are held at their peak values longer than in the test points at lower normal load factors. Not unexpectedly, all surfaces experience some rate limiting during the abrupt transient portions of the pilot command inputs. The rudders are both position limited at their maximum deflection of 30° at time equals 7.8 seconds, and rate limited thereafter at the maximum rate of 56 degrees per second.

All of the surfaces on the generic F-18A experience rate limiting to some extent while performing the T_{RC180} maneuver. Rate limiting occurs not only at the test points at high angles of attack and elevated normal load factors, but at all of the test points. However, only the rate limiting of the rudders significantly affect the performance of the maneuver and the value of T_{RC180}. During

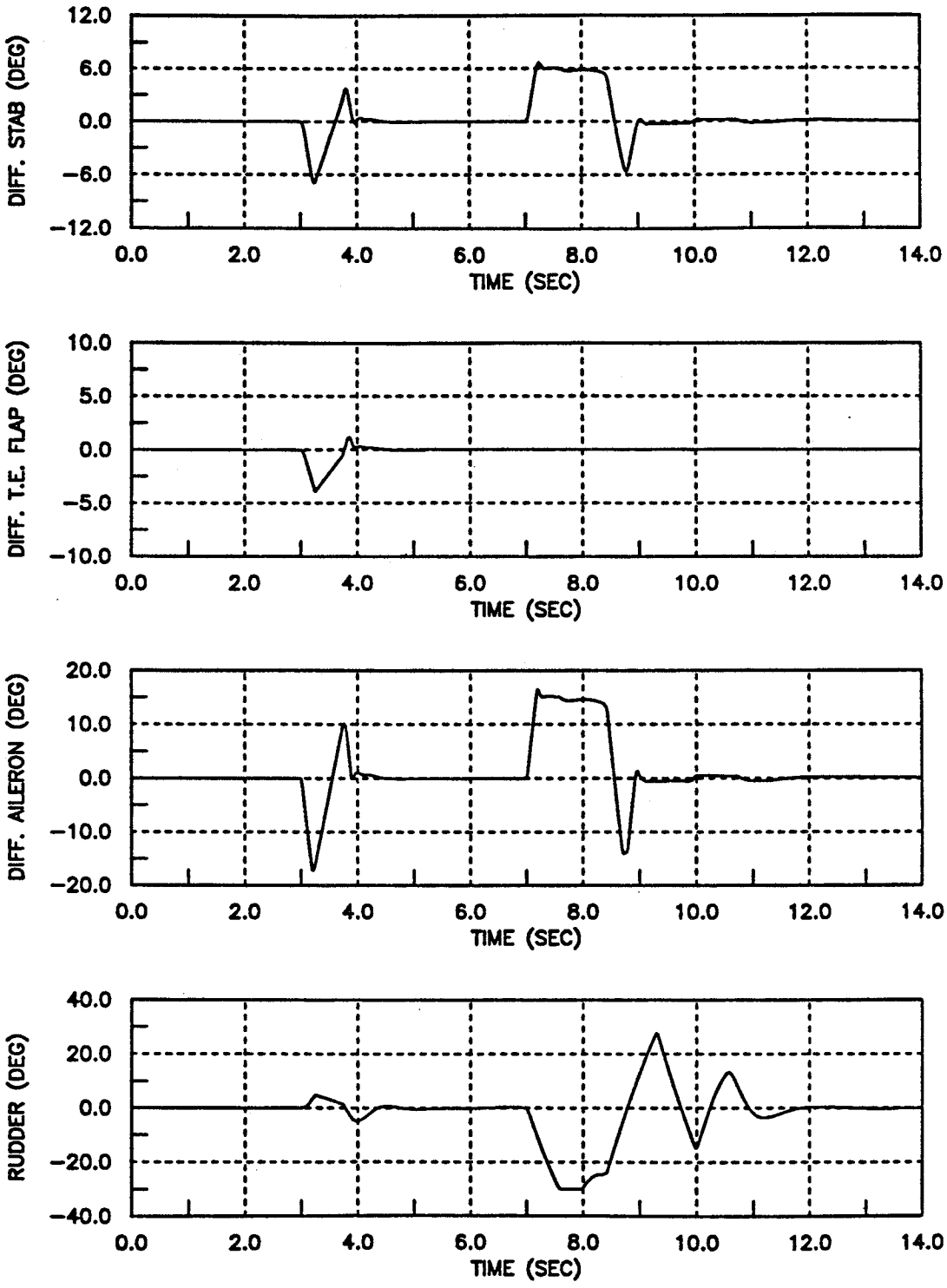

Figure 4.23 Generic F-18A Control Surface Activity During A *180° Roll Angle Capture*, Average Angle Of Attack 16°, 0.7/15k (REF. 7)

this investigation, this effect only occurs at the 16° average angle of attack test point. Though not commanded by the pilot, the rudders are used extensively by the FCS of the generic F-18A. Rather than using the rudder to drive sideslip to zero, the FCS instead tracks lateral acceleration because of the N_Y feedback system used for turn coordination. While this architecture ensures that lateral accelerations remain within tolerable levels, it does not eliminate all sideslip during uncoordinated maneuvers, and may not be utilizing all of the roll capability in the airframe. This is probably a result of lateral agility, i.e. rolling at high angle of attack, not being a stringent requirement during the design of the F-18A flight control system. It is not a matter of concern when rolling at low normal load factors, but it is at elevated normal load factors and high angles of attack where roll control power decreases and adverse yaw can become large.

Although the T_{RC180} metric is normally measured without any rudder inputs from the pilot, Reference 38 investigated the utility of these inputs to enhance performance of the maneuver. Two different pilot rudder command input schemes were used. The first scheme tracked sideslip and used the rudder to generate an opposing yawing moment which reduces the buildup of adverse yaw. The presumed benefit of this scheme is that the aircraft is able to perform the maneuver in a more coordinated fashion. The pilot rudder commands for this scheme consist of a series of doublets. The second scheme used the rudder to generate and maintain a large proverse yawing moment. Provided that sufficient rudder control power is available, this has the anticipated effect of inhibiting the buildup of adverse yaw for at least a short time.

Reference 38 concluded that no practical advantage in improving T_{RC180} is to be gained from using pilot rudder command inputs. The pilot rudder command inputs are not pilot friendly, as the inputs are of short duration and perturb the aircraft sufficiently as to require additional pilot command input compensation. The only observed benefit of using the rudders in this manner was a reduction in sideslip angle and lateral accelerations. No significant increase in bank angle rate was achieved

by applying either of these pilot rudder command schemes, and a bank angle response which satisfied the capture criteria of Section 4.3.3 could not be generated. Any advantages which pilot rudder command inputs offer toward improvement in the performance of the maneuver must be weighed against the possibility that i) these inputs may be difficult or awkward for the pilot to execute; and ii) they are likely excessive in terms of additional pilot workload. Reference 26 demonstrated that even an existing FCS could be modified to relieve the pilot of this burden and improve lateral agility.

4.4.3.3 180° Roll Angle Capture Sensitivity

The sensitivity of the *180° roll angle capture* metric to deviations in pilot stick input commands is shown in Figure 4.24. The sensitivities presented here are for a Mach number of 0.7, and an altitude of 15,000 feet. All time points for the deviations in pilot stick input commands listed in Table 4.1 are identical to the nominal generic F-18A inputs. The T_{RC180} metric is relatively insensitive to 50% reductions in aft stick position during the capture portion of the maneuver. The only significant differences occur at average angles of attack of five degrees and 16 degrees. The 0.8 second difference in time to capture at five degrees compared to the nominal is attributable to transients which perturb the response to just outside the ± 3° error band. Both the nominal and aft stick error responses achieve the 90° bank angle at the same time, but the latter introduces angle of attack transients due to a somewhat sharp 0.5g reduction in normal load factor. The nominal response for the five degree test point lies at the extreme upper limit of the error band. Introduction of the transient pushes the response 1.5° outside the upper limit of the error band. As a result, the time for the oscillation to decay into the range of the error band increases the capture time. Angle of attack transients do not alter the nominal four degree response, because of the greater inherent damping than the nominal five degree response. The nominal eight degree response is already oscillatory, and thus

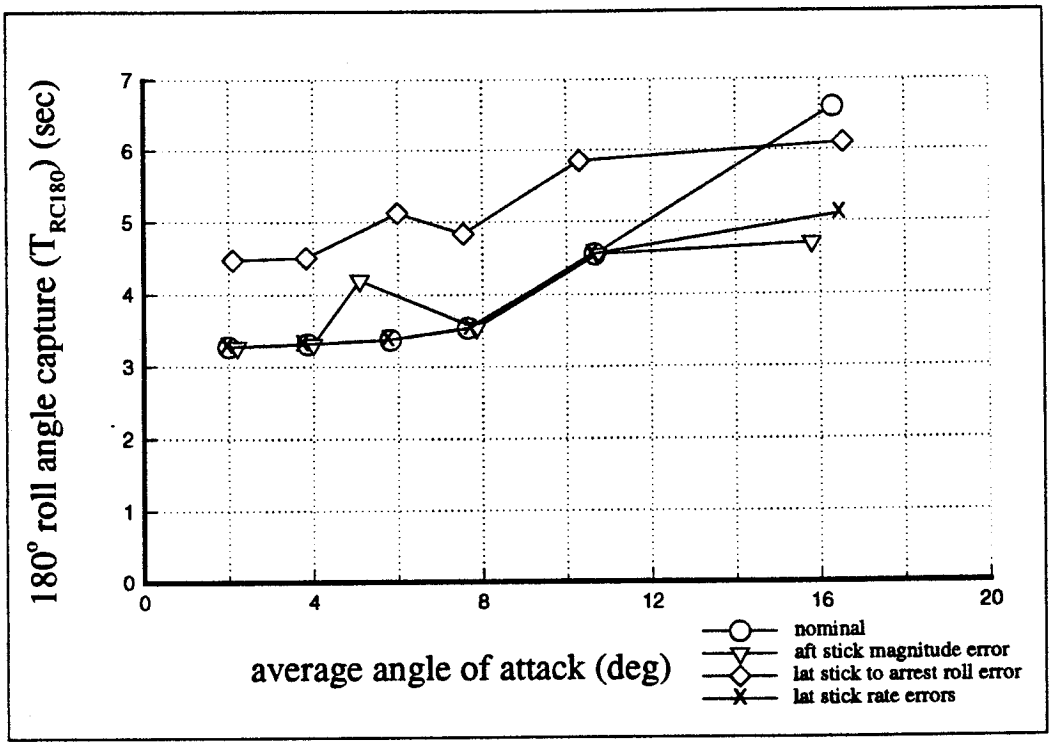

Figure 4.24 Generic F-18A *180° Roll Angle Capture* Sensitivity, Mach = 0.7, H = 15000 feet

not overly sensitive to small transients. The 28.8% error for the 16 degree test case is attributable to an increase in roll rate caused by a reduction in normal load factor of 3g. Reducing normal load factor by this amount generates a bank angle response which does not overshoot and is nonoscillatory, significantly reducing the time to capture.

Figure 4.24 indicates that the T_{RC180} metric is sensitive to errors from the application of less than maximum deflections of the lateral stick to arrest roll rate and capture the target bank angle. This is to be expected since roll rate is not arrested as quickly as it would be by application of maximum lateral stick. Averaged over all six test points, the error is a significant 32.9%. At first glance the 16 degree test point appears to be an anomaly; it is however consistent since this test point is characterized by a lightly damped oscillatory response. Reducing lateral stick magnitude during capture as is done in the error test case does not perturb bank angle response as much as in the

nominal case. Although the maximum bank angle achieved is the same in both cases at 16 degrees, the error response is more damped and requires less time to satisfy the capture criterion. As with the aft stick error cases, the only seemingly inconsistent trends occur in the higher angle of attack range.

Errors in lateral stick input and output rates do not appreciably affect the test results (Figure 4.24). Averaged over all the test points, this error is only 3.8%. The only standout is the 16 degree test point, which is in error by 22.7%. It has already been indicated that the nominal 16 degree test point exhibits light damping and is sensitive to perturbations. The same is true when this error is introduced, as the smaller input and output stick rates produce smaller perturbations than the larger input and output stick rates of the nominal test case.

The *180° roll angle capture* metric 16 degree test point is sensitive to errors due to relaxing aft stick position during capture, and reduced lateral stick magnitudes during capture. The generic F-18A has little difficulty satisfying the capture criterion of Section 4.3.3 at the lower angles of attack, but has trouble in the 16 test points due to kinematic coupling, reduction in damping in all three axes, and a heightened sensitivity to perturbations.

4.4.3.4 Summary

Although the *180° roll angle capture* is similar to the *90° roll angle capture*, the longer duration of the maneuver and the larger bank angle displacement tend to result in a larger buildup of adverse yaw. This has the effect of making a successful capture increasingly difficult. There appears to be no specific advantage over the *90° roll angle capture* metric; it is simply a more challenging task for the aircraft as explained above. Use of the capture criteria identified a flight condition (test point for 16 degrees angle of attack) where the generic F-18A could not satisfy the capture criteria. For other test cases, the capture criteria gave an indication of how easy (or difficult) accomplishing the

capture can be. Although more realistic than the normalization algorithm, it is considerably more demanding and time consuming to use because of the iterative nature of determining the command sequence that generates the desired results.

When measured using the generic F-18A, the *180° roll angle capture* metric is recognized to be sensitive to reductions in aft stick magnitude in the higher range of normal load factors. Comparing the characteristics of the two aircraft, the generic F-5A appears to be better damped in all three axes, but suffers from being below corner speed at this flight condition. However, the capability of performing this maneuver over a greater range of angles of attack and near the design limit normal load factor, may **not** be tactically significant. Although the normal load factor for the generic F-5A is limited at this flight condition, it still performs the maneuver quite well. The generic F-18A, on the other hand, is less damped in all three axes than the generic F-5A, yet is slightly better in performing the maneuver at all the angles of attack tested.

4.5 SUMMARY

In summary, the suitability of three candidate lateral agility metrics were tested to determine for suitability in measuring lateral agility. The maneuvers required to test the lateral agility metrics are somewhat unique from the standpoint of traditional flight test maneuvers, and could promote pilot disorientation due to the atypical aircraft attitudes encountered. Disorientation problems can be partially alleviated through adequate cockpit instrumentation. During this investigation none of the aircraft exhibited roll reversal or roll ratcheting tendencies, and execution of the maneuvers did not impose any intolerable linear accelerations upon the pilot.

The *time through roll angle* metrics, e.g. T_{TR90}, as a class are suitable for measuring the transient performance aspect of lateral agility. The main advantage of this class of metrics is that they

measure the same transient performance as the *roll angle capture* class of metrics (T_{RC90}, T_{RC180}), but are easier to fly and simulate. The pilot, being relieved of the task of capturing a bank angle, can concentrate more on holding longitudinal quantities (angle of attack or normal load factor) constant during the roll. The maneuver is an open-loop type, and is much less susceptible to pilot technique as a source of data scatter.

The sensitivity analysis using the generic F-18A determined that by using the normalization algorithm of Section 4.3.2, the introduced deviations in pilot inputs resulted in average T_{RC90} errors of less than 3%. The normalization algorithm was not used for the T_{RC180} metric sensitivity. The T_{RC180} metric is quite sensitive to deviations in maximum deflections of the lateral stick. The other deviations produced an average error of approximately 5% over the range of angles of attack tested.

To obtain an estimate of the flying qualities during the maneuvers, the *roll angle capture* class of metrics should be used. Both classes of metrics together with conventional handling qualities measurements can provide a basic measure of lateral agility. The interaction of flying qualtities and lateral agility metrics becomes especially important when manned simulators and actual flight testing are used instead of the unmanned non real-time simulations used for these investigations. For coverage of this aspect of lateral agility the reader is encouraged to consult Reference 34.

5. AXIAL AGILITY

5.1 BACKGROUND

This chapter introduces the axial agility metrics and demonstrates how they are used to assess the axial agility of different aircraft. Traditional methods of quantifying the axial capability (longitudinal translation capability) of fighter aircraft have generally consisted of thrust-to-weight ratio, maximum Mach number in level flight, maximum rate of climb and specific excess power (P_s). These point performance measures of merit quantify performance only at discrete aircraft states only and are not indicative of the capability of an aircraft to rapidly change its energy rate. Axial agility metrics are intended to provide a measure of this capability.

The following analysis and results reveal some of the not immediately obvious aspects of axial agility. Results are presented for the axial agility of the generic F-16A and generic F-18A. No results are presented for the generic F-5A because that simulation program does not model the speedbrakes. The utility or acceptability of the maneuvers to an operational pilot and the flying qualities he would encounter during the maneuver are not addressed in his report.

5.2 CANDIDATE AXIAL AGILITY METRICS

The *power onset parameter* and the *power loss parameter* have been proposed to quantify axial agility. They basically consist of the time rate of change of P_s, and account for the combined effects of engine spool time, maximum thrust and drag due to speed brakes. A traditional comparison of energy maneuverability levels will not reflect these interactions. For example, consider two aircraft with similar energy maneuverability levels, but significantly different engine spool times. Simply measuring the P_s of the aircraft will not highlight the

advantage of quicker engine response and more effective speedbrakes. However, measuring both the positive and negative time rate of change of P_s should. It should be noted that the axial agility metrics do **not** quantify the acceleration or deceleration performance of an aircraft. This result is shown in Appendix D.

5.3 AXIAL AGILITY TESTING AND DATA REDUCTION TECHNIQUES

Both the *power onset parameter* and the *power loss parameter* are tested at altitudes of 500 feet, 15,000 feet and 30,000 feet, and at Mach numbers from 0.4 to 0.9. The Mach numbers are selected to be representative of the range of speeds at which fighter aircraft would most likely be engaged in close air combat. The altitudes are selected with air combat in mind also. While it is possible to generate large amounts of drag very quickly by pitching to high angles of attack, such a maneuver is not considered here. Non real-time simulations of the generic F-18A and generic F-16A are used to generate the results.

The test case for the *power onset parameter* begins with the aircraft setting-up at steady level trimmed flight with speedbrake extended at a Mach number slightly greater than the test Mach number; typically $M_{START} = M_{TEST} + 0.03$. The throttle is then ramped down to the flight idle setting over one second. A one second ramp was used to reduce unwanted, large transitory thrust responses. The aircraft begins decelerating in a minimum thrust/maximum drag configuration. When the test Mach number is reached, a step command is applied to the throttle, from the flight idle setting to maximum afterburner, while simultaneously retracting the speedbrake (Figure 5.1). The resulting acceleration is maintained, holding altitude constant, until the net axial force reaches a maximum value. This typically requires approximately three seconds from the beginning of the maneuver. The entire test case from dynamic settling (trim), set-up,

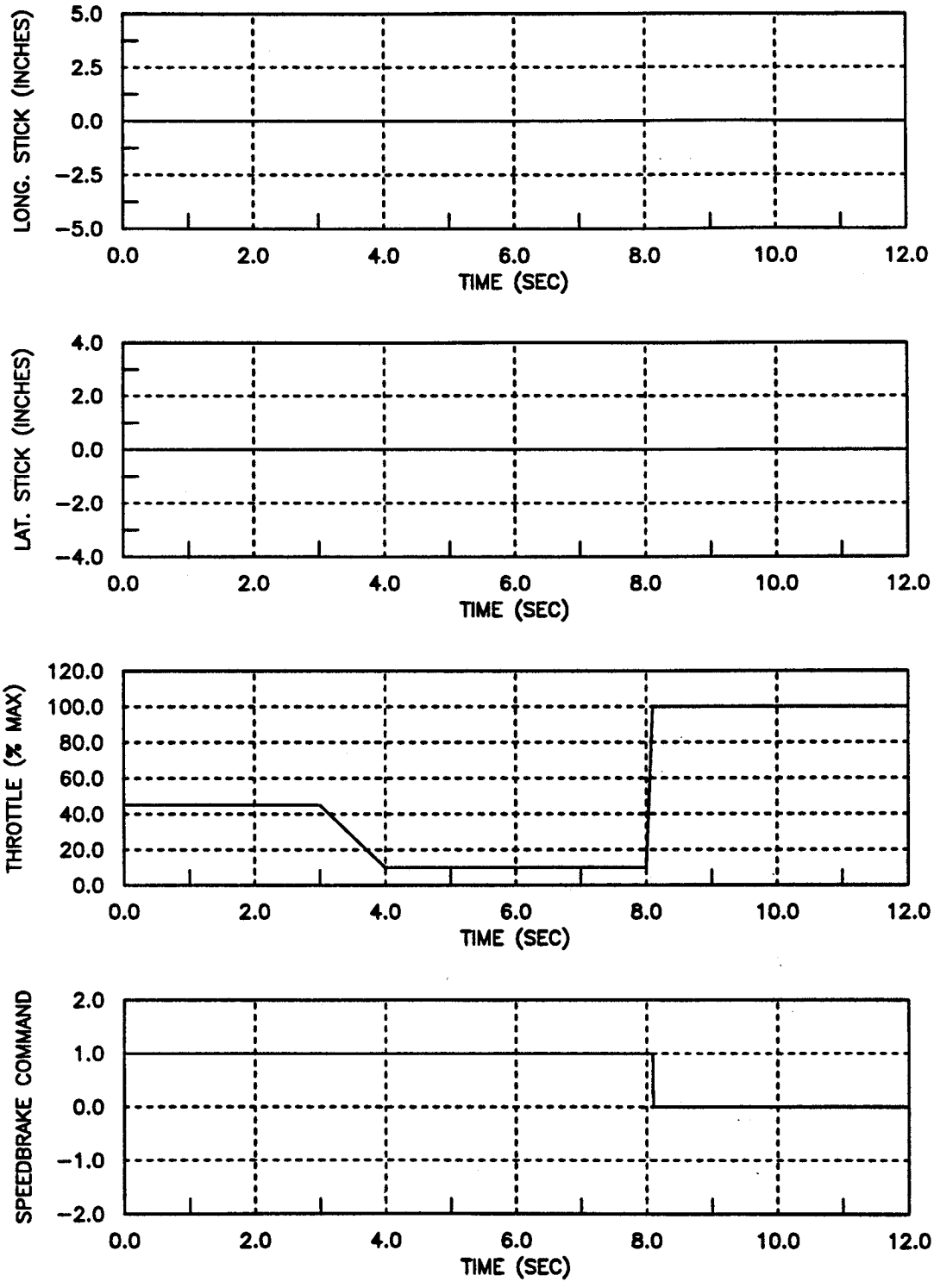

Figure 5.1 Command Time Histories For Testing The *Power Onset Parameter*

and maneuver requires approximately ten seconds of flight time.

The *power loss parameter* is basically the opposite of the *power onset parameter*, so testing it is similar to testing the *power onset parameter*. The aircraft accelerates up to the test Mach number at maximum throttle setting with the speedbrake retracted. Upon reaching M_{TEST}, the throttle command is stepped from maximum setting to flight idle while simultaneously extending the speedbrake (Figure 5.2). Thrust reversing would be also engaged at this point if the aircraft was so equipped. Altitude is held constant during the deceleration (using an altitude hold autopilot if necessary) until the net axial force reaches a minimum. This requires approximately three seconds. The entire test case from dynamic settling, set-up, and maneuver requires approximately ten seconds of flight time.

The data reduction method for quantifying axial agility is straightforward in concept but can contain some degree of uncertainty. In order to automate the data reduction process, the simulations are programmed to output values of P_s and thrust minus drag (net axial force) every 25 milliseconds. Consider the equation for the *power onset parameter*:

$$\frac{\Delta P_s}{\Delta t} = \frac{P_{s_f} - P_{s_i}}{t_f - t_i} \tag{5.1}$$

where

P_{S_i} = P_S at the minimum value of thrust minus drag
P_{S_f} = P_S at the maximum value of thrust minus drag
t_i = time at which thrust minus drag is minimum
t_f = time at which thrust minus drag is maximum

Whereas thrust minus drag usually attains easily identifiable minimum values, the maximum values in many instances are approached asymptotically. Criteria are thus required to define the maximum value in such instances. A method which is easy to use and is found to give good results is to examine the difference between successive values of net axial force. When four

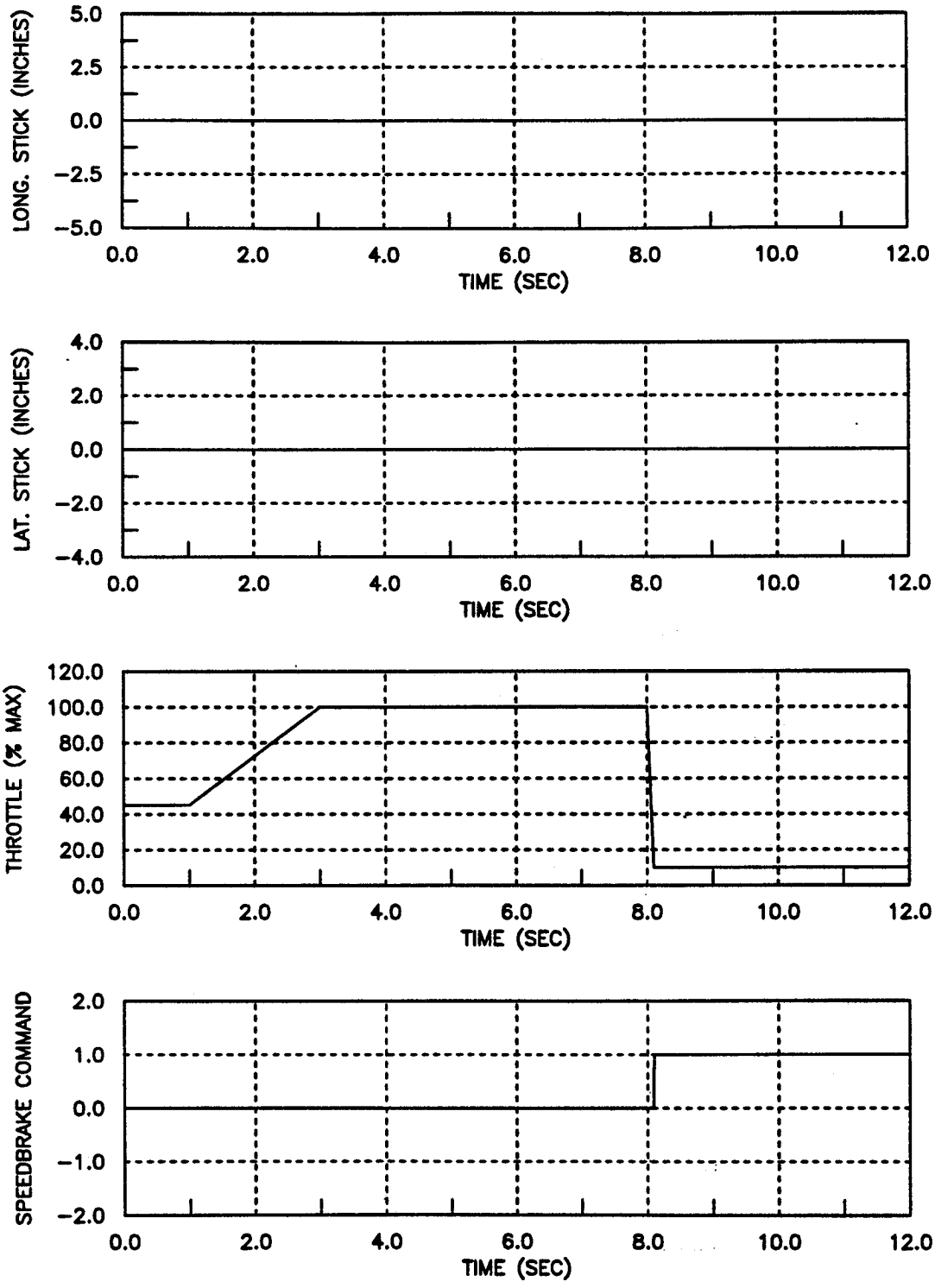

Figure 5.2 Command Time Histories For Testing The *Power Loss Parameter*

successive data points (at 25 millisecond intervals) are identified which do not differ by more thanapproximately ten pounds between any successive point, the fourth point is selected to represent the maximum value. The value of ten pounds is chosen because the maximum as calculated using this value correspond well to the visually determined maximum values in the graphs. The ten pounds of net axial force per 25 milliseconds corresponds to a change in net axial force of 400 pounds per second. With respect to the magnitudes and time intervals of the data, 400 pounds per second is only a small percentage of the maximum thrust of the generic F-18A.

5.4 CANDIDATE AXIAL AGILITY METRICS RESULTS

In this section each of the axial agility metrics are presented. First the metric will be defined and then typical results will be presented.

5.4.1 **Power Onset Parameter** (REF. 18)

5.4.1.1 Definition

The increment of specific excess power (ΔP_s) resulting in going from a minimum power/maximum drag condition, to a maximum power/minimum drag condition, divided by Δt, the time in seconds required to complete the transition:

$$\text{Power Onset Parameter} = \frac{\Delta P_s}{\Delta t} = \frac{P_{s\,\text{final}} - P_{s\,\text{initial}}}{t_{\text{final}} - t_{\text{initial}}}$$

5.4.1.2 Discussion and Results

Figure 5.3 displays values for the *power onset parameter* computed for the generic F-16A and generic F-18A at altitudes of 500 feet, 15,000 feet, and 30,000 feet. The generic F-18A exhibits larger (better) values of the *power onset parameter* than the generic F-16A at the high

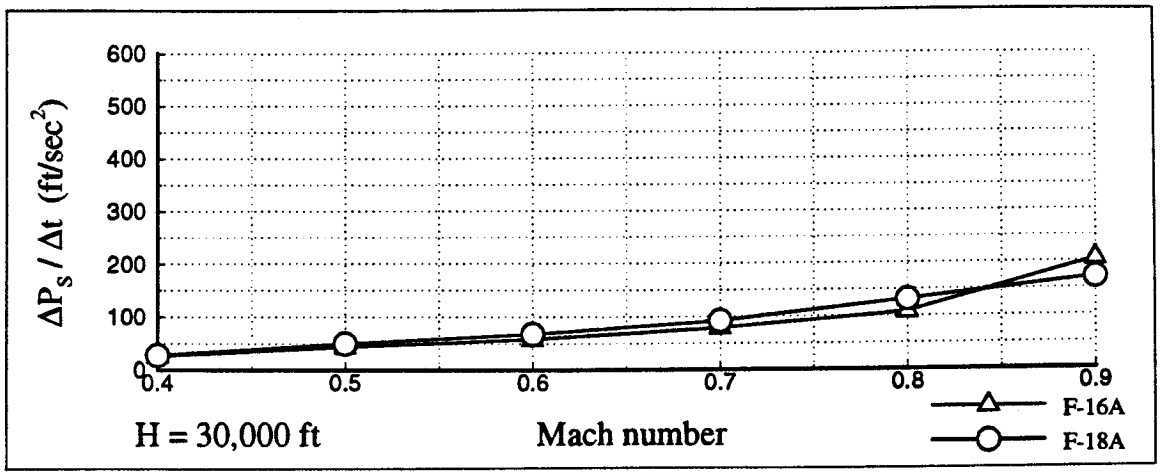

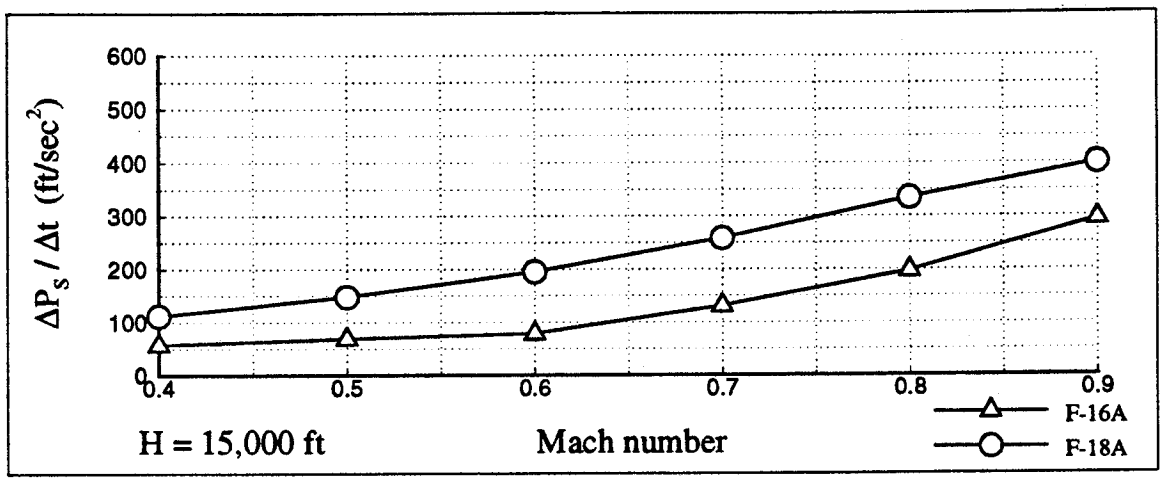

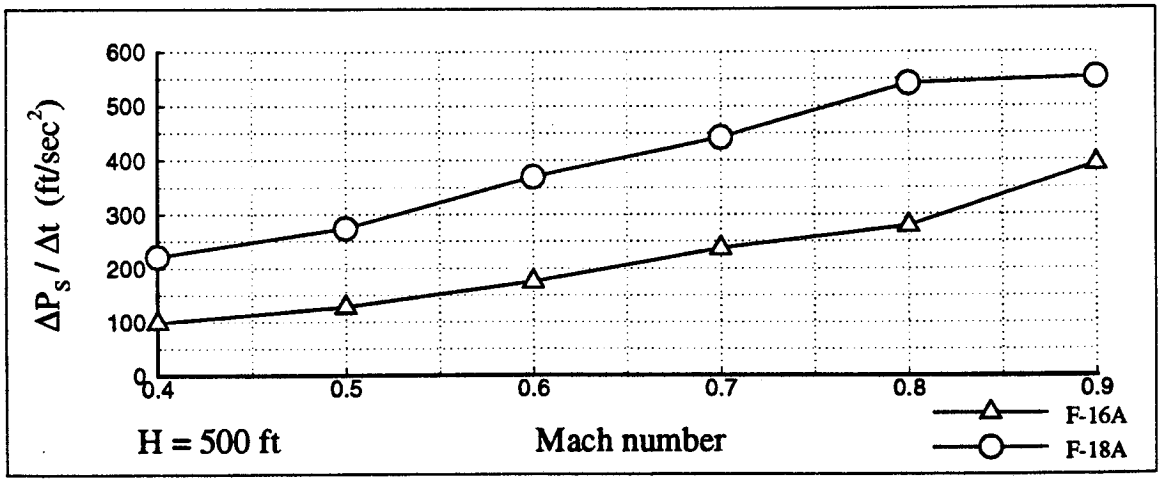

Figure 5.3 *Power Onset Parameter* For The Generic F-16A and Generic F-18A

dynamic pressure flight conditions, i.e. low level, high speed. Although the generic F-18A transitions a smaller difference in initial and final levels of P_s than the generic F-16A, it does so in approximately one-half the time. The generic F-16A surpasses the generic F-18A in the *power onset parameter* only at Mach 0.9 at 30,000 feet. At this flight condition, the generic F-18A transits a smaller ΔP_s in only two thirds the time required by the generic F-16A. However, ΔP_s for the generic F-16A is 1.8 times that of the generic F-18A and is sufficiently great enough to offset the advantage of the shorter transit time.

The importance of the transition time is demonstrated by the following example. Consider aircraft A and aircraft B in Figure 5.4 Although aircraft A generates a larger ΔP_s compared to aircraft B, aircraft B can transition across its smaller ΔP_s in a correspondingly shorter time ΔT_B than the time required for aircraft A (ΔT_A). Therefore, according to the definition of the *power onset parameter*, aircraft B is said to have better axial agility.

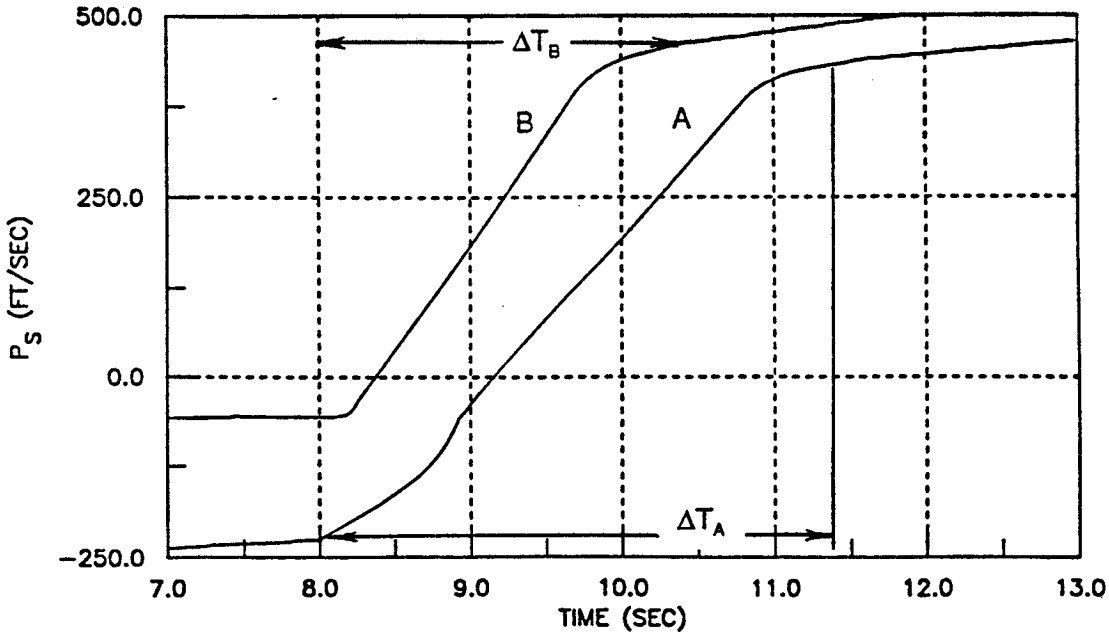

Figure 5.4 Effect of Transition Times on The *Power Onset Parameter*

5.4.1.3 Summary

The *power onset parameter* is simple to test, but measurement of the final P_S level can be difficult in certain cases. The initial or final value of P_s itself usually does not dominate this metric, but the **transition** times between the initial and final values usually does. In a few situations the value ΔP_s can be important, but normally to a lesser extent.

5.4.2 **Power Loss Parameter** (REF. 18)

5.4.2.1 Definition

The increment of specific excess power (ΔP_s) resulting in going from a maximum power/minimum drag condition, to a minimum power/maximum drag condition, divided by Δt, the time in seconds required to complete the transition:

$$\text{Power Loss Parameter} = \frac{\Delta P_s}{\Delta t} = \frac{P_{s\ final} - P_{s\ initial}}{t_{final} - t_{initial}}$$

5.4.2.2 Discussion and Results

Figure 5.5 displays values for the *power loss parameter* for the generic F-16A and generic F-18A at altitudes of 500 feet, 15,000 feet and 30,000 feet. Note that unlike the results for the *power onset parameter*, Figure 5.5 shows that the generic F-18A does not have better axial agility than the generic F-16A over most of the test points. At all altitudes, the generic F-18A is superior in the low subsonic Mach number range, while the generic F-16A is superior in the high subsonic Mach range. The generic F-18A achieves both larger differences in P_s levels and shorter transition times than the generic F-16A over all low subsonic Mach numbers, at all the altitudes tested. The *power loss parameter* values for the two aircraft are similar at 0.7 Mach at 500 feet and 15,000 feet, after which the generic F-16A is able to transition a larger ΔP_s and having a shorter transition

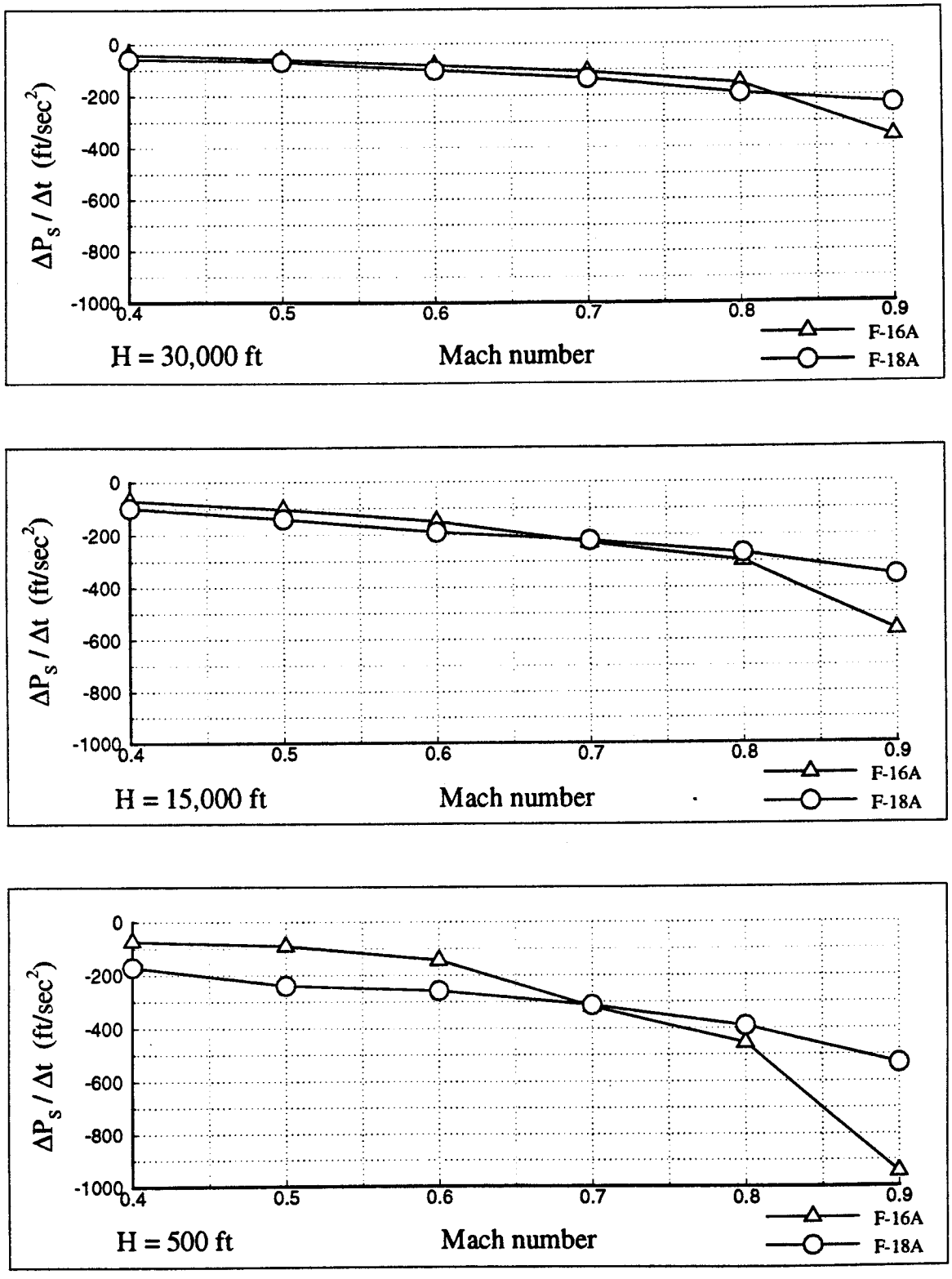

Figure 5.5 *Power Loss Parameter* For The Generic F-16A and Generic F-18A

time than the generic F-18A. The generic F-16A is superior at 30,000 feet only because of its larger P_s level.

5.4.2.3 Summary

Although the *power loss parameter* is very similar to the *power onset parameter*, the results have shown that an aircraft which is superior in terms of one of the axial agility metrics is not necessarily superior in terms of the other metric also. The *power loss parameter* is simple to test, and is generally affected by the same parameters as the *power onset parameter.*

5.5 SUMMARY

Axial agility metrics measure the capability of an aircraft to transition between maximum and minimum P_s levels. Instead of knowing only what level of P_s an aircraft possesses at a particular point, axial agility reflects how fast the aircraft can transition to another P_s level. The time required to make the transition tends to be the most important aspect, while the magnitude of the P_s change involved in transitioning is important to a lesser extent. Thus both the time rate of change of thrust and the time rate of change of drag are influential. Overall, the time rate of change of thrust, i.e. engine spool time, tends to have a more pronounced effect on these metrics than the time rate of change of drag, i.e. effectiveness and deployment times of speedbrakes. In terms of axial agility, an agile aircraft is characterized as having high thrust engines with very short spool times, and fast deploying, effective speedbrakes.

The *power onset parameter* and *power loss parameter* are not measures of the acceleration capability of an aircraft. In fact, the acceleration of the aircraft has a negligible impact on the values of the *power onset parameter* and *power loss parameters*, meaning that the weight of the

aircraft does not affect the values (Appendix D). Therefore, a lighter aircraft is not advantageous in terms of axial agility.

The axial agility of a fighter is also affected by the engine's transient performance at elevated angles of attack and sideslip. The transient behavior of the engine during large scale maneuvers and high angle of attack flight is an important contributor to overall combat effectiveness. However, the *power onset parameter* and the *power loss parameter* do not address this aspect of engine performance.

The *power onset parameter* and *power loss parameter* could be easily extended to account for any unique capabilities which may be used to effect changes in P_s. These capabilities may consist of engines with very fast response to throttle commands, thrust vectoring or thrust reversing nozzles, or even nozzles which permit vectoring in forward flight (VIFFING).

6. FUNCTIONAL AGILITY

6.1 BACKGROUND

Functional agility metrics are intended to quantify how fighter aircraft execute rapid changes in heading or rotations of the velocity vector. This class of metrics is concerned with a time scale on the order of ten to twenty seconds. These metrics as a class tend to place emphasis on energy lost during turns through large heading angles, and the time required to recover kinetic energy after unloading to zero normal load factor. Many of the functional agility metrics involve maneuvers composed of brief transient segments. The effect of these transient segments are measured best by the class of transient agility metrics, e.g. pitch agility and lateral agility. However, metrics are needed to quantify an entire maneuver. These are the functional agility metrics.

This chapter demonstrates how to test, measure, and compare the functional agility of fighter aircraft using several of the candidate functional agility metrics. For the results contained in this chapter, functional agility is quantified using nonlinear, non real-time, six degree-of-freedom generic flight simulation computer programs. Results and analysis are presented for the F-5A, F-16A, F-18A, and X-29A aircraft to show how characteristics of the aircraft and flight control system (FCS) can influence the metrics. The maneuvers and results are intended to quantify the agility of the aircraft being tested. The acceptability of such maneuvers to an operational pilot, the associated issues of flying qualities, pilot discomfort, and g-induced loss of consciousness are not addressed in this report.

6.2 CANDIDATE FUNCTIONAL AGILITY METRICS

In recent years agility researchers have proposed numerous metrics to quantify functional agility of fighter aircraft. The proposed metrics include:

1) combat cycle time 180° heading change
2) combat cycle time 90° heading change
3) dynamic speed turn
4) relative energy state
5) energy-agility concept
6) time-energy penalty
7) DT parameter
8) pointing margin
9) one-circle pointing quotient

All nine candidate functional agility metrics are defined in Appendix A. Results for the *DT parameter*, *pointing margin*, and *one-circle pointing quotient* metrics are not presented in the current study, since these metrics have been previously analyzed and tested. For a discussion and results from these metrics, the reader should consult References 35, 30, and 41 respectively.

6.3 FUNCTIONAL AGILITY TESTING AND DATA REDUCTION TECHNIQUES

Metrics one through six listed above are tested at Mach equals 0.8 at 15,000 feet. The Mach number is selected to at or near corner speed for the aircraft tested, and the altitude is selected to be representative of that at which fighter aircraft are most likely be engaged in within

visual range air combat. The maneuver sequence used to test the *combat cycle time* metric (CCT) is sufficient for testing the *dynamic speed turn*, *relative energy state*, *energy-agility concept*, and *time-energy penalty* metrics. Data for all of these metrics can be obtained by post-processing a single CCT test case for a given aircraft.

Although not explicitly a part of the definition of any metric, a set of constraints is established in order to define an acceptable or realistic maneuver. This consideration is particularly important for the functional agility metrics from an energy management standpoint. The constraints also provide a level of standardization and repeatability. Referring to Figure 6.1, the CCT metric is a series of segments consisting of the time to pitch from one g to the limit normal load factor (t_1), plus the time to turn to a specified new heading angle at maximum normal load factor ($t_{21} + t_{22}$), plus the time to unload the aircraft to a normal load factor of either one or zero (t_3), plus the time to accelerate to the original energy level (t_4). The enforced test constraints for the CCT maneuver sequence consist of the following:

1. altitude excursion during any phase: ± 1500 feet
2. altitude excursion during unload and roll: ± 200 feet
3. captured heading angle excursion: ± 5°

The altitude band is imposed during the transition from the unloading phase (t_3) to the start of the acceleration phase (t_4) to insure that the aircraft is using a straight-line acceleration to regain the original energy, and not climbing to gain altitude or descending to gain airspeed. This isolates the ability of the aircraft to accelerate without using beneficial gravity effects. The heading angle capture criterion of ±2° is arbitrarily selected, and insures that the acceleration phase of the maneuver occurs at the desired heading.

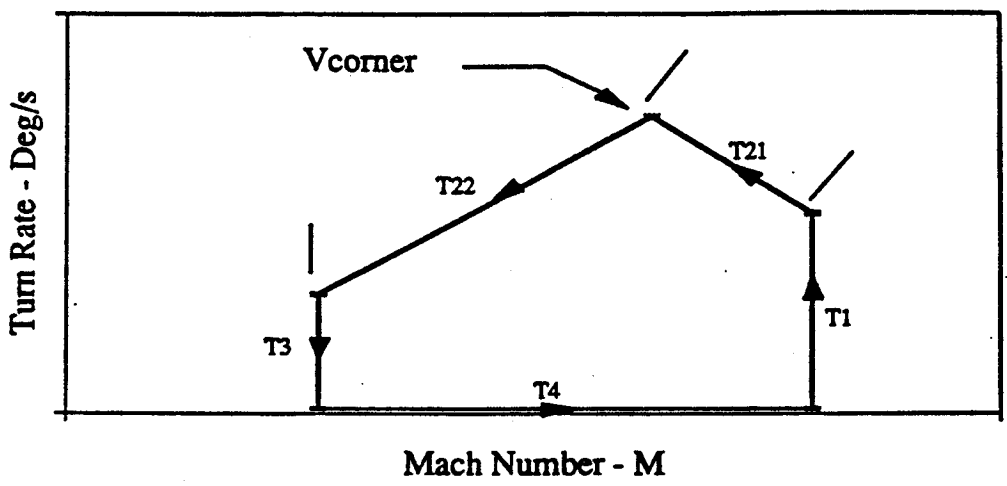

Figure 6.1 Maneuver Segments Of A Typical *Combat Cycle Time* Plot (REF. 42)

The pilot control inputs for the CCT maneuver consist of longitudinal and lateral stick and throttle commands only. All pilot command inputs are ramped in and ramped out over a minimum of 0.1 seconds. The speedbrake was not extended as each aircraft decelerated rapidly with the onset of elevated angle of attack. Figure 6.2 is an example time history of the pilot control input strategy used for the CCT metric. To perform the maneuver, the aircraft first sets up in steady level 1g flight, with a zero P_s level. The maneuver is initiated with a full deflection lateral stick doublet to capture a 90° bank angle. Upon capturing the 90° bank angle, full aft stick is then applied to initiate the heading change, while throttle is simultaneously ramped up from flight idle to full afterburner. Full aft stick is held continuously throughout the heading change, until the final heading is captured. Longitudinal stick is then brought out to unload the aircraft, and lateral stick is then commanded to roll the aircraft out of the turn and back into level flight.

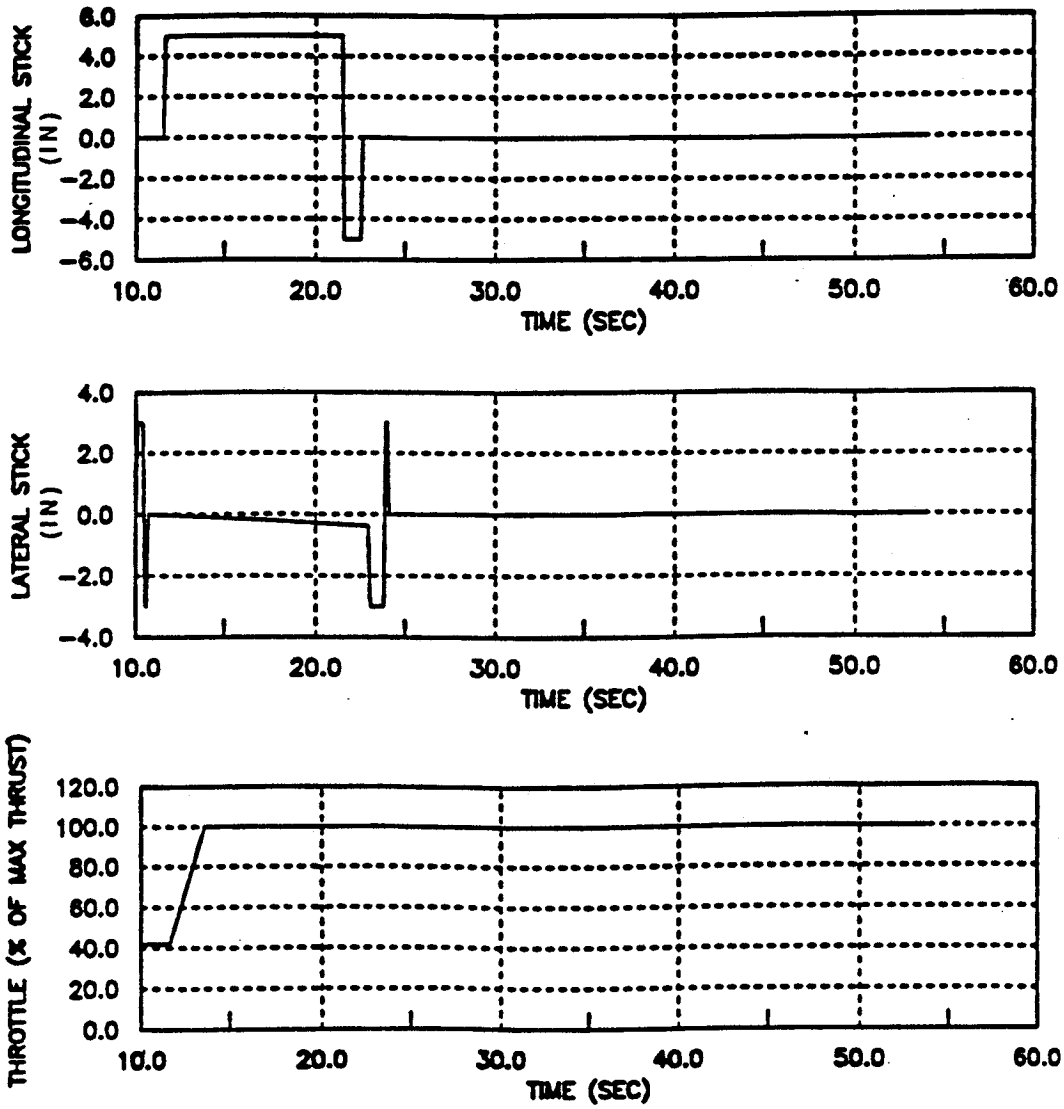

Figure 6.2 Typical Pilot Stick And Throttle Input Commands
Used For Testing The *Combat Cycle Time* Metric (REF. 43)

Heading angle change is the independent variable for selecting test points for the CCT metric. Heading angle changes of 180° and 90° are selected for this study. A 180° heading change is selected because previous studies involving minimum time turns consider 180° heading changes as a baseline maneuver (REF. 44, 45, 46). A 90° heading angle change is selected as an attempt to reduce the influence of sustained maneuvering.

The *dynamic speed turn* plots are by definition cross-plots from the energy-maneuverability doghouse plot (REF. 47). Rather than developing the entire energy-maneuverability diagram for each aircraft, the turn rate versus airspeed data from the CCT maneuver is used to obtain data for this metric. The equation for specific excess power (P_s) is used to calculate the amount of acceleration and deceleration. Since the CCT maneuver does not employ a level turn, the acceleration and bleed rates for the *dynamic speed turn* plots are calculated by differentiating true airspeed in knots. Airspeed changes are indicated using Mach number.

The data for the *relative energy state* metric is obtained from the CCT maneuver by dividing the velocity of the aircraft during the turn by the corner velocity (V_c). It is suggested that at least two 90° turns be completed before the velocity of the aircraft falls below corner speed.

The *energy-agility* plot is generated by plotting P_s as a function of time during the CCT maneuver. The time to kill (t_k) is then defined as the time required to reach a heading angle of 180°.

The generic F-18A simulation is used to assess the sensitivity of the functional agility metrics. It is important to note that *these sensitivity results are specific to the generic F-18A **only**, and cannot be generalized to all fighter aircraft.* The intent here is simply to determine in a broad sense how sensitive the functional agility metrics can be to pilot inputs, and to demonstrate one way in which an analysis of this type can be conducted. Since this analysis is simply

intended to show typical behavior, the sensitivity tests are limited to a single altitude of 15,000 feet.

The sensitivities are determined by generating optimal trajectories for the 180° and 90° CCT maneuvers using the Optimal Trajectories by Implicit Simulation (OTIS) program (Appendix B). Angle of attack and bank angle are the control parameters which the OTIS program uses to generate the optimal CCT maneuver. The angle of attack and bank angle time histories specified by the OTIS program are then used as schedules for determining a sequence of pilot stick input commands. This command sequence is then used to reproduce the optimal CCT maneuver using the generic F-18A simulation. The optimal CCT maneuver is also used to determine sensitivities for the *dynamic speed turn*, *relative energy state*, *energy-agility concept*, and *time energy penalty* metrics.

Three variations of the 180° and 90° CCT maneuvers form the basis for the sensitivity analysis:

1) heading change at maximum angle of attack

2) optimal turn; defined here as a minimum time turn without the final velocity defined, and using the angle of attack schedule specified by OTIS

3) optimal total time; defined here as a minimum time turn with the final velocity = initial velocity, and using angle of attack schedule specified by OTIS

The constraints enforced on the nominal CCT are applied to the three maneuvers listed above. The first variation, heading change at maximum angle of attack, is tested by maintaining full aft stick deflection after the aircraft captures the initial 90° bank angle, until the aircraft achieves the new heading. A full aft stick deflection is typically used in flight testing agility parameters (REF. 25, 48).

The second variation, optimal turn, is generated in a similar fashion. Instead of applying full aft stick after capturing the 90° bank angle, the aft stick is deflected so that angle of attack tracks the angle of attack schedule specified by the OTIS program. Figure 6.3 demonstrates that the angle of attack schedule specified by OTIS can be reasonably reproduced by the generic F-18A simulation. After capturing the new heading, the aircraft is permitted to accelerate back to the initial Mach number.

The third variation, optimal total time, also uses the angle of attack schedule specified by the OTIS program, but requires that the velocity as the heading angle is achieved be equal to the initial velocity. Thus, the OTIS program generates a trajectory which results in the aircraft possessing its initial velocity when the new heading angle is reached. Therefore, the 1g acceleration back to the initial velocity is unnecessary.

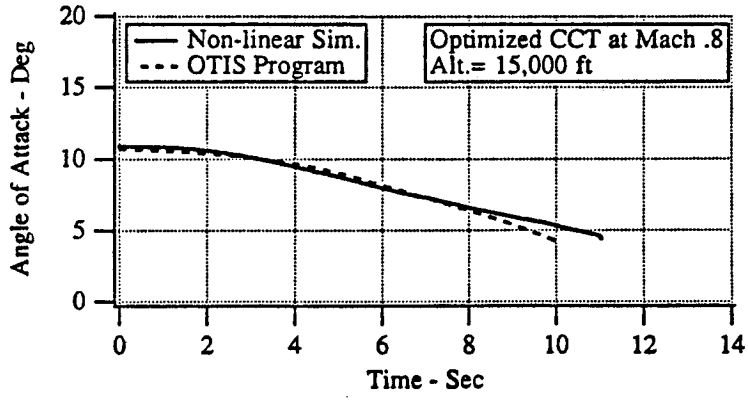

Figure 6.3 Angle Of Attack Time History Match
For The OTIS and Generic F-18A Simulations (REF. 42)

Sensitivity to errors in optimal bank angle were also investigated using the OTIS program in Reference 42. Bank angle errors have little influence on the total maneuver time, since limiting bank angle to ± 100° only added about 0.7% to the total CCT for each case. Therefore, only the angle of attack schedule is used for generating the optimal CCT maneuver.

6.4 CANDIDATE FUNCTIONAL AGILITY METRICS RESULTS

In this section results for the candidate functional agility metrics are presented. Each metric is defined and then typical results are given.

6.4.1 **Combat Cycle Time 180° Heading Change** (REF. 30)

6.4.1.1 Definition

This metric is defined as the sum of: $t_1 + t_{21} + t_{22} + t_3 + t_4$

where t_1 = time to pitch from one g to the limit normal load factor

$t_{21} + t_{22}$ = time to turn to a specified new heading angle at maximum normal load factor

t_3 = time to unload to a normal load factor of either one or zero g

t_4 = time to accelerate to the original energy level

6.4.1.2 Discussion and Typical Results

This metric is characterized by a continually changing flight condition constrained within structural, lift, and power limits. It is calculated for a given set of starting conditions and some specified heading angle change. The 180° turn specified by the CCT metric highlights the capability and importance of transitioning between sustained maneuvering conditions. It provides insight into these transient capabilities by addressing the transitions between steady state conditions. The acceleration to regain the original energy level is important to the CCT metric, and so an aircraft with a high thrust-to-weight ratio would be expected to have a small CCT value.

The 180° CCT plot for the generic F-5A is shown in Figure 6.4. This aircraft does not maneuver along its normal load factor limit since the initial Mach number for this evaluation (0.8) is below this aircraft's corner speed. The peak in the turn rate is a direct result of a spike in the

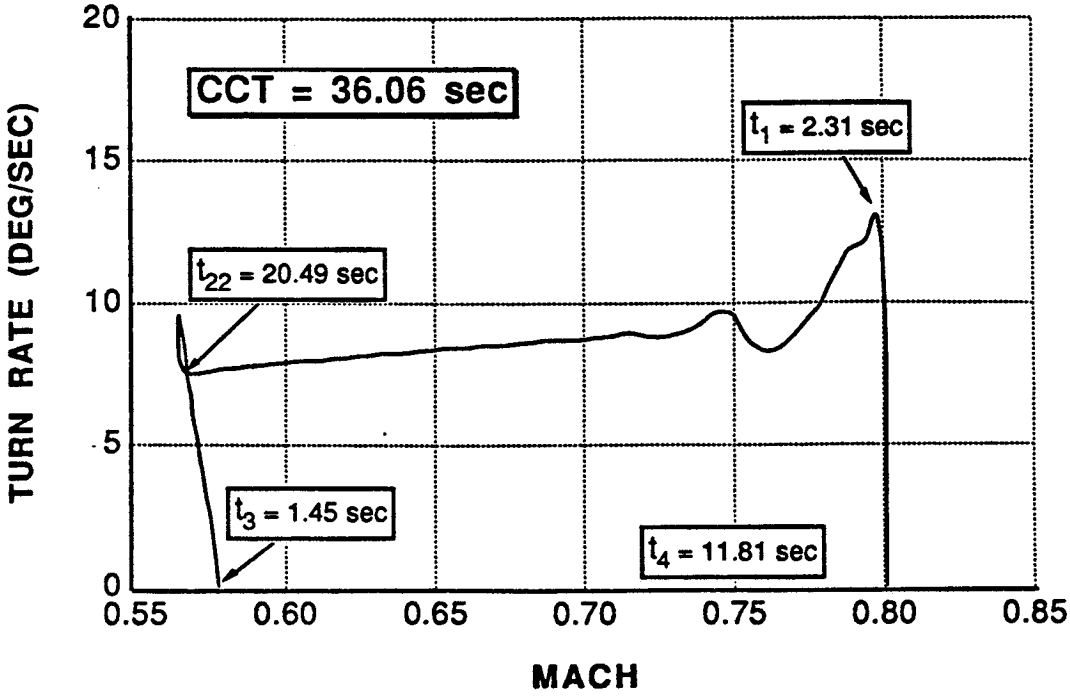

Figure 6.4 Generic F-5A 180° *Combat Cycle Time* Plot,
Mach = 0.8, H = 15,000 feet (REF. 49)

load factor response as a result of commanding full aft stick. The relatively low sustained normal load factor of approximately 3g's for this aircraft is a result of operating below corner speed. This low sustained normal load factor translates into mediocre turn rates of 5 to 10 degrees per second, such that the turning phase (t_2) dominates the total CCT for this aircraft.

The CCT plot for the generic F-16A is shown in Figure 6.5. Limiters in the flight control system of this aircraft have a strong influence on the CCT and prevent the plot from having the doghouse shape. The effect of the limiters on the CCT is three-fold. First, the limiting prevents the generic F-16A from achieving its angle of attack for maximum lift (approximately 35°). Second, bleed rate is kept to a minimum with the result that large energy losses are avoided. Third, due to limiting the corner speed consists of a bandwidth of velocities ranging between 340 to 440 KIAS (REF. 51). The total result of this limiting on the generic F-16A CCT is that the overall CCT is smaller and the times are balanced, with the turning (t_2) and acceleration (t_4)

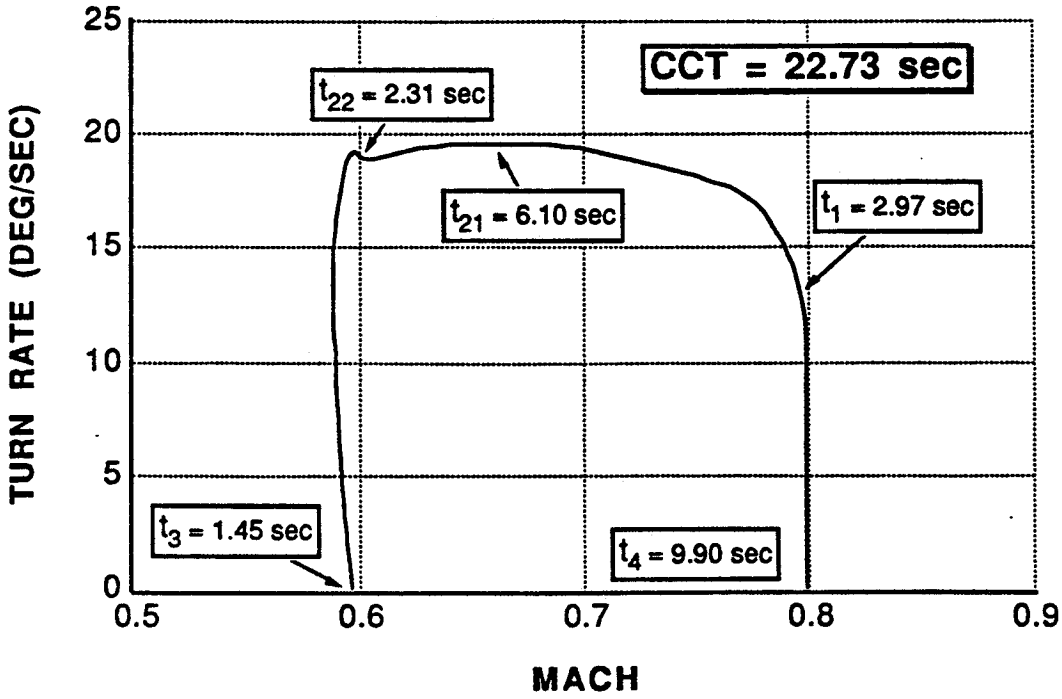

Figure 6.5 Generic F-16A 180° *Combat Cycle Time* Plot,
Mach = 0.8, H = 15,000 feet (REF. 49)

phases equally dominating the metric.

Figure 6.6 is the 180° CCT plot for the generic F-18A. The aircraft starts the maneuver at Mach equals 0.8 with zero turn rate (point 1). It then proceeds to maneuver along the normal load factor limit (t_1 to t_{22}), bleeding airspeed and losing turn rate as the lift limit is reached and exceeded. The time t_4 required to accelerate from point 3 back to the original energy level at point 4 dominates the total time for the metric. Because full aft stick is commanded throughout the turn, this aircraft exceeds its angle of attack for maximum lift (approximately 38°). It must be noted that this aircraft is not **required** to attain such a high angle of attack during the turn, but that this is simply a result of the selected pilot control input strategy. The consequence of commanding the aircraft to the high angle of attack during the turn is shown in Figure 6.7 to be a large drag penalty which causes a rapid deceleration to a low speed condition. Upon completing the turn, the aircraft pitches down from an angle of attack of 57° in approximately two seconds

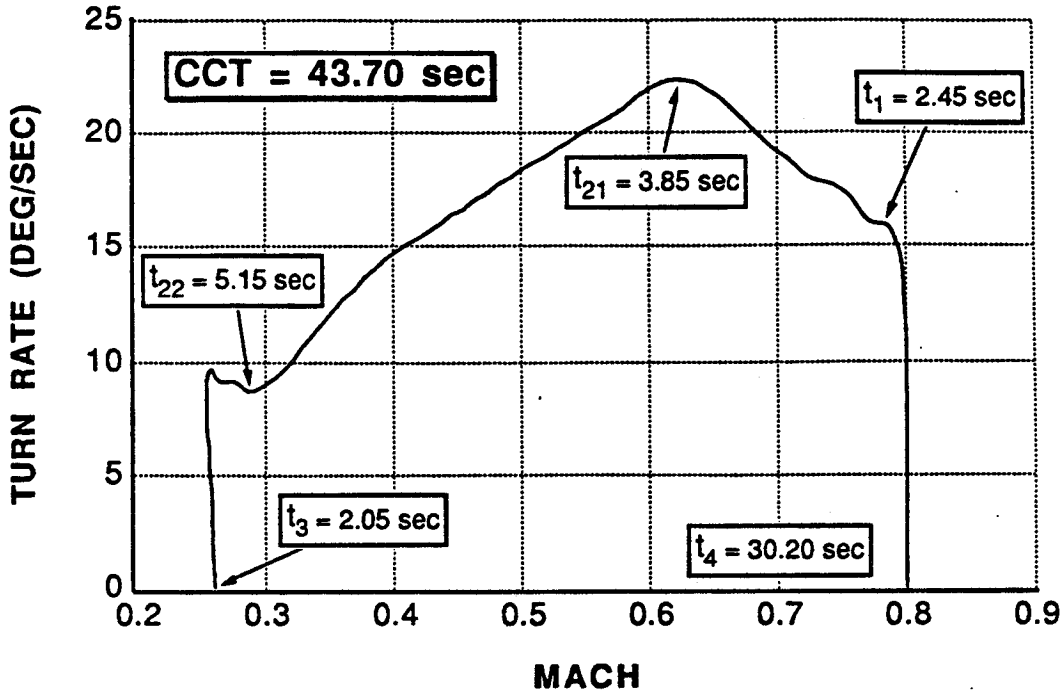

Figure 6.6 Generic F-18A 180° *Combat Cycle Time* Plot,
Mach = 0.8, H = 15,000 feet (REF. 49)

(t_3), and begins the acceleration phase. A superior transient pitch capability can be equated to a reduction in the thrust required for the acceleration phase, since the mass of an aircraft is accelerated by a force due to net thrust, i.e. thrust minus drag (REF. 50).

The 180° CCT plot for the generic X-29A is shown in Figure 6.8. The time for the total combat cycle (as well as the individual segment times) are very similar to the generic F-18A, since the acceleration phase dominates the metric. Unlike the generic F-16A, the generic X-29A does not have limiters which directly prevent it from achieving higher turn rates. However, the shape of the plot is similar to the generic F-16A since turn rate is relatively constant across the range of subsonic Mach numbers. This is because the rapid onset of elevated angles of attack bleeds airspeed, causing the normal load factor to decrease. As a result the turn rate remains constant with Mach number, regardless of the reduction in normal load factor, since the aircraft decelerates appreciably during the turn.

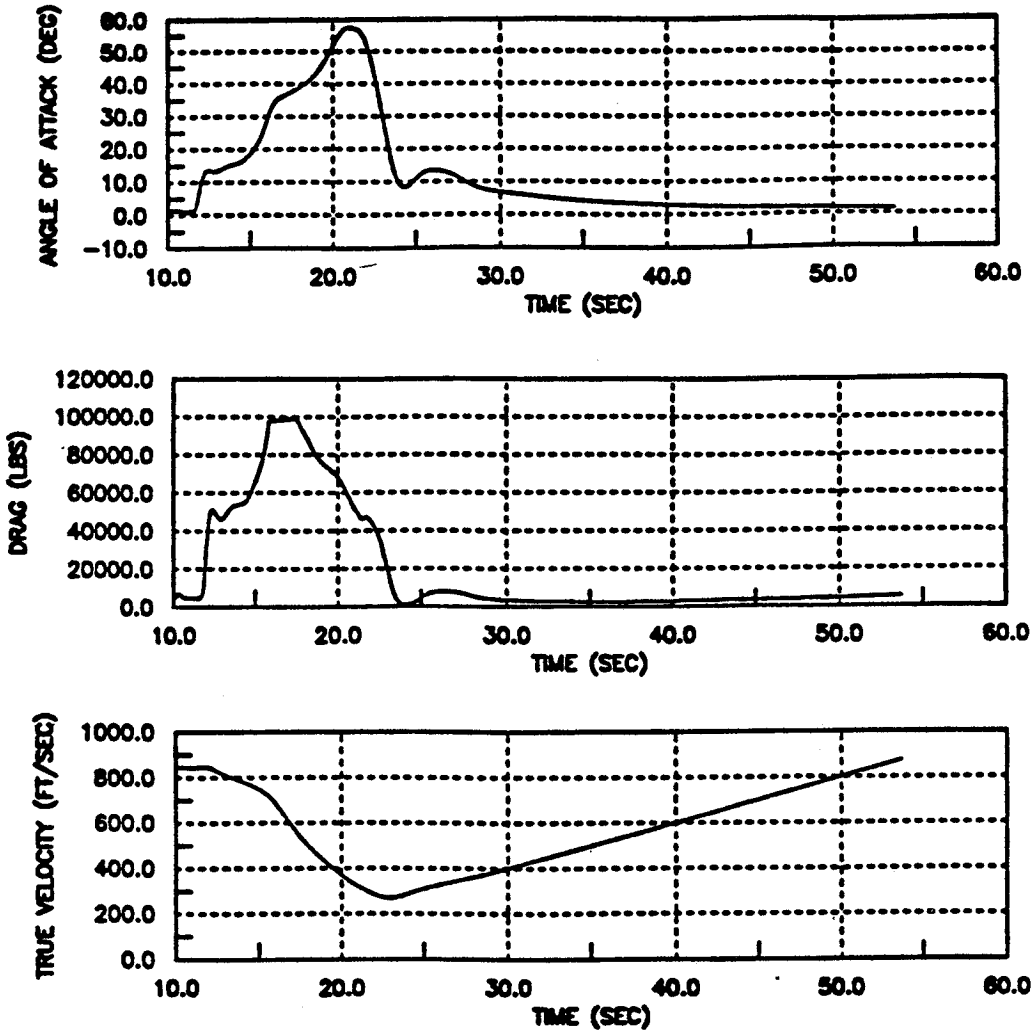

Figure 6.7 Generic F-18A Drag Build-Up And
Speed Loss During 180° Heading Change (REF. 43)

The maneuver segment times for each aircraft tested are presented graphically in Figure 6.9. The interested reader should consult Reference 49 for specific numeric values of the maneuver segment times. The only valid CCT comparison *between* aircraft is in the total numerical value for the complete combat cycle. The percentages of individual maneuver segment times to the total time for the combat cycle cannot be compared fairly between aircraft. This is due to differences in flight conditions for each aircraft during the maneuver segments. For example, referring to Figure 6.9 the generic F-18A and generic X-29A require nearly 70% of their

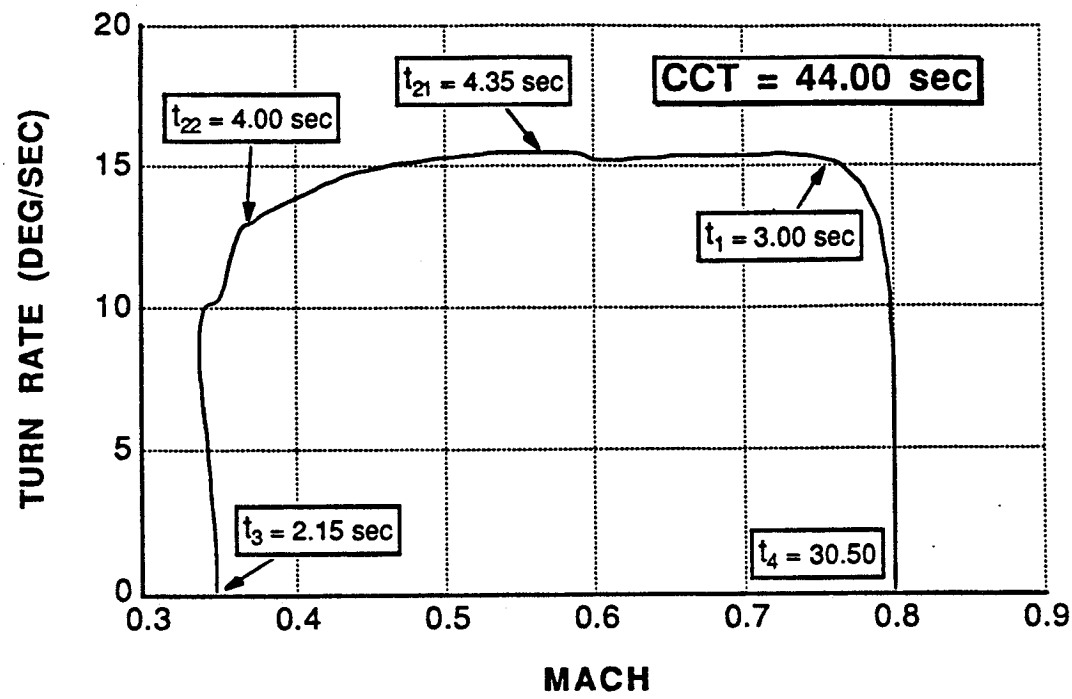

Figure 6.8 Generic X-29A 180° *Combat Cycle Time* Plot,
Mach = 0.8, H = 15,000 feet (REF. 49)

total CCT to accelerate back to the original energy level. Compare this to the approximately 35% for the generic F-5A and generic F-16A. This is not because the generic F-18A and generic X-29A are poorly accelerating aircraft, but because they begin the acceleration phase at a Mach number less than 0.35. In comparison, the generic F-5A and generic F-16A begin the acceleration phase at approximately Mach equals 0.55. This example highlights the drawback of attempting to determine relative advantages based solely on a comparison of maneuver segment times.

The total time required for each aircraft to complete the 180° combat cycle is shown in Table 6.1. The generic F-16A is indicated to be superior to the other three aircraft based on the total time to complete the maneuver. The generic F-16A achieves this advantage due to the angle of attack and normal load factor limiters. These limiters prevent the aircraft from experiencing large energy losses during the maneuver. The generic F-5A is the next best performer, in spite of suffering a reduction in turn rate from being below corner speed at the test Mach number.

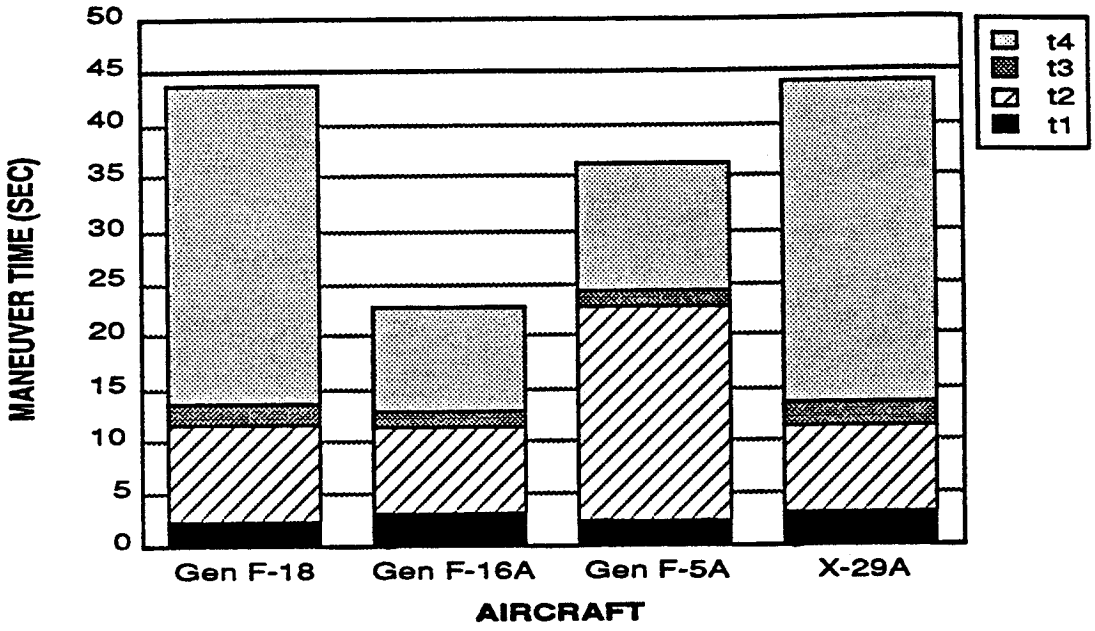

Figure 6.9 Maneuver Segment Times Of The Generic F-5A, F-16A, F-18A, and X-29A During A 180° *Combat Cycle Time* Maneuver Sequence (REF. 43)

Had the initial Mach number been higher, the generic F-5A would probably have performed better. Consequently, an even lower CCT value for the generic F-5A might have resulted had the initial Mach number been even lower. This result demonstrates that corner speed has a strong influence on the outcome of the CCT.

In spite of a longer CCT, the generic F-18A is nearly equal in performance to the generic F-16A during the first two phases of the combat cycle (t_1 and t_2). However, at the start of the acceleration phase both the generic F-18A and generic X-29A suffer from severe energy losses. This is largely due to the pilot command input scheme used for testing these aircraft, since angle of attack is permitted (unrealistically) to exceed that for maximum lift. Thus, the generic F-18A and generic X-29A are forced to perform in a manner which is disadvantageous for them.

Table 6.1 180° *Combat Cycle Times* For The Generic F-5A, F-16A, F-18A, and X-29A, Mach = 0.8, H = 15,000 feet

aircraft	Combat Cycle Time (sec)
generic F-5A	36.06
generic F-16A	22.73
generic F-18A	43.7
generic X-29A	44.

6.4.1.3 Combat Cycle Time 180° Heading Change Sensitivity

Figure 6.10 shows the generic F-18A 180° CCT plots for the three cases of heading change at maximum angle of attack, optimal total turn, and optimized total CCT. The data in Figure 6.10 is generated by the generic F-18A simulation using the angle of attack schedules specified by the OTIS program. The angle of attack time histories for each of the three sensitivity test cases is displayed in Figure 6.11. Considering the heading change at maximum angle of attack, although the new heading is reached in a very short time, the time spent regaining energy is almost 70% of the total maneuver time of 41.8 seconds. The energy is lost primarily during the turning segment to the new heading. During that segment, the angle of attack reached a maximum value of 50° (Figure 6.11), which is well above $C_{l\,max}$ for the F-18A.

Compared to the maximum angle of attack case, the optimal total turn test case results in

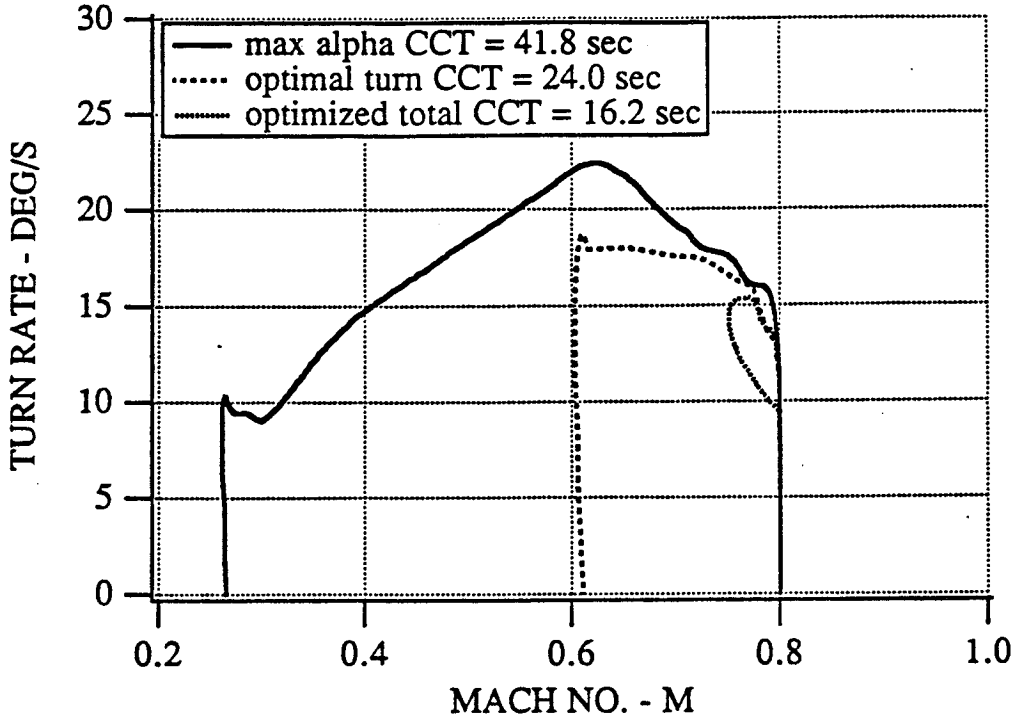

Figure 6.10 Generic F-18A 180° *Combat Cycle Time* Sensitivity, Mach = 0.8, H = 15,000 feet (REF. 42)

a 43% reduction in CCT by limiting the maximum angle of attack. Figure 6.11 shows that the angle of attack schedule specified by the OTIS program limits angle of attack to the range $11° \leq \alpha \leq 20°$, as opposed to the 50° maximum for the previous maneuver. The flattened appearance of the "doghouse" is due to the scheduling of angle of attack during the turn. The benefit of the scheduling is lower drag through the turn and therefore less energy loss. The Mach number is higher when the aircraft unloads and reaches 1g, reducing the amount of time it takes to regain the lost energy by 60%. The penalty for using the angle of attack schedule is a reduction in maximum turn rate. Since the aircraft must maintain a reduced turn rate longer, it is 20% slower in achieving the new heading than the maximum angle of attack case.

The total CCT for the optimal total time maneuver is 16.2 seconds, a 60% reduction compared to the maximum angle of attack case. The constraints for this case required that the

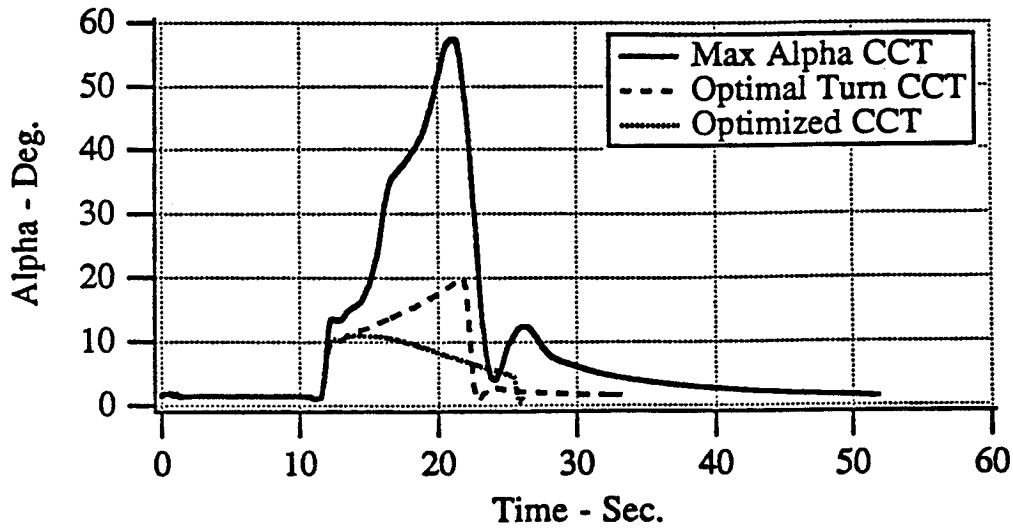

Figure 6.11 Generic F-18A 180° *Combat Cycle Time* Sensitivity
Angle Of Attack Comparison, Mach = 0.8, H = 15,000 feet (REF. 42)

velocity as the new heading is reached be equal to the initial velocity. This eliminates the 1g acceleration segment by combining the time to unload and the time to accelerate into one value. For the optimal total time test case, the "doghouse" plot no longer has its characteristic shape because the aircraft is decelerating in the first half of the turn, and accelerating in the second half. The CCT values for the generic F-18A nominal, heading change at maximum angle of attack, optimal turn, and optimal total time test cases are summarized Table 6.2.

6.4.1.4 Summary

In summary, the results presented here demonstrate that the turning (t_2) and acceleration (t_4) phases dominate the total CCT. The generic F-16A benefits from the angle of attack and normal load factor limiter, since it prevents the aircraft from experiencing large energy losses during the maneuver. The generic F-5A suffers a reduction in turn rate from being below corner

Table 6.2 Generic F-18A 180° *Combat Cycle Time*
Sensitivity Results, Mach = 0.8, H = 15,000 feet

test case	Combat Cycle Time (sec)
nominal	43.7
maximum angle of attack	41.8
optimal turn	24.
optimal total CCT	16.2

speed at the test Mach number. Had the initial Mach number been higher, the generic F-5A would probably have performed better. Consequently, a lower initial Mach number would probably result in a worse performance. These considerations demonstrate that corner speed has a strong influence on the outcome of the CCT, and should be kept firmly in mind when evaluating results obtained using this metric. At the start of the acceleration phase, both the generic F-18A and generic X-29A suffer from severe energy losses. This is largely due to the pilot command input strategy used for testing these aircraft, since angle of attack is permitted to (unrealistically) exceed that for maximum lift. Thus, the generic F-18A and generic X-29A are forced to perform at a disadvantage.

These results support the hypothesis in Reference 1 that the CCT metric is dominated by sustained capabilities such as turn rate and level acceleration. These capabilities are in turn dependent upon the traditional measures of merit of wing loading and thrust-to-weight ratio. Although it does not quantify transient agility, the CCT metric is useful in that it: i) provides a

measure of the ability of an aircraft to transition between sustained maneuver states and ii) stresses the importance of minimizing the time required to point the nose while keeping the significant energy losses associated with hard nose pointing maneuvers to a minimum.

The CCT metric is highly sensitive to the particular type of maneuver (nominal, maximum angle of attack, optimal turn, optimal total time) used to test it. The maneuver is dictated by the angle of attack schedule which is followed, which significantly affects measured values of the metric. Additionally, which maneuver is best from an operational standpoint is highly dependent on the combat situation. For example, from the context of operations the turn segment might likely involve a pitch up to bleed airspeed, followed by a descending slice back for gravity assist to help tighten the turn (REF. 52). Naturally, this technique might also vary somewhat according to the aircraft being flown.

Therefore when drawing conclusions, the combat utility of all three types of maneuvers must be carefully weighed against the particular objective or task the pilot is trying to accomplish. This also underscores the need to standardize test procedures in agility flight testing. If the optimal maneuvers had been used, the generic F-5A and generic F-18A would compare more favorably to the other aircraft since they would not have been forced into large energy loss situations.

6.4.2 **Combat Cycle Time 90° Heading Change** (REF. 30)

6.4.2.1 Definition

This metric is defined as the sum of: $t_1 + t_{21} + t_{22} + t_3 + t_4$

where t_1 = time to pitch from one g to the limit normal load factor

$t_{21} + t_{22}$ = time to turn to a specified new heading angle at maximum normal load factor

t_3 = time to unload to a normal load factor of either one or zero g

t_4 = time to accelerate to the original energy level

6.4.2.2 Discussion and Typical Results

This metric is completely analogous to the 180° CCT of Section 6.4.1, except that the specified new heading angle is 90 degrees. Results for the generic X-29A are not presented for the 90° CCT since the simulator was not available at the time the investigation was being conducted. The 90° CCT plot for the generic F-5A is shown in Figure 6.12. The 90° CCT for this aircraft is very similar to the results for the 180° CCT, in that all of the maneuvering occurs along the normal load factor limit line. This is because the 90 degree heading angle is captured before corner speed is reached.

Figure 6.13 shows the 90° CCT plot for the generic F-16A. Like the generic F-5A, this aircraft also maneuvers only along its normal load factor limit line, since the 90 degree heading angle is captured before corner speed is reached. The segment t_{22} is not applicable for the generic F-16A when performing the 90° CCT.

Figure 6.14 shows the 90° CCT plot for the generic F-18A. Like the generic F-5A and generic F-16A, the generic F-18A is seen to maneuver only along its normal load factor limit line for the same reason.

6.4.2.3 Combat Cycle Time 90° Heading Change Sensitivity

The sensitivity analysis for the 90° CCT metric is performed using the angle of attack schedules specified by the OTIS program. Because of the short time scale involved with the 90°

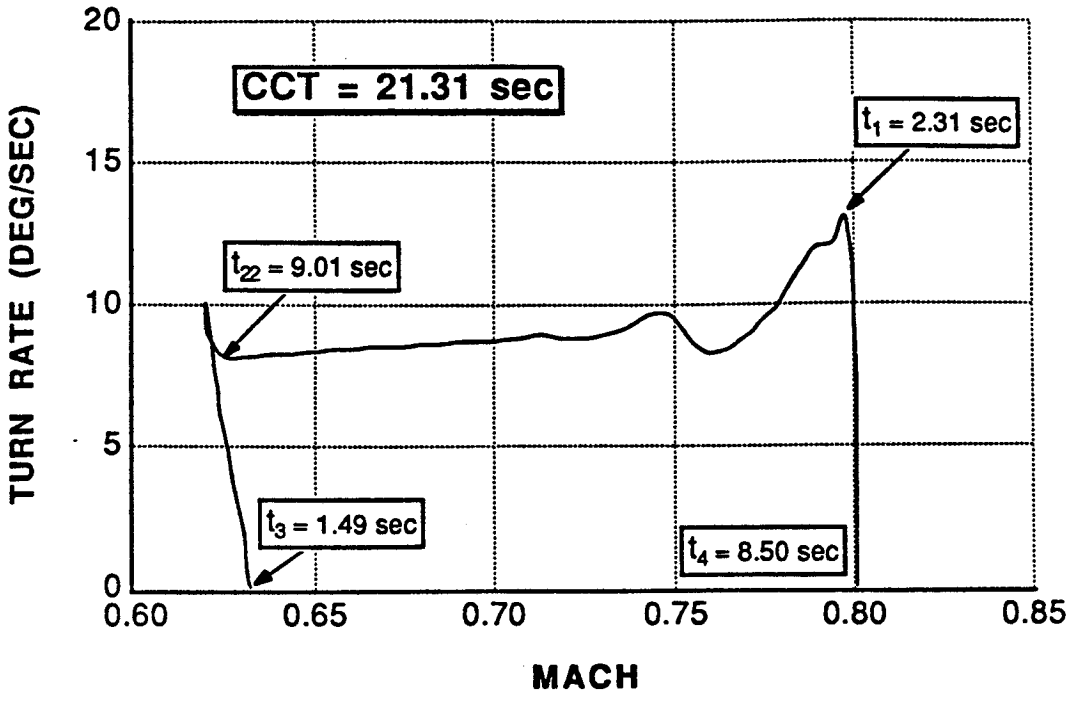

Figure 6.12 Generic F-5A 90° *Combat Cycle Time* Plot, Mach = 0.8, H = 15,000 feet (REF. 43)

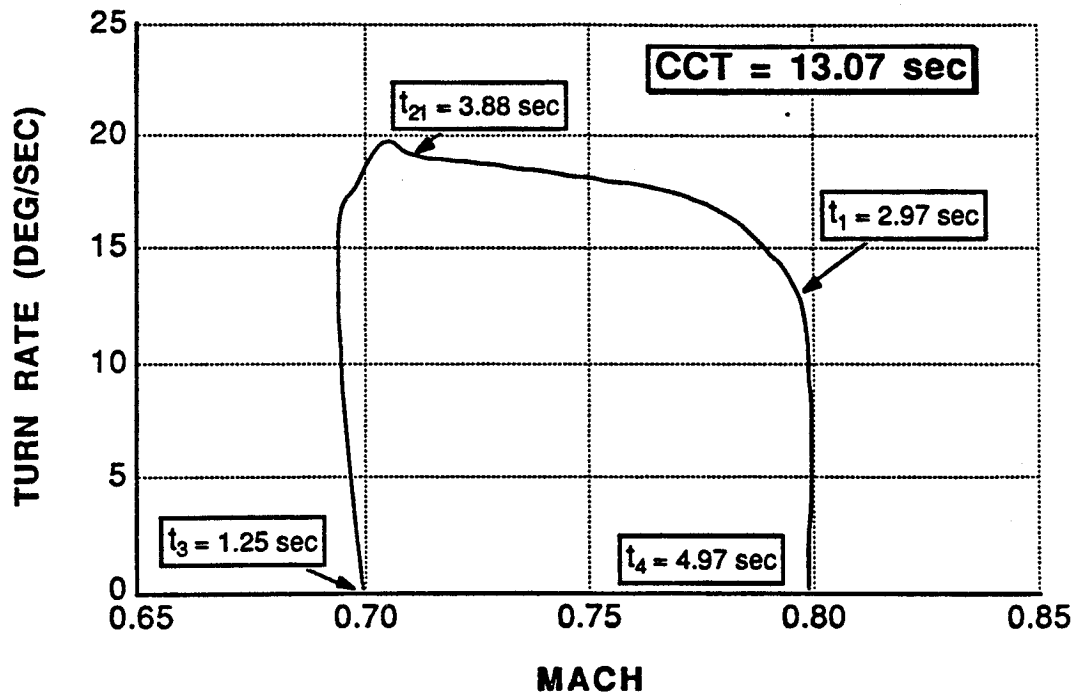

Figure 6.13 Generic F-16A 90° *Combat Cycle Time* Plot, Mach = 0.8, H = 15,000 feet (REF. 43)

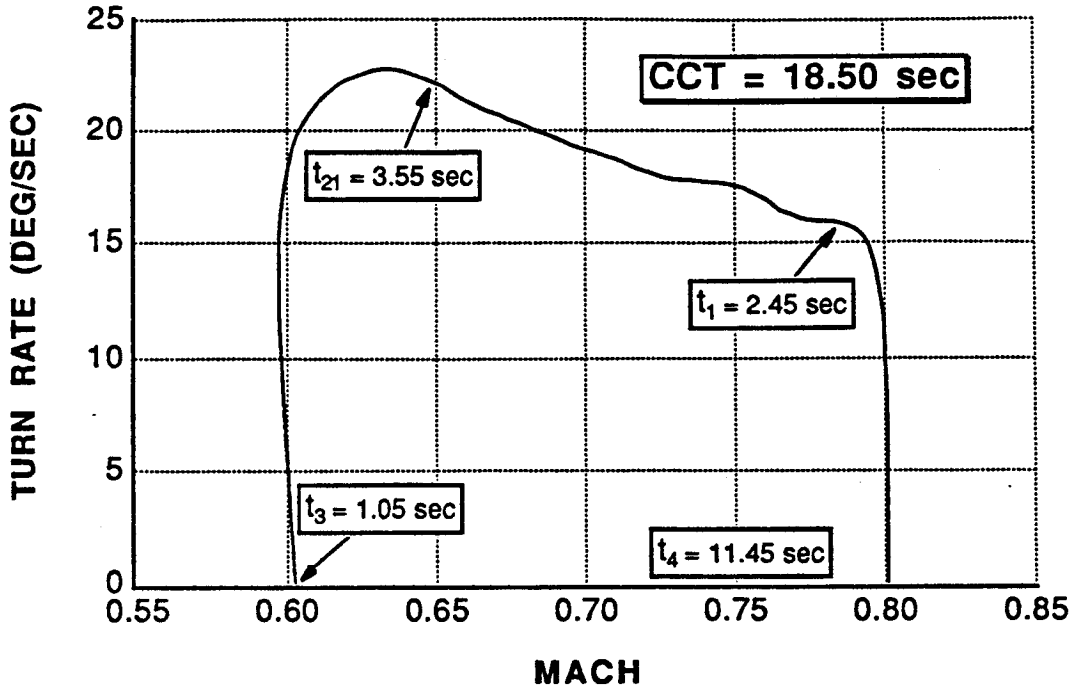

Figure 6.14 Generic F-18A 90° *Combat Cycle Time* Plot, Mach = 0.8, H = 15,000 feet (REF. 43)

maneuvers, changes in maneuver time for the different control strategies are not as pronounced. By turning only 90 degrees less energy is expended than in the 180 degree cases, and less time is needed to regain the lost energy. This has the effect of reducing the influence of the changes in angle of attack. The resulting maneuvers showed the same trends for the 90° CCT as for the 180° CCT sensitivity cases. For this reason data for the 90° CCT sensitivities are not presented in this report. The interested reader should consult Reference 53.

6.4.2.4 Summary

The 90° CCT metric does not appear to offer any distinct advantages over the 180° CCT metric. Comparing the 90° CCT results for the three aircraft, the generic F-18A fares much better

against the generic F-16A and F-5A for the 90 degree heading angle change because it is not commanded to as high an angle of attack as it was for the 180 degree case, thereby avoiding high energy bleed rates. The overall 90° CCT performance of the generic F-5A once again suffers because of its reduced turn rate capability, as it requires roughly twice as long as the other aircraft to complete the 90° turn.

6.4.3 **Dynamic Speed Turn** (REF. 47, 54)

6.4.3.1 Definition

plot of P_s versus maximum turn rate at a given starting airspeed.

6.4.3.2 Discussion and Typical Results

The intent of the *dynamic speed turn* metric is to capture the dynamic maneuvering capability of fighter aircraft (agility) as viewed from a pilots perspective, and to present that capability in a form which can be readily used by pilots and engineers. *Dynamic speed turn* plots show the dynamics of turning and acceleration over a wide range of speeds, combine the ability of the aircraft to point its nose, continue pointing its nose, and accelerate. This is accomplished by presenting information in the form of two distinct plots: one clearly showing the bleed rate for maximum acceleration turns, and another showing the straight and level acceleration capability at various airspeeds.

The *dynamic speed turn* plots for the generic F-5A, F-16A, F-18A, and X-29A are derived from the nominal 180° CCT maneuvers of Section 6.4.1. The generic F-5A *dynamic speed turn* plots are shown in Figure 6.15. Maneuvering along the normal load factor and lift limit lines is represented by Figure 6.15a, which plots turn rate versus bleed rate. The straight line acceleration

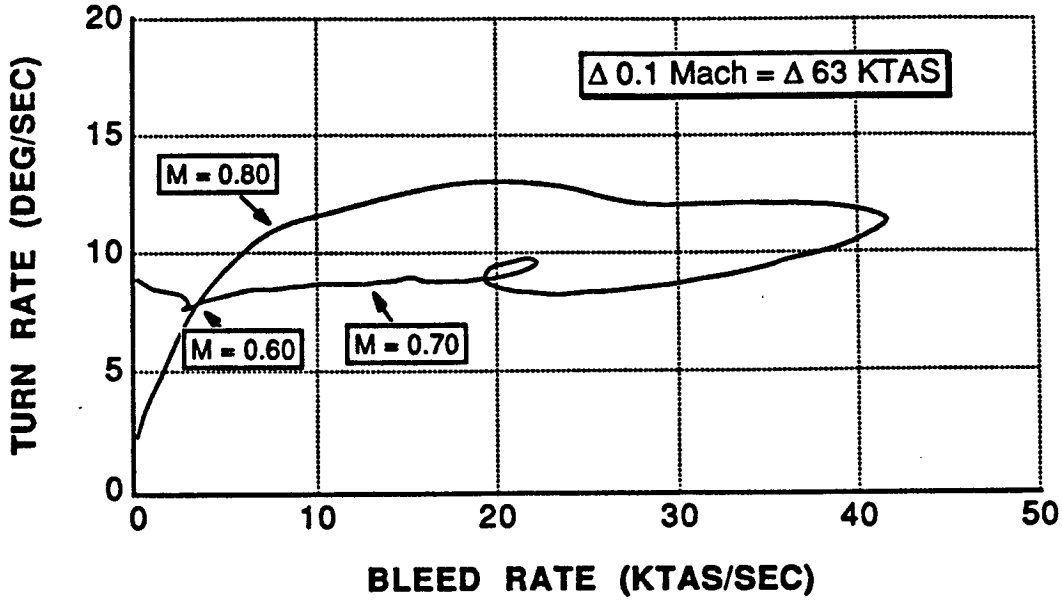

a) Turn Rate as a Function of Bleed Rate

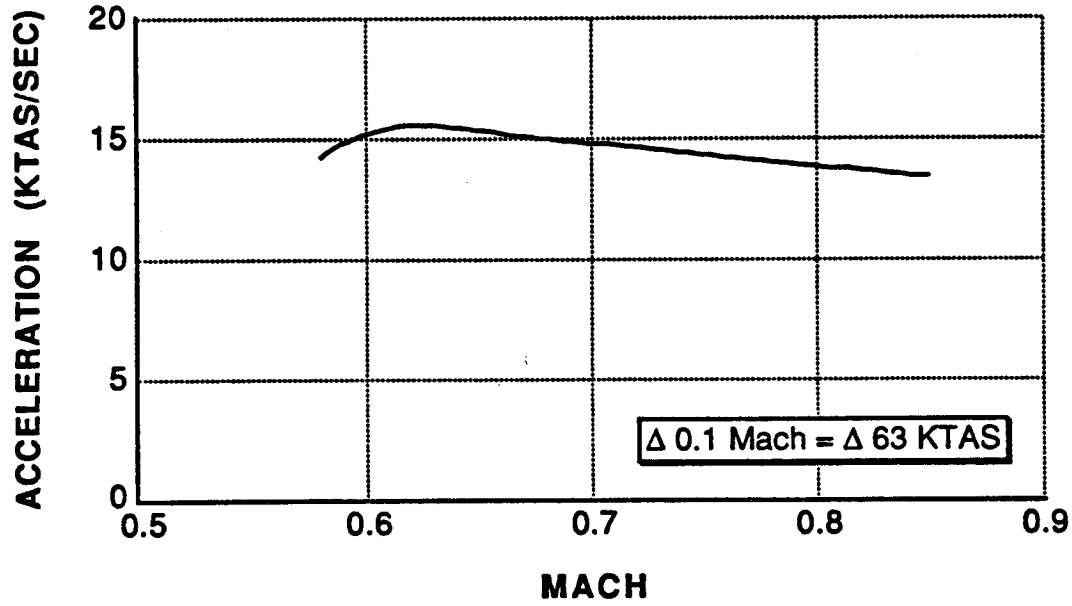

b) Acceleration as a Function of Mach Number

Figure 6.15 Generic F-5A *Dynamic Speed Turn* Plots, Mach = 0.8, H = 15,000 feet (REF. 43)

capability is shown by Figure 6.15b, which plots acceleration versus Mach number. Upon the initial full aft stick command, a large spike in normal load factor is generated causing a rapid onset of bleed rate. The generic F-5A quickly decelerates and the second smaller spike in load factor causes the loop in the plot just before Mach equals 0.7. The reduced maximum normal load factor at this flight condition not only reduces turn rate capability but also reduces bleed rates. Although the generic F-5A does not incur a large energy penalty, it cannot generate and maintain large turn rates during this maneuver. The level acceleration capability is approximately 15 KTAS per second, decreasing slightly at the high end of the subsonic Mach number range.

The *dynamic speed turn* plots for the generic F-16A are shown in Figure 6.16. The effect of the normal load factor limiting is exhibited in two features of the turn rate versus bleed rate plot. First, turn rate is increasing while the aircraft is decelerating. This is because the turn is performed essentially at a constant normal load factor. Second, since the limiter prevents the aircraft from attaining high angles of attack, flight regimes of excessive bleed rates are avoided, enabling the aircraft to maneuver at a nearly fixed bleed rate (15 KTAS per second). Upon decelerating to near corner speed, maximum turn rate is reached and is maintained for prolonged maneuvering. Figure 6.16 shows that the generic F-16A is capable of an essentially constant 15 KTAS per second acceleration capability across the high subsonic Mach number range.

Figure 6.17 shows the *dynamic speed turn* plots for the generic F-18A. The particular pilot command input strategy used for this investigation commanded the aircraft to a maximum angle of attack of 57° during the maximum performance turn. This lead to excessively large bleed rates in excess of 60 KTAS per second. At the higher Mach numbers, the aircraft is maneuvering along its normal load factor limit, and has a higher turn rate capability than at the lower Mach numbers. The notch in the bleed rate plot is caused by the increase in thrust as the throttle is ramped into afterburner.

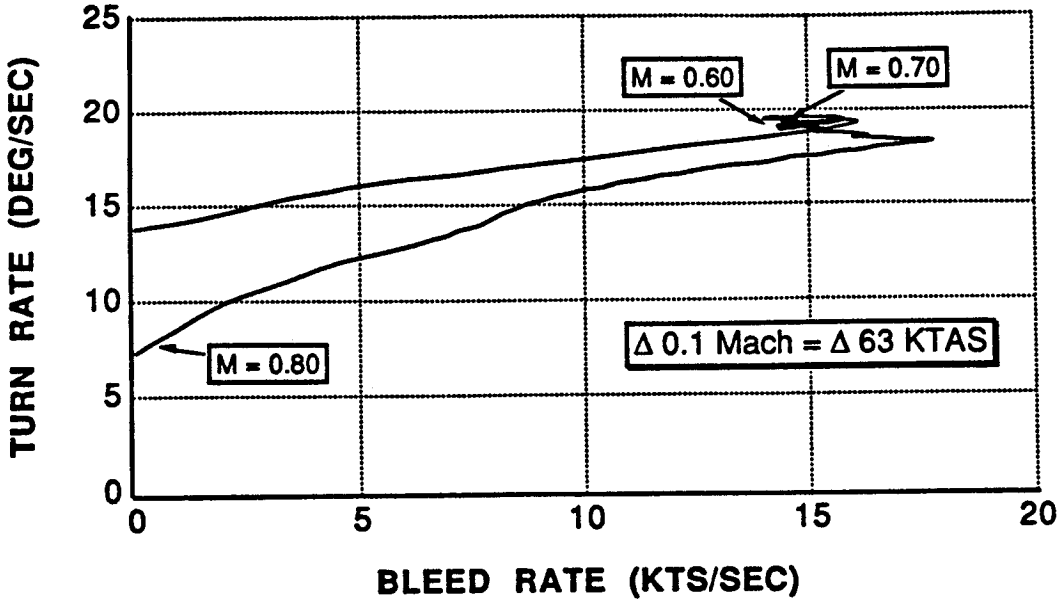

a) Turn Rate as a Function of Bleed Rate

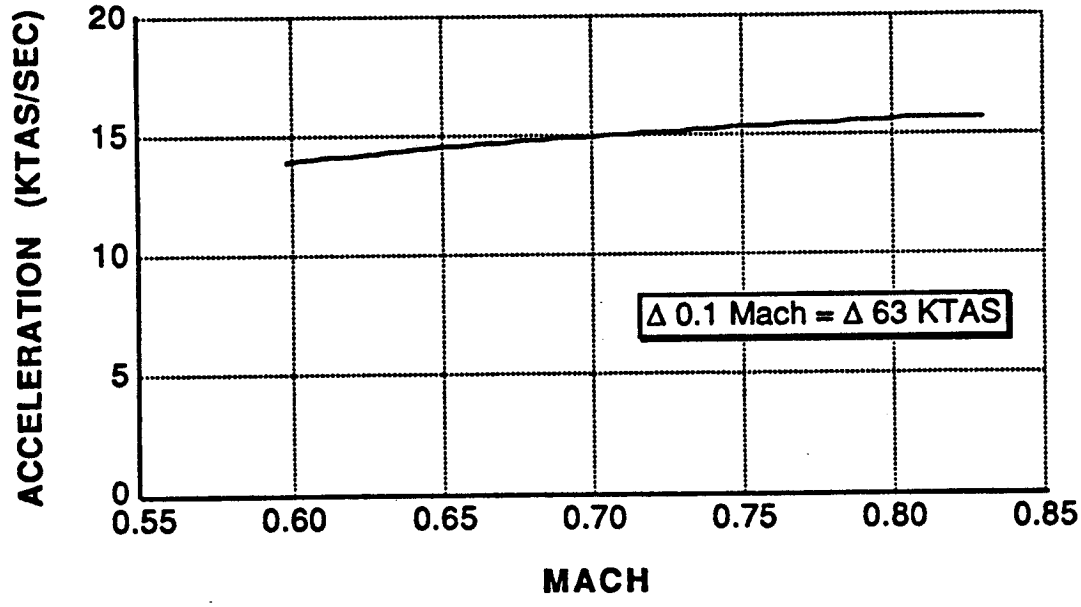

b) Acceleration as a Function of Mach Number

Figure 6.16 Generic F-16A *Dynamic Speed Turn* Plots, Mach = 0.8, H = 15,000 feet (REF. 43)

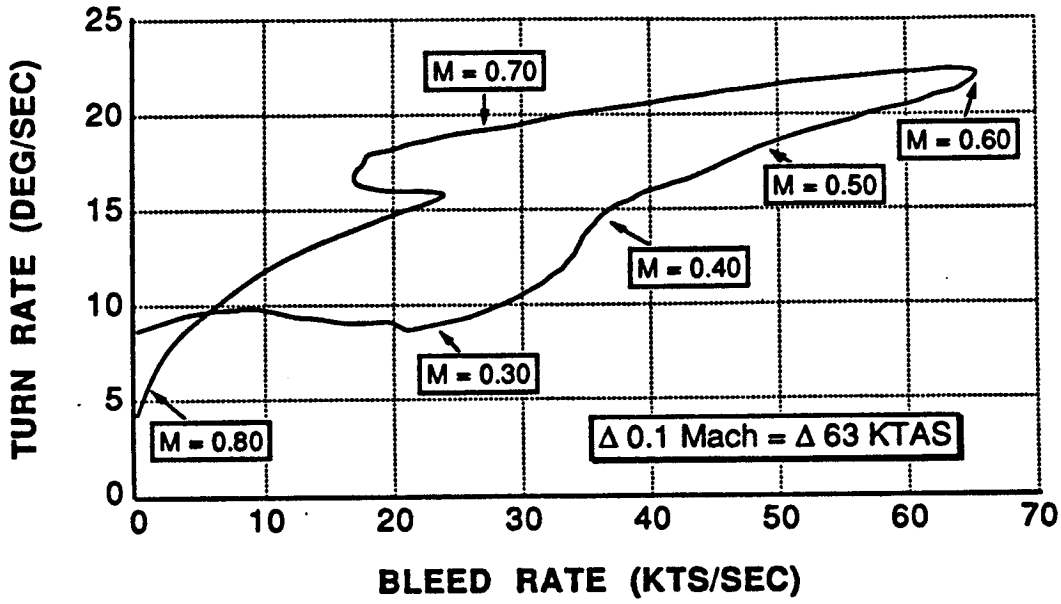

a) Turn Rate as a Function of Bleed Rate

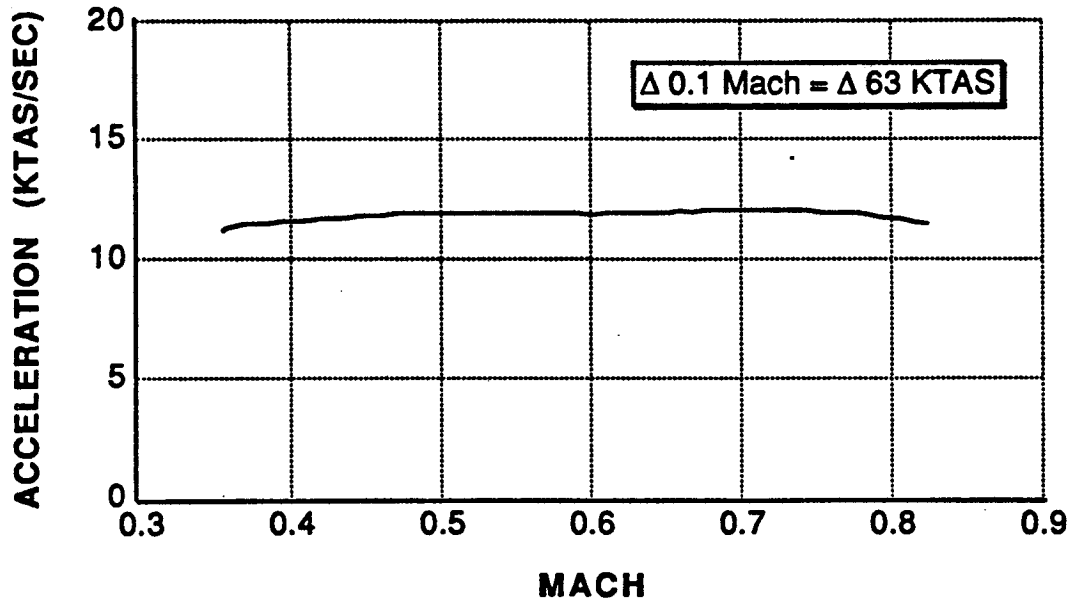

b) Acceleration as a Function of Mach Number

Figure 6.17 Generic F-18A *Dynamic Speed Turn* Plots, Mach = 0.8, H = 15,000 feet (REF. 43)

The generic X-29A *dynamic speed turn* plots in Figure 6.18 highlight the difference between the maneuver capability of that aircraft and the generic F-16A. Although both aircraft have a flattened doghouse plot, the 30 KTAS per second bleed rate of the generic X-29A is nearly twice that of the generic F-16A during the entire turn. This comparison demonstrates that the generic X-29A may not be capable of achieving its maximum (theoretical) turn rate, whereas the generic F-16A could do so were it not for the angle of attack and normal load factor limiters. To a large extent the inability of the generic X-29A to sustain a high normal load factor is due to the higher angles of attack (and thus higher drag) attained by the generic X-29A during the turn, and to a lesser extent by thrust-to-weight considerations (REF. 43). The generic X-29A level acceleration capability is approximately 10 to 12 KTAS per second across the mid to high subsonic Mach number range.

Perhaps the most useful feature of the *dynamic speed turn* plots is the ability to clearly compare the maneuver capability of dissimilar aircraft. For the purpose of relative comparison between the four aircraft, the respective *dynamic speed turn* plots are superimposed into a single combined *dynamic speed turn* plot in Figure 6.19. The turn rate versus bleed rate plot shows that an aircraft maneuvering in the region upwards and to the left side of the plot is desirable as this indicates a high turn rate capability at low bleed rates. The generic F-16A appears to dominate as it has a higher turn rate and lower bleed rate than either the generic F-5A, F-18A, or X-29A. In terms of acceleration capability the generic F-5A and generic F-16A are comparable, exceeding the generic F-18A and generic X-29A by approximately 2 to 3 KTAS per second. Although the X-29A exhibits lower bleed rates than the generic F-18A, its acceleration capability is several KTAS per second less than the generic F-18A for the low subsonic Mach numbers. This results in equivalent values for the CCT.

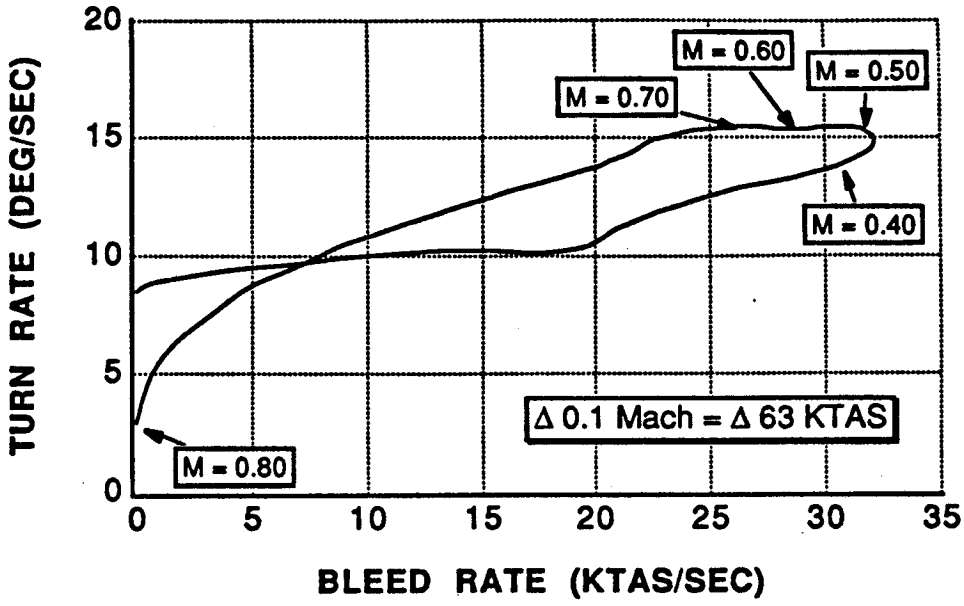

a) Turn Rate as a Function of Bleed Rate

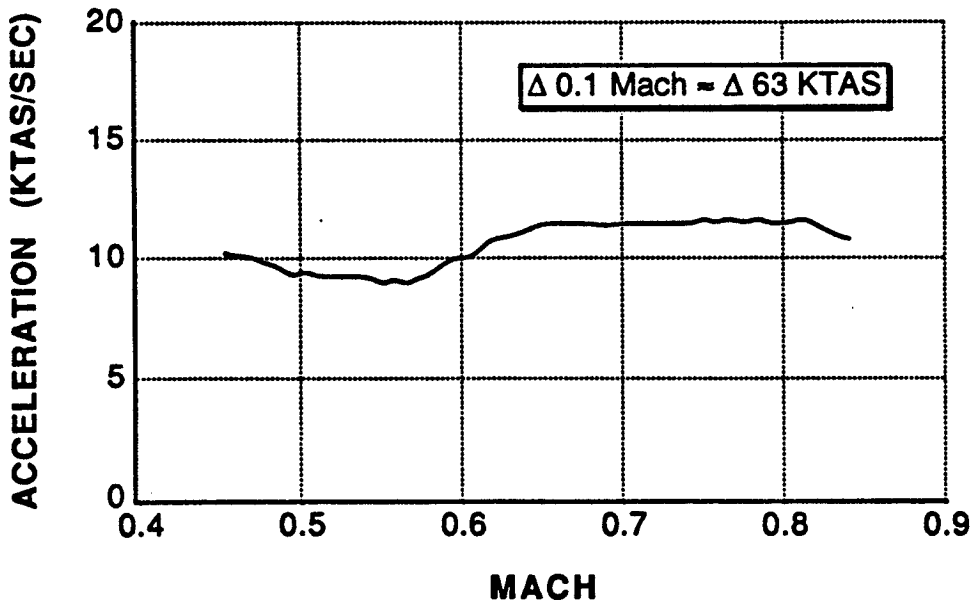

b) Acceleration as a Function of Mach Number

Figure 6.18 Generic X-29A *Dynamic Speed Turn* Plots, Mach = 0.8, H = 15,000 feet (REF. 43)

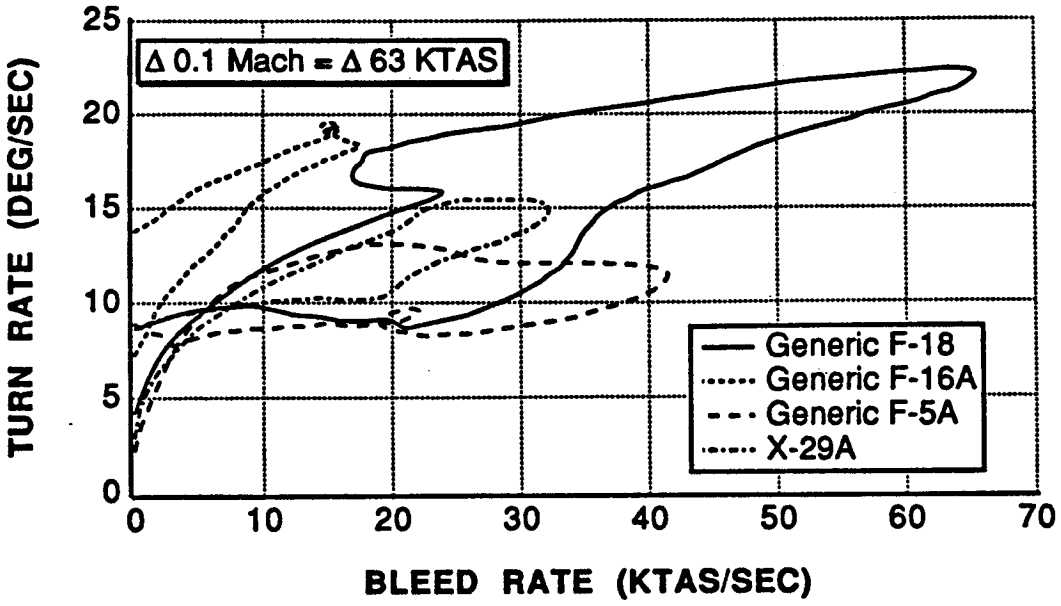

a) Turn Rate as a Function of Bleed Rate

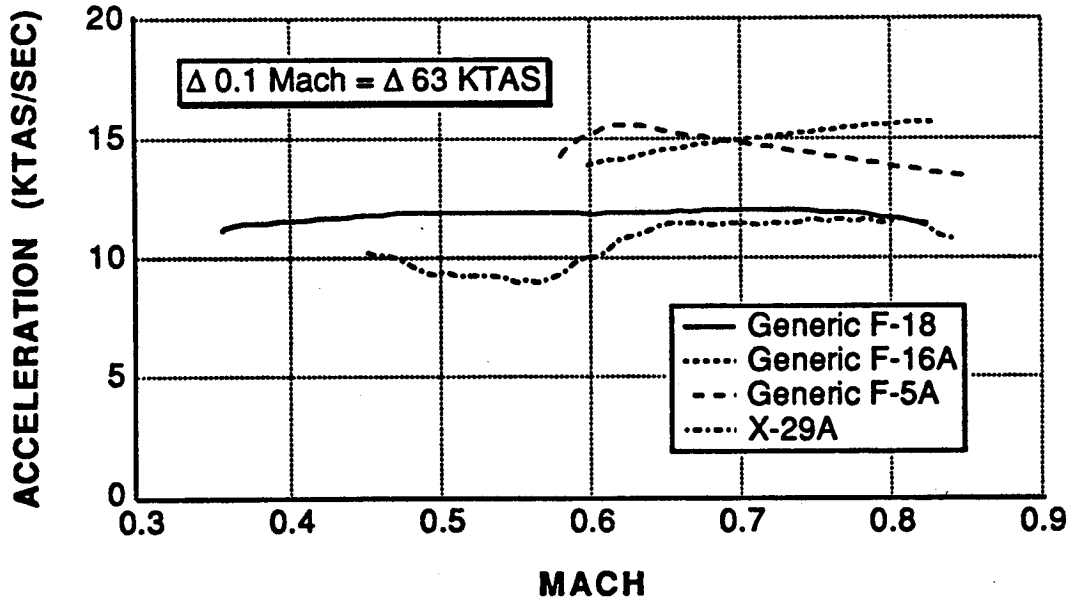

b) Acceleration as a Function of Mach Number

Figure 6.19 Comparison Of Generic F-5A, F-16A, F-18A, and X-29A *Dynamic Speed Turn* Plots, Mach = 0.8, H = 15,000 feet (REF. 49)

6.4.3.3 Dynamic Speed Turn Sensitivity

The sensitivity of the *dynamic speed turn* metric to pilot command input strategy is determined using the generic F-18A and the OTIS program. Figure 6.20 shows the generic F-18A *dynamic speed turn* plots for the three cases of heading change at maximum angle of attack CCT, optimal total turn CCT, and optimized total CCT. The data in Figure 6.20 is generated by the generic F-18A simulation using the angle of attack schedules specified by the OTIS program for the 180° CCT.

Considering the turn rate versus bleed rate plot first, the desirable test case is defined here as the one which results in minimal bleed rates but still allows a high turn rate. This produces a good combination of low maneuver time and low energy loss. The maximum angle of attack CCT test case demonstrates the consequence of maneuvering at high angle of attack. The bleed rates are in excess of 60 KTAS per second during the maneuver, since the aircraft decelerates from Mach equals 0.8 to Mach equals 0.25. It is evident from Figure 6.20 that the optimal turn CCT test case achieves a high value of turn rate, yet produces a lower bleed rate than the maximum angle of attack CCT test case. The optimal total CCT test case reduces bleed rates even further, but does not achieve maximum turn rate until the end of the maneuver. The flat appearance of the slope is due to the scale used to plot the graph. The energy efficiency is evidenced by the very small loss of airspeed during the turning portion of the maneuver. The optimal total CCT test case also shows that the maximum bleed rate for this maneuver is only 12 KTAS per second, compared to the 60 KTAS per second for the maximum angle of attack CCT test case. The optimal total CCT test case and the optimal turn CCT test case both show that by performing the maneuver at lower angles of attack, the maximum bleed rate is approximately 20 KTAS per second, compared to the 60 KTAS per second for the maximum angle of attack CCT test case.

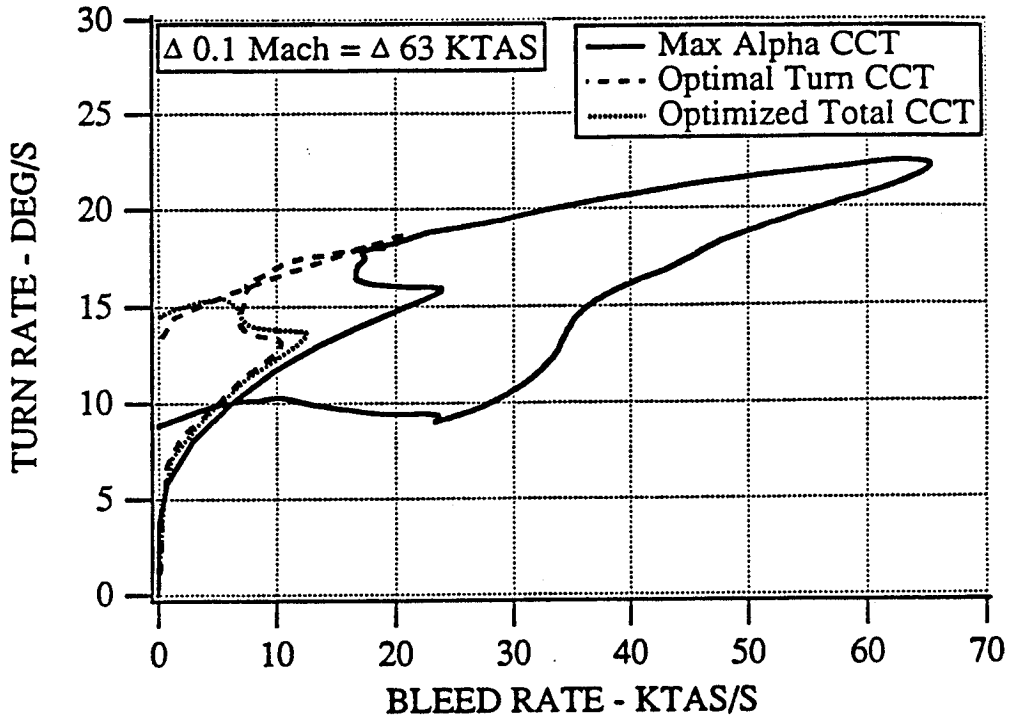

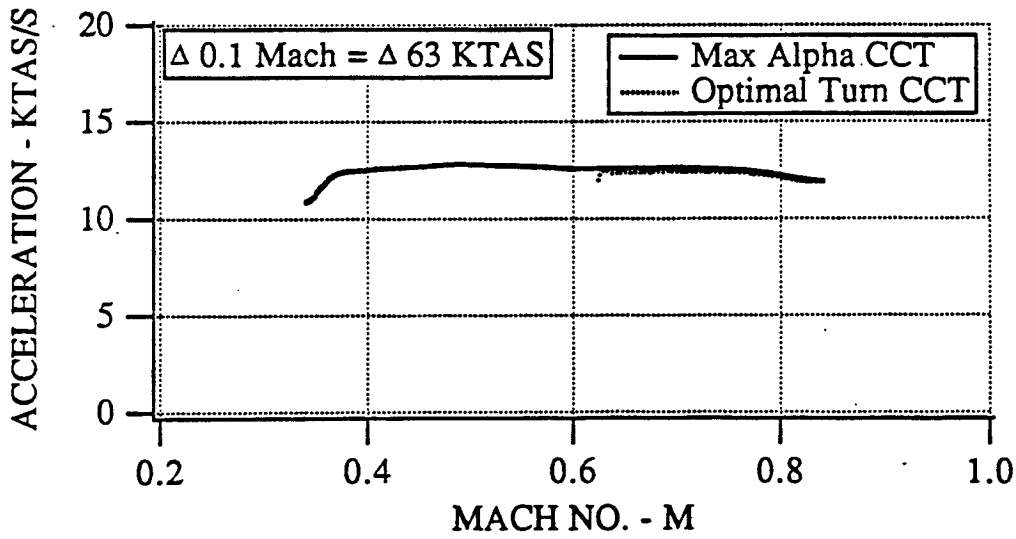

Figure 6.20 Generic F-18A *Dynamic Speed Turn* Sensitivity, Mach = 0.8, H = 15,000 feet (REF. 42)

The acceleration versus Mach number plot in Figure 6.20 for the maximum angle of attack CCT test case shows that the generic F-18A is capable of a straight and level acceleration of 12 KTAS per second, or a sustained acceleration of approximately 0.6 g. This information is useful for estimating how long it will take the pilot to regain lost energy at a given flight condition. The optimal turn CCT test case shows that the generic F-18A accelerates straight and level at about 12 KTAS per second for this maneuver. This test case matches the plot for the maximum angle of attack CCT test case since the generic F-18A is at full throttle, indicating that the maximum straight and level acceleration for the generic F-18A at 15,000 ft is approximately 12 KTAS per second. The optimal total CCT test case shows the generic F-18A to be accelerating at its maximum capability of approximately 12 KTAS per second for this test case, which is again virtually identical to the other two test cases. It is interesting to note that this angle of attack schedule results in a maximum bleed rate of 12 KTAS per second, which is equal to the maximum level acceleration of the aircraft.

In terms of the *dynamic speed turn* metric, the 180° optimal total CCT is judged to be the best command input strategy. This is in spite of the fact that the optimal total CCT test case is actually slower in reaching the final heading angle.

A similar *dynamic speed turn* analysis using the 90° CCT cases (REF. 53) showed that the maneuver time is too small to allow the bleed rate to increase to a significant level. The turn rate versus bleed rate plots for these maneuvers are not included since they are almost identical to Figure 6.20. The acceleration of the aircraft is not changed appreciably from the previous test cases, and the different control strategies do not yield significant changes in the shape of the plots.

6.4.3.4 Summary

The *dynamic speed turn* metric provides useful information regarding maneuver capabilities. The two plots relate maneuverability to three combat relevant tasks:

1. The ability to point the nose of the aircraft
2. The ability to continue pointing the aircraft quickly, i.e. residual turn rate.
3. The capability to disengage or regain speed.

As indicated in Section 6.4.3.3, the generic F-18A and generic X-29A incur large energy losses during the 180° turn reversal because they are commanded to maneuver at high angles of attack. These high angles of attack are a direct result of the pilot command input strategy used. The generic F-16A is able to avoid incurring large energy losses with the same basic pilot command input strategy because of its angle of attack limiter. However, this same angle of attack limiter also restricts the maximum maneuver potential of the generic F-16A. In limiting the maximum angle of attack for this maneuver, a trade-off occurs between energy preservation (lower bleed rates) versus the effectiveness of high angle of attack maneuvering (rapid heading angle changes). Another consideration is that these maneuvers generate significant downrange and crossrange distances, which could be significant.

The pilot command input strategy to use for the best *dynamic speed turn* results is defined as that which results in the maximum angle of attack for which increasing turn rates at the expense of increased bleed rates results in diminshing returns (REF. 47). Performing the *dynamic speed turn* at this angle of attack maximizes maneuver potential while minimizing energy losses. The sensitivity analysis for this metric shows that the 180° optimal total CCT test case produces the angle of attack schedule for the best *dynamic speed turn* performance.

6.4.4 **Relative Energy State (V/V_c)** (REF. 30)

6.4.4.1 Definition

The ratio of the aircraft's speed to its corner speed at the completion of a 180° turn at maximum normal load factor from a given starting position (altitude and airspeed). This ratio, V/V_c, should be as close to 1.0 as possible.

6.4.4.2 Discussion and Typical Results

The *relative energy state* metric is intended to quantify the capability of an aircraft engaged in WVR air combat to execute multiple 90 degree turns. The presentation of this metric consists of plots of the ratio of aircraft speed to corner speed for various heading angle changes. In testing the *relative energy state* metric, the number of 90 degree turns an aircraft is required to execute is not specified by the definition of the metric. However, the author of this metric suggests in Reference 30 that at least two 90 degree turns be completed before the speed of the aircraft falls below corner speed. When an aircraft is flying below corner speed, it has in essence maximized pointing capability, while exhausting maneuvering potential. Conversely, when flying above corner speed, an aircraft retains energy for future maneuvering while sacrificing maximum pointing capability (REF. 49).

Data for the *relative energy state* metric is obtained directly from the 180° CCT maneuver of Section 6.4.1. The *relative energy state* for the generic F-5A, generic F-16A, generic F-18A, and generic X-29A is plotted versus heading angle in Figure 6.21. From Figure 6.21 it is seen that the generic F-18A loses speed during the turn reaching a *relative energy state* of 0.62 at 180°, whereas the generic F-16A is seen to maintain its speed relatively well with a final *relative energy state* of 0.92. The X-29A loses airspeed at a constant rate throughout the heading change with the *relative energy state* remaining above 1.0 for the first 90° turn, and then reaching a value of 0.70 by the end of the second turn.

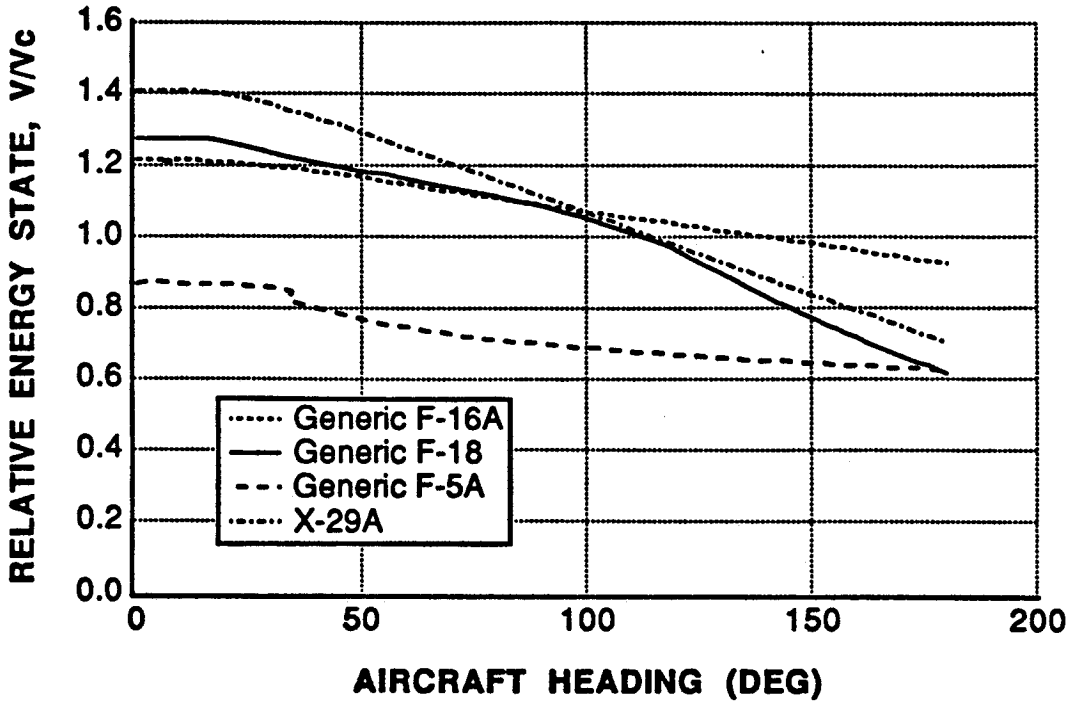

Figure 6.21 Generic F-5A, F-16A, F-18A, And X-29A *Relative Energy State* For Various Heading Angles, Mach = 0.8, H = 15,000 feet (REF. 49)

Comparison of the generic F-5A to the other three aircraft is difficult using *relative energy state* in this speed range since the generic F-5A has a much higher corner speed.

During the maneuver, the generic F-16A and generic F-5A retain nearly 75% of their original velocity, whereas the generic F-18A and generic X-29A lose over one half of their initial velocity. The primary cause is the difference in angle of attack (and therefore induced drag) during the turn for each aircraft (Figure 6.22).

6.4.4.3 Relative Energy State Sensitivity

The sensitivity of the *relative energy state* metric to pilot command input strategy is determined using the generic F-18A and the OTIS program. Figure 6.23 shows the generic F-

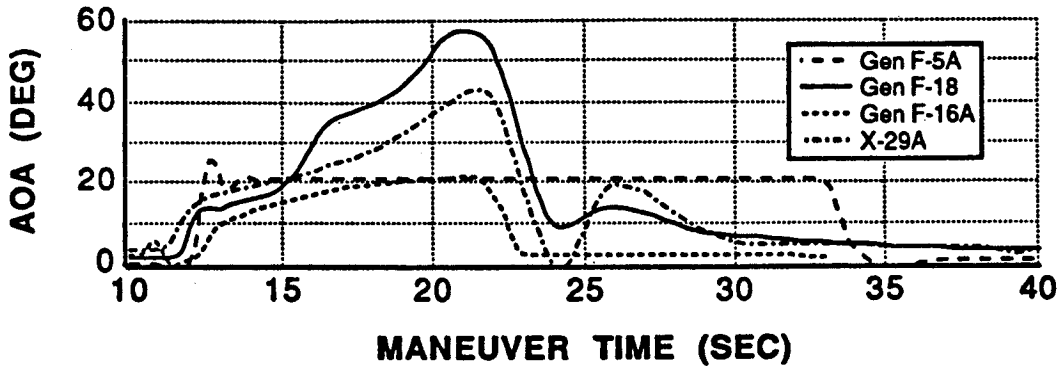

Figure 6.22 Comparison Of Generic F-5A, F-16A, F-18A, And X-29A Angle Of Attack Time Histories For A 180° Turn, Mach = 0.8, H = 15,000 feet (REF. 43)

F-18A *relative energy state* plots for the three cases of heading change at maximum angle of attack CCT, optimal total turn CCT, and optimized total CCT. The data in Figure 6.23 is generated by the generic F-18A simulation using the angle of attack schedules specified by the OTIS program for the 180° CCT.

Figure 6.23 indicates that the maximum angle of attack CCT test case allows the generic F-18A to execute only one 90 degree turn before speed drops below corner speed. The heading angle at which corner speed is reached is approximately 110 degrees. The ramification of this result is that by pulling and holding full aft stick, only one turn will be completed before the pilot will have to unload and accelerate to regain the depleted energy.

By limiting angle of attack as in the optimal turn CCT test case, the generic F-18A does not drop below corner speed until the heading angle has changed by 180 degrees. The optimal turn CCT test case indicates that the generic F-18A can perform two 90 degree heading changes (two turns) before falling below maximum turn rate and degrading the nose pointing ability.

The angle of attack schedule specified by the optimal total CCT test case ensures that the generic F-18A stays above corner speed throughout the maneuver, and returns back to the initial ratio of just over 1.2. This is because the OTIS program is asked to provide a trajectory which

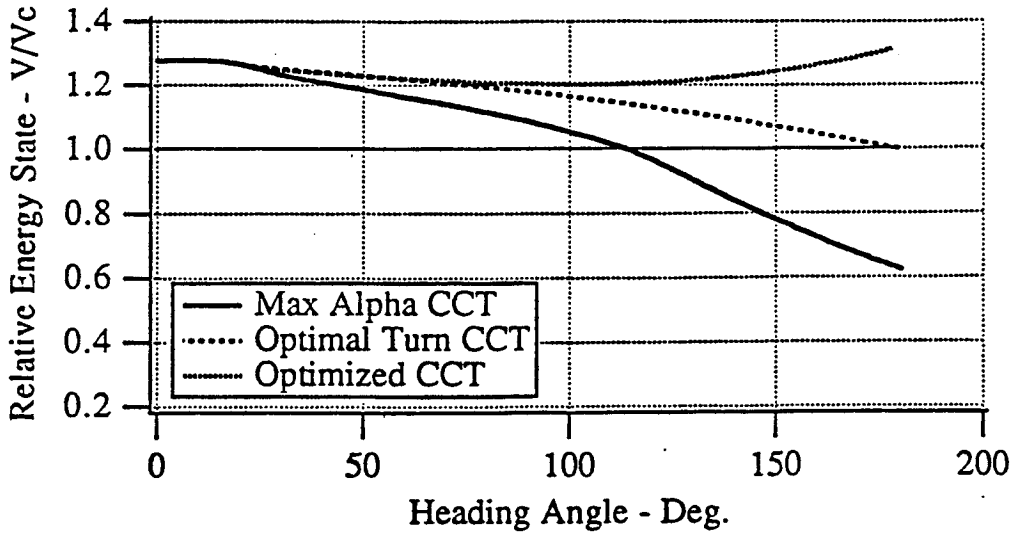

Figure 6.23 Generic F-18A *Relative Energy State* Sensitivity, Mach = 0.8, H = 15,000 feet (REF. 42)

both changes the heading angle by 180 degrees, and has the same initial and final velocity.

In terms of the *relative energy state* measure of merit, the optimal total CCT test case is the most desirable pilot command input strategy. This result is consistent with those in Sections 6.4.1 through 6.4.3, and demonstrates that these metrics all heavily weigh maneuver time and energy loss, even at the expense of turn radius.

6.4.4.4 Summary

The *relative energy state* metric provides a means for comparing the energy conservation of dissimilar aircraft that have similar corner speeds. This comparison typifies the need for an aircraft to quickly decelerate to corner speed while controlling its bleed rate. The benefit of this capability is the larger heading angle changes possible with extended maneuvering at or near corner speed. This metric is dominated by thrust and drag characteristics, but neglects turn rate

and thus the time required to complete the 180 degree turn.

The *relative energy state* metric is sensitive to the pilot command input strategy used to test it. The best values of *relative energy state* are obtained when using an angle of attack schedule like that specified by the optimal total CCT test case. Although it is possible to test in flight, the *relative energy state* metric seems best suited for early design studies. It would most appropriately be used in optimization routines to examine parameter variation effects on maneuvering performance.

6.4.5 **Energy-Agility** (REF. 5)

6.4.5.1 Definition

The specific energy of an aircraft during the time required to complete a maneuver, plotted as a function time.

6.4.5.2 Discussion and Typical Results

The *energy-agility* metric attempts to model the time to kill (t_k), defined as the time required to reach a heading angle of 180 degrees, the time to recover, and the energy compromised, as an engineering tool. The author of this metric defines *energy-agility* as characterizing the capability of minimizing both the time and energy penalties, while directly seeking a useful positional advantage. The graphical display of *energy-agility*, presented in the form of a plot of specific energy versus time, indicates both the amount of energy lost, and at what point in the maneuver the energy losses occur. The task associated with the *energy-agility* metric has relevance because it is a quantitative outgrowth of the traditional angles and energy fight scenario of air combat (REF. 55).

Data for the *energy-agility* metric is obtained directly from the 180° CCT maneuver of Section 6.4.1. The *energy-agility* of the generic F-5A, generic F-16A, generic F-18A, and generic X-29A is plotted in Figures 6.24 through 6.27. Figure 6.24 indicates that the generic F-5A performs most of its turn at low bleed rates. However, the extended time at these conditions (i.e., low turn rate) still results in a considerable energy loss. The better energy efficiency of the generic F-16A in Figure 6.25 can be attributed to the angle of attack and normal load factor limiters which help it avoid the high energy bleed rate regions of the doghouse plot. Consistent with the discussion of excessive bleed rates in Sections 6.4.3 and 6.4.4, the generic F-18A (Figure 6.26) and generic X-29A (Figure 6.27) quickly deplete a large amount of energy respectively. Comparing *energy-agility* results between each aircraft, the generic F-16A expends approximately 50% less energy-time as the generic F-5A, and 25% less energy-time than either the generic F-18A or the generic X-29A.

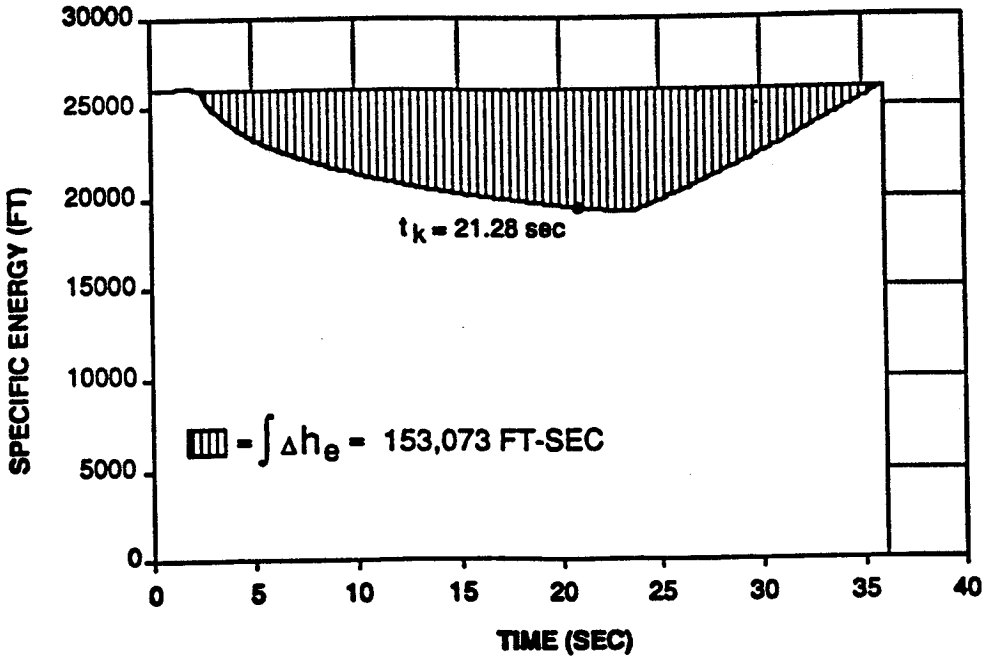

Figure 6.24 Generic F-5A *Energy-Agility* Plot, Mach = 0.8, H = 15,000 feet (REF. 43)

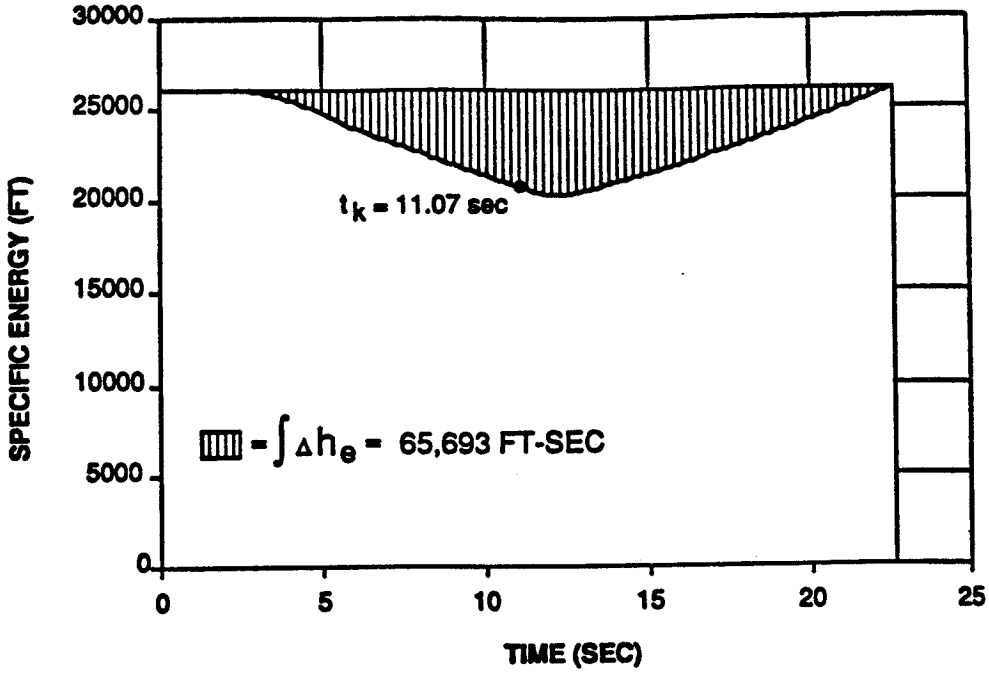

Figure 6.25 Generic F-16A *Energy-Agility* Plot, Mach = 0.8, H = 15,000 feet (REF. 43)

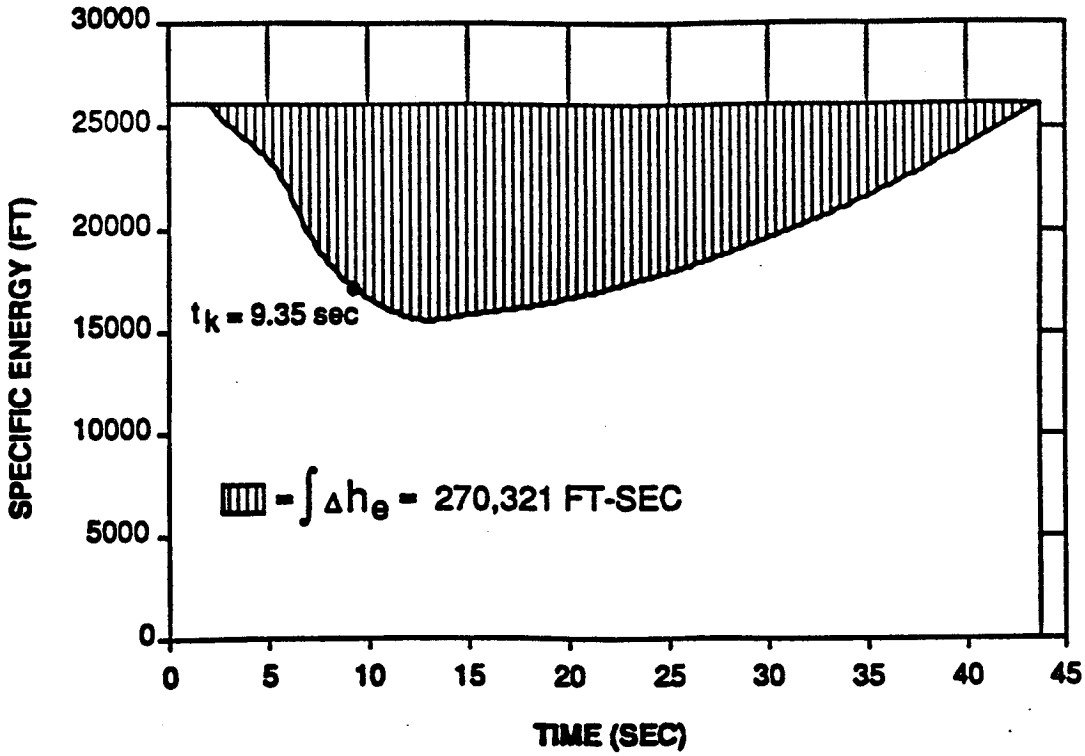

Figure 6.26 Generic F-18A *Energy-Agility* Plot, Mach = 0.8, H = 15,000 feet (REF. 43)

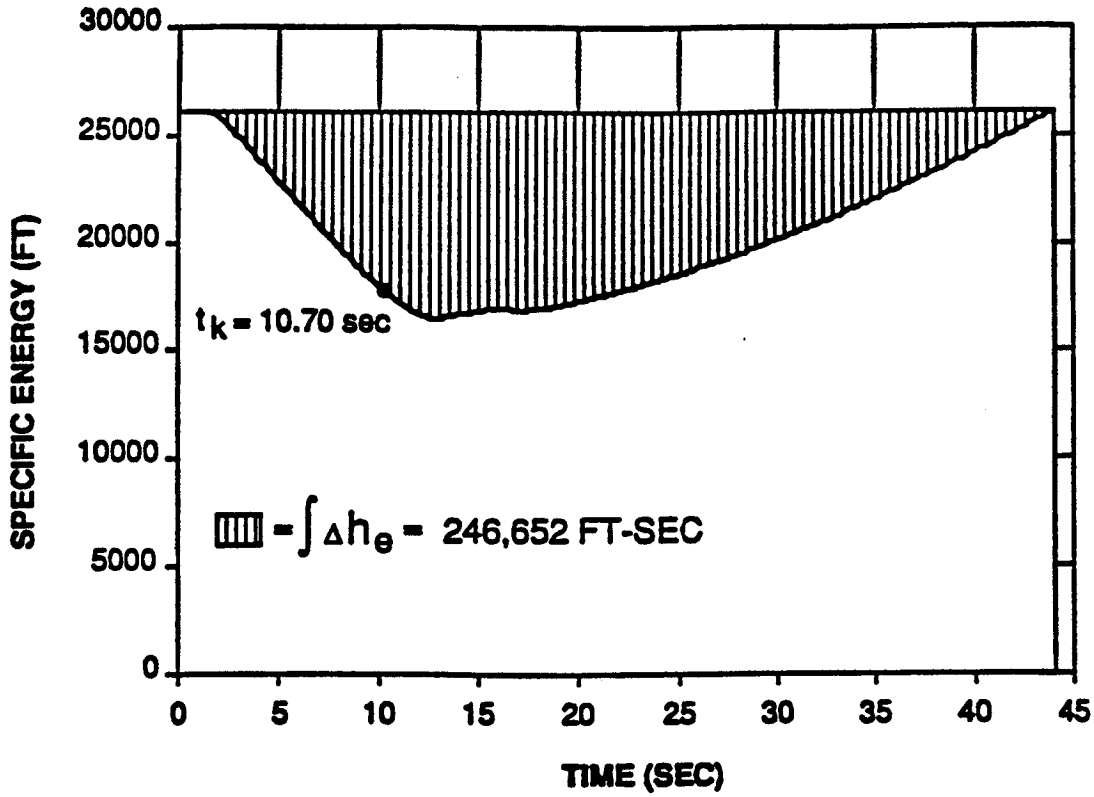

Figure 6.27 Generic X-29A *Energy-Agility* Plot, Mach = 0.8, H = 15,000 feet (REF. 43)

As shown in each of Figures 6.24 through 6.27, the time to kill is not necessarily coincident with the time for minimum energy. Overshoot is required so that upon unloading from the elevated angle of attack or normal load factor condition, the flight path vector is aligned at $\Psi = 180°$. This fact is evidenced by Figure 6.28. The overshoot (the amount of which depends on the angle of attack achieved during the turn) is the cause of the time difference between the time to kill and the point of minimum energy.

6.4.5.3 Energy-Agility Sensitivity

The sensitivity of the *energy-agility* metric to pilot command input strategy is determined

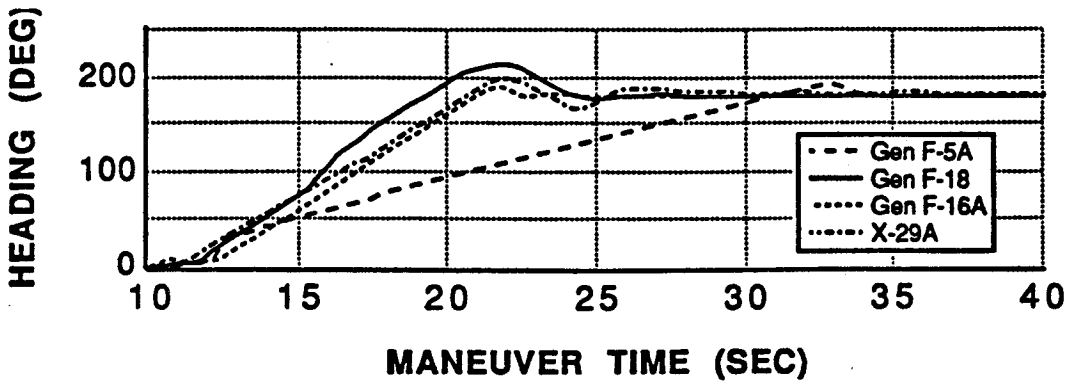

Figure 6.28 Comparison Of Generic F-5A, F-16A, F-18A, And X-29A Overshoot Of Heading Angle Required To Capture 180°, Mach = 0.8, H = 15,000 feet (REF. 43)

using the generic F-18A and the OTIS program. The generic F-18A *energy-agility* sensitivity results for the 180° CCT maximum angle of attack, optimal turn, and optimal total time test cases are displayed in Figure 6.29. For the maximum angle of attack CCT test case, Figure 6.29 demonstrates that the generic F-18A completes the maneuver in 41.8 seconds. This is the same total time as the nominal 180° CCT for this maneuver, but 23% of the total available energy is lost. The time to kill occurs in only 9.35 seconds, illustrating that a maximum angle of attack maneuver utilizes the maximum nose pointing ability of the aircraft. The time to kill does not occur at the point corresponding to the lowest energy state since a slight heading overshoot is needed.

Figure 6.29 shows that the optimal turn CCT test case results in a slight increase in the time to kill (t_k), despite a decrease in the total maneuver time. The time to kill is 11.6 seconds, which represents a 25% increase over the maximum angle of attack CCT test case. The total amount of energy expended for this maneuver is 63,163 ft-sec, which is only 10% of the total energy available. This represents a 56% saving over the maximum angle of attack CCT test case. These results indicate that limiting the maximum angle of attack for the turning portion of the

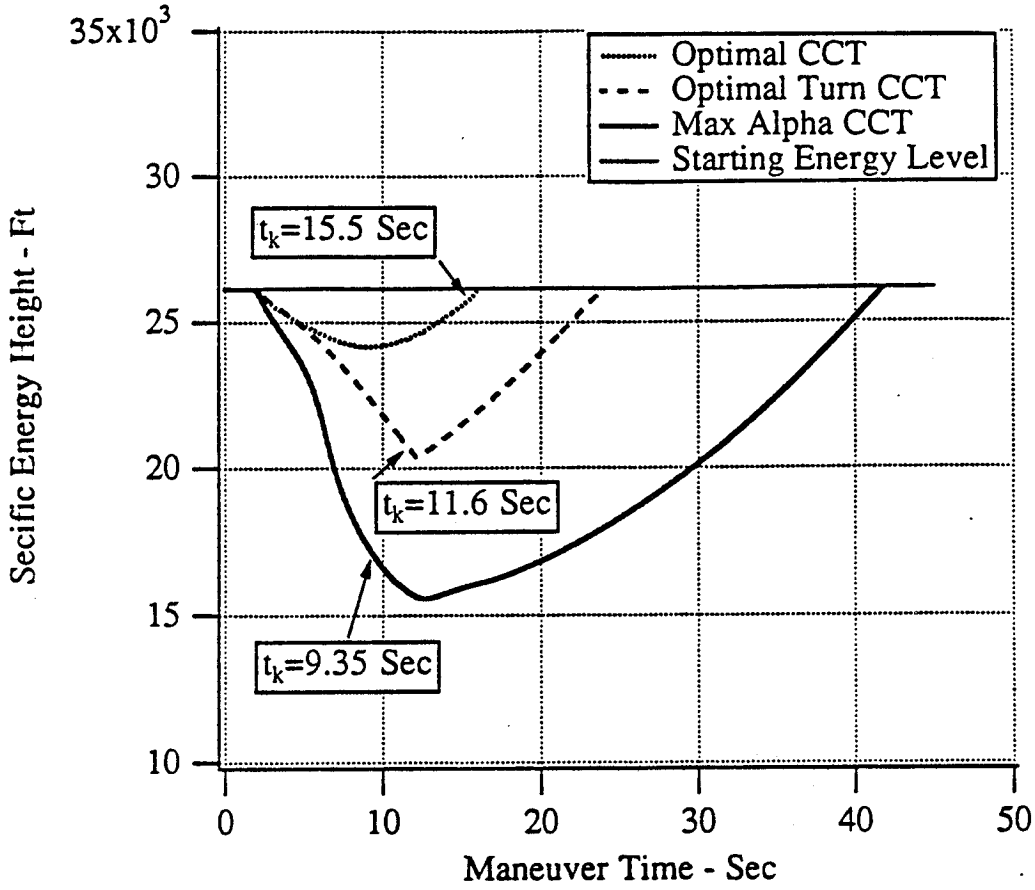

Figure 6.29 Generic F-18A *Energy-Agility* Sensitivity, Mach = 0.8, H = 15,000 feet (REF. 53)

CCT maneuver by flying an optimal angle of attack schedule can significantly decrease the amount of energy lost, with only a relatively small increase in the time to kill.

The optimal total CCT can further reduce the energy lost and the maneuver time (Figure 6.29). The total energy loss is only 18,139 ft-sec. This is 4% of the total energy available, which represents an 83% improvement over the maximum angle of attack CCT test case. However, the time to kill is increased 66% compared to that test case.

Figure 6.30 shows the heading angle time histories for the three sensitivity test cases. The objective is to decrease the amount of energy expended for the 180 degree turn and minimize

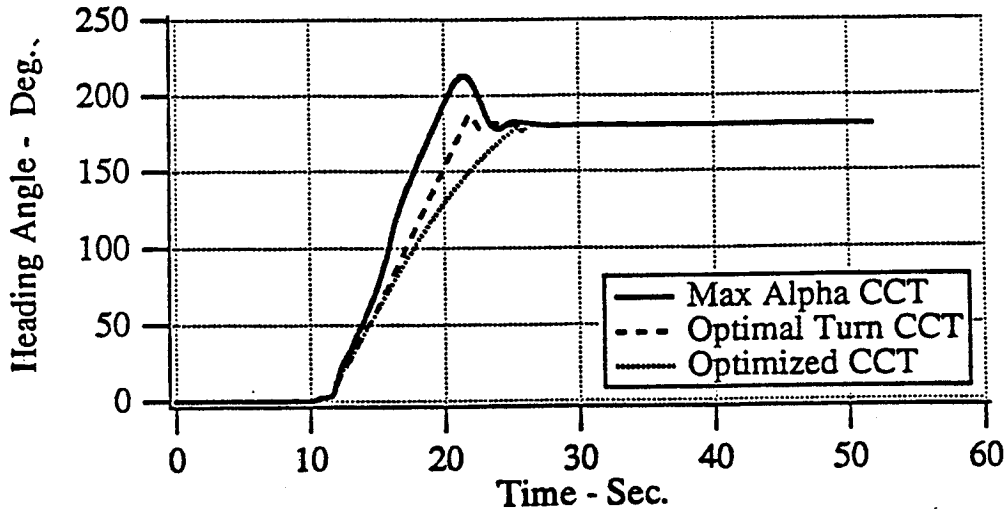

Figure 6.30 Comparison Of Generic F-18A Heading Angle Overshoots From *Energy-Agility* Sensitivity, Mach = 0.8, H = 15,000 feet (REF. 53)

maneuver time. This plot clearly shows that the maximum angle of attack CCT test case reaches the 180 degree heading angle first. The drawback of this quick nose pointing ability is the large energy loss which is incurred, since nearly 30 seconds is required to regain the energy lost during the turn. The integrated area over the curve represents the total amount of energy lost during the maneuver. This value is a very large 252,870 ft-sec. If the initial energy level is multiplied by the total maneuver time (the time to kill and recover), the total amount of available energy can be compared to the amount lost during the maneuver. From the foregoing, it seems evident that concluding which command input strategy is best based solely on the *energy-agility* metric is unsuitable. This is because of the many factors involved, such as the task objective and combat situation.

It can also be proved that the optimal total time CCT test case is an optimal combination of maneuver time and energy efficiency (REF. 53).

6.4.5.4 Summary

The *energy-agility* concept is a useful graphical technique to view the energy loss during a combat relevant task. This metric is well suited to comparing the energy compromised during the task by different aircraft, since each aircraft can be rated by its ability to minimize the energy loss penalty while directly seeking a positional advantage. Determining the best pilot command input strategy to use for testing the *energy-agility* metric is difficult because of the many inter-related effects.

6.4.6 **Time-Energy Penalty** (REF. 43)

6.4.6.1 Definition

This metric is defined as

$$\text{Time Energy Penalty} = t_{\Delta\psi} \times \Delta h_e$$

where $t_{\Delta\psi}$ is the time to complete a specified heading angle change and (if required) the time to pitch down to achieve missile envelope firing parameters, and Δh_e is the change in specific energy height during the maneuver.

6.4.6.2 Discussion and Typical Results

The time $t_{\Delta\psi}$ consists of the sum of the time to roll 90 degrees and pitch to maximum normal load factor (t_1 of *combat cycle time*), plus the time to obtain a specified heading angle (t_2 of *combat cycle time*), plus the time to pitch down and reduce angle of attack or normal load factor so that an air-to-air missile can be fired within its envelope. The missile envelope is based on the all-aspect AIM-9L Sidewinder which can be fired up to 25 degrees angle of attack and approximately six to seven g (REF. 56). The change in specific energy height, Δh_e, is measured

from the start of the maneuver until the time at which the heading angle is reached and the missile envelope parameters are satisfied. An aircraft capable of executing a short duration turn with minimal energy loss is desirable. Conversely, an aircraft which turns slowly and depletes large amounts of energy is undesirable.

Data for the *time-energy penalty* metric is obtained directly from the test cases used to measure both the 180° and 90° CCT. For the 180° heading angle change, Figure 6.31 shows the generic F-16A completes the turn in less time and with less energy loss than the other three aircraft. The generic F-18A actually reaches the target heading before the generic F-16A, but requires time to unload to satisfy the missile firing parameters.

Discretion must usually be exercised when interpreting *time-energy penalty* results. Attempting to determine relative advantages based solely on values of the metric without regard

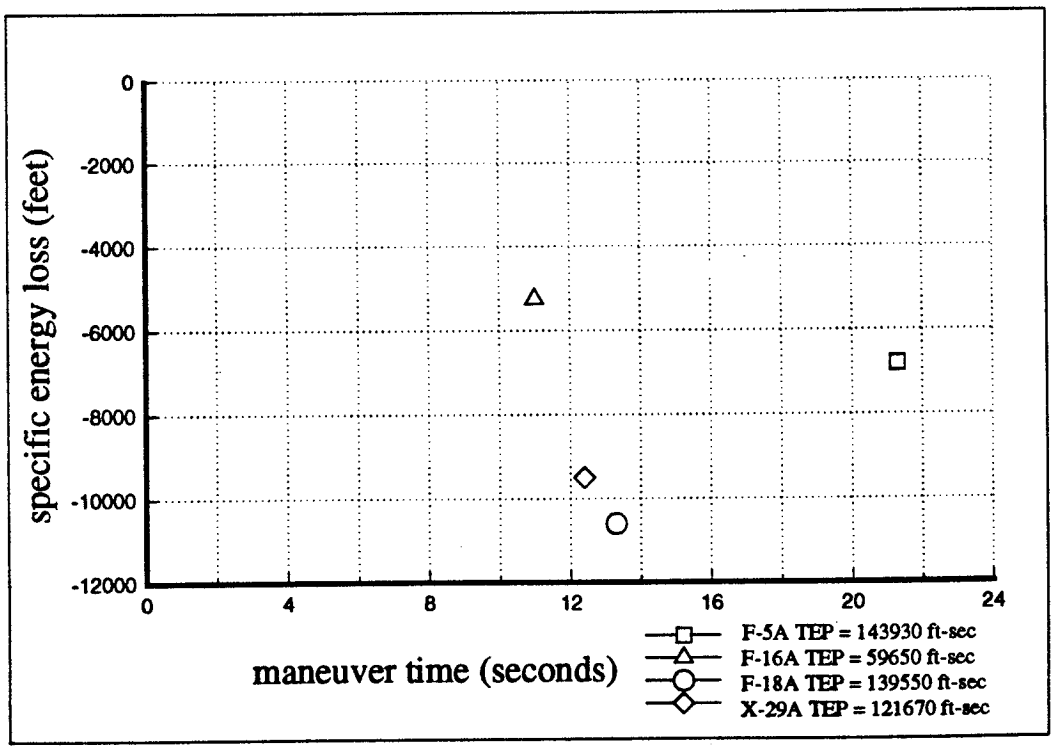

Figure 6.31 Generic F-5A, F-16A, F-18A, And X-29A 180° *Time-Energy Penalty* Plot, Mach = 0.8, H = 15,000 feet

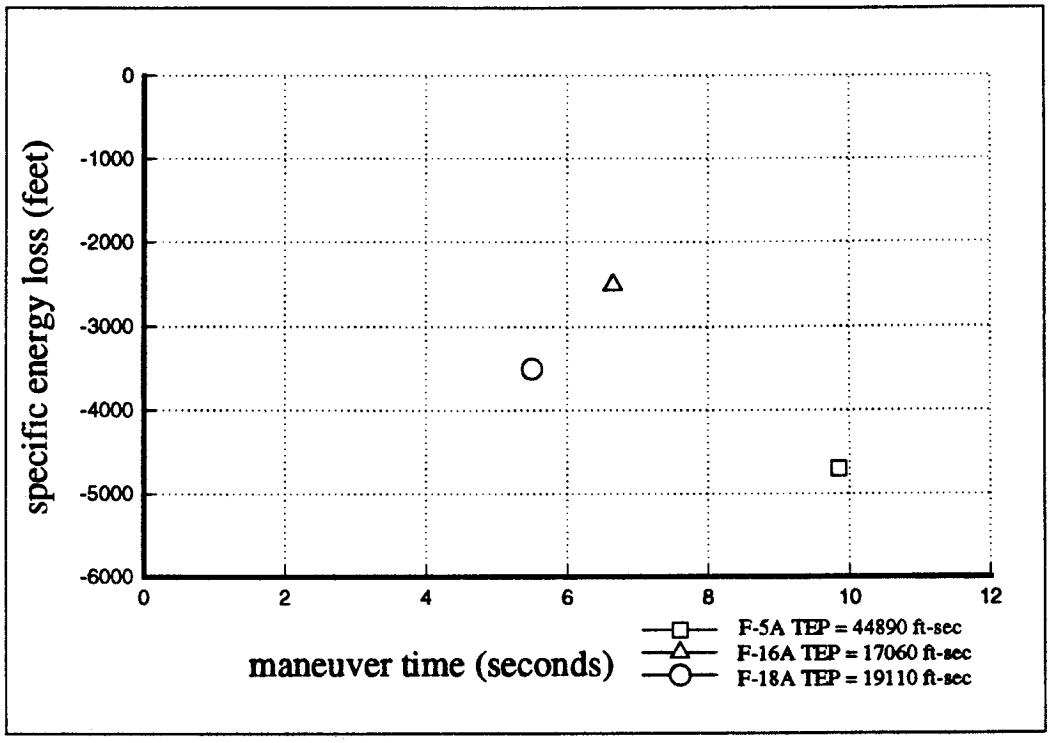

Figure 6.32 Generic F-5A, F-16A, F-18A, And X-29A 90°
Time-Energy Penalty Plot, Mach = 0.8, H = 15,000 feet

for combat effectiveness can lead to gross errors. For example, consider the 90° heading change *time-energy penalty* plot of Figure 6.32. The value of *time-energy penalty* for the generic F-18A is 19,110 feet-seconds, and for the generic F-16A 17,060 feet-seconds. Based solely on this result, the generic F-16A would appear to be have an advantage over the generic F-18A, based upon its lower *time-energy penalty* value. Whether or not this does in fact translate into an advantage must be determined by cross-checking the regions on the *time-energy penalty* plot which correlate with different levels of combat effectiveness. Referring to Figure 6.32, an additional consideration is whether a one second advantage for the generic F-18A is worth the nearly 1000 feet per second specific energy loss incurred. The advantage of a quicker turn at the expense of more energy loss may deteriorate as the duration of the engagement is extended. The *time-energy penalty* plot can be a useful aid for arriving at these decisions.

6.4.6.3 Time-Energy Penalty Sensitivity

The sensitivity of the *time-energy penalty* metric to pilot command input strategy is determined using the generic F-18A simulation and the OTIS program. The data for the *time-energy penalty* sensitivity study presented here is condensed from Reference 53. The generic F-18A *time-energy penalty* sensitivity results for the 180° CCT maximum angle of attack, optimal turn, and optimal total time test cases are displayed in Figure 6.33. The desirable position on the plot is to be as close to the origin as possible, or in the region of low energy loss and low maneuver time. At a *time-energy penalty* of 135,225.6 feet-seconds, the maximum angle of attack CCT test case loses a considerable amount of energy compared to the optimal turn CCT test case, which has a *time-energy penalty* of only 62,506 feet-seconds. Not unexpectedly, the optimal total CCT test case reduces the *time-energy penalty* further still to 5,852.8 feet-seconds. According to

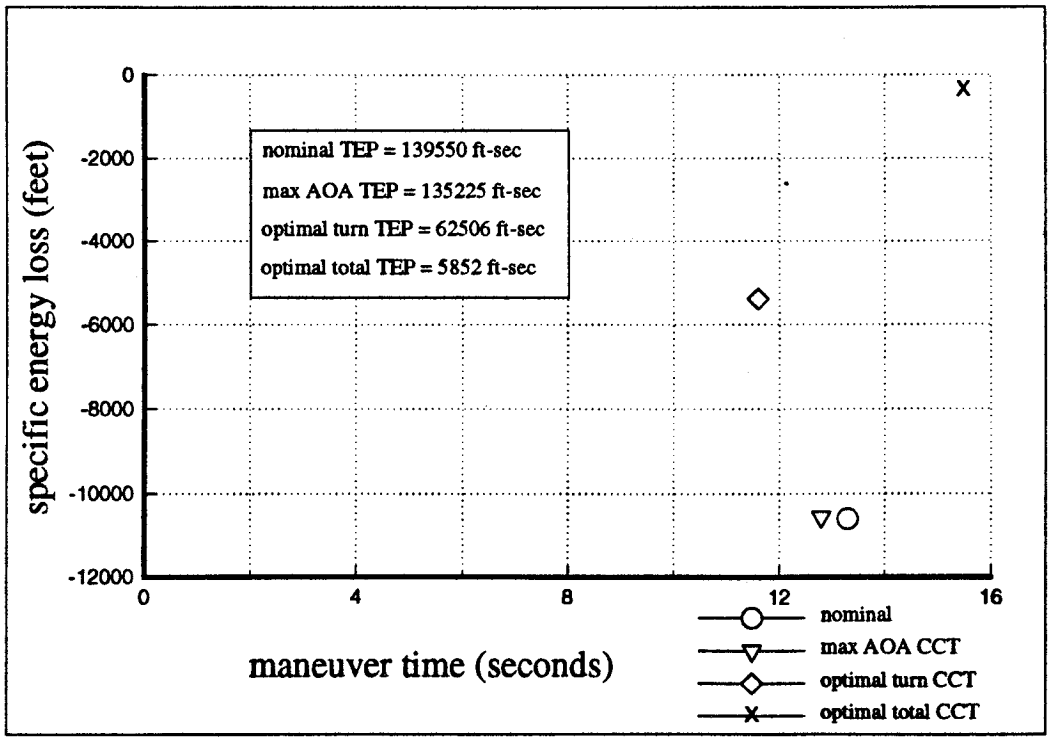

Figure 6.33 Generic F-18A 180° *Time-Energy Penalty* Sensitivity, Mach = 0.8, H = 15,000 feet

the *time-energy penalty* criteria, the optimal turn CCT test case is judged to be the best. All of these trends are substantiated by the energy losses results of Sections 6.4.1 through 6.4.5 for these test cases.

Figure 6.34 is a plot of the *time-energy penalty* values for the three 90° *combat cycle time* test cases. The same trends are evident using the 90° CCT, though the short time scales for the turns make the three test cases very similar.

6.4.6.4 Summary

The *time-energy penalty* metric is basically an extension of the *combat cycle time* and *energy-agility* metrics with its name taken from Reference 57. It is intended to address the tactically significant maneuver of heading angle changes by correlating combat effectiveness with regions on the *time-energy penalty* plot. The result of a direct multiplication between $t_{\Delta\psi}$ and Δh_e is a single parameter which equally weighs the importance of minimizing time and preserving energy during a heading change maneuver. The optimum balance between time to point the nose of the aircraft and the energy lost while doing so may be determined and used as a design guide.

The *time-energy penalty* metric is sensitive to the pilot command input strategy used to test it. The best *time-energy penalty* results are obtained when the test aircraft uses the angle of attack schedule corresponding to the optimal turn CCT test case.

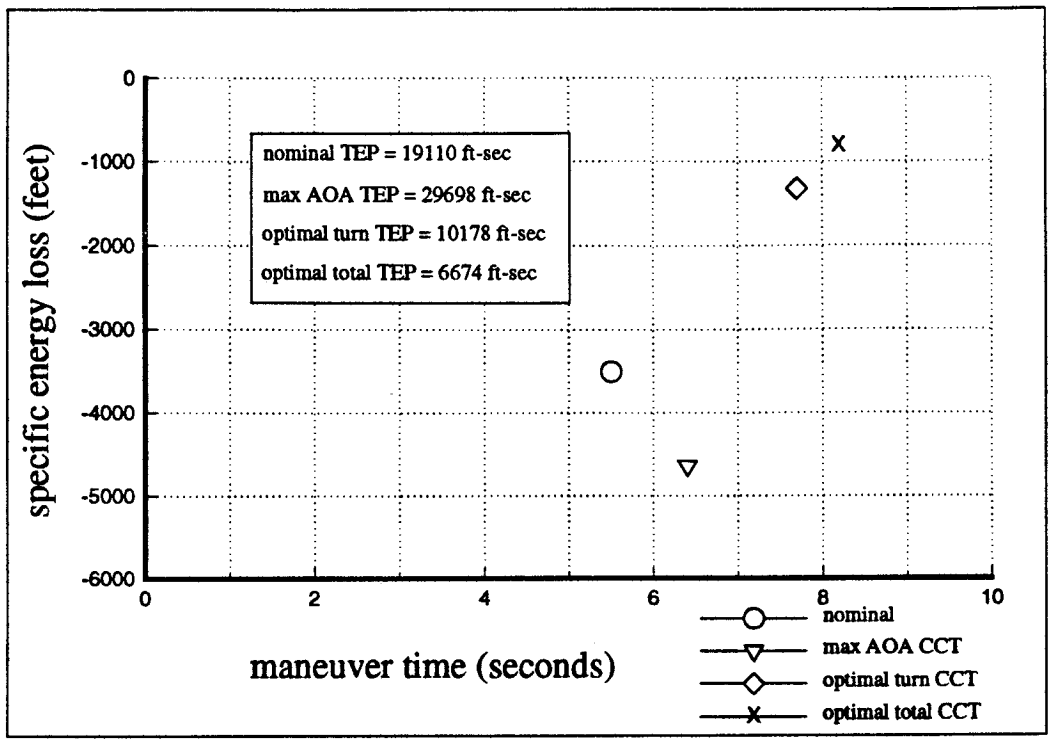

Figure 6.34 Generic F-18A 90° *Time-Energy Penalty* Sensitivity, Mach = 0.8, H = 15,000 feet

6.5 SUMMARY

The functional agility metrics are dominated by energy management capabilities and therefore the energy maneuverability (EM) traditional measure of merit. High angle of attack maneuvers are good for maximizing nose pointing ability, but can result in unacceptable energy losses. The low angle of attack maneuvers result in lower energy losses and improved total maneuver times, but result in a larger turn radius and larger distances traveled in downrange and crossrange. Which type of maneuver to use to achieve a desired heading angle change depends on the task objective and the combat situation.

The functional agility metrics tested here cannot fully address the high angle of attack controllability issue and its effect upon maneuvering capability. This is demonstrated by the inability of the functional agility metrics to highlight the unconventional design features incorporated in the X-29A, e.g. good high angle of attack lateral control, and reduced trim drag in the transonic and supersonic flight regimes. These aspects tend to lend themselves better to analysis using the lateral agility metrics in Chapter 4. However, the functional agility metrics did indicate that the generic X-29A has energy bleed rates at elevated angles of attack similar to other fighter aircraft.

None of the functional agility metrics studied take into account the turn radius of a given maneuver, which is an important parameter. A metric that directly combines the turn radius, maneuver time, and energy efficiency for a given maneuver into one parameter would be very useful but is beyond the scope of the current study.

Within their limitations, the functional agility metrics are useful measures of maneuvering capability. The strength of this class of metrics is:

1. the direct measurement of the capability to quickly transition between two distinct maneuvering states
2. representation of tasks relevant to air combat maneuvering, in a format readily accessible to pilots
3. measurement of the efficiency of a given maneuver, in addition to assessing the agility of the airframe.

The results presented for each of the functional agility metrics tested in Section 6.4 demonstrate that they are **highly** sensitive to the particular pilot command input strategy used. These sensitivities can cause large changes in the measured value for each metric, but also offer

insight into the efficiency of different air combat maneuvers for a given aircraft. The sensitivity also makes it difficult to use these metrics for direct comparisons between aircraft without establishing a common test strategy, not just a common test pilot command input strategy. The example of using the 180° *combat cycle time* metric to compare the generic F-16A and generic F-18A illustrates that a standardized command input strategy can inadvertently favor a given aircraft and bias the results. This is because the aircraft which does not have an angle of attack limiter (e.g. the generic F-18A) might be judged inferior due to large energy losses during the 180 degree heading angle change, compared to an aircraft which has an angle of attack limiter (e.g. the generic F-16A). The use of an optimal angle of attach schedule resulted in marked improvements in the measured agility of the generic F-18A, while still complying with the test criteria.

From results obtained using the generic F-18A, the sensitivities of the functional agility metrics as a class can be summarized as follows:

1. the measured values of the functional agility metrics are a strong function of angle of attack, while bank angle errors and throttle setting have only a small effect.

2. low angle of attack maneuvers provide the lowest measured values of the metrics, but may not best the "best" maneuvers for a given combat situation.

3. high angle of attack nose pointing maneuvers result in large measured values of the metrics, but maximize nose pointing capability (small time to kill).

4. by following an optimal angle of attack schedule, it is possible to reduce total energy losses and bleed rates as much as 80%, and improve the measured value of some metrics by 60%.

5. the time to capture a 180° heading angle change (time to kill) can be reduced 40% by using the maximum available angle of attack.

7. CONCLUSIONS

Instead of supplying specific, detailed conclusions about the relevance or utility of one candidate metric versus another one, the authors have attempted to provide sufficient data and analyses for readers to formulate their own conclusions. Readers are ultimately responsible for judging exactly which metrics are "best" for their particular needs. The following general conclusions on fighter agility, based upon the experiences of all researchers who participated in the investigation, are as follows.

1) The study of agility uses conventional airplane dynamics that are well known and understood. It does not require a "new look" at the airplane equations of motion. Agility is some unspecified combination of transient performance and flying qualities. Besides the obvious impact of transient performance on agility, flying qualities serve to identify the fastest dynamics that pilots can use effectively.

2) Agility metrics are most useful when they measure combat relevant tasks. The task oriented measures of agility are usually straightforward to test and measure since they are well defined. Metrics which emphasize large instantaneous rates and accelerations are not true reflections of the quicker time to complete a task. Acceleration is just one aspect of transient performance. Emphasizing maximum values ignores the associated problem of reductions in controllability. However, it has been shown that task oriented metrics can in some cases be unintentionally aircraft specific, usually due to prescribed initial and final conditions.

3) No single candidate agility metric investigated in this report is completely adequate, by itself, for quantifying the combat capabilities of fighter aircraft in a modern, within visual range (WVR) air combat environment. Each candidate metric provides a different insight into the complex issue of agility.

4) With the exception of the functional metrics and instantaneous metrics, each candidate agility metric is categorized according to a single aircraft axis. The axis selected represents the axis in which the (intended) motion occurs. However, the metrics categorized according to axis tend not to be truly uncoupled from the other axes.

5) The usefulness and/or relevance of any one candidate agility metric cannot be determined by applying it to only one type of aircraft. The results in this report clearly demonstrate that results can vary widely between aircraft types for the same metric.

6) In addition to the sometimes obvious contributions of the airframe and powerplant to the overall agility level of an aircraft, the details of the flight control system have a major impact on the agility (or lack of agility) that an aircraft possesses.

7) Aircraft design involves compromises between many conflicting requirements. Once a particular class or set of candidate agility metrics is selected, it is possible to incorporate them as performance requirements when specifying airframe/flight controller design specifications, even if not as a formal specification such as a military specification. Using only minor changes (increased rudder rate, larger rudder on the same vertical tail, and modified roll command limiters), aircraft which were designed without an specific agility requirement can in some cases have their existing level of agility improved. An example of how the existing agility of an aircraft can be improved is given in Reference 26.

8) The sensitivity of the candidate agility metrics to deviations in pilot command inputs varies widely. The range is from low sensitivity (pitch metrics), to medium sensitivity and reliance on algorithms (lateral metrics), to highly sensitive (functional metrics). Therefore agility metrics as a whole cannot reliably be classified as having a single, common degree of sensitivity.

9) All of the candidate agility metrics investigated in this report are straightforward to measure and test using non real-time flight simulation. Since the metrics are well defined and existing standard flight test instrumentation is sufficient, extension of the testing and measurement procedures in this report to piloted simulators and actual flight testing should not impose requirements for instrumentation or sensors currently available on high performance test aircraft.

10) The axial agility metrics (power onset parameter and the power loss parameter) do not quantify the acceleration capability of an aircraft. They highlight instead the desirable qualities of short engine spool up and down times and the effectiveness of drag producing devices. In general, the aircraft with the faster spooling engine and the more effective speedbrakes tends to have greater axial agility than the aircraft which is superior in acceleration.

11) With the exception of the time to maximum normal load factor metric, the pitch agility metrics as a class apply to dissimilar aircraft comparisons, and are straightforward for pilots to flight test. Extraction of useable data from flight test for measuring the load factor rate metric may require unique data reduction methods. As tested on the generic F-18A, all of the pitch agility metrics investigated are largely insensitive to deviations in pilot command inputs.

12) Lateral agility metrics tend to be representative of the pilot tasks and nonsymmetrical maneuvering demands of modern air combat. The time through roll angle metrics are useful for measuring the transient performance aspect of agility, and the roll angle capture metrics incorporate flying qualities to a certain extent. Although the lateral agility metrics tend to become more sensitive to deviations in pilot command inputs with increasing angle of attack, the effects can be largely corrected by the data reduction algorithm discussed in Chapter 4.

13) The functional agility metrics are measures of the efficiency of a given maneuver, in addition to measures of airframe agility. The use of high angle of attack command input strategies for evaluating the functional agility metrics provides good nose pointing ability, but tends to result in unacceptable energy losses. Trajectory optimization routines can provide command input strategies (optimal angle of attack schedules) which lead to significant reductions in the functional agility metric values for a given aircraft. Maneuvers which track an optimal angle of attack schedule result in lower energy losses and improved total maneuver times, but result in larger turn radius values and larger distances traveled in downrange and crossrange. The task objective and combat situation would dictate which strategy is best to use for a given situation. The functional agility metrics as a class are very sensitive to variations in pilot command input strategy.

14) The instantaneous agility metrics, curvature agility and Herbst torsional agility, are of the open loop, maximum value, "more is better" type. Since no practical upper limits on the measured values of these two metrics are imposed, care must be taken when interpreting results and drawing conclusions based upon them. Curvature agility and Herbst torsional agility are well approximated by maximum rate of change of normal load factor and maximum wind axis roll rate respectively.

8. RECOMMENDATIONS

Based on the results of this report, several promising areas for further investigation have been identified.

1) The value that increased agility holds for air combat effectiveness should be investigated. The differences in levels of agility must be correlated with the experiences of the pilots who employ the aircraft in operational air-to-air and air-to-ground missions. Further study of the promising candidate agility metrics studied so far under this project should be conducted on a manned fight simulator. This information can then be used to help set priorities and goals for designing more agility into fighter aircraft.

2) The airframe design compromises necessary to achieve various levels of agility should be investigated, especially large control surfaces and fast actuator rates. With regard to lateral agility, focus on ways to increase both roll and yaw control power and how to coordinate them during a rolling maneuver. A study of the generic F-18A showed that lateral agility on that aircraft can be improved through better coordination of the ailerons and rudders (REF. 26). A similar analysis on a different aircraft, one which already possesses good aileron-rudder coordination, might highlight different areas for improvement.

3) Flight control system design can directly enhance the agility of fighter aircraft. Techniques which appear promising for improving agility include:

   i) striving for control harmony by trying various combinations of rudder and actuator rates until a combination which enhances agility is obtained.

   ii) feedbacks to the rolling surfaces to coordinate rolls at high angles of attack.

   iii) using rudder to generate proverse yawing moments and to damp lateral and directional oscillations at high angles of attack.

4) The benefits of increased nose down pitch agility on air combat effectiveness should be determined. NASA Langley has also expressed renewed interest (May 1991) in the capability of pitching down to zero g from a high angle of attack attitude.

5) Standardized test procedures for testing different aircraft types should be developed, especially for the functional agility metrics. In this regard, the OTIS program can be used to study the feasibility of automatically flying agility maneuvers. These optimal maneuvers could also be used to provide information for designing flight control limiters and pilot displays. The OTIS program can also be used for optimization of high angle of attack maneuvers, such as the Herbst maneuver. By calculating the functional agility metrics for this maneuver, it could be compared to other conventional maneuvers to study energy loss, heading capture time, and total maneuver time.

6) Determine whether axial acceleration capabilities or axial agility capabilities is most important in modern air combat. The less desirable characteristic can probably be discarded all together.

7) Most of the candidate agility metrics investigated in this report exhibited significant multi-axis effects. These multi-axis effects should be carefully examined and given due consideration when interpreting results and drawing conclusions.

8) Aerodynamic data that includes unsteady and aero-elastic effects should be incorporated into flight simulation programs which are used for studying agility metrics. This can help determine what influence these nonlinear aerodynamic effects might have on the values of the metrics.

9) The functional agility metrics studied in this report do not take into account the turn radius of a given maneuver, which can be a significant consideration. A new metric, or a modified version of an existing one, that directly combines the turn radius, maneuver time, and energy efficiency for a given maneuver into one parameter might be useful.

9. REFERENCES

1. Liefer, Randall K., Valasek, John, Eggold, David P., and Downing, David R., "Fighter Agility Metrics, Research and Test," *Journal Of Aircraft*, Vol. 29, No. 3, May-Jun. 1992, pp. 452-457.

2. Liefer, Randall K., Valasek, John, Eggold David P., and Downing, David R., "Assessment of Proposed Fighter Agility Metrics," AIAA-90-2807-CP, AIAA Atmospheric Flight Mechanics Conference, Portland, OR, Aug. 1990.

3. Liefer, Randall K., "Fighter Agility Metrics," University Of Kansas Flight Research Laboratory, KU-FRL-831-2, Lawrence, KS, Jun. 1990.

4. Skow, Andrew M., and Hamilton, W. L., "Advanced Fighter Agility Metrics," Eidetics International Technical Report TR84-05, Hawthorne, CA, Sept. 1984.

5. Dorn, Matthew D., "Aircraft Agility: The Science and the Opportunities," AIAA-89-2015-CP, AIAA/AHS/ASEE Aircraft Design, Systems and Operations Conference, Seattle, WA, Jul. 1989.

6. Valasek, John, and Eggold, David P., "Fighter Agility Metrics Research At The University Of Kansas," AIAA Wichita Section XVI Annual Technologyfest, Wichita, KS, Nov. 1989.

7. Valasek, John, "A Study Of A Proposed Modified Torsional Agility Metric," AIAA-91-2883-CP, AIAA Atmospheric Flight Mechanics Conference, New Orleans, LA, Aug. 1991.

8. Valasek, John, "SIM-II Generic F-18 Flight Simulation Program Documentation," University Of Kansas Flight Research Laboratory, KU-FRL-831-1, Lawrence, KS, Jun. 1990.

9. Paris, S.W., Hargraves, C.R., and Martens, P.J., "Optimal Trajectories By Implicit Simulation Version 2.0 Formulation Manual," Boeing Aerospace and Electronics, Seattle, WA, 1990.

10. Vlases, W.G., "Optimal Trajectories By Implicit Simulation Version 2.0 User's Manual," Boeing Aerospace and Electronics, Seattle, WA, 1990.

11. Foltyn, R.W., et. al., "Development of Innovative Air Combat Measures of Merit for Supermaneuverable Fighters," Air Force Wright Aeronautical Laboratories, Dayton, OH, AFWAL-TR-87-3073, Oct. 1987.

12. Lynch, Urban H.D., et. al., "Tactical Evaluation of the Air-to-Air Combat Effectiveness of Supermaneuverability," WRDC-TR-90-3035, Jun. 1990.

13. Herbst, Wolfgang B., and Krogull, B., "Design For Air Combat", *Journal Of Aircraft*, Vol. 10, No. 4, Apr. 1973, pp. 247-253.

14. Herbst, Wolfgang B., "Supermaneuverability," Joint Automatic Control Conference, Charlottesville, VA, Jun. 1981.

15. Herbst, Wolfgang B., "Dynamics of Air Combat," *Journal of Aircraft*, Vol. 20, No. 7, Jul. 1983, pp. 594-598.

16. Herbst, Wolfgang B., "Future Fighter Maneuverability for Air Combat," AIAA Design, Systems and Operations Meeting, Oct. 1983.

17. Hodgkinson, John, et. al., "Relationships Between Flying Qualities, Transient Agility, and Operational Effectiveness of Fighter Aircraft," AIAA-88-4329-CP, AIAA Atmospheric Flight Mechanics Conference, Minneapolis, MN, Aug. 1988.

18. Skow, Andrew M., et. al., "Transient Agility Enhancements for Tactical Aircraft, Vol. III," Eidetics International Technical Report TR89-001, Hawthorne, CA., Jan. 1989.

19. Riley, David R., and Drajeske, Mark H., "An Experimental Investigation of Torsional Agility in Air-to-Air Combat," AIAA-89-3388, AIAA Atmospheric Flight Mechanics Conference, Boston, MA, Aug. 1989.

20. Small, Lester L., and Liston, Glenn W., "Impact of Pitch/Yaw Vectoring Nozzles on Close-In Fighter Combat," Wright Research and Development Center, Oct. 1990.

21. Herbst, Wolfgang B., "X-31A," SAE-871346, IEEE National Aerospace Electronics Conference, 1987.

22. Ray, B.S. and Cord, Thomas J. "Supermaneuverability and Flying Qualities Issues," IEEE National Aerospace Electronics Conference, 1986.

23. Sweetman, Bill "X-31; Through the Grape Barrier," *Interavia*, Oct. 1987, pp. 475-476.

24. Brown, Paul T., Hardeman, J.W., Ross, M.L., Albrecht, B.R., Fortmann, K.M., and Zeis, J.E. Jr., "T-38A/F-16B Agility Metrics Evaluation (Agile Lightning)," USAF Test Pilot School Technical Report USAFTPS-TR-87A-SO4, Dec. 1987.

25. Butts, Stuart L. and Lawless, Alan R. "Flight Testing for Aircraft Agility," AIAA-90-1308-CP, AIAA/SFTE/DGLR/SETP Fifth Biannual Flight Test Conference, May 1990.

26. Eggold, David P., Valasek, John, and Downing, David R., "Measurement and Improvement of the Lateral Agility of the F-18," *Journal of Aircraft*, Vol. 30, No. 6, Nov.-Dec. 1993.

27. Eggold, David P., Valasek, John, and Downing, David R., "The Measurement and Improvement of the Lateral Agility of the F-18," AIAA-91-2880-CP, AIAA Atmospheric Flight Mechanics Conference, New Orleans, LA, Aug. 1991.

28. Eggold, David P., "The Assessment and Quantification of Lateral Agility Metrics Using an F-18 Simulation," University Of Kansas Flight Research Laboratory, KU-FRL-831-4, Lawrence, KS, Sept. 1990.

29. Dorn, Matthew D., "The Science of Aircraft Agility: A Framework for Classification and Exploration," AIAA Aerospace Engineering and Conference Show, Feb. 1989.

30. Tamrat, B.F., "Fighter Agility Assessment Concepts and Their Implications on Future Agile Fighter Design," AIAA-88-4400-CP, AIAA Aircraft Systems, Design and Operations Meeting, Sept. 1988.

31. Spearman, M. Leroy, "Some Fighter Aircraft Trends," AIAA-84-2503-CP, AIAA Aircraft Design, Systems and Operations Meeting, San Diego, CA, Nov. 1984.

32. Bitten, Robert, "Qualitative and Quantitative Comparison of Government and Industry Agility Metrics," AIAA-89-3389-CP, AIAA Atmospheric Flight Mechanics Conference, Boston, MA, Aug. 1989.

33. Herbst, Wolfgang B., "Agility," Workshop On Agility Metrics, Air Force Flight Test Center, Edwards AFB, CA, Mar. 1988.

34. Riley, David R., and Drajeske, Mark H., "Relationships Between Agility Metrics and Flying Qualities," SAE Paper 901003, SAE Aerospace Atlantic, Dayton, OH, Apr. 1990.

35. Kalviste, Juri, "Measures of Merit for Aircraft Dynamic Maneuvering," SAE Paper 901005, SAE Aerospace Atlantic, Dayton, OH, Apr. 1990.

36. Schweikhard, William G., Kohlman, D.L., "Flight Test Principles and Practices Short Course Notes," University Of Kansas Division of Continuing Education, May 1990.

37. Hoffler, Keith, Ogburn, M., and Nguyen, L., "High-Alpha Control Requirements," NASA High-Alpha Technology Program Workshop, Dryden Flight Research Facility, Nov. 1989.

38. Valasek, John, "A Study Of A Modified Torsional Agility Metric Using Simulation Methods," University Of Kansas Flight Research Laboratory, KU-FRL-831-3, Lawrence, KS, Oct. 1990.

39. Anonymous, "F-5A/E Technical Description," Northrop Corporation Aircraft Division, Northrop Report 71-20, Hawthorne, CA, Jul. 1973.

40. Anonymous, "Military Standard - Flying Qualities of Piloted Vehicles," MIL-STD-1797-A, Mar. 1987.

41. Cannon, John D., "Predicting The Victor," AIAA-91-0418-CP, 29th AIAA Aerospace Sciences Meeting, Reno, NV, Jan. 1991.

42. Ryan, George W. III, and Downing, David R., "The Evaluation of Several Functional Fighter Agility Metrics Using Optimal Trajectory Analysis Techniques," AIAA-92-4488-CP, AIAA Atmospheric Flight Mechanics Conference, Hilton Head Island, SC, Aug. 1992.

43. Cox, Brian W., "Evaluation of Several Functional Agility Metrics For Fighter Class Aircraft," MS Thesis, University of Kansas Department of Aerospace Engineering, Lawrence, KS, Aug. 1991

44. Humphreys, Robert P., Hennig, G.R., Bolding, W.A., and Helgeson, L.A., "Optimal 3-Dimensional Minimum Time Turns for an Aircraft," *The Journal of the Astronautical Sciences*, Vol. XX, No. 2, Sept.-Oct. 1972, pp. 88-112.

45. Well, K.H., and Berger, E., "Minimum-Time 180° Turns of Aircraft," *Journal of Optimization Theory and Applications*, Vol. 38, No. 1, Sept. 1982, pp. 83-97.

46. Schneider, Garret L., and Watt, George W., "Minimum Time Turns Using Vectored Thrust," *Journal of Guidance, Control, and Dynamics*, Vol. 12, No. 6, Nov.-Dec., 1989.

47. McAtee, Thomas P., "Agility-Its Nature And Need in the 1990's," The Society of Experimental Test Pilots Symposium, Sept. 1987.

48. Lawless, Alan R., "Aircraft Agility Measurement Research and Development," AFFTC-TIM-91-01, Jun. 1991.

49. Cox, Brian W., and Downing, David R., "Evaluation of Functional Agility Metrics For Fighter Class Aircraft," AIAA-92-4487-CP, AIAA Atmospheric Flight Mechanics Conference, Hilton Head Island, SC, Aug. 1992.

50. Skow, Andrew M., "Agility As A Contributor To Design Balance," *Journal Of Aircraft*, Vol. 29, Jan.-Feb. 1992, pp. 34-46.

51. Personal Conversation with Major Bob Vosburgh, USAF, Iowa State University Air Force ROTC, Oct. 1990.

52. Personal Conversation with Major Dale A. Nagy, USAF, United States Air Force Academy, Nov. 1990.

53. Ryan, George Wesley III, "The Evaluation of Several Functional Agility Metrics Using Optimal Trajectory Analysis Techniques," MS Thesis, University of Kansas Department of Aerospace Engineering, Lawrence, KS, Apr. 1992

54. McAtee, Thomas P., "Agility in Demand," Aerospace America, May 1988, pp. 36-38.

55. Shaw, Robert L., **FIGHTER COMBAT Tactics and Maneuvering**, Naval Institute Press, Annapolis, MD, 1985.

56. Personal Conversation with Joe Wilson, NASA-Ames Dryden Flight Research Facility (XRDD), May 1991.

57. Dorn, Matthew D., "EIGHT IDEAS Toward an Aircraft Agility Theory," a USAF Flight Dynamics Laboratory White Paper, 1989.

58. Anonymous, "Military Specification, Flying Qualities of Piloted Airplanes," MIL-F-8785C, Nov. 1980.

59. Anonymous, "Military Specification, Flying Qualities of Piloted Airplanes," MIL-F-8785, Sept. 1954.

60. Anonymous, "Military Specification, Flying Qualities of Piloted Airplanes," MIL-F-8785B, Aug. 1969.

61. Lockenour, Jerry L., "Northrop Review of MIL-F-8785B Proposed Revisions," *Proceedings of AFFDL Flying Qualities Symposium Held at Wright State University 12-15 Sep. 1978*, AFFDL-TR-78-171, Dec. 1978, pp. 260-282.

62. Moorehouse, David J., Woodcock, R.J., and Sweeney, T.P., "Discussion and Status of the Proposed Revision (1978) to MIL-F-8785B," *Proceedings of AFFDL Flying Qualities Symposium Held at Wright State University, 12-15 Sept. 1978*, AFFDL-TR-78-171, Dec. 1978, pp. 236-250.

63. Chalk, Charles R., Neal, T.P., Harris, T.M., Pritchard, F.E., and Woodcock, R.J., "Background Information and User Guide For MIL-F-8795B(ASG)," Air Force Flight Dynamics Laboratories, Dayton, OH, AFFDL-TR-69-72, Aug. 1969.

64. Lipschutz, M. M., **Differential Geometry**, Mc-Graw Hill, New York, NY 1969.

65. Stoker, J. J., **Differential Geometry**, Wiley Interscience, New York, NY, 1969.

66. Baker, Dick, "Aircraft Time History Program," Sperry Support Services, Langley Operations, Report Number SP-205-, Hampton, VA, Jan. 1979.

67. Angelucci, Enzo, and Bowers, P., **The American Fighter**, Orion Books, New York, NY, 1985.

68. Linn, Don, **The F-18 Hornet In Detail & Scale**, Tab Books Inc., Blue Ridge Summit, PA, 1982.

69. Reports and Presentations Branch, NASA-Ames Dryden Flight Research Facility, Edwards, CA.

70. Etkin, Bernard, **Dynamics of Atmospheric Flight**, John Wiley & Sons, New York, 1972.

71. Anonymous, "USAF Test Pilot School FLYING QUALITIES TEXTBOOK VOLUME II Part 2," USAF-TPS-CUR-86-03, Apr. 1986.

72. Blakelock, John, **Automatic Control of Aircraft and Missiles**, John Wiley & Sons, New York, 1965.

73. Nguyen, Luat T., Gilbert, William P., and Ogburn, Marilyn E., "Control-System Techniques For Improved Departure/Spin Resistance For Fighter Aircraft," NASA TP-1689, Aug. 1980.

74. Chalk, Charles R., "The Ideal Controlled Element for Real Airplanes is Not K/s," Calspan FRM No. 554, Aug. 1981.

75. Monagan, Stephen J., Smith, R.E., and Bailey, R.E., "Lateral Flying Qualities of Highly Augmented Fighter Aircraft," Air Force Wright Aeronautical Laboratories, Dayton, OH, AFWAL-TR-81-3171, Vol. I, Jun. 1982.

76. Hoh, Roger H., Mitchell, D.G., Ashkenas, I.L., Klein, R.H., Heffley, R.K., and Hodgkinson, J., "Proposed MIL Standard and Handbook -Flying Qualities of Air Vehicles, Volume II: Proposed MIL Handbook," Air Force Wright Aeronautical Laboratories, Dayton, OH, AFWAL-TR-82-3081 VOLUME II, Nov. 1982.

77. Whitley, Phillip B., "Human Capabilities in Highly Agile Aircraft," SAE Aerospace Atlantic Conference, Dayton, OH, Apr. 1990.

78. Lan, Chuan-Tau, and Roskam, J., **Airplane Aerodynamics and Performance**, Roskam Aviation and Engineering Corporation, Ottawa, Kansas, 1980.

In addition to the numbered references, the researchers and contributors to this report have found the following reports and documents useful in the study of agility, and recommend them to the interested reader:

Aircraft Agility WORKshop," Air Force Wright Research and Development Center, Aug. 1989.

Anderson, John, "Agile Fighter Aircraft Simulation," AIAA-89-0015-CP.

Barnes, A.G., "The Study of Combat Aircraft Manoeuvrability by Air To Air Combat Simulation," British Aerospace Public Limited Company, Warton Division, Preston, Lancashire, England.

Beaufrere, Henry, "Integrated Flight Control System Design for Fighter Aircraft Agility," AIAA-88-4503-CP, Aircraft Design, Systems and Operations Meeting, Sep. 1988.

Bihrle, William Jr., and Barnhart, B., "Departure Susceptibility and Uncoordinated Roll-Reversal Boundaries for Fighter Configurations," *Journal of Aircraft*, Vol. 19, No. 11, Nov. 1982.

Bise, Michael E., Black, Thomas G., "Is Agility Implicit in Flying Qualities?," *Proceedings of the 1990 IEEE National Aerospace and Electronics Conference*, Dayton, OH, May 1990.

Bratt, R.W. and Johnston, E.W., "Technology Analysis - Candidate Advanced Tactical Fighters," AIAA-78-1451-CP, AIAA Systems and Technology Meeting, Aug. 1978.

Chin, J., "X-29A Flight Control System Performance During Flight Test," AIAA-87-2878-CP, AIAA Aircraft Design, Systems and Operations Meeting, Sep. 1987.

Chin, Hubert H, "A Knowledge Based System for Supermaneuver Selection for Pilot Aiding," AIAA-88-4442-CP, AIAA Aircraft Design, Systems and Operations Meeting, Sep. 1988.

Chody, Joseph R., Hodgkinson, John, and Skow, Andrew M., "Combat Aircraft Control Requirements for Agility," *Aerodynamics of Combat Aircraft Controls and of Ground Effects*, AGARD-CP-465, Apr. 1990.

Conrady, Neal, Baron, Timothy, and Fu, Johnny S., "Local Adaptive Maneuvering Optimization for Fighter Aircraft," AIAA-90-3453-CP, AIAA Atmospheric Flight Mechanics Conference, Portland, OR, Aug. 1990.

Cord, Thomas J., Detroit, Mark J. and Multhopp, Dieter, "Is An Agility Requirement Needed for Fighter Agility," SAE Aerospace Atlantic Conference, Dayton, OH, Apr. 1990.

Cord, Tom J., "A Standard Evaluation Maneuver Set for Agility and the Extended Flight Envelope - An Extension to HQDT," AIAA-89-3357-CP, AIAA Atmospheric Flight Mechanics Conference, Boston, MA, Aug. 1989.

Ethell, Jeffrey L., "Radar Combat and the Illusion of Invincibility," *Aerospace America*, Jan. 1990, pp. 14-18.

Foltyn, R.W., et al., "Innovative Cockpit Display and Cuing Systems for Operation in an Extended Flight Envelope." NASA-TR-87-215.

Gilbert, W.P., "Overview of NASA High-Alpha Technology Program (HAPT)," High Alpha Technology Program Workshop, Nov. 1989.

Henri, A.W., "Review of Practical Experience on Combat Aircraft Maneuverability," Royal Netherlands Air Force.

Herbst, Wolfgang B., "Future Fighter Technologies," *Journal of Aircraft*, Vol. 17, No. 8, Aug. 1980.

Herrick, Paul W., "Propulsion Influences on Air Combat," AIAA-85-1457-CP, AIAA Joint Propulsion Conference, Jul. 1985.

Innocenti, Mario, "Metrics for Roll Response Flying Qualities," *Flying Qualities*, AGARD-CP-508, Feb. 1991, pp. 14-1 to 14-11.

Juang, Jyh-Ching and Yussef, Hussein M., "Aircraft Agility," Lockheed Aeronautical Systems Company, Burbank, CA, 1990.

Johnston, Donald E., "High AOA Lateral-Directional Design Guides and Criteria - A Piloted Simulation Assessment," *Proceedings of AFFDL Flying Qualities Symposium Held at Wright-Patterson Air Force Base in October 1979*, AFWAL-TR-80-3067, May 1980, pp. 9-28.

Kalviste, Juri, "Spherical Mapping and Analysis of Aircraft Angles for Maneuvering Flight," *Journal of Aircraft*, Vol. 24, No. 8, Aug. 1987.

Kalviste, Juri, "Roll Reversal Agility Parameter," Air Force Flight Dynamics Laboratories, Dayton, OH, AFFDL Aircraft Agility Workshop Summary Booklet, Aug. 1989.

Kato, Osamu, "Attitude Projection Method for Analyzing Large-Amplitude Airplane Maneuvers," *Journal of Guidance, Control, and Dynamics*, Vol. 13, No. 1, Jan.-Feb. 1990, pp. 22-29.

Kocher, James A., "Integrated Control and Avionics for Air Superiority: A Program Overview," SAE Paper 901049, SAE Aerospace Atlantic Conference, Dayton, OH, Apr. 1990.

Liu, Hung-Chi, "Development of Trim States and Linear Models From Nonlinear Simulations," MS Thesis, University of Kansas Department of Aerospace Engineering, Lawrence, KS, Dec. 1991

Madelung, Gero, "Characteristics of Fighter Aircraft," AIAA-77-1219-CP, AIAA Aircraft Systems and Technology Meeting, Seattle, WA, Aug. 1977.

Mayer, John P., and Hamer, H.A., "A Study of Service-Imposed Maneuvers of Four Jet Fighter Airplanes in Relation to Their Handling Qualities and Calculated Dynamic Characteristics," NACA RM L55E19, Aug. 1955.

Mazza, C.J., "Agility: A Rational Development of Fundamental Metrics and their Relationship to Flying Qualities," *Flying Qualities*, AGARD-CP-508, Feb. 1991, pp. 27-1 to 27-7.

McKay, K., and Walker, M.J., "A Review of High Angle of Attack Requirements for Combat Aircraft," *Flying Qualities*, AGARD-CP-508, Feb. 1991, pp. 28-1 to 28-12.

Myers, T.T., McRuer, D.T., and Johnston, D.E., "Flying Qualities Analysis for Nonlinear Large-Amplitude Maneuvers," AIAA-87-2904-CP, AIAA/AHS/ASEE Aircraft Design, Systems and Operations Meeting, St. Louis, MO, Sept. 1987.

Neal, T.P. and Smith, R.E., "An In-flight Investigation to Develop Control System Design Criteria for Fighter Airplanes," Air Force Flight Dynamics Laboratories, Dayton, OH, AFFDL-TR-70-74, Dec. 1970.

Polumbo, Jake, "Lethal at the Merge...Kill and Survive," *USAF Fighter Weapons Review*, Summer 1992, pp. 23-25.

Raymer, Daniel P., "Post-Stall Maneuver and the Classic Turn Rate Plot," AIAA-91-3170-CP, AIAA/AHS/ASEE Aircraft Design, Systems and Operations Meeting, Baltimore, MD, Sept. 1991.

Roskam, Jan, "A Simplified Method to Identify and Cure Roll Coupling," *Journal of the Aerospace Sciences*, Vol. 29, No. 5, May 1962.

Rutowski, Edward, "Energy Approach to the General Aircraft Performance Problem," *Journal of the Aeronautical Sciences*, Vol. 21, No. 3, Mar. 1954, pp. 187-195.

Skow, Andrew M., "An Analysis of the Su-27 Flight Demonstration at the 1989 Paris Air Show," SAE Paper 901001, SAE Aerospace Atlantic Conference, Dayton, OH, Apr. 1990.

Talty, P.K. and Caughling, D.J., "F-16XL Demonstrates New Capabilities in Flight Test at Edwards AFB," *Journal of Aircraft*, Vol. 25, No. 3., May-Jun. 1988.

Twisdale, T. and Franklin, D., "Tracking Task Techniques for Handling Qualities Evaluations," AFFTC-TD-75-1, May 1975.

Walker, H.C., AFFTC Agility Flight Test Committee Meeting Minutes, Jun. 1987.

Woodcock, Robert J., "Estimation of Flying Qualities of Piloted Airplanes," Air Force Flight Dynamics Laboratories, Dayton, OH, AFFDL-TR-65-218, Apr. 1966.

A. CANDIDATE AGILITY METRICS

A.1 BACKGROUND

This appendix contains a list of most of the published agility metrics and the references in which they may be found. Each metric in this section is classified according to type, defined, and in most cases discussed briefly. The definition used for each metric is the definition according to the author(s) of each metric.

A.2 CANDIDATE PITCH AGILITY METRICS

Pitch agility metrics involve only pitching motion and normal acceleration.

A.2.1 **Time Derivative of Load Factor** (REF. 32)

Definition:

The time rate of change of normal load factor for a given maneuver.

Discussion:

The *time derivative of load factor*, though difficult to measure directly, can, in theory, be extracted from flight test or simulation time histories. Since both pitch up and pitch down capability are tactically important, the rate of change of normal load factor during both types of maneuvers should be investigated. It has been shown in Reference 32 that time histories of normal load factor derivative and the *curvature agility* metric of Reference 33 are virtually identical when scaled to account for different units.

A.2.2 **Time to Capture a Specified Angle of Attack** (REF. 18)

Definition:

The time required to attain (pitch up and stop) maximum lift angle of attack from various initial angles of attack.

Discussion:

During subsequent discussion of pitch agility (at the AFFDL Agility Workshop, Aug 89, for example), *time to capture a specified angle of attack* was generally rejected as a useful metric. Its primary disadvantage is the difficulty in accurately capturing a specified angle of attack during flight test. A secondary disadvantage is that the time to capture angle of attack is not an appropriate quantity for comparison among dissimilar aircraft. Also, aircraft normal acceleration is generated by lift, which is a function angle of attack and lift curve slope. This metric neglects the lift curve (lift versus angle of attack) characteristics of the aircraft. For these reasons, the *time to capture a specified angle of attack* is not studied in this report.

A.2.3 **Time to Change Pitch Attitude** (REF. 24)

Definition:

The ability of an aircraft to change it's pitch angle as rapidly and precisely as possible.

Discussion:

Time to change pitch attitude has been flight tested by students at the USAF Test Pilots School (REF. 24). During that study, pitch angle changes of -45° to 45° and -30° to 30° were flown. Pilots and flight test engineers involved in that evaluation concluded that time to change pitch attitude was unsuitable due to the large changes in airspeed and altitude that occurred during the maneuver.

A.2.4 **Maximum Nose-Up and Nose-Down Pitch Rate** (REF. 18)

Definition:

The maximum value of positive pitch rate attainable in transitioning from a 1g flight condition to maximum lift angle of attack; the maximum value of negative pitch rate attainable in transitioning from maximum lift angle of attack to a 0g flight condition.

A.2.5 **Pitch Agility** (REF. 18)

Definition:

The sum of:

(time to pitch from a 1g flight condition to maximum lift coefficient or normal load factor)

and

(Time to pitch down from maximum lift coefficient or normal load factor to 0g)

Discussion:

The authors of this metric observed that both nose up and nose down pitch agility are important. However, a number of questions about pitch agility remain are not addressed in Reference 18.

1. If the times associated with nose up and nose down pitch maneuvers are to be summed, should the two be equally weighted?
2. Is the time to pitch up significantly different than the time to pitch down?
3. Does an aircraft with better positive pitch agility necessarily have better negative pitch agility?

Since these questions remain to be resolved by flight testers, engineers and fighter pilots, values associated with positive pitch maneuvers and those associated with nose down pitching are treated as separate metrics through out this report rather than summed into a single figure

of merit. Though the time to achieve maximum normal load factor and the time to unload to zero normal load factor are conceptually simple, several difficulties arise when these metrics are evaluated with realistic aircraft models. While it is easy to initiate the pitch up from steady level flight conditions, the pitch down from positive normal load factor may start from a condition where airspeed and altitude are rapidly changing. If pitch agility is to be plotted against flight condition, the choice of flight condition may often be somewhat arbitrary.

A.2.6 **Average Pitch Rate**

Definition:

This metric is defined as

$$\text{Average Pitch Rate} = \frac{\int_{t_1}^{t_2} q \, dt}{t_2 - t_1}$$

where q is pitch rate, t_1 is the time at which the pitch-up is executed, and t_2 is the time at which the pitch-up maneuver is completed. The completion time t_2 is selected at the discretion of the tester. Usually, t_2 is selected from a common sense point of view for the particular task which is being performed.

Discussion:

A pilot usually commands pitch rate to point the nose of the aircraft or to achieve a desired load factor/turn rate. Ideally, pitch agility metrics should be task oriented. Measuring maximum pitch rate capability does not relate directly to either of these tasks. Most pitch agility metrics measure only the peak value of pitch rate that an aircraft can generate. This is often misleading for the purpose of comparing aircraft since aircraft can only momentarily generate very large values of pitch rate. From a task oriented point of view, it is the *average pitch rate* which is desirable to measure. This metric gives some indication of how quickly

a change in pitch angle can be acheived. It penalizes an aircraft which can briefly generate a large pitch rate, and rewards the aircraft which can sustain maintain the largest values of pitch rate over a period of time. Presentation of the *average pitch rate* metric are plots of average pitch rate versus Mach number, for a specified altitude.

A.2.7 **Pitch Agility Criteria** or **Maximum Initial Pitch Acceleration Parameter** (REF. 18)

Definition:

This metric is defined as

$$\text{Pitch Agility Criteria} = \frac{S\,\bar{c}\,C_{m_\delta}}{I_{yy}}$$

where C_{m_δ} is the nondimensional pitching moment produced by maximum deflection the aircraft's pitch control surfaces. Here, S, $\bar{c}$ and I_{yy} are standard notation for reference wing area, mean aerodynamic chord and pitch axis moment of inertia.

Discussion:

This parameter is extracted from the expression for the dimensional pitching moment derivative

$$M_\delta = \frac{\bar{q}\,S\,\bar{c}\,C_{m_\delta}}{I_{yy}}$$

and is a measure of the airframe's potential to generate pitch acceleration. It can be calculated directly from aerodynamic coefficients and configuration data but does not reflect any flight control system limits.

A.3 CANDIDATE LATERAL AGILITY METRICS

Lateral agility metrics deal primarily with rolling motion, especially rolling at high angles of attack and/or elevated normal load factors.

A.3.1 **Lateral Agility, T_{RC90}** (REF. 18)

Definition:

The time required to roll 90° and stop while maintaining an angle of attack.

Discussion:

This metric is a closed loop maneuver which is a function of Mach number, altitude, and normal load factor or angle of attack. No criteria is supplied as to what constitutes the "stop" which terminates the maneuver. How (or should) this maneuver be compared to the more common technique of unloading first, then rolling at one or zero g and then pitching to re-establish the initial angle of attack is not specified. The unload-roll-load method is probably faster especially for high angle of attack conditions. Using the loaded roll method, i.e. holding angle of attack as constant as possible during the roll, the aircraft heading angle is changed during the rolling maneuver. However, with the unloaded roll method the aircraft orientation is changed but the heading angle is not rotated since the roll is accomplished while unloaded. Manned simulation or flight test may be required to determine which pilot technique is both easiest to test and most meaningful to the tactical (as opposed to the test) pilot. It is the opinion of Reference 55 and others that the loaded roll is important in the study of fighter agility since it measures the ability of the aircraft to maneuver at high angles of attack even though it is not as commonly used by current fighters engaged in air combat maneuvering.

A.3.2 **Lateral Agility, T_{RC180}** (REF. 18)

Definition:

The time required to roll 180° and stop while maintaining an angle of attack.

Discussion:

This metric may be more representative of actual tactics than T_{RC90}. T_{RC180} is also a more demanding test of the flight control system since the build up of adverse yaw will be more pronounced over the longer maneuver.

A.3.3 **Roll Angle Capture** (REF. 25)

Definition:

The time required to roll and capture delta phi = 90°, 180°, and 360°.

Discussion:

The T_{RC90} and T_{RC180} metrics introduced above are subsets of the roll angle capture metric. The discussion involving the T_{RC90} and T_{RC180} metrics can generally be applied to the roll angle capture metric.

A.3.4 **Time Through Roll Angle** (REF. 58)

Definition:

The time required to roll through a target bank angle at elevated normal load factor levels.

Discussion:

Unlike the lateral agility metrics described above, the *time through roll angle* metric is measured using open loop pilot command inputs. This metric specifies the time to achieve

a specific bank angle change, initiated from a load factor of 1g with wings level. The specification states that the inputs shall be abrupt, and the pitch control input shall be fixed throughout the maneuver. This metric has evolved into its present form from several metrics which had appeared in earlier versions of the military specification for flying qualities of piloted airplanes (REF. 59, 60). It is a well defined metric which specifies the class of aircraft, the flight phase, and the speed range. These conditions were imposed on the metric to i) account for the reduction in roll response at low and high airspeeds, ii) account for the reduction in roll response at elevated load factors, iii) require higher response rates in the middle of the envelope for 1g flight (REF. 61). Thus the bank angle requirements were adjusted such that the bank angle change was modified to be compatible with the speed at which the roll performance was to be demonstrated (REF. 62). The roll performance for 360° rolls were proposed to apply only at 1g. This was done because it agreed with the current requirement in the loads specification, and could be tested without special planning in a typical test program. Unlike the *roll angle capture* metrics, the *time through roll angle* metric does not address the controllability aspect of arresting the roll after the specified bank angle change has been achieved. In spite of this, the metric is testable, repeatable, and is useful in the study of agility. Results using this metric are presented in Chapter 4.

A.3.5 **Roll Reversal Capture** (REF. 25)

Definition:

> The time required to roll from a 90° bank angle to the opposite 90° bank angle and then back to capture the original bank angle.

Discussion:

> The *roll reversal capture* metric is a variation of the *roll angle capture* metric and most likely highlights slightly different qualities of an aircraft's transient performance. It is assumed that

this metric is to apply for rolling maneuvers at elevated normal load factor levels. No criteria has been supplied defining the capture of the original bank angle.

A.3.6 **Defensive Roll Reversal Agility Parameter** (REF. 35)

Definition:

This metric is defined as

$$\text{Defensive Roll Reversal Agility Parameter} = Y^n T$$

where Y is the cross range generated during the maneuver, T is the time required to perform the maneuver, and n is a weighting factor on the distance parameter. The data is obtained by executing a maneuver consisting of an initial steady, level turn at constant velocity with a bank angle for horizontal flight, followed by a roll through zero bank angle until the same bank angle as the initial bank angle is reached (not captured) except with an opposite sign. Angle of attack is to be held constant during the maneuver. Y and T are measured when the flight path heading angle is equal to the initial heading angle, not the time when the roll reversal is completed.

Discussion:

The *defensive roll reversal agility parameter* uses essentially the same maneuver as the *roll reversal capture* metric, except that cross range is also accounted for. The smaller the value of the *defensive roll reversal agility parameter*, the more agile the aircraft is judged to be. The weighting on the distance parameter (n) is assumed to be unity for an initial approximation in defensive maneuvers. The weighting is less than unity in offensive situations where the task is to change the direction of flight, since angular advantage due to cross range would not be as great as for the typical "point and shoot" maneuver. The actual value of the weighting parameter is obtained empirically (REF. 35). Once the weighting parameter has been established, the *defensive roll reversal agility parameter* can be used to compare the agility of different aircraft for the roll reversal maneuver.

A.3.7 **Torsional Agility, TR/T_{RC90}** (REF. 18)

Definition:

Turn rate (TR) divided by the lateral agility metric, T_{RC90}, as defined above. Resulting units are degrees per second squared.

Discussion:

This metric is referred to as torsional because the maneuver encompasses rolling while turning, and thus is loosely analogous to the familiar solid mechanics example of the torsion of a rod due to an applied moment. The authors of this metric felt that measuring agility in this way captures not only the roll rate capability but also the roll acceleration/deceleration dynamics of the aircraft. The time to bank and stop is computed at all angles of attack to characterize lateral agility at elevated normal load factors. The values of this metric can be obtained from the same flight test results used to obtain T_{RC90} data so all the issues associated with that metric apply here also. Turn rate is not measured directly during the flight test but is calculated from test results based on airspeed and normal load factor as

$$\text{turn rate} = \frac{g\sqrt{n_z^2 - 1}}{V}$$

When these quantities change during the rolling maneuver the choice of which speed and normal load factor to use in calculating turn rate is unresolved. This metric also indicates that turn rate and T_{RC90} are equally critical to agility. For example, an aircraft with twice the normal acceleration for a given angle of attack and airspeed is exactly as torsionally agile as one with half the T_{RC90} at the same conditions.

A.3.8 **Roll Transient** (REF. 25)

Definition:

The maximum stability axis roll acceleration achieved when reversing a full stick 360° roll.

Discussion:

Roll acceleration metrics have several inherent problems. Specifically, acceleration is just one aspect of transient performance and measuring just the maximum value ignores the many other factors that are important in performing a roll quickly. Reference 34 points out that in a single degree-of-freedom approximation, roll acceleration is related to maximum roll rate P_{max} and roll mode time constant τ_r through the equation

$$\dot{P} = \frac{P_{max}}{\tau_r}$$

A given value of $\dot{P}$ could come from a wide range of values of P_{max} and τ_r, corresponding to either Level 1 dynamics, sluggish dynamics, or sensitive dynamics with poor controllability.

A.4 CANDIDATE AXIAL AGILITY METRICS

Axial agility metrics are intended to quantify the ability of an aircraft to transition between energy states or specific excess power (P_s) levels. They involve only translational motion.

A.4.1 **Axial Agility** (REF. 18)

Definition:

The increment of specific excess power (ΔP_s) resulting in going from a minimum power/maximum drag condition, to a maximum power/minimum drag condition, divided by Δt, the time in seconds required to complete the transition (REF. 18).

$$\frac{\Delta P_s}{\Delta t} = \frac{P_{s\ final} - P_{s\ initial}}{t_{final} - t_{initial}} \qquad (1)$$

Transition from minimum to maximum power is called the *power onset parameter* and transition from maximum to minimum power is termed the *power loss parameter.*

Discussion:

Traditional methods of quantifying the axial capability (i.e. longitudinal translation capability) of fighter aircraft have generally consisted of thrust-to-weight ratio, maximum level Mach number, maximum rate of climb and specific excess power (P_s). These point performance measures of merit only quantify performance at discrete aircraft states and are not indicative of the capability of an aircraft to change its energy state rapidly. Axial agility metrics are intended to provide a measure of this capability. The axial agility metrics measure the rate of change of P_s and conform well to the idea of agility being the rate of change of maneuverability (REF. 4). Instead of knowing only what level of P_s an aircraft possesses at a particular point, axial agility reflects how effectively the aircraft can **transition** to another P_s level. The *power onset* and *power loss parameters* measure the combined effects of engine spool time, maximum thrust and drag due to speed brakes. An aircraft with good axial agility is characterized by superior velocity control (both acceleration and deceleration).

A.5 CANDIDATE FUNCTIONAL AGILITY METRICS

Functional agility metrics deal with time scales of ten to twenty seconds. This class of metrics seeks to quantify how well the fighter executes rapid changes in heading or rotations of the velocity vector. The emphasis is on energy lost during turns through large heading angles and the time required to recover kinetic energy after unloading to normal load factor of zero. Many of these functional agility metrics involve maneuvers made up of a sequence of brief segments of the transient agility metrics.

A.5.1 **Combat Cycle Time** (REF. 30)

Definition:

$t_1 + t_{21} + t_{22} + t_3 + t_4$ where:

t_1	=	time to pitch from one g to the limit normal load factor
$t_{21} + t_{22}$	=	time to turn to a specified new heading angle at maximum normal load factor
t_3	=	time to unload the aircraft to a normal load factor of one (or zero)
t_4	=	time to accelerate to the original energy level

Discussion:

The *combat cycle time* metric is characterized by a continually changing flight condition constrained within structural, lift, and power limits. It is calculated for a given set of starting conditions and some specified heading angle change, usually either 90 or 180 degrees. The plot of this metric conveniently shows the relationships of normal load factor, velocity, turn rate, and turn radius for a level turn. It is not clear whether the author of the metric intends for the aircraft to be at the same Mach number and altitude at the end of the combat cycle or only to have the same total energy. Times t_1 and t_3 might be negligible relative to the others

so this parameter is probably dominated by turn rate and P_s. Another useful feature of the *combat cycle time* metric is that its maneuver cycle allows for measuring the *dynamic speed turn*, *relative energy state*, *energy-agility*, and *time-energy penalty* metrics.

A.5.2 **Dynamic Speed Turns** (REF. 47, 54)

Definition:

plot of specific excess power (P_s) versus maximum turn rate at a given starting airspeed.

Discussion:

This intent of this metric is to capture the dynamic maneuvering capability of fighter aircraft (agility) as viewed from a pilots perspective, and to present that capability in a form which can be readily used by pilots and engineers. This is accomplished by clearly showing the bleed rate for maximum acceleration turns and the straight and level acceleration capability at various airspeeds. *Dynamic speed turn* plots show the dynamics of turning and acceleration over a wide range of speeds, combine the ability of the aircraft to point its nose, continue pointing its nose, and accelerate.

A.5.3 **Relative Energy State,** (V/V_c) (REF. 30)

Definition:

The ratio of the aircraft's speed to its corner speed at completion of a 180 degree turn at maximum g from a given starting position (altitude and airspeed). This ratio, V/V_c, should be as close to 1.0 as possible.

Discussion:

Relative energy state is classified as a functional agility metric because it is dominated by

thrust and drag characteristics. The author of this metric suggests that at least two 90 degree turns must be made before falling below corner speed. Any speed below corner indicates that the fighter has maximized pointing capability while exhausting maneuvering potential and conversely, any speed above corner indicates that a fighter has not yet achieved its maximum pointing ability in favor of retaining energy for future maneuvering. Turn rate and thus the time required to complete the 180 degree turn are not addressed by this metric.

A.5.4 **Energy-Agility** (REF. 5)

Definition:

The specific energy of an aircraft during the time required to complete a maneuver, plotted as a function time.

Discussion:

This metric was developed as an attempt to model the time to kill, the time to recover, and the energy compromised as an engineering tool. The concept for this metric was inspired by the description of an angles fight and an energy fight (REF. 55). An angles fight is one in which a positional advantage is sought first at the expense of energy. The purpose of the energy fight is to garner an energy advantage over the adversary and then convert this energy into a lethal positional advantage. The author of this metric coined the terms *angles-agility* (the ability to rapidly and efficiently convert a given energy advantage into a useful positional advantage) and *energy-agility* (the ability to minimize the time-energy penalty while directly seeking a useful positional advantage) from which this metric derives its name.

A.5.5 **Time-Energy Penalty** (REF. 43)

Definition:

This metric is defined as

$$\text{Time Energy Penalty} = t_{\Delta\psi} * \Delta h_e$$

where $t_{\Delta\psi}$ is the time to complete a specified heading angle change and (if required) the time to pitch down to achieve missile envelope firing parameters, and Δh_e is the change in specific energy height during the maneuver.

Discussion:

The *time-energy penalty* metric examines the tactically significant maneuver of heading angle changes. This metric is essentially an extension of the *combat cycle time* and *energy-agility* metrics with its name taken from Reference 57. The result of a direct multiplication between $t_{\Delta\psi}$ and Δh_e is a single parameter which equally weighs the importance of minimizing time and preserving energy during a heading change maneuver. The ideal situation is a maneuvering aircraft which completes a short duration turn with minimal energy loss. Conversely, an aircraft which turns slowly and depletes a large amount of energy is undesirable. The time $t_{\Delta\psi}$ consists of the sum of the time to roll 90 degrees and pitch to maximum normal load factor (t_1 of *combat cycle time*), plus the time to obtain a specified heading angle (t_2 of *combat cycle time*), plus the time to pitch down and reduce angle of attack or normal load factor so that the missile can be fired within its envelope. The change in specific energy height, Δh_e, is measured from the start of the maneuver until the time at which the heading angle is reached and the missile envelope parameters are attained.

A.5.6 **DT Parameter** (REF. 35)

Definition:

This metric is defined as

$$\text{DT Parameter} = D^n T$$

where D is the cross range distance of the maneuver, T is the time required to perform the maneuver, and n is a weighting factor on the distance parameter. The maneuver is initiated from straight and level flight at constant velocity. The aircraft then pitches, rolls into a limit normal load factor level turn, and then decelerates to corner speed to achieve maximum instantaneous turn rate. The turn is continued at constant angle of attack until the body X-axis of the aircraft has been turned through 180°.

Discussion:

The *DT parameter* is analogous to the *defensive roll reversal agility parameter* defined in Section A.3.6, except that the maneuver for the *DT parameter* is a level 180 degree turn. This metric is a function of Mach number, altitude, and the heading angle change of the maneuver. It is intended to predict the "point and shoot" firing solution in engagements consisting of aircraft which have different initial velocities and relative heading angles. Also, the difference in *DT parameters* for two aircraft performing the same maneuver (ΔDT) predicts an advantage for one of the aircraft, but does not relate directly to a time advantage, which is the most important parameter. The time advantage can be computed from

$$\Delta T = \frac{(DT)_{\text{aircraft B}} - (DT)_{\text{aircraft A}}}{D_{\text{aircraft A}}} = \frac{\Delta DT}{D_{\text{aircraft A}}}$$

The ΔT is an approximation of the time advantage that aircraft A has over aircraft B based on the difference in the *DT parameters* for the two aircraft. An important assumption which has been made in defining a "point and shoot" maneuver such as the *DT parameter* is that both aircraft have similar weapons and flying qualities so that the time increment for "capture"

(or termination of the maneuver) will be the same. The capture is defined in terms of the envelope of the weapon carried. Thus the termination of the maneuver is not defined in terms of capturing a desired angle, but rather in tracking a target, i.e when the weapon is within firing parameters. These parameters will be distinctly different for missiles and guns. The *DT parameter* encompasses some aspects of transient agility, and assumes both aircraft are to be constrained to a single maneuver plane, essentially 2-D maneuvering in the horizontal plane. As such, the metric is heavily dependent upon the traditional performance measure of sustained level turn performance. Like the *relative energy state* metric, the *DT parameter* is dominated largely by pitch rate and thrust and drag characteristics.

A.5.7 **Pointing Margin** (REF. 30)

Definition:

The angle between the nose of the adversary and the line of sight at the instant the friendly fighter is aligned with the line of sight.

Discussion:

This metric requires the definition of some standard adversary turn performance (normal load factor, speed loss, altitude change, etc). Reference Liefer 30 implies that both aircraft are to be constrained to a single maneuver plane. This metric incorporates the effects of pitch rate, thrust and drag transient characteristics but long term performance (seven to ten seconds) tends to have a greater impact than transient agility. Similar aircraft capabilities can possibly be assessed using the *DT parameter.*

A.5.8 **One-Circle Pointing Quotient** (REF. 41)

Definition:

This metric is defined as:

$$O_p = D + \sigma_* \left(d_r + \frac{d_o}{2} \right) \ln \left(T - t_r \right)$$

where O_p is the pointing quotient, D is the distance component of the one-ship pointing turn, σ_* is the flight path displacement angle required in the one-ship pointing turn, d_r is the length of the roll-in segment, d_o is the initial separation in the one-ship duel, T is the time component of the one-ship pointing turn, and t_r is the time of the roll-in segment. The one-ship pointing turn refers to a turn performed by an aircraft during a one-circle engagement (REF. 41).

Discussion:

The *one-circle pointing quotient* is a function of quickness and positioning in the one-circle engagement, thereby determining the relative importance of these two factors. The validity of the *one-circle pointing quotient* as a measurement of agility is independent of the tightness and quickness in the turn and hence independent of tactics and technologies. The author of this metric intended to provide a single agility number that quantifies the pointing capability of aircraft in the one-circle duel.

A.6 CANDIDATE AGILITY POTENTIAL METRICS

Agility potential metrics are independent of time and serve to highlight the (sometimes obvious) relationships between thrust, weight, inertia, control power and agility. They deal not with the aircraft characteristics demonstrated via flight test or simulation, but with the agility potential that results from sizing and configuration choices.

A.6.1 **Agility Potential and Maneuvering Potential** (REF. 31)

Definition:

> *Agility potential* is defined as the aircraft's maximum thrust to weight ratio divided by its wing loading. *Maneuvering potential* is not explicitly defined in Reference 31, but is described only as a function of the thrust to weight ratio, the lift to drag ratio, the maximum lift coefficient and wing loading.

Discussion:

> These two parameters relate aircraft size and configuration to agility using traditional measures of merit, wing loading and thrust to weight ratio. It is not the intention of these metrics to address transient aircraft agility, flight control characteristics, high angle of attack capability, and body rate controllability.

A.7 CANDIDATE INSTANTANEOUS AGILITY METRICS

The instantaneous agility metrics as a class are intended to quantify the instantaneous angular acceleration capabilities of aircraft. They are obtained by writing the aircraft equations of motion with respect to the aircraft velocity vector, and then differentiating with respect to time. The result is acceleration and jerk of the velocity vector, when taking the second and third derivatives with respect to time.

A.7.1 **Curvature Agility** (REF. 18, 33)

Definition:

This metric is defined as

$$\text{Curvature Agility} = 2\,\omega\,\dot{v} + v\,\dot{\omega}$$

where v is aircraft velocity, and ω is turn rate.

Discussion:

The *curvature agility* metric is intended to quantify the instantaneous pitch agility of aircraft. It is based upon the second derivative with respect to time of the aircraft velocity vector. For a complete derivation and further discussion of this metric, see Appendix E.

A.7.2 **Herbst Torsional Agility** (REF. 18, 33)

Definition:

This metric is defined as

$$\text{Torsional Agility} = \frac{d}{dt}\left(\dot{\Psi} - \dot{\chi}\sin\gamma\right)$$

where all variables are defined in the Serret-Frenet reference system (REF. 64, 65).

Discussion:

Like the *curvature agility* metric, the *Herbst torsional agility* metric is based upon the second derivative with respect to time of the aircraft velocity vector. Although this is a lateral agility metric, it bears no real similarity to the *torsional agility parameter* defined in Section A.3.7 other than by name. For a complete derivation and further discussion of this metric, see Appendix E.

B. FLIGHT SIMULATION PROGRAMS

B.1 BACKGROUND

This appendix contains descriptions of the flight simulation computer programs used to obtain the results in this report. The aircraft models consist of a generic F-5A, generic F-16A, generic F-18A, and generic X-29A. Brief descriptions of the simulation programs, summaries of the mass properties used for the test cases, and physical descriptions are provided.

B.2 GENERIC F-5A SIX DEGREE-OF-FREEDOM AIRCRAFT SIMULATION (ATHP)

The flight simulation program used to model the generic F-5A Freedom Fighter is the University of Kansas Flight Research Laboratory's version of the Aircraft Time History Program (ATHP) (REF. 66). The ATHP simulation is a high fidelity non real-time, nonlinear six degree-of-freedom aircraft simulation. It contains full flight control system, engine, and aerodynamic models. The flight control system is representative of the generic F-5A, consisting of pilot command inputs and a stability augmentation system. The aerodynamic data base contains nonlinear, steady aerodynamic data for up-and-away flight at angles of attack up to and including 40°. The aerodynamic data base was obtained from wind tunnel data. The engine model is nonlinear and is representative of the F-5A's powerplants. User interface to ATHP is through input and output files. The input files contain initial attitude and flight condition, and pilot commands in the form of longitudinal and lateral stick commands, rudder, and throttle time histories. Output files consist of tabular time history data which is plotted using standard plotting routines. Any special processing such as filtering or estimation is performed within the simulation itself when possible. All data collection runs for the generic F-5A were performed at the following mass properties.

1) Aircraft weight: 12,000 (lbf)

2) Inertias: I_{XX} = 2,620 (slug-ft^2)
I_{YY} = 30,300 (slug-ft^2)
I_{ZZ} = 32,300 (slug-ft^2)
I_{XZ} = -190 (slug-ft^2)

The external physical characteristics of the F-5A are displayed in Figure B.1.

B.3 GENERIC F-16A SIX DEGREE-OF-FREEDOM AIRCRAFT SIMULATION (F-16SIM)

The flight simulation program used to model the generic F-16A Fighting Falcon is the University of Kansas Flight Research Laboratory's F-16SIM. The F-16SIM simulation is a high fidelity non real-time, nonlinear six degree-of-freedom aircraft simulation. It contains full flight control system, engine, and aerodynamic models. The flight control system is representative of the generic F-16A. The aerodynamic data base contains nonlinear, steady aerodynamic data for up-and-away flight. The aerodynamic data base was obtained from wind tunnel data. The engine model is nonlinear and is representative of the F-16A's powerplant. User interface to F-16SIM is through input and output files. The input files contain initial attitude and flight condition, and pilot commands in the form of longitudinal and lateral stick commands, rudder, and throttle time histories. Output files consist of tabular time history data which is plotted using standard plotting routines. Any special processing such as filtering or estimation is performed within the simulation itself when possible. All data collection runs for the generic F-16A were performed at the following mass properties:

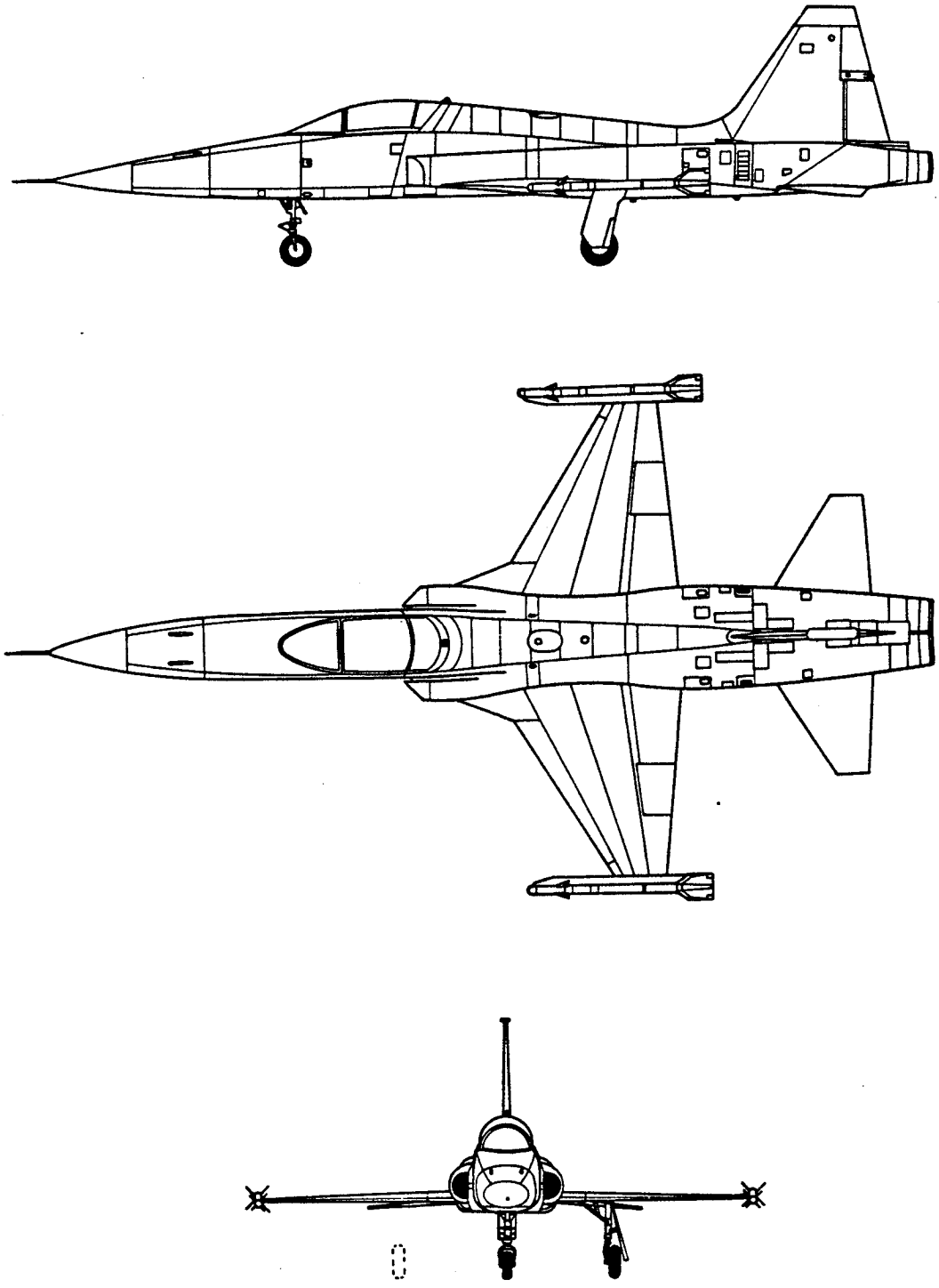

Figure B.1 F-5A External Physical Characteristics (REF. 67)

1) Aircraft weight: 20,048 (lbf)

2) Inertias: I_{XX} = 7,035 (slug-ft^2)
I_{YY} = 52,372 (slug-ft^2)
I_{ZZ} = 57,160 (slug-ft^2)
I_{XZ} = 52.2 (slug-ft^2)

3) Center of gravity location: 35.0% MGC

The external physical characteristics of the F-16A are displayed in Figure B.2

B.4 GENERIC F-18A SIX DEGREE-OF-FREEDOM AIRCRAFT SIMULATION (SIM-II)

The generic F-18A Hornet flight simulation computer program is the University of Kansas Flight Research Laboratory's version of Sim-II (REF. 8). The Sim-II program is a high fidelity, non real-time, nonlinear six degree-of-freedom aircraft simulation which has been used throughout the industry to model a wide range of aircraft. It contains full flight control system, engine, and aerodynamic models. The flight control system model is of version 8.3.3, and runs multi-rate with gain scheduling. All limiters and nonlinearities in the flight control system are present. The aerodynamic data base contains nonlinear, steady aerodynamic data for up-and-away flight at angles of attack up to and including 70 degrees. The aerodynamic data base was obtained from wind tunnel data and is corrected to flight test data, including flexibility effects. The engine model is nonlinear and is representative of the F-18A powerplant. User interface to Sim-II is through input and output files. The input files contain initial attitude and flight condition, and pilot commands in the form of longitudinal and lateral stick position, rudder, and throttle time histories. Output files consist of tabular time history data which is plotted using standard plotting routines. Any special processing such as filtering or estimation is performed within the simulation itself when possible. All simulation

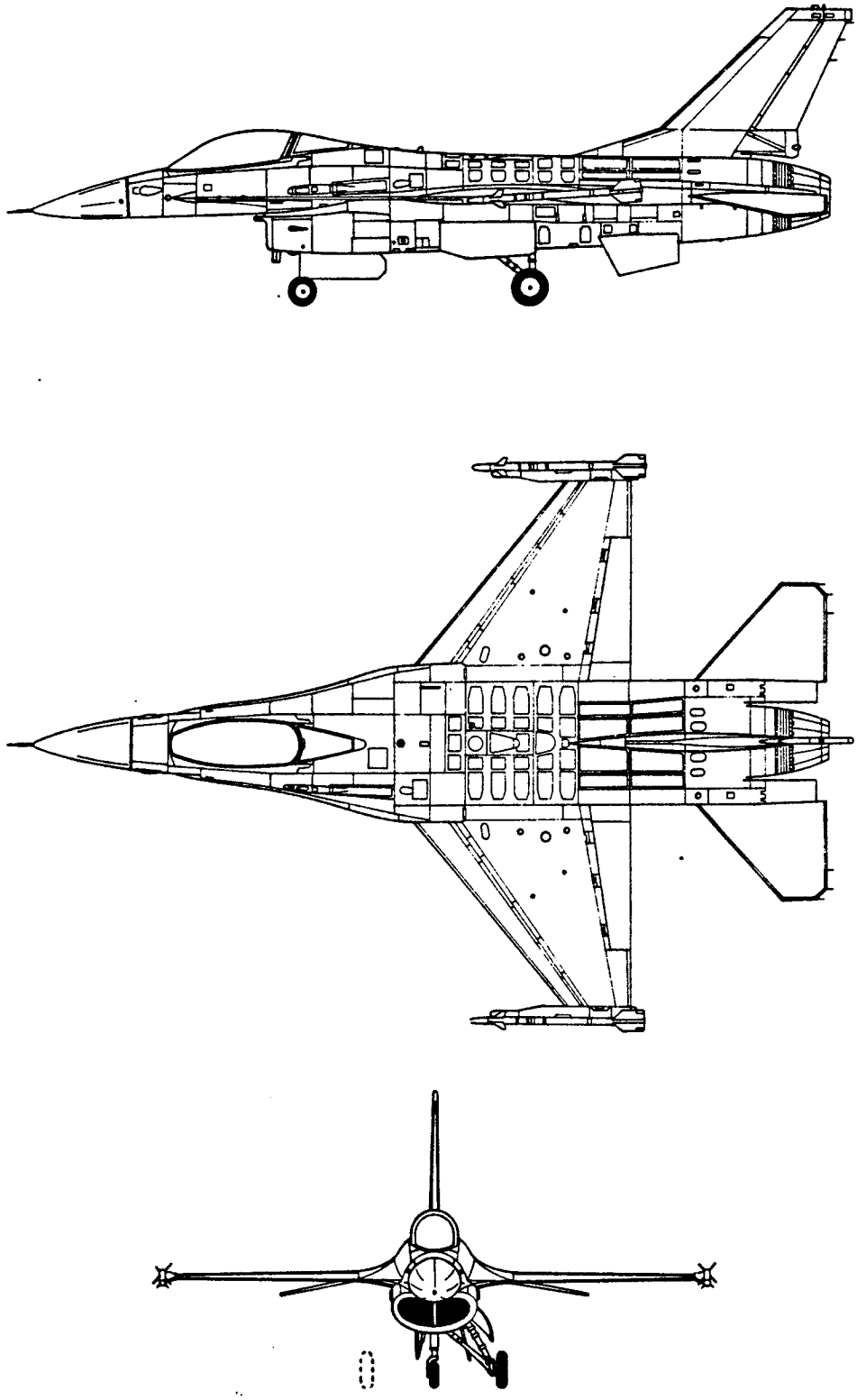

Figure B.2 F-16A External Physical Characteristics (REF. 67)

data collection runs for the generic F-18A were performed with the following mass properties:

1) Aircraft weight: 30,540 (lbf)

2) Inertias: I_{XX} = 21,957 (slug-ft^2)
I_{YY} = 122,506 (slug-ft^2)
I_{ZZ} = 137,339 (slug-ft^2)
I_{XZ} = 1,912 (slug-ft^2)

3) Center of gravity location: 23.3% MGC
FS 456.17 inches

The external physical characteristics of the F-18A are displayed in Figure B.3.

B.5 GENERIC X-29A SIX DEGREE-OF-FREEDOM AIRCRAFT SIMULATION

The generic X-29A flight simulation computer program at the NASA-Ames Dryden Flight Research Facility was used to obtain all of the generic X-29A data for this report. All simulation data collection runs for the generic X-29A were performed with the following mass properties:

1) Aircraft weight: 15,000 (lbf)

2) Inertias: I_{XX} = 4,600 (slug-ft^2)
I_{YY} = 53,600 (slug-ft^2)
I_{ZZ} = 56,000 (slug-ft^2)
I_{XZ} = 2,500 (slug-ft^2)

3) Center of gravity location: between FS 443.5 and 454. inches

The external physical characteristics of the X-29A are displayed in Figure B.4.

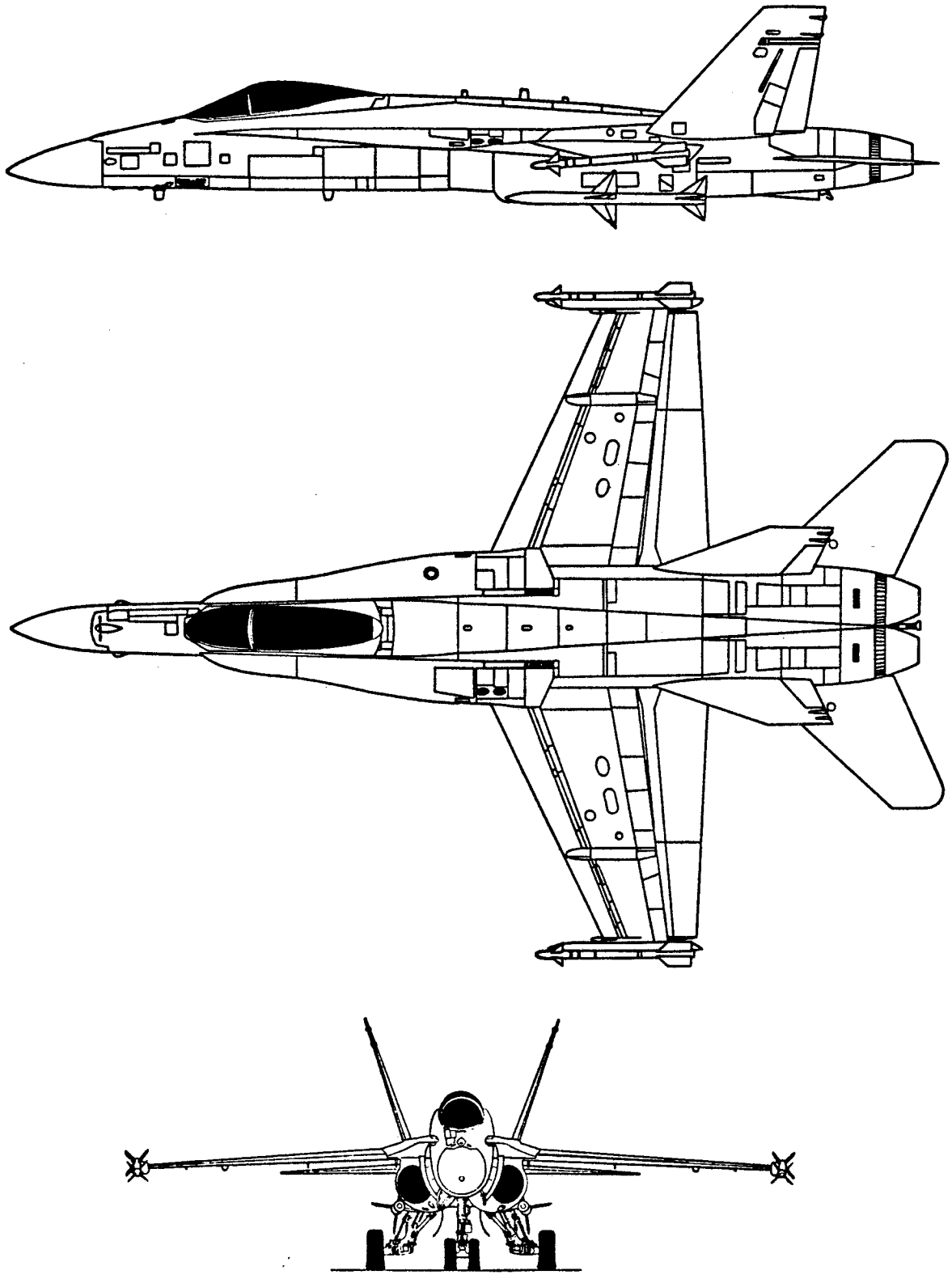

Figure B.3 F-18A External Physical Characteristics (REF. 68)

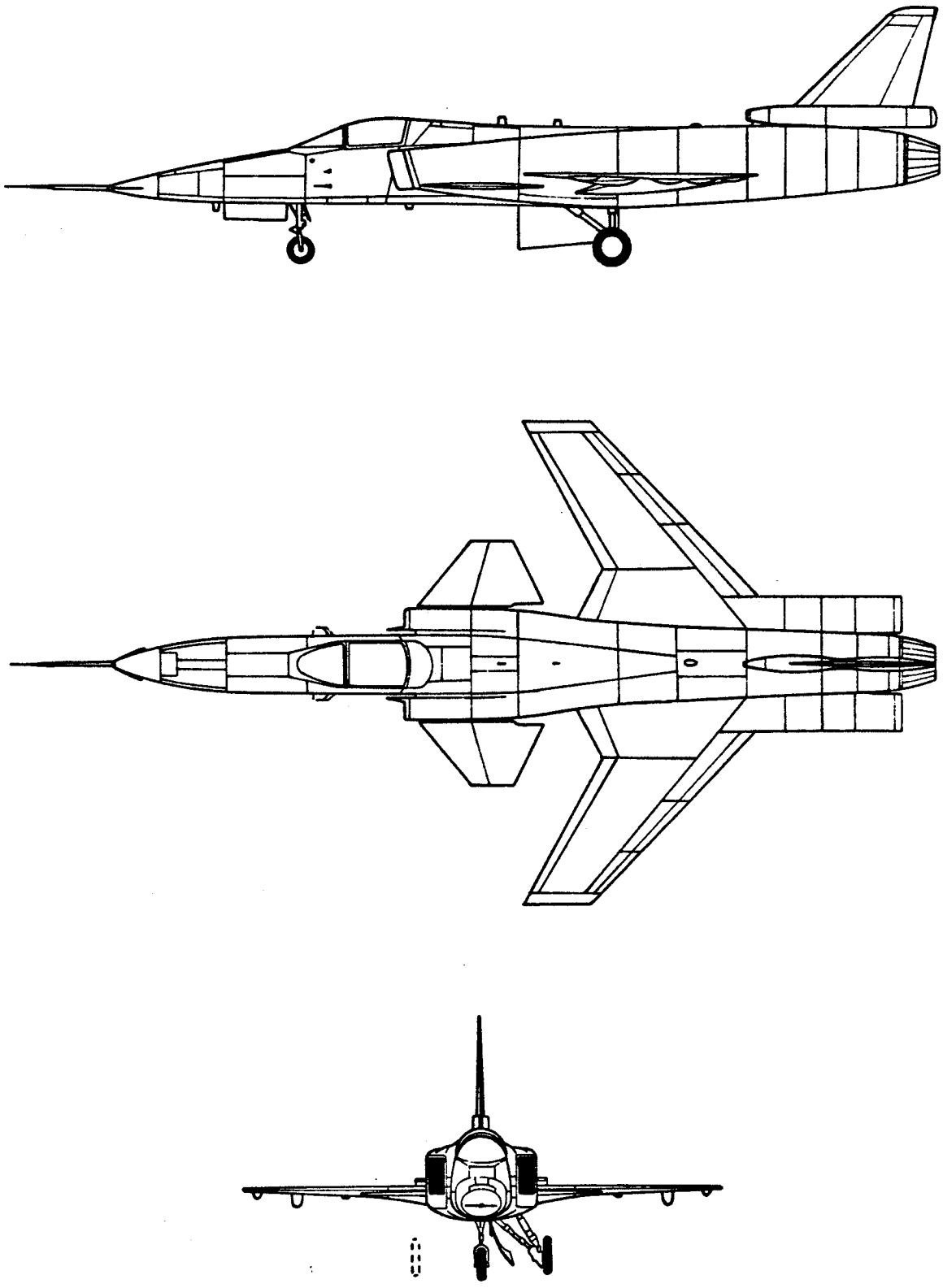

Figure B.4 X-29A External Physical Characteristics (REF. 69)

B.6 OPTIMAL TRAJECTORIES BY IMPLICIT SIMULATION PROGRAM (OTIS)

The following description is condensed from Reference 53. OTIS is a general purpose FORTRAN program for simulating and optimizing point mass trajectories for a wide variety of aerospace vehicles. The code was written by the Boeing Aerospace and Electronics company in Seattle, Washington for the Aeronautical Systems Division of the Wright Research and Development Center (REF. 9, 10). The code consists of over 400 subroutines with a total of over 74000 lines and can estimate aerodynamic heating for a vehicle and develop propulsion models for the vehicle, in addition to optimal trajectory development. The OTIS program can be run in one of four different modes to solve any of the following problems:

1) Generate a discrete trajectory for a set of predefined controls and fixed initial conditions (Mode 1-Explicit Trajectory Integration).

2) Solve targeting problems by varying the values of a set of specified independent variables to provide a trajectory which passes through a set of waypoints and/or satisfies preset boundary conditions (Mode 2 - Explicit Trajectory Integration With Targeting).

3) Compute an optimal trajectory by varying a set of independent variables, usually less than 10 in number. Constraints can be imposed. For optimization, the number of independent variables must be greater than the number of active constraints. If the number is less, a solution is not possible unless the constraints are dependent in some way on each other. If the number is equal, a feasible solution is possible but there is no freedom for optimization (Mode 3 - Explicit Trajectory Integration With Optimization).

4) Optimize trajectories by generating control functions and varying discrete parameters. The major difference between this problem and the previous one is that the optimal control problem has, in theory, an infinite number of degrees of freedom since control functions are being sought, rather than just discrete parameters. Also, path constraints which encompass the entire trajectory can be imposed (Mode 4 - Implicit Trajectory Optimization).

The above problems are complimentary because a discrete trajectory generated using Mode 1 can be used as an input for generating targeting and optimal trajectory solutions in Modes 2-4. In addition, Mode 1 trajectories can be used to verify the accuracy of Mode 4 results. The above problems can be solved for a wide variety of vehicles, such as aircraft, missiles, or spacecraft. The vehicle type os defined by user inputs that are read into the program through a namelist file. The inputs for the program consist of the following:

1) General inputs to describe the number of phases to divide the trajectory into, the type of atmospheric model to be used, and what coordinate system is to be used for integration.

2) Initial conditions and final conditions for trajectory to be simulated. This includes initial conditions for the states and controls and the starting and ending time constraints to be placed on the trajectory.

3) Constraints to be enforced at every point along the trajectory, such as limits on load factor, angle of attack, or altitude.

4) Scaling factors to be used to dimension all the states and controls in the program. This is done to bring all the variables within the same order of magnitude to allow the program to equally weigh all the variables in the solution process.

5) Definition of the objective function. This is a combination of any of the variables within the program, independent or dependent. For most problems in this thesis, maneuver time was the optimized parameter.

6) Inputs to describe the vehicle to be modeled, including the number of engines, the reference areas to be used for aerodynamic calculations, and the number of stages. Also, a tabular data file is used to input the aerodynamic and propulsion models for the vehicle.

7) Details of the parameters to be output by the program. This includes the generation of plots and tabular data files. The routines used in the code include techniques to convert the objective function to be minimized into a quadratic approximation, methods to estimate Lagrange multipliers for the quadratic function, and an algorithm to calculate the active set of constraints applicable to the problem. Once the active set is found and the constraints are determined, the problem is sent to a nonlinear quadratic programming algorithm to solve for the states and controls that minimize the objective function.

A sample namelist input file and printout of the tabular data file is available in Reference 53.

C. ADDITIONAL LATERAL AGILITY CONSIDERATIONS

C.1 BACKGROUND

This appendix contains detailed developments of several topics which are fundamental to the analysis and understanding of lateral agility.

C.2 AXIS SYSTEMS

Three different axis systems are required to adequately represent the translations and rotations of an aircraft during rolling maneuvers: body axes, stability axes, and wind axes. The body axes (X_B, Y_B, Z_B) are situated along the longitudinal (X_B), lateral (Y_B), and vertical (Z_B) axes of the aircraft as shown in Figure C.1 and remain rigidly attached to the airframe.

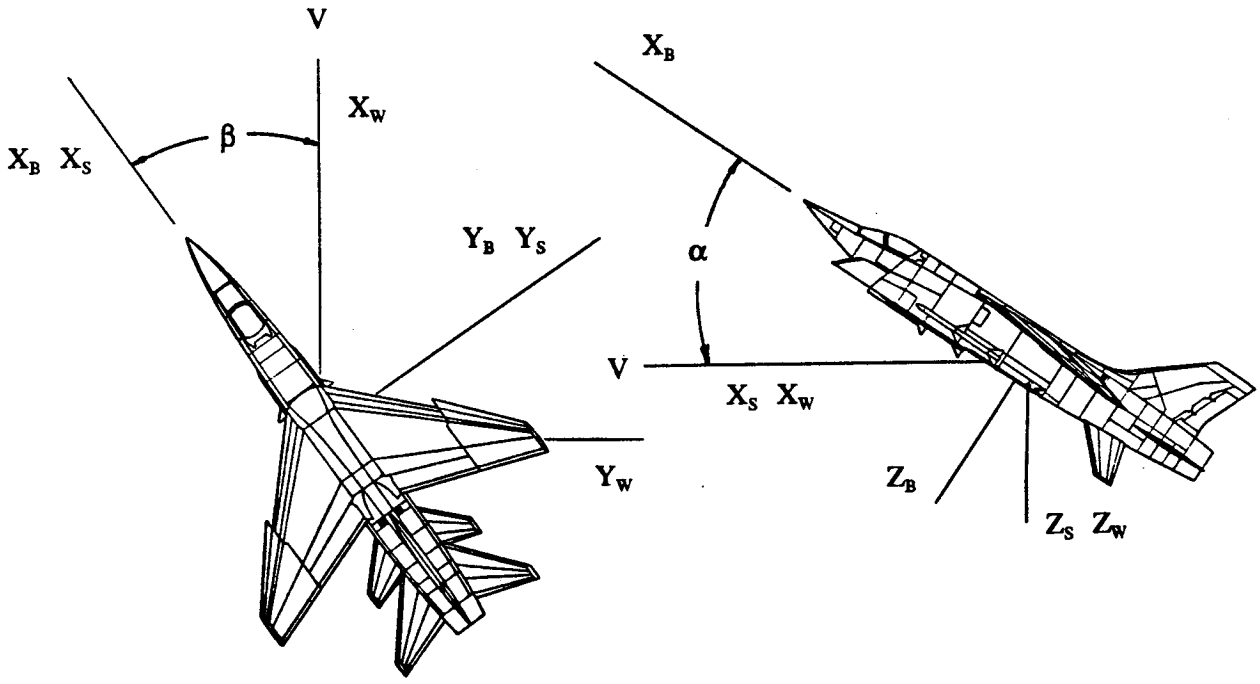

Note: Positive Senses Shown

Figure C.1 Geometric Relationships Between Body Axes, Stability Axes, And Wind Axes (REF. 38)

The stability axes (X_S, Y_S, Z_S) is itself a body fixed axis system. The X_S axis is obtained by rotating the X_B axis through the steady state angle of attack until it lies along the velocity vector. Wind axes (X_W, Y_W, Z_W) differ from stability axes in that the X_W axis is coincident with the velocity vector in the presence of steady state sideslip (Figure C.1), whereas the X_S axis always remains in the aircraft's X_B-Z_B plane (REF. 70). Although for some analyses the distinction between stability axes and wind axes is unimportant, the open literature largely tends to prefer the use of wind axes when discussing lateral agility, and that convention is followed in this report.

Since agility typically involves some amount of nose pointing, the rotation about the X_B axis is usually of only secondary importance to the rotation about the velocity vector. Physically, the motion consists of nonequivalent rotations about the aircraft X_B axis, and the velocity vector. Additionally, since adverse yaw and therefore sideslip is typically generated during these rotations, the roll rate about the X_W axis (P_W) should be measured instead of the roll rate about the X_S axis (P_{stab}). Stability axis roll rate in terms of body axis pitch, roll, and yaw rates, and angle of attack, and sideslip angle is defined as

$$P_{stab} = P\cos\alpha + R\sin\alpha \tag{C.1}$$

Similarly, wind axis roll rate is defined as

$$P_w = P\cos\alpha\cos\beta + R\sin\alpha\cos\beta + Q\sin\beta \tag{C.2}$$

C.3 ROLLING ABOUT THE VELOCITY VECTOR

Rolls should be coordinated to prevent roll oscillations due to the dihedral effect. These oscillations are more prevalent at high angles of attack where lateral-directional control power and

directional stability are reduced. A *coordinated roll* is defined here as a roll which occurs with zero sideslip angle. Roll coordination should not be confused with turn coordination, which is defined by lateral acceleration being equal to zero. Note that while a turn changes the direction of the velocity vector, a roll rotates the airframe about the velocity vector. The source of nonzero sideslip angles during a roll can be identified by considering the equation for sideslip rate:

$$\dot{\beta} = P\sin\alpha - R\cos\alpha + \sin\phi\cos\theta\frac{g}{V_t} + n_y\frac{g}{V_t} \tag{C.3}$$

For simplicity, Equation C.3 assumes the sideslip angle to be zero. Equation C.3 is however a good approximation to the complete equation used by nonlinear six degree-of-freedom aircraft simulations such as Reference 8 for values of sideslip angle at least as large as those encountered in this research. This was verified by comparing the sideslip rate from the generic F-18A simulation to that calculated by Equation C.3.

Sideslip rate can be divided into kinematic, gravitational and lateral g terms:

$$\dot{\beta}_{kinematic} = P\sin\alpha - R\cos\alpha \tag{C.4}$$

$$\dot{\beta}_{grav} = \sin\phi\cos\theta\frac{g}{V_t} \tag{C.5}$$

$$\dot{\beta}_{lateral\ g} = n_y\frac{g}{V_t} \tag{C.6}$$

Sideslip due to the kinematic term, called kinematic coupling, occurs when body axis roll and yaw rates are proportioned such that the axis of airframe rotation is not parallel to the velocity vector. The other two terms describe the sideslip rate caused by the forces acting on the airplane. During a roll

these two terms cannot be held to zero. Gravity effects sideslip rate in all attitudes except $\phi = 0°$, 180° and $\theta = \pm 90°$, while the control surface deflections required to roll the airplane produce lateral acceleration. Therefore, in order to roll with sideslip rate equal to zero, there needs to be just enough kinematic coupling to cancel the effects of gravity and lateral acceleration. To get a general idea of the body axis roll and yaw rates needed for roll coordination, Equation C.3 is set to zero and the effects of gravity and lateral g's are neglected:

$$0 = P\sin\alpha - R\cos\alpha \tag{C.7}$$

Solving for body axis yaw rate,

$$R = P\tan\alpha \tag{C.8}$$

Substituting Equation C.8 into Equation C.1 and multiplying by $\cos\alpha$, the body axis roll rate (P) can be expressed as a function of stability axis roll rate (P_{stab}) and angle of attack as

$$P = P_{stab}\cos\alpha \tag{C.9}$$

Then using Equation C.8, body axis yaw rate can be expressed as

$$R = P_{stab}\sin\alpha \tag{C.10}$$

tEquations C.9 and C.10 are used to construct Figure C.2 which indicates combinations of the body axis roll rates (P) and yaw rates (R) as a percent of P_{stab} which are required at zero sideslip over a range of angles of attack. Although these are simple relationships, they are important in understanding the roll and yaw rate requirements for lateral agility, especially at high angles of attack. For example, in order to be capable of a P_{stab} of 100 degrees per second at 20° angle of attack, a body axis roll rate of 87 degrees per second, and a body axis yaw rate of 27 degrees per second are required. Although a 100 degree per second body axis roll rate is typically very easy to achieve for most any jet fighter, the same fighter may not be able to achieve the same rate of stability and/or wind axis roll. This is

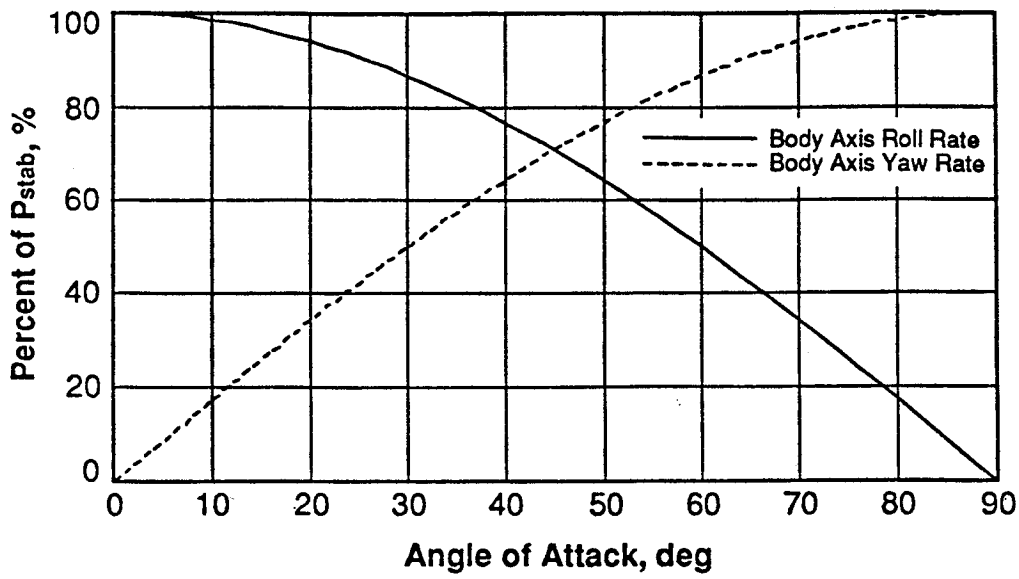

Figure C.2 Required Combinations Of Body Axis Roll And Yaw Rates For Stability Axis Roll Rates (REF. 28)

because the body axis yaw rate requirement increases with angle of attack. Additionally, notice that at 30° angle of attack, yaw rate must be half the value of P_{stab}, and at 45° angle of attack body axis roll and yaw rate must be equal. Reference 37 suggests that modern fighter aircraft be capable of achieving a minimum desirable wind axis roll rate of 60 degrees per second across the subsonic Mach number range of 0.2 to 0.6. This capability requires fighter aircraft to have a large degree of directional stability and directional control power at moderate to high angles of attack. For typical fighter aircraft there exists an angle of attack above which body axis yaw rate capability becomes the limiting factor in performing wind axis rolls. This is because yaw rate capability is typically much lower than roll rate capability, and decreases with angle of attack. To determine the body axis roll rate needed to coordinate the available body axis yaw rate above this angle of attack, Equation C.3 is solved for P:

$$P = R\cot\alpha - \sin\phi\cos\theta\frac{g}{V_t\sin\alpha} - n_y\frac{g}{V_t\sin\alpha} \qquad (C.11)$$

Equation C.11 represents the roll control surface contribution to roll rate which is required to maintain roll coordination as a function of the available yaw rate. It is important that rolls be coordinated to avoid oscillations in the lateral-directional axis which tend to reduce controllability. The equations presented here allow the cause of sideslip during a roll to be isolated and identified.

As an example of roll coordination analysis, consider the generic F-18A response to a full lateral stick roll at Mach equals 0.4 at an altitude of 15,000 feet (Figure C.3). Full positive lateral stick is input at time equals six seconds, while aft stick is held constant at 1.5 inches, which is 30% of full aft stick deflection. Figure C.3 shows that although the rudders generate a large amount of yaw rate, they saturate quickly, and adverse sideslip builds up to seven degrees. The cause of the adverse sideslip can be found by plotting sideslip rate (Equation C.3) along with the three terms for sideslip rate (Equations C.4, C.5, and C.6). This is done in Figure C.4, which demonstrates that the kinematic term is dominant. In the first half second, the kinematic term reaches over twice the magnitude reached by the next largest term, the gravitational term. Plotting the roll rate required for coordination (Equation C.9) with the actual roll rate shows the cause of the kinematic coupling. Figure C.5 shows that too much roll rate was commanded in the first 1.25 seconds for the amount of yaw rate that was available. Methods to improve the roll coordination would be in the form of a faster rudder, to allow the yaw rate to "keep up" with the roll rate; or a reduced roll rate, in proportion to the available yaw rate. The interested reader should consult Reference 26 for more details on these aspects.

Controlling and maintaining angle of attack is another concern when performing rolls about the velocity vector. By examining the equation for time rate of change of angle of attack,

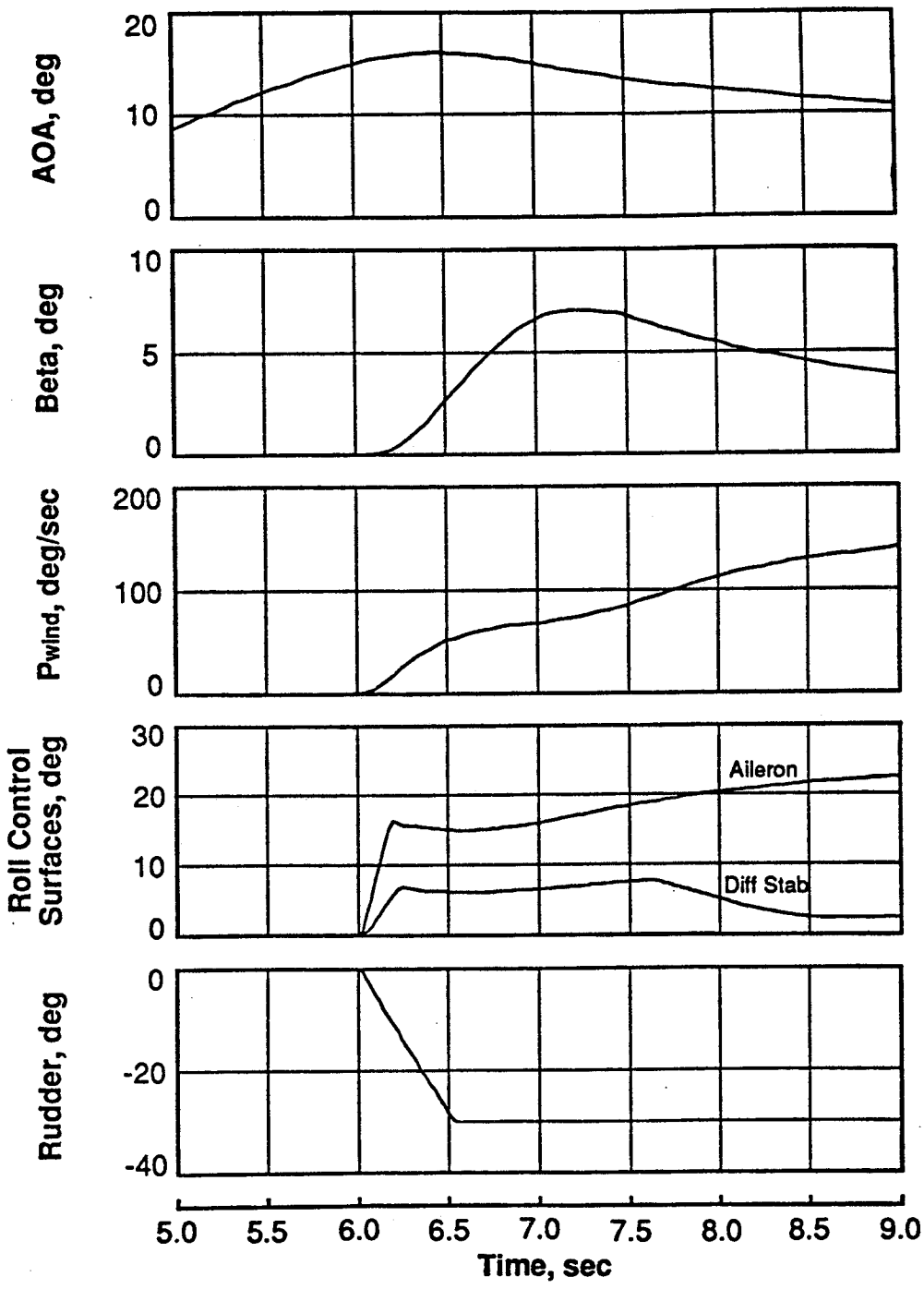

Figure C.3 Generic F-18A Response To Full Lateral Stick Command, Aft Stick = 1.5 inches, Mach = 0.4, H = 15,000 feet (REF. 28)

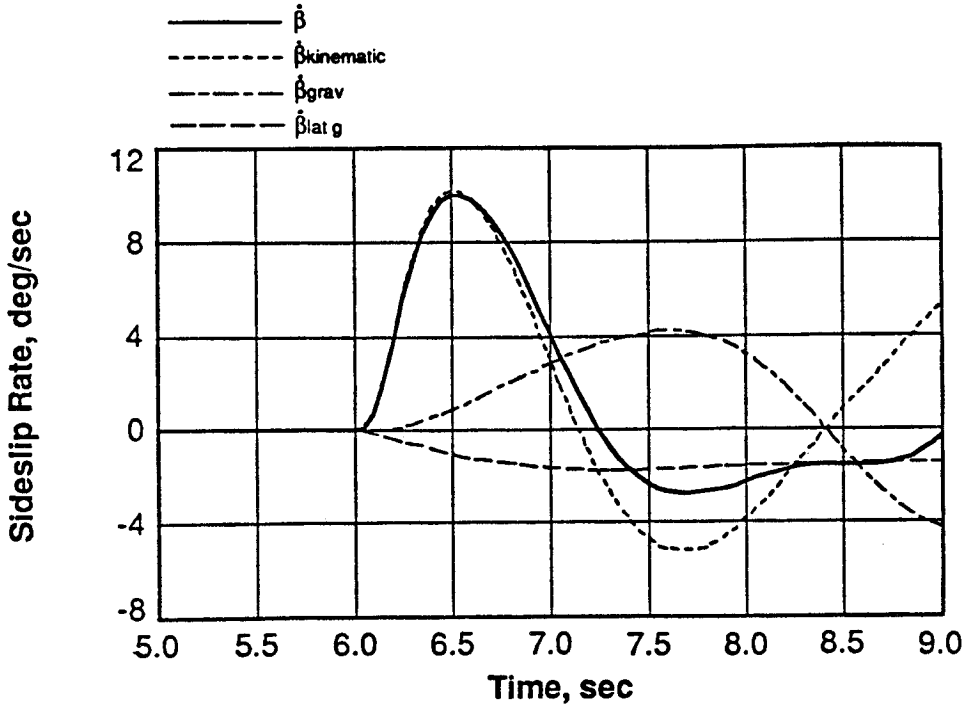

Figure C.4 Components Of Sideslip Rate Resulting From A Full Lateral Stick Command, Generic F-18A, Aft Stick = 1.5 inches, Mach = 0.4, H = 15,000 feet (REF. 28)

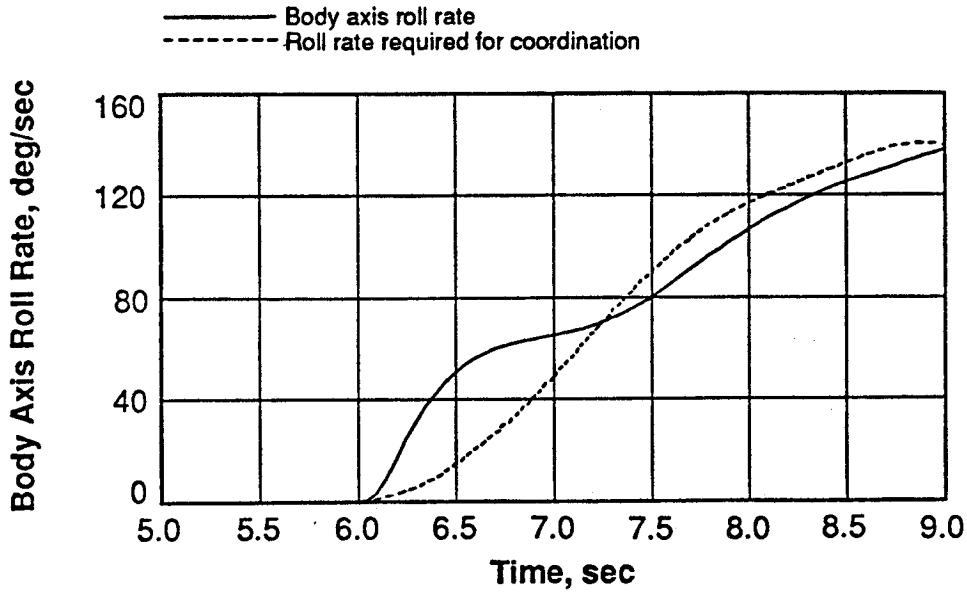

Figure C.5 Source Of Kinematic Coupling Into Sideslip Resulting From A Full Lateral Stick Command, Generic F-18A, Aft Stick = 1.5 inches, Mach = 0.4, H = 15,000 feet (REF. 28)

$$\dot{\alpha} = Q - P_{stab}\tan\beta - (L + T\sin\alpha)\frac{g}{W V_t \cos\beta}$$

$$+ (\cos\theta\cos\phi\cos\alpha + \sin\theta\sin\alpha)\frac{g}{V_t\cos\beta} \qquad \text{(C.12)}$$

it is seen that there are four contributors:

1. pitch rate

$$\dot{\alpha}_{\text{pitch rate}} = Q \qquad \text{(C.13)}$$

2. kinematic coupling

$$\dot{\alpha}_{\text{kinematic}} = P_{stab}\tan\beta \qquad \text{(C.14)}$$

3. lift

$$\dot{\alpha}_{\text{lift}} = (L + T\sin\alpha)\frac{g}{W V_t\cos\beta} \qquad \text{(C.14)}$$

4. gravity

$$\dot{\alpha}_{\text{gravity}} = (\cos\theta\cos\phi\cos\alpha + \sin\theta\sin\alpha)\frac{g}{V_t\cos\beta} \qquad \text{(C.15)}$$

Figure C.6 shows an example of how these terms contribute to angle of attack rate for the same full lateral stick roll maneuver shown in Figure C.3. When the aircraft is rolling, the kinematic coupling term (Equation C.13) shows that adverse sideslip contributes a negative value to angle of attack rate. The lift term (Equation C.14) remains essentially constant during the maneuver, while the gravitational term (Equation C.15) switches sign as the aircraft rolls to an inverted attitude. Note that while the aft stick command was held constant, the flight control system commanded additional pitch rate to counter the effects of the kinematic and gravitational terms.

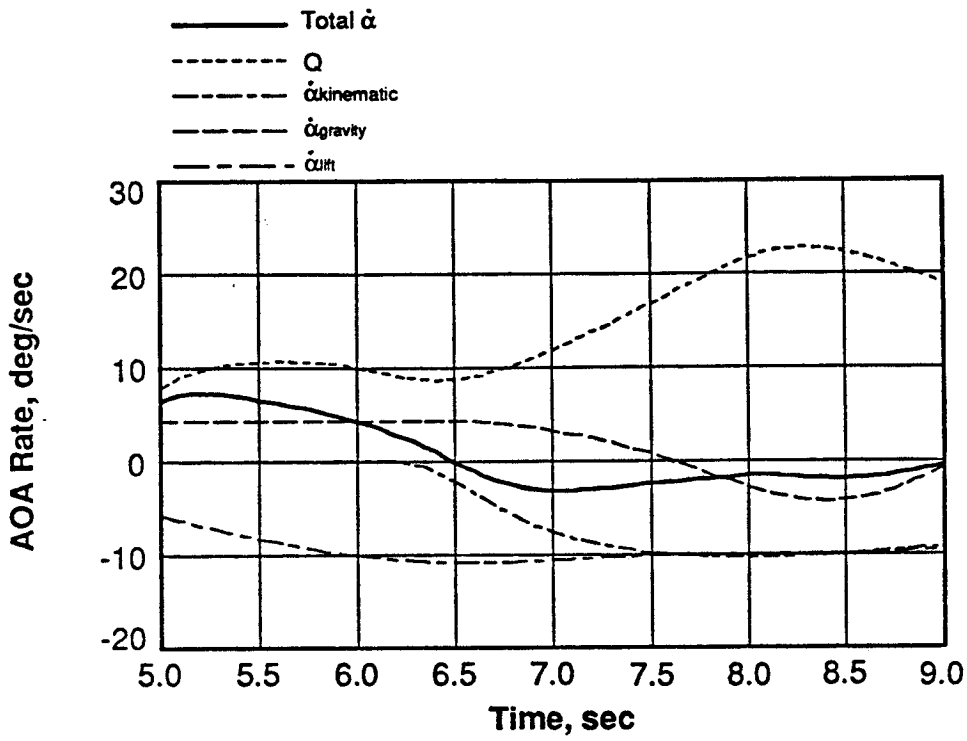

Figure C.6 Components Of Angle Of Attack Rate
Resulting From A Full Lateral Stick Command, Generic F-18A,
Aft Stick = 1.5 inches,Mach = 0.4, H = 15,000 feet (REF. 28)

C.4 COUPLING EFFECTS

Stability is of major importance at high roll rates because the roll response of the aircraft may not consist of only a pure rolling motion. The combined motion can also be divergent, such that the aircraft may depart from controlled flight due to uncommanded or unexpected responses. Four factors which dominate roll coupling effects are (REF. 71):

1) kinematic coupling

2) inertial coupling

3) I_{xz} effect

4) engine gyroscopic effect

The engine gyroscopic effects are only significant at very low airspeeds, where aerodynamic moments are small. Specifically, a departure in the longitudinal axis can occur as a result of executing a roll about the velocity vector. Equation C.16 is the aircraft pitch acceleration, without engine gyroscopic terms.

$$\dot{Q} = \frac{\Sigma M}{I_y} - PR\frac{(I_x - I_z)}{I_y} - (P^2 - R^2)\frac{I_{xz}}{I_y} \qquad (C.17)$$

Equation C.17 relates aerodynamic (first term), inertial (second term), and I_{XZ} (third term) contributions to pitch acceleration. Kinematic coupling occurs when the aircraft is rolled about an axis other than the velocity vector. The interchange of angle of attack and sideslip angle causes the aerodynamic moment in Equation C.17 to alternate between pitching and yawing moments, and leads to coupling (REF. 72).

Inertial coupling typically occurs when the magnitude of the roll moment of inertia, I_X, is much smaller than the pitch moment of inertia, I_Y, and the yaw moment of inertia, I_Z. For aircraft configurations in which significantly more mass is distributed in the fuselage along the X_B axis, as opposed to in the wing along the Y_B axis, i.e. $I_X << I_Y$, the second term in Equation C.17 is usually the dominant term. Since P and R have the same sign during a velocity vector roll at a positive angle of attack, their product is always positive, and the effect of inertial coupling is a nose-up pitching moment. This can be visualized by representing an airplane as a dumbbell aligned along the body x-axis as shown in Figure C.7. When the axis of rotation has the orientation as shown, the dumbbell wants to rotate clockwise (nose-up). It is therefore imperative that this inertial coupling does not overpower the available nose-down authority of the control effectors.

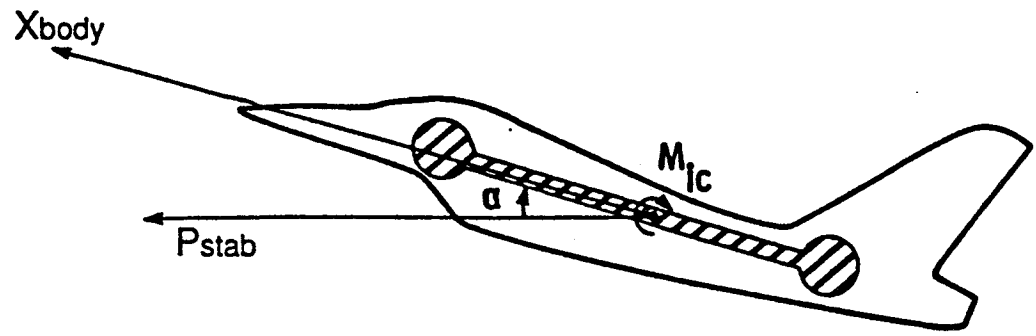

. Figure C.7 Pitching Moment Due To Inertial Coupling (REF. 73)

Although the product of inertia I_{XZ} is also an inertial parameter, it influences coupling in a different way. When an aircraft is rolled about an axis other than a principal axis, such as the stability axis or wind axis, I_{XZ} is nonzero and pitching and yawing rates contribute to pitch rate through the third term in Equation C.17. The contribution of I_{XZ} to pitch rate may not be very significant since it is normally small in magnitude compared to the moments of inertia.

C.5 PILOT CONSIDERATIONS

Executing a lateral agility maneuver such as a wind axis roll in a prescribed manner may result in sufficient pilot discomfort to prohibit or discourage its use. It is not uncommon for the incremental angles of attack and sideslip that are attained during these rolling maneuvers to produce accelerations which are disturbing to the pilot (REF. 71). The results of a study of piloting behavior presented in Reference 74 indicated that "the roll angular acceleration and the lateral linear accelerations at the pilot station are important considerations in flying qualities. The angular and linear accelerations can become objectionable when the roll damping (τ_R < .15 seconds), the height above the roll axis, or the product of these factors becomes very large". This also becomes a problem when the aircraft is prone to *roll ratcheting*, a condition described by evaluation pilots as the roll

response having "square corners" or being very "jerky" (REF. 75). In addition to being merely objectionable, the accelerations impose sometimes severe bending moments on the pilot's neck during such maneuvers. This problem is not easily overcome because the pilot's head is not restrained in the lateral direction of motion and current pilot helmets and associated headgear weigh in excess of three pounds.

Lateral acceleration at the pilot's station comes from three sources: lateral acceleration at the airplane center of gravity, body axis roll acceleration, and body axis yaw acceleration. The equation for lateral acceleration (n_y) at the pilot station is

$$g_{pilot} = n_y + \frac{P\Delta z}{g} + \frac{R\Delta x}{g} \qquad \text{(C.18)}$$

where:

Δz = distance of pilot above the center of gravity

Δx = distance of pilot ahead of the center of gravity

Figure C.8 shows the three terms in equation C.18 for the rolling maneuver of Figure C.3. Adverse sideslip and rudder deflection produce lateral g's at the center of gravity in the opposite sense of the initial roll and yaw accelerations. This causes g_{pilot} to begin in one direction and then switch sign in the steady state portion of the roll.

A requirement for acceptable levels of lateral accelerations has been proposed in Reference 76 in order to limit lateral accelerations to acceptable levels. This is done by forming the ratio of maximum lateral acceleration at the pilot station to maximum roll rate as measured during the first two and one half seconds following a step roll control input. Table C.1 shows the recommended $n_{Y\,MAX} / P_{MAX}$ values.

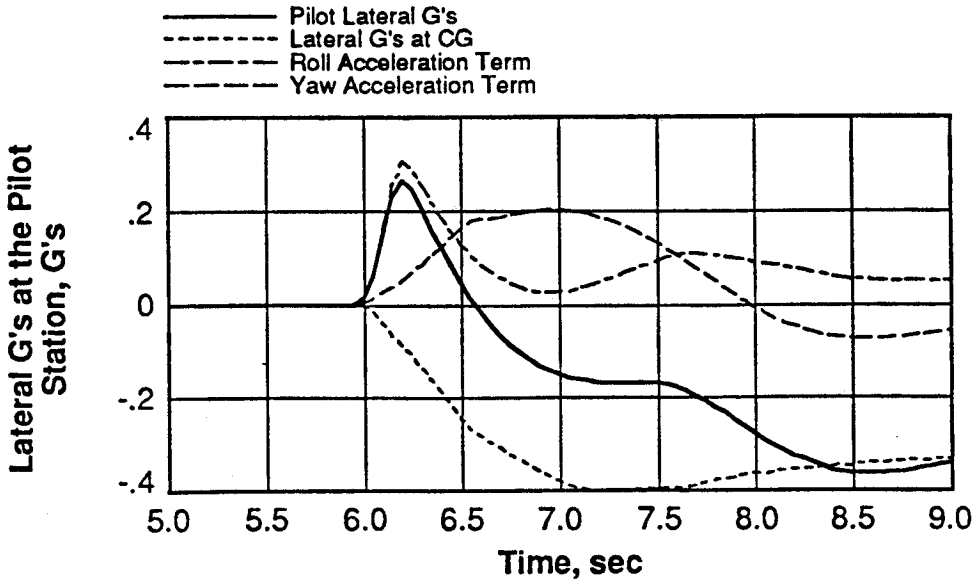

Figure C.8 Components Of Lateral Acceleration At The Pilot Station During A Full Lateral Stick Command, Generic F-18A, Aft Stick = 1.5 inches, Mach = 0.4, H = 15,000 feet (REF. 28)

Table C.1 Lateral Acceleration at Pilot Station Requirement (REF. 76)

Level	n_Y pilot max / P_{MAX} (g/deg/sec)
1	.012
2	.035
3	.058

The criteria of Table C.1 was applied to the "optimum" stability axis roll rate of 200 degrees per second suggested by Reference 19 and the 100 degrees per second wind axis roll rate discussed above. Solving for the maximum permissible n_Y max for each level, the following ranges were obtained:

Level	100 deg/sec	200 deg/sec
1	$n_Y \leq 1.2$	$n_Y \leq 2.4$
2	$1.2 < n_Y \leq 3.5$	$2.4 < n_Y \leq 7.0$
3	$5.8 < n_Y$	$7.0 < n_Y$

The Level 1 n_Y values for both the 100 and 200 degree per second roll rates appear to be reasonable when compared with the levels contained in Reference 77. The Level 2 values are arguably acceptable for the 100 degree per second roll rate since exposure to n_Y of up to 5g for short durations impairs but not does not prohibit pilot tracking tasks. The respective values for the 200 degree per second roll rate would have to be of very short duration if impairment of tracking tasks and ill effects on the pilot are to be avoided. The Level 3 values are unacceptably high for even extremely short durations. As a result, it appears that an applicable requirement for lateral accelerations at the pilot station will need to account for duration of exposure in addition to maximum acceleration levels.

Since lateral agility typically comprise rolling motions at elevated normal load factors, the possibility of g induced loss of consciousness (GLOC) due to large lateral accelerations at the pilot station is a concern. The consideration of large lateral accelerations is important not only for the determination of flying qualities, but also because of degrading effects on pilot motor and cognitive performances for demanding tasks such as air-to-air tracking during combat.

Recent research demonstrates that the physiological effect of high lateral accelerations ($n_Y >$ 2.0) on pilot mission effectiveness is a function of both the *magnitude* of the imposed acceleration and the *duration* of the exposure (REF. 77). Table C.2 indicates the levels of physiological impairment and effects on pilot mission effectiveness as a result of imposed high lateral accelerations during an air-to-air combat tracking task.

Table C.2 Effect of High Lateral Accelerations on
Pilot Physiology and Mission Effectiveness (REF. 77)

$\pm n_Y$	Duration (seconds)	Effect
2	15	impairment; tracking tasks difficult but possible
5+	10+	discomfort, headaches; tracking tasks not possible

Clearly, even relatively mild lateral acceleration levels such as 2g over short periods of time should be avoided if possible. Even though the physiological effect may consist only of discomfort, it can distract the pilot's attention from critical flying tasks in situations when pilot workload is already heavy. Limiting the duration of exposure to only very short intervals will not prevent the effects, but is crucial for keeping them within tolerable and manageable levels. Exposure to very high accelerations for periods of less than one second will impair the pilot temporarily, can cause serious injury and in some instances will result in death (REF. 77).

The issues discussed above are important when studying agility, although much insight can be gained through the study of flying qualities and flying qualities parameters, especially when considering the roll axis (REF. 34). Investigation of lateral agility and its relationship to flying qualities using real time manned flight simulators is beyond the scope of this report. The reader should consult Reference 19 for results concerning this important facet of lateral agility.

D. ADDITIONAL AXIAL AGILITY CONSIDERATIONS

D.1 BACKGROUND

A prevalent misconception concerning axial agility is that the axial agility metrics quantify the level acceleration/deceleration capability of aircraft. This appendix contains an analysis that elucidates the distinct differences between level acceleration capability and axial agility. An example result is presented using the generic F-18A.

D.2 THE COMPONENTS OF AXIAL AGILITY

Axial agility metrics do **not** quantify the acceleration or deceleration performance of an aircraft. This can be shown by starting with the relation for specific excess power (REF. 78)

$$P_S = \frac{V\,(T - D)}{W} \qquad \text{(D.1)}$$

where

V = total velocity	(ft/sec)
T = thrust	(lbf)
D = drag	(lbf)
W = weight	(lbf)

Since $\Delta P_s / \Delta t$ is approximately the derivative of P_s with respect to time, Equation D.1 is differentiated to obtain

$$\frac{\Delta P_S}{\Delta t} \cong \frac{dP_S}{dt} = \left(\frac{(T-D)}{W}\right)\frac{dV}{dt} + \left(\frac{V}{W}\right)\frac{dT}{dt} - \left(\frac{V}{W}\right)\frac{dD}{dt} \qquad \text{(D.2)}$$

where the weight is assumed to be constant. The first term in Equation D.2 is the component of

$\Delta P_s/\Delta t$ due to acceleration of the airframe; the second and third terms are the components due to time rate of change of thrust and drag respectively. Acceleration (dV/dt) does not have a pronounced effect on the values of $\Delta P_s/\Delta t$. This is because the very short spool times of fighter aircraft engines (generally between three and five seconds), and the rapid drag rise due to deployment of speedbrakes cause the time rate of change of the thrust and drag terms to be much larger than the acceleration term. As a result the second and third terms in Equation D.2 achieve their respective maximum/minimum values before acceleration becomes large enough to contribute significantly to $\Delta P_s/\Delta t$. These relationships are displayed in Figure D.1, which is a plot of the three terms in Equation D.2 during a typical data collection run. Note that each term is plotted on a different scale.

The time history of the first term, the contribution of the time rate of change of velocity, is considerably smaller in magnitude relative to the second and third terms (time rate of change of thrust and drag respectively). This demonstrates that axial agility is not dominated by acceleration capability. The time history of the second term shows the thrust level increasing at a constant rate from time equals 8.3 seconds to 10.3 seconds, during the engine spool up time, before leveling off at maximum thrust. The time rate of change of drag, the third term, reflects the change (decrease) in drag due to retraction of the speedbrake over a period of one second, starting at time equals eight seconds. This time history is less intuitive at first glance due to the sign convention. When retracting the speedbrake, the time rate of change of drag increases in magnitude, but is negative in sign (since drag is decreasing).

The axial agility of a fighter is also affected by the engine's transient performance during large scale maneuvering, and at elevated angles of attack and sideslip. Although this engine behavior is an important contributor to overall combat effectiveness, the *power onset parameter* and the *power loss parameter* do not address this aspect.

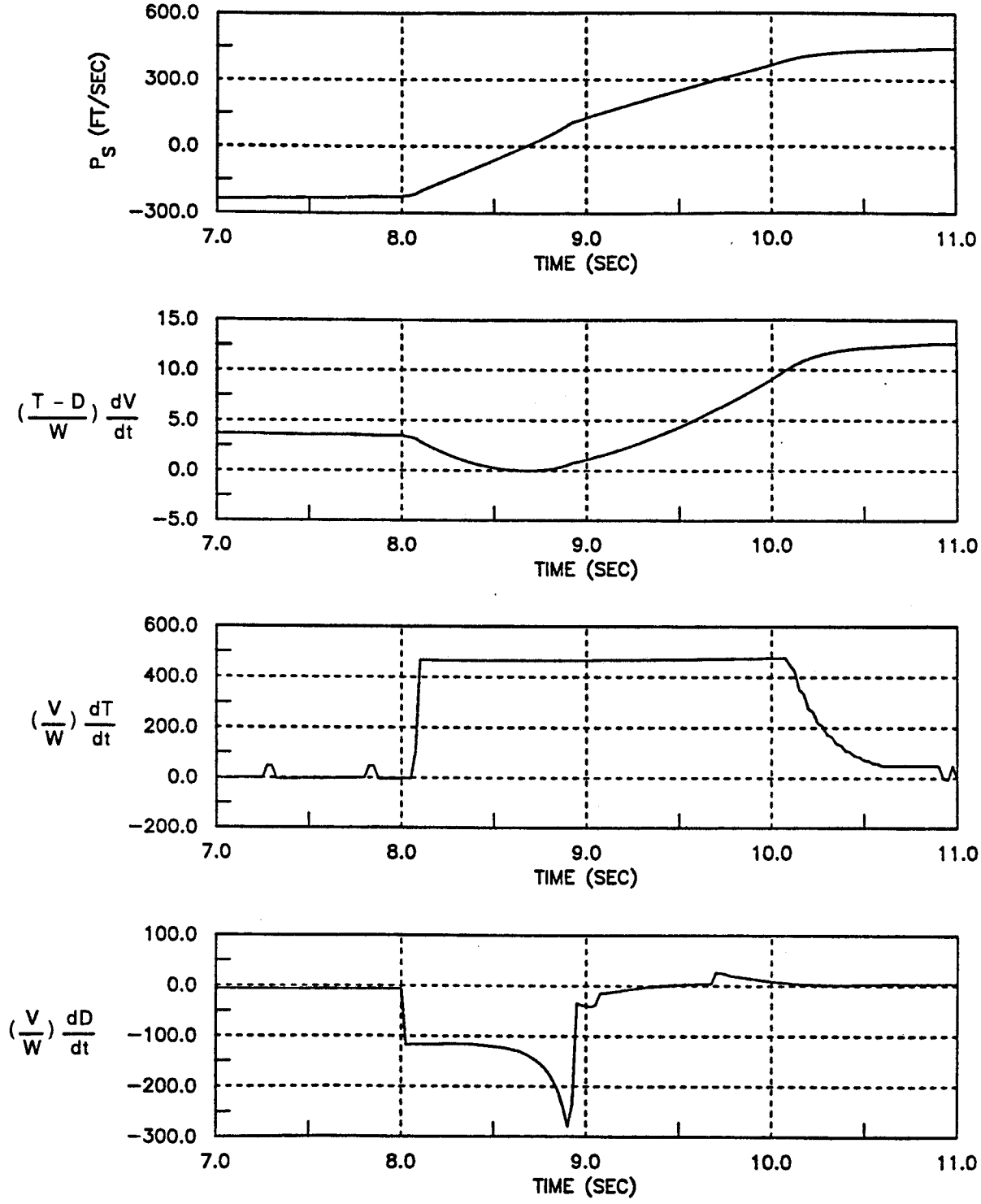

Figure D.1 Terms In Approximation of $\Delta P_s/\Delta t$, *Power Onset, Parameter*, Generic F-18A, Mach = 0.7, H = 15,000 feet

E. DERIVATION OF INSTANTANEOUS AGILITY METRICS

E.1 BACKGROUND

Instantaneous agility is concerned with the instantaneous angular acceleration capabilities of aircraft. The candidate instantaneous agility metrics are obtained by writing the aircraft equations of motion with respect to the aircraft velocity vector and then differentiating with respect to time. The result is acceleration and jerk of the velocity vector, when taking the second and third derivatives with respect to time. While the derivations of these metrics have remained proprietary and unpublished in the open literature, the metrics themselves have been published. The purpose of this chapter is to clearly demonstrate the derivation of these metrics, derive approximations to the metrics which aid in their physical understanding, and outline the scope of their applicability.

E.2 CANDIDATE INSTANTANEOUS AGILITY METRICS

E.2.1 **Curvature Agility** (REF. 18, 33)

Definition:

This metric is defined as

$$\text{Curvature Agility} = 2\,\omega\,\dot{v} + v\,\dot{\omega}$$

where v is aircraft velocity, and ω is turn rate.

Discussion:

The *curvature agility* metric is intended to quantify the instantaneous pitch agility of aircraft. It is based upon the second derivative with respect to time of the aircraft velocity

vector. This metric is not task oriented but rather an essentially open loop metric, since there is no specified initial or terminal state, nor any upper or lower limit on it's value.

E.2.2 **Herbst Torsional Agility** (REF. 18, 33)

Definition:

This metric is defined as

$$\text{Torsional Agility} = \frac{d}{dt}\left(\dot{\text{Я}} - \dot{\chi}\sin\gamma\right)$$

where the variables are defined in the Serret-Frenet reference system of References 64 and 65:

γ	=	pitch angle (or flight path angle)
χ	=	heading angle
Я	=	roll angle

Like the *curvature agility* metric, *Herbst torsional agility* is open loop and based upon the second derivative with respect to time of the aircraft velocity vector. Although this is a lateral agility metric, it bears no real similarity to the *torsional agility parameter* defined in Section A.3.7 of Appendix A other than by name.

E.3 DERIVATION AND APPROXIMATION TO THE INSTANTANEOUS AGILITY METRICS

The Serret-Frenet reference system is briefly introduced to make clear the physical meaning of the terms in the *Herbst torsional agility* metric. The pitch angle (or flight path angle) Γ and heading angle χ of the Serret-Frenet system are identical to γ and ψ respectively in the

familiar stability axis system. The angle Я, however, is the angle from the horizontal plane to a plane called the *maneuver plane*. Figure E.1 shows the geometry of a steady level turn to demonstrate the definition of the maneuver plane and the angle Я.

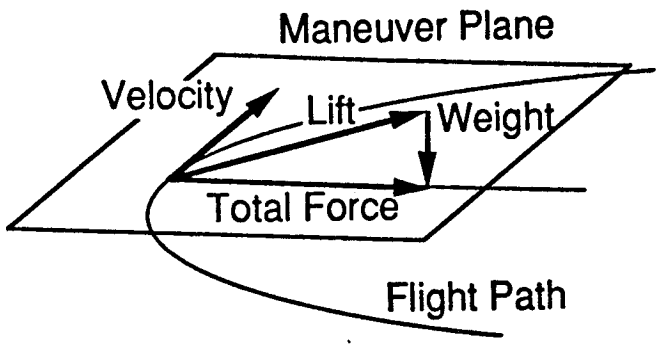

Figure E.1 Geometry of the Maneuver Plane in a Steady Level Turn

The maneuver plane is the plane that contains both the velocity vector and the total force vector. It is sometimes referred to as the *osculating plane*. The total force vector is the vector sum of all forces acting on the airplane, including gravity. In this example it is assumed that thrust equals drag (T+D=0) so the total force is the vector sum of lift and weight. In a steady level turn the total force vector, and the maneuver plane, are in the horizontal plane. The roll angle Я is defined in Figure E.2.

Roll rate $P_{man\ plane}$ is the angular rate of the maneuver plane about the velocity vector and can be written in terms of the Serret-Frenet Euler angles as

$$P_{man\ plane} = \dot{Я} - \dot{\chi} \sin \gamma \qquad \text{E.1}$$

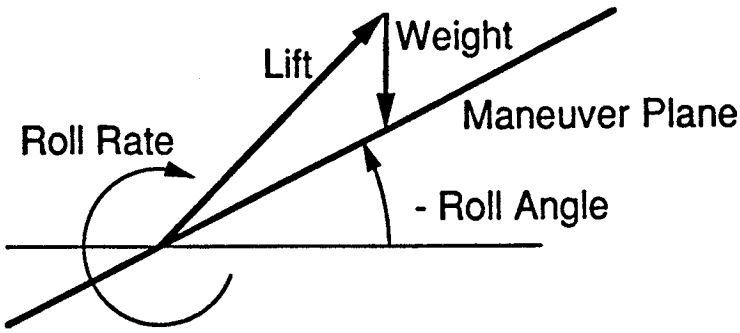

Note: Velocity Vector Points Into the Page

Figure E.2 Definition of Serret-Frenet Roll Angle $\Re$ and Roll Rate $P_{man\ plane}$

This is directly analogous to body axis roll rate P_{body} written in terms of the body axis Euler angles:

$$P_{body} = \dot{\phi} - \dot{\psi}\sin\theta \qquad \text{E.2}$$

It is possible to write these metrics in terms of more familiar parameters. The turn rate ω can be written as

$$\omega = \frac{A_{cent}}{V} \qquad \text{E.3}$$

where A_{cent} is the centripetal acceleration due to the total force acting perpendicular to the velocity vector. Taking the derivative of ω,

$$\dot{\omega} = \frac{\dot{A}_{cent}}{V} - \frac{\dot{V}\,A_{cent}}{V^2} \qquad \text{E.4}$$

and substituting this and equation E.1 into the defintion of the *curvature agility* metric, provides the following relationship for *curvature agility*:

$$\text{curvature agility} = \frac{\dot{V}\, A_{cent}}{V} + \dot{A}_{cent} - \frac{\dot{V}\, A_{cent}}{V} \qquad \text{E.5}$$

or

$$\text{curvature agility} = \dot{A}_{cent}$$

An approximation for $\dot{A}_{cent}$ and therefore *curvature agility* can be devised in terms of a combination of body axis accelerations (A_x, A_y, A_z) as measured by accelerometers and the acceleration due to gravity. The accelerations are then transformed to the stability axis system where the normal and lateral accelerations are added vectorially. Thus assuming that the sideslip angle β is small, $\dot{A}_{cent}$ can be approximated as

$$\dot{A}_{cent} = \frac{d}{dt}\sqrt{[\,(-A_n + \cos\theta\cos\phi)\cos\alpha - (A_x - \sin\theta)\,]^2 + (A_y + \cos\theta\sin\phi)^2} \qquad \text{E.6}$$

Equation E.6 can be simplified by assuming that the force of gravity is small compared to the body axis normal and axial forces (A_n and A_x), and that the lateral accelerations (A_y) are small. This results in

$$\dot{A}_{cent} \approx \frac{d}{dt}\sqrt{(-A_n\cos\alpha - A_x\sin\alpha)^2} \qquad \text{E.7}$$

As a final simplification, it is assumed that the first term is much larger than the second so that

$$\text{curvature agility} \approx -\dot{A}_n \qquad \text{E.8}$$

To construct an approximation to the *Herbst torsional agility* metric, the inclination of the maneuver plane is determined using the direction of the lift vector alone. This assumes that lateral accelerations, A_y, on the airplane are small and that the addition of the gravity vector to the lift vector makes a small change in the inclination of the total force vector. Therefore the maneuver plane roll rate is approximated by wind axis roll rate, i.e.

$$P_{man\,plane} \approx P_{wind} = P\cos\alpha\cos\beta + R\sin\alpha\cos\beta + Q\sin\beta \qquad \text{E.9}$$

Therefore, *Herbst torsional agility* can be approximated as wind axis roll acceleration.

$$\text{Herbst torsional agility} = \frac{d}{dt} P_{man\,plane} \approx \frac{d}{dt} P_{wind} \qquad \text{E.10}$$

E.4 INSTANTANEOUS AGILITY RESULTS

The approximations for *curvature agility* (equation E.8) and *Herbst torsional agility* (equation E.10) respectively are compared to the definitions of the *curvature agility* and *Herbst torsional agility* metrics using flight test data and simulation data for a single aircraft. For comparing the *curvature agility* approximation to the complete metric, flight test data of a -15° to 10° pitch angle capture maneuver performed at 200 knots and 15° angle of attack is used. The data used to construct the *Herbst torsional agility* comparison is obtained from computer flight simulation data of a 5g roll maneuver performed at Mach equals 0.7 at an altitude of 15,000 feet.

E.4.1 Curvature Agility Results

Figure E.3 demonstrates how well the approximation of equation E.8 matches the definition of the *curvature agility* metric. The actual maneuver commences at time equals six

seconds. Except for some slight disagreement near the peaks at time equals ten seconds and time equals eleven seconds respectively, the approximation is excellent.

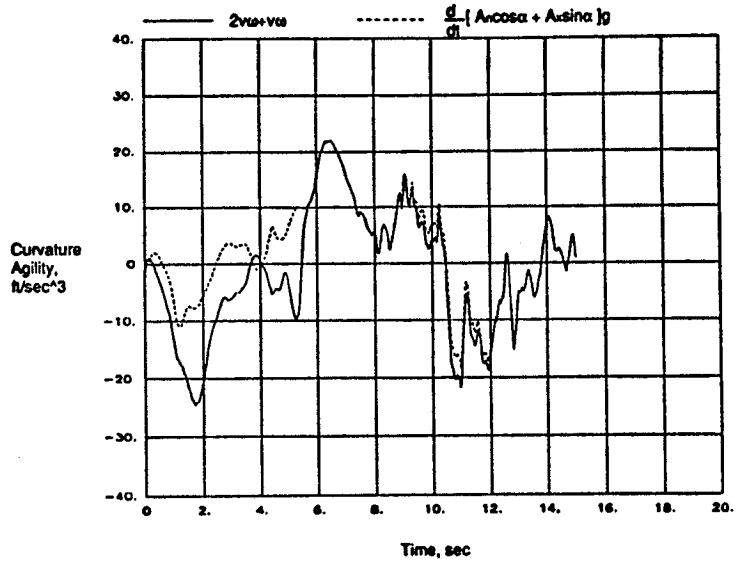

Figure E.3 Comparison Of Approximation To The *Curvature Agility* Metric, -15° To 10° Pitch Capture, 200 KTAS, Angle Of Attack = 15°

E.4.2 Herbst Torsional Agility Results

Figure E.4 demonstrates how well equation E.10 matches the definition of the *Herbst torsional agility* metric. The actual maneuver commences at time equals two seconds. Although not an exact match, the approximation captures the main features of the metric.

E.5 SUMMARY

The *curvature agility* metric and the *Herbst torsional agility* metric are shown to be approximated by the time rate of change of normal acceleration and roll acceleration in the wind

axis respectively. Both approximations appear to be satisfactory for obtaining quantitative information about *curvature agility* and *Herbst torsional agility.* Since both metrics are open loop and not task oriented they are subject to the pitfalls inherent of maximum rate type metrics, specifically, that "more is better".

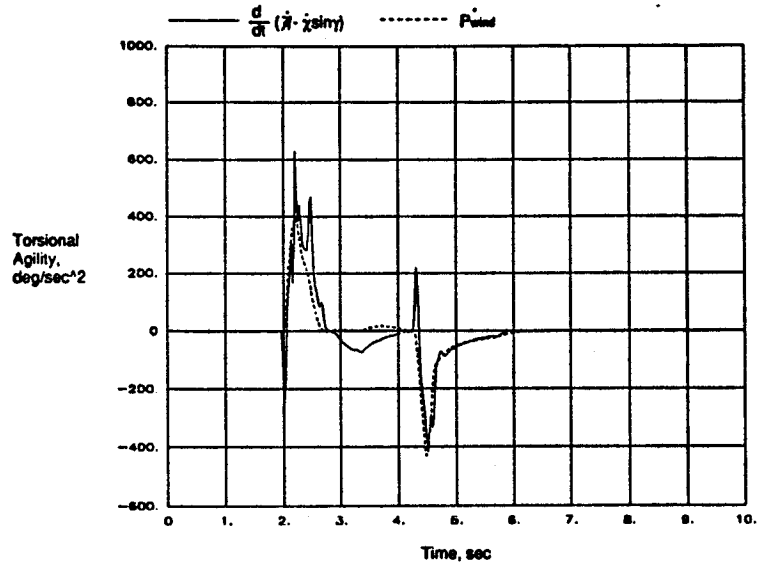

Figure E.4 Comparison Of Approximation To The *Herbst Torsional Agility* Metric, 5g Roll Maneuver, Mach = 0.7, H = 15,000 feet